THE ACTIVITY OF AMYLOID BETA BINDING ALCOHOL DEHYDROGENASE IN ALZHEIMER'S DISEASE

Zoe Eleanor Allen

A Thesis Submitted for the Degree of MPhil
at the
University of St. Andrews

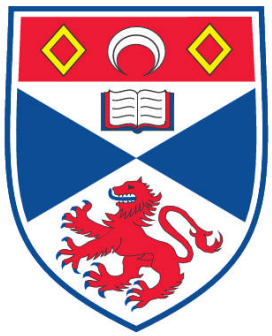

2012

THE ACTIVITY OF AMYLOID BETA BINDING ALCOHOL DEHYDROGENASE IN ALZHEIMER'S DISEASE

ZOE ELEANOR ALLEN

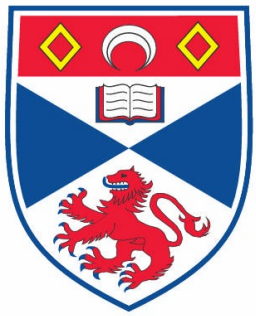

This thesis is submitted to the University of St Andrews in partial fulfilment for the degree of Master of Philosophy

School of Biology

January 2012

ABSTRACT

The mitochondria are a vibrant hub for many problems that occur in Alzheimer's disease. The enzyme amyloid-β binding alcohol dehydrogenase (ABAD) and Cyclophilin D (CypD) are two key mitochondrial proteins that have essential functions in Alzheimer's disease. ABAD is crucial in the generation of energy via the β-oxidation of fatty acids, and CypD has been linked to Alzheimer's disease through the initiation of necrosis.

Changes in glucose metabolism have been observed in the brains of Alzheimer's disease sufferers. This suggests that neurons require an alternative energy source that can bypass glycolysis in order to produce energy. The oxidation of fatty acids is crucial at this point as the products of this catabolism can feed into the second stage of the respiratory cycle. In Alzheimer's disease, Amyloid-β (Aβ) has been found to bind to ABAD distorting the catalytic site changing its activity.

The first objective of this thesis was to investigate a potential previously reported interaction between ABAD and CypD. To explore this further, FRET analysis and immunoprecipitation studies were conducted. Though no strong interactions were observed from the immunoprecipitation studies, live cell FRET analysis did reveal a small/weak interaction between CypD and ABAD. Additional studies also showed a decrease in ABAD activity in the presence of CypD, suggesting that there could be functional consequences from this interaction between CypD and ABAD.

I also explored the effect of changing cellular energy sources on the activity of ABAD. ABAD activity was found to increase under conditions of reduced glucose in both HEK 293 and SK-N-SH cells expressing ABAD. In addition, Alois Alzheimer initially reported changes in lipids. These reported changes in lipids were explored under conditions where there was increased expression of ABAD and in the presence of Aβ. On the whole, the changes suggested that there was a shift in the metabolism of fatty acids when ABAD was expressed further implying a change in energy sources in the Alzheimer's disease brain.

DECLARATION

I, Zoe Allen hereby certify that this thesis, which is approximately 39,000 words in length, has been written by me, that it is the record of work carried out by me and that it has not been submitted in any previous application for a higher degree.

I was admitted as a research student in September 2010 and as a candidate for the degree of Master of Philosophy in January 2011; the higher study for which this is a record was carried out in the University of St Andrews between 2010 and 2011.

Date…… Signature of candidate ……

I hereby certify that the candidate has fulfilled the conditions of the Resolution and Regulations appropriate for the degree of Master of Philosophy in the University of St Andrews and that the candidate is qualified to submit this thesis in application for that degree.

Date…… Signature of supervisor ……

COPYRIGHT DECLARATION

In submitting this thesis to the University of St Andrews I understand that I am giving permission for it to be made available for use in accordance with the regulations of the University Library for the time being in force, subject to any copyright vested in the work not being affected thereby. I also understand that the title and the abstract will be published, and that a copy of the work may be made and supplied to any bona fide library or research worker, that my thesis will be electronically accessible for personal or research use unless exempt by award of an embargo as requested below, and that the library has the right to migrate my thesis into new electronic forms as required to ensure continued access to the thesis. I have obtained any third-party copyright permissions that may be required in order to allow such access and migration, or have requested the appropriate embargo below.

The following is an agreed request by candidate and supervisor regarding the electronic publication of this thesis:

Access to printed copy and electronic publication of thesis through the University of St Andrews.

Date …….. signature of candidate …….. signature of supervisor ……

ACKNOWLEDGEMENTS

Science has brought me close to many amazing people I fear I would not have met otherwise.

To my Professor, Dr Frank Gunn-Moore, I owe the most humongous thank you, words cannot describe how grateful I am for your support and guidance. Thank you for your time, your encouragement and your friendship.

Many thanks to Terry Smith for your time, input and generous teaching of all things lipid!

To my mum, apologies for the stress and anxiety caused! Thank you for your constant reassurance and for giving me the conviction to carry on when things were rough. Thank you both mum and dad for the love and support throughout the year, and most of all for your understanding and patience.

A big thank you to the girls in the lab: Laura, Lotte, Susana, Eva, Elaine and Kirsty. Thank you for all the laughs, your listening ears and your wise words of advice.

Finally, thank you to Em and Marcus for the most ridiculous moments and silly carry ons throughout the year. Em, thank you for your scientific integrity, thought provoking questions and most of all for being there.

Marcus without you I honestly do not think I would have finished the introduction. You have been there at every point with words of encouragement and overwhelming faith in me.

Gandhi once said

'Whatever you do in life will be insignificant but it is very important that you do it'

I am determined that whatever I do in life will have an impact and consequently be important.

TABLE OF CONTENTS

FIGURES AND TABLES

APPENDIX

ABBREVIATIONS

^{18}FDG-PET	(^{18}F) Fluorodeoxyglucose positron emission tomography
2D-DIGE	Two dimensional-difference gel electrophoresis
4-HNE	4-hydroxynoneal
8-OHG	8-hydroxyguanosine
AA	Arachidonic acid
ABAD	Amyloid-β binding alcohol dehydrogenase
ABAD-DP	Amyloid-β binding alcohol dehydrogenase – decoy peptide
AD	Alzheimer's disease
ADP	Adenosine diphosphate
ANT	adenine nucleotide translocase
ApoE ε4	Apolipoprotein ε4
APP	Amyloid precursor protein
APS	Ammonium persulphate
ATP	Adenosine triphosphate
Aβ	Amyloid β
BACE	β-site APP cleavage enzyme
BSA	bovine serum albumin
CDP-DAG	cytidine diphosphate-diacylglycerol
CFP	cyan fluorescent protein
CLU	Clusterin

CMRg	Cerebral metabolic rate $_{glucose}$
COX	Cytochrome C oxidase
CRC	Calcium retention capacity
CsA	Cyclosporin A
CSF	Cerebrospinal fluid
C-terminus	carboxy terminal
CypD	Cyclophilin D
DHA	Docoashexanoic acid
DMEM	Dulbecco's minimal essential medium
DMSO	Dimethyl sulfoxide
DNA	Deoxyribonucleic acid
dNTP	deoxy nucleoside triphosphate
DTT	Dithiothreitol
E.coli	*Escherichia coli*
ECFP	enhanced cyan fluorescent protein
EDTA	Ethylenediaminetetraacetic acid
Ep-1	Endophilin 1
ER	Endoplasmic reticulum
ERAB	Endoplasmic reticulum amyloid-β binding protein
ESI	Electrospray ionisation
ESI-MS	Electrospray ionisation- mass spectrometry
ETC	electron transport chain

EYFP	enhanced yellow fluorescent protein
FAD	Familial Alzheimer's disease
FCS	Foetal calf serum
FLIM	Fluorescence lifetime imaging microscopy
FRET	Förster/ Fluorescent resonance energy transfer
GFP	green fluorescent protein
GLUT	Glucose transporters
GWAS	Gene wide association study
HADH II	L-3-hydroxyacyl-CoA dehydrogenase type II
HADH	3-hydroxyacyl-CoA dehydrogenase
HEK 293	Human embryonic kidney cell line
HIV-1 TAT	Human immunodeficiency virus 1-transactivator
HRP	horseradish peroxidase
HSD10	17β-hydroxysteroid dehydrogenase type 10
IMM	Inner mitochondrial membrane
JNK	c-jun N-terminal kinase
KGDHC	α-ketoglutarate dehydrogenase
LB	Luria Bertani
MDA	Malondialdehye
MEF	mouse embriyonic fibroblasts
MEM	Minimum essential medium eagle
MMSE	Mini mental State Examination

mPTP	mitochondrial permeability transition pore
MRI	magnetic resonance imaging
MS	Mass spectrometry
MTT	3-(4,5-Dimethylthiazol-2-yl)-2,5-diphenyltetrazolium bromide
mutABAD	mutated ABAD
MVB	Multivesicular bodies
NAD	Nicotinamide adenine dinucleotide
NFT	Neurofibrillary tangles
N-terminus	amino terminus
OMM	outer mitochondrial membrane
PA	phosphatidic acid
PAGE	polyacrylamide gel electrophoresis
PBS	Phosphate buffered saline
PC	phosphatidylcholine
PCR	polymerase chain reaction
PDHC	Pyruvate dehydrogenase complex
PE	phosphatidylethanolamine
PET	Positron emission tomography
PFA	Paraformaldehyde
PI	phosphatidylionositol
PIB-PET	Pittsburgh compound B - positron emission tomography
PICALM	Phosphatidylinositol-binding clatharin assembly lymphoid-myeloid

PKC	protein kinase C
PLA_2	phospholipase A_2
PLC	Phospholipase C
PMSF	Phenylmethulsuflonylfluoride
Prdx-2	Peroxiredoxin 2
PS	phosphatidylserine
PSB	Protein sample buffer
Q1	Quadropole 1
Q2	Quadropole 2
Q3	Quadropole 3
ROI	regions of interest
ROS	reactive oxygen species
SAT	Serine acetyltransferase
SCHAD	short chain L-3-hydroxyacyl-CoA dehydrogenase
SDS	Sodium Dodecyl Sulphate
SDS-PAGE	Sodium Dodecyl Sulphate-polyacrylamide gel electrophoresis
SK-N-SH	human neuroblastoma cell line
SM	Sphingomyelin
SOC	super optimal catabolite repression broth
SOD	superoxide dismutase
SPR	surface plasmon resonance
TBE	tris-borate-EDTA buffer

TBS	Tris buffered saline
TBS-T	Tris buffered saline with Tween 20
TEM	transmission electron microscopy
TEMED	tetramethylethylenediamine
Tg	Transgenic
TIM	Translocase of the inner membrane
TLC	thin layer chromatography
TNFα	Tumour necrosis factor α
TOM	Translocase of the outer membrane
Tween 20	polyoxyethylenesorbitan monolaurate
UV	ultra violet
VDAC	voltage dependent anion channel
Wt	wild type
YFP	yellow fluorescent protein

Chapter 1: INTRODUCTION

1.1 ALZHEIMER'S DISEASE

Alzheimer's disease (AD) is a debilitating progressive disorder, initially characterised clinically by abnormalities in memory, language, judgement and orientation, which all stem from a gradual deficit in declarative memory (Muirhead et al., 2010a, Alzheimer's Research Trust, 2010). Dementia symptoms such as memory loss appear many years after the onset of the disease, as the decline in memory is attributed to the loss of neuronal cells. Neuronal loss occurs in specific regions of the brain, starting with degeneration of the entorhinal cortex, hippocampus and the cerebral cortex. The progressive loss of neurons in the AD brain leads to a notably large reduction in brain mass post mortem.

AD is present in two forms, Familial Alzheimer's Disease (FAD) and Sporadic Alzheimer's Disease. FAD is most commonly known as early onset AD, as symptoms of dementia start around 40 years of age. FAD is passed through generations via mutations in genes involved in specific chemical pathways associated with the biochemical hallmarks of the disease. In comparison, sporadic AD occurs past the age of 65 and has less strongly associated links to genetic mutations; but an increased prevalence of the Apolipoprotein ε4 (ApoE ε4) allele has been shown to increase the likelihood of developing AD (Rebeck et al., 1993). Due to the population of individuals studied and the selection of control participants, the risk of developing AD and having ε4 homozygotes varies between studies. Reported findings have suggested that heterozygote carriers of ApoE ε4 have a 20-70% increased risk of developing AD (Tsai et al., 1994, Ertekin-Taner, 2007) Recent genome-wide association studies (GWAS) have reported two new genes linked to AD: Clusterin gene (*CLU*, also known as Apolipoprotein J) found on chromosome 8 and involved in pathways that lead to inflammation within the brain; Phosphatidylinositol-binding clatharin assembly lymphoid-myeloid

(*PICALM*) gene, which is implicated in the trafficking mechanisms in cells, particularly the release of synaptic vesicles from the pre-synaptic terminal (Harold et al., 2009, Kamboh et al., *in press,* Borovecki et al., 2011)

Early stage diagnosis of sporadic AD is very difficult as 'forgetfulness' is a common occurrence in aging. However, one of the main tests conducted to define dementia is the Mini Mental State Examination (MMSE) which tests memory based on a scoring system (Dajani, 2011). Further diagnostic procedures include neuroimaging using MRI (magnetic resonance imaging), measuring glucose metabolism using (^{18}F) Fluorodeoxyglucose positron emission tomography (FDG-PET) and the presence of specific biomarkers such as amyloid-β_{42} ($A\beta_{42}$), total tau and hyperphosphorylated tau in the cerebrospinal fluid (CSF) of AD patients (Blennow, 2006, Blennow et al., 2010, Jack et al., 2008).

Since the first recorded case of AD in 1906, it has now become the most prevalent form of neurodegeneration in the UK and as the greatest risk factor for AD is age, the growing population of elderly people indicates a quickly developing social and economic problem (Alzheimer's Research Trust, 2010). In addition to the risk of aging as a precursor to AD, poor diet and lack of exercise are all seen to exacerbate the risk of developing AD (Judd, 2011).

1.2 NEUROPATHOLOGY OF ALZHEIMER'S DISEASE

Three pathologies seen in AD brains distinguish AD from other forms of dementia and are thought to be the key contributing factors of the disease. Neurofibrillary tau 'tangles', Amyloid- β 'plaques' and lipoid granules were first identified by Alois Alzheimer upon post-mortem of Auguste Deter, later diagnosed as the first reported case of AD (Foley, 2010). The two former, distinct histopathological features have been widely investigated since their initial discovery, and the presence of both allow for a definitive diagnosis of AD at post-mortem.

1.2.1 LIPID GRANULES

The occurrence of lipid granules in the AD brain signifies an accumulation of insoluble materials. Lipid deposits are commonly seen in aged brains but are excessively present in AD (Foley, 2010). Liposomic phagocytosis of highly oxidised cellular components form these lipid granules (Foley, 2010, D'Andrea et al., 2002). Analysis of the lipid components in AD brains highlights two key lipid classes, ceramide and sphingomyelin (see section 1.4.2) at abnormal levels, and the change in these lipids has been hypothesised to have effects on neuronal functioning (Han et al., 2011).

Although it has not been widely studied, the role for lipids in AD is mainly through membrane composition. In AD brains, the lipid content of membranes is of particular importance in the generation of Amyloid β (Aβ) and consequently changing the lipid composition and their relative levels modifies Aβ production (see section 1.4.2). Additionally, particular lipids have been seen to have protective roles in attenuating Aβ accumulation, again through changes in the lipid membrane composition (Florent-Bechard et al., 2009).

1.2.2 NEUROFIBRILLARY TANGLES

Neurofibrillary tangles (NFT) are made from a microtubule-associated protein called tau which becomes hyperphosphorylated and subsequently aggregates into paired helical cores that are the precursors of larger aggregates known as tangles (Goedert et al., 1988). The tau protein is part of the neuronal cytoskeleton, and hyperphosphorylated tau is particularly located in the frontal cortex and the hippocampus, which are expressly affected in AD (Goedert et al., 1988, Pooler et al., 2011). Tau binds to and stabilises microtubules in neuronal processes i.e. when abnormal phosphorylation of tau occurs, synaptic and neuronal functioning are compromised as axonal transport is affected due to its involvement on the function of microtubules (Stoothoff and Johnson, 2005, Avila, 2006). Specifically excessive phosphorylation prevents tau from binding to microtubules and it is hypothesised that the aggregation of tau, seen in AD, causes transportation along neuronal axons

to be reversed, consequently increasing movement of cell components into the cell body (Mandelkow et al., 2003). This is supported by the finding that neuronal axon processes in the hippocampus of AD transgenic mouse models have reduced number of mitochondria implying a shift in their localization (Pigino et al., 2003).

Tau localization is crucial to its function. It has recently been shown that de-phosphorylation of tau causes it to be trafficked to the neuronal membrane, away from the cytosol suggesting a stabilizing role for tau at the cell membrane (Pooler et al., 2011). This finding is important as it suggests that hyperphosphorylation of tau, in AD, could potentially alter any effects tau exerts on the neuronal membrane. Research supporting this has found that the accumulation of hyperphosphorylated tau occurs within the cytosol and not at the neuronal membrane (Iqbal et al., 2005).

1.2.3 β-AMYLOID PLAQUES

Highly fibrillated neuritic plaques, found initially in the extracellular environment of post-mortem AD brains, are made from an aggregated peptide called Aβ. Aβ is present in multiple forms in AD, including monomers, oligomers and fibrils and in differing amino acid lengths (e.g. $A\beta_{40}$ and $A\beta_{42}$). Indeed, Ahmed et al. (2010) showed that Aβ is much more toxic in its oligomeric state in comparison to the more stable Aβ fibrils, which implies that the smaller forms of Aβ are able to affect more cellular activities than the larger aggregates . Zhang et al. (2002) also investigated the toxicity of the multimeric forms of Aβ using microinjection, inserting different forms of Aβ into the cytosol of neurons. Analysis of the results showed that $A\beta_{42}$ was the most toxic form, both in its non-fibrillized (monomers, dimers, oligomers and polymers) and fibrillized forms (Zhang et al., 2002).

1.2.3.1 GENERATION OF AMYLOID-β PEPTIDE

The differing lengths of Aβ are produced by sequential cleavage of a larger transmembrane glycoprotein called the amyloid precursor protein (APP). APP is known to be localised within the endoplasmic reticulum (ER), Golgi body, lipid rafts and cell membranes (Zhong et al., 1994, Culvenor et al., 1997). This membrane-spanning protein can undergo two cleavage pathways rendering either insoluble Aβ peptides of either 40 or 42 amino acids length or a soluble peptide called P3 (Figure 1.1)(Blennow, 2006, Haass et al., 1993):

NON-AMYLOIDGENIC PATHWAY: Once APP has reached maturation and its C-terminus is embedded in the membrane, the long N-terminal region is proteolytically cleaved by α-secretase, releasing a large soluble APP ectodomain (Haass et al., 1993, Blennow, 2006, Zhong et al., 1994). The remaining 10kDa C-terminal fragment is further cleaved by γ-secretase to produce P3. Primary cleavage by α-secretase prevents the formation of toxic Aβ, as the cleavage site is present within the Aβ fraction of the APP protein (Mattson, 2004a). One hypothesis for Aβ formation suggests that decreased α-secretase activity is at fault, as lower levels of the soluble APP ectodomain have been measured in AD patients (Lannfelt et al., 1995).

AMYLOIDGENIC PATHWAY: Differences in APP processing during the initial cleavage, causes the formation of the different Aβ isoforms. In the generation of Aβ the first enzyme to cleave APP is β-secretase which leaves a 99 amino acid fragment in the membrane (Blennow, 2006). This is then cleaved by γ-secretase to form the insoluble Aβ peptide either of 40 or 42 amino acids, the differing lengths are dependent on the original isoform of APP and the intramembranous cleavage by γ-secretase (Citron et al., 1995, Wolozin, 2001). In sporadic AD an elevation in levels of the β-secretase active component, β-site APP cleavage enzyme (BACE), increases the production and accumulation of Aβ (Cruts et al., 2001, Li et al., 2004a). The preference of the amyloidgenic pathway increases levels of Aβ and further explanations below (and section 1.4.2) give evidence for this preference in AD.

The production of Aβ was discovered to occur under normal cell functioning, suggesting that Aβ peptide can be broken down or used elsewhere in a non-toxic form (Haass et al., 1992). A recent study suggests that one method for breakdown of Aβ is by a mitochondrial peptidase which specifically degrades 'short unstructured peptides', such as Aβ. This peptidase has been named PreP peptidasome (Falkevall et al., 2006). Transgenic mice overexpressing mutant APP (Tg mAPP) show an accumulation of Aβ, implying that PreP is unable to function fully in degrading an abundance of Aβ, resulting in the build-up of Aβ observed in AD (Yao et al., 2011). Furthermore small quantities of Aβ are less likely to aggregate and could be broken down by PreP peptidasome.

There are a number of gene mutations in FAD, which are derived from missense mutations in the APP gene, causing APP processing problems and enhanced Aβ production. Particularly mutations of APP linked to the activity of γ-secretase, which is dependent on its active component Presenilin (Wisniewski and Sigurdsson, 2010). Over 100 mutations have been found in the encoding gene (PSEN) and they are seen to enhance Aβ production (Sastre et al., 2001, De Strooper, 2007).

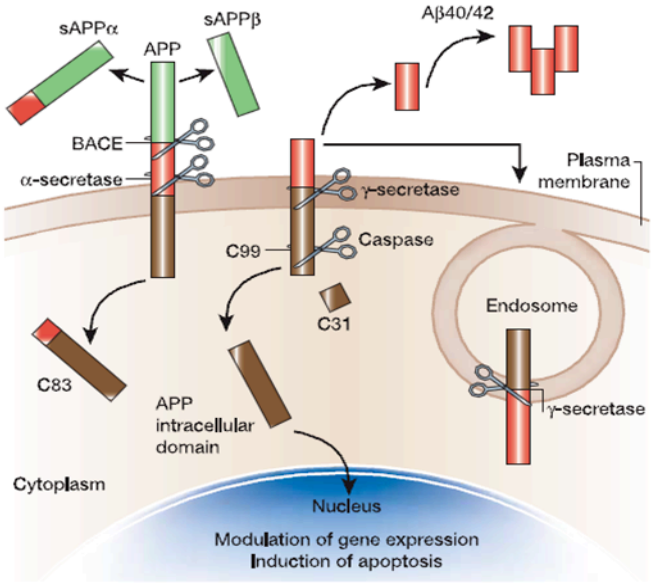

Figure 1-1: APP processing occurs in cellular membranes. Initial cleavage occurs out with the membrane, whereas in both the non-amyloidgenic and the amyloigenic pathways γ-secretase cleaves within the membrane (Mattson, 2004b)

Aβ AND LIPID MEMBRANES

As well as gene mutations that can influence Aβ production, lipid composition within the plasma membrane is also seen to influence Aβ generation in AD. Indeed key lipids that are reportedly linked in AD include cholesterol, fatty acids, sphingomyelin and phospholipids. The lipid membrane bilayer of cells is thought to be heavily involved in the trafficking and regulation of membrane spanning proteins. Significantly the cleavage processes that lead to the production of Aβ include the transmembrane protein APP which is influenced by the balanced composition of lipids in the membrane. The lipid membrane content is crucial for the fluidity of the membrane which in turn determines the activities of the membrane (Vestergaard et al., 2008). For example, the presence of cholesterol and sphingolipids in lipid membranes decrease its fluidity, due to the rigidity of cholesterol and the stabilising properties of sphingolipids (Wolozin, 2001).

Early studies into lipid membrane composition in AD brains, reported that levels of phospholipids, specifically phosphatidylcholine (PC), in the membrane were inclined to be lower compared in AD tissue samples to controls (Nitsch et al., 1992). The effect of changes in the lipid content of membranes has large consequences in AD as the membrane associated proteins seen in Aβ production such as γ-secretase and β-secretase occupy cholesterol rich lipid membranes in comparison to the non-amyloidgenic processing pathway, where α-secretase preferentially occupies phospholipid membranes (Vestergaard et al., 2008). This favouritism of lipid rich membranes is shown by the increased Aβ production from cholesterol rich lipid rafts.

Ehehalt et al. (2003) suggested that APP processing occurs in two main areas within the cell, at the cell membrane and lipid rafts. Lipid rafts consist mainly of cholesterol and sphingolipids making the membrane very rigid (Wolozin, 2001, Vestergaard et al., 2008). Using cholesterol reducing drugs, statins, Ehehalt et al. (2003) decreased cholesterol levels in mouse neuroblastoma N2a cells and found that APP generation of Aβ was prevented . Statins work to inhibit the intracellular production of cholesterol from the ER. Further investigations found that by

increasing α-secretase activity and depleting cholesterol, Aβ production was greatly reduced and the activity of β- and γ- secretase was also reduced (Kojro et al., 2001). Also observed was the increased fluidity of the lipid membrane when α-secretase activity was expressed (Kojro et al., 2001). The use of statins in AD appears to shift the cleavage of APP to the non-amyloidgenic pathway reducing the generation of Aβ (Kojro et al., 2001). The reaction of primary hippocampal neurons and animal models to statins shows a significant decrease in $A\beta_{40}$ and $A\beta_{42}$ levels (Fassbender et al., 2001).

To determine if the reduction in Aβ caused by decreasing cholesterol would be a beneficial therapeutic target, transgenic mice were treated with statins and their memory assessed. The results revealed that statins did improve learning and memory impairments; however, there appeared to be no reduction in Aβ levels in comparison to controls (Li et al., 2006). This suggests that by reducing Aβ production by increasing membrane fluidity does not have any effect on the degradation of Aβ accumulation and by slowing the generation of Aβ memory improvements occur. Indeed cholesterol has been found to have effects other than altering membrane fluidity and enhancing Aβ production, as cholesterol micelles were found to bind to Aβ directly using transmission electron microscopy (TEM) and consequently induce fibrillisation (Harris, 2008).

1.2.3.2 INTRACELLULAR ACCUMULATION OF AMYLOID-β PEPTIDE

The original theory for AD implied that the problem stemmed from the extracellular accumulation of Aβ plaques. It was hypothesised that insoluble Aβ aggregates accumulated within the endosomes and lysosomes, unable to be degraded they were then released into the extracellular environment (Golde et al., 1992, Yang et al., 1999, Gouras et al., 2005). However, Wirths et al. (2001) established that Aβ accumulation also occurs within hippocampal neurons of double-transgenic mice (expressing human mAPP and human mutant presenilin-1) before any extracellular plaque deposits develop (Wirths, 2001). Many other studies report similar findings of Aβ accumulation within neurons, specifically in

patients with FAD and preceding NFT generation (Gouras et al., 2000, Gouras et al., 2005, Rovelet-Lecrux et al., 2006).

The presence of Aβ before any other AD symptoms or pathologies suggests that Aβ is having an effect intracellularly that could cause cytotoxicity, necrosis or apoptosis to instigate neuronal loss. From this it can be deduced that intracellular Aβ is one of the earliest factors in the development of AD.

Regions of Intracellular Aβ Accumulation

Aβ has been found in many different sites within neurons mainly areas associated with membranes such as the ER, lipid rafts, synapse, multivesicular bodies (MVB) and the mitochondrial membrane (Buckig et al., 2002, Takahashi et al., 2002, Kawarabayashi et al., 2004, Manczak et al., 2006).

Cook et al. (1997) found that APP co-localised with the ER as APP was discovered to have an ER targeting sequence and is modified here before transportation to the Golgi apparatus (Cook et al., 1997, Salminen et al., 2009). When membrane trafficking from the ER was inhibited, so that APP was retained in the ER, Aβ was still seen to be generated providing evidence that the ER is a site for Aβ production and that full-length of APP is present at this point and is capable of being cleaved within the ER (Cook et al., 1997).

In addition to spanning the ER membrane, APP is also present in cholesterol rich lipid rafts and as such these are increasingly linked to Aβ production (Wolozin, 2001). The low fluidity of the lipid raft membrane, caused by elevated levels of cholesterol and sphingolipids, are connected to enhanced Aβ generation in these lipid rafts, whereas P3 production is favoured in membranous regions containing low cholesterol with increased membrane fluidity (Kojro et al., 2001). In conjunction with this, BACE cleavage activity has been found to decrease upon reduction in the level of cholesterol within the neuronal cell line, SH-SY5Y implying that Aβ production is reduced when cholesterol levels are low (Cordy et al., 2003).

It has been shown by electron microscopy that Aβ accumulates on both the outside and inside of MVB (Takahashi et al., 2002). It is thought that after APP

cleavage, Aβ is invaginated into MVB and transported to the plasma membrane, where these MVB accumulate at the synapses of neurons and disrupt synaptic transmission (Almeida et al., 2006).

As well as the ER targeting sequence, full-length APP also contains a mitochondrial targeting sequence, and was first discovered to localise with mitochondria in 1992 (Yamaguchi et al., 1992, Park et al., 2004, Chen and Yan, 2007). APP was found to reside with its N-terminus embedded in the mitochondrial membrane and the C-terminal end within the cytoplasm of the cell (Anandatheerthavarada et al., 2003). This may signify that cleavage of APP would allow for the release of Aβ into the cell cytoplasm and not into the mitochondria.

In addition to localising in the mitochondrial membrane, APP was also shown to associate with the import machinery of the mitochondria (translocase of the outer/inner membrane, TOM/TIM) giving rise to the theory that APP could enhance mitochondrial dysfunction, by obstructing these pores (Anandatheerthavarada et al., 2003, Lin and Beal, 2006). However, the smaller Aβ fragment has been seen to accumulate directly within the mitochondria and therefore due to the orientation of the APP, questions arose of how does Aβ enter the mitochondria and what effects occur due to its presence?

1.3 ALZHEIMER'S DISEASE AND THE MITOCHONDRIA

1.3.1 MITOCHONDRIAL CONSEQUENCES OF INTRACELLULAR AMYLOID-β

As indicated above Aβ has been found to be localised both in the mitochondria of human AD brains and in AD animal models. In mutant APP transgenic mice, cortical mitochondria were isolated and immunoblotting carried out, the results showed expression of $A\beta_{40}$ and $A\beta_{42}$ in comparison to control mitochondria (Manczak et al., 2006). Additionally Aβ has been shown to accumulate in the neuronal mitochondria of AD patients (Caspersen et al., 2005, Hansson Petersen et al., 2008).

These studies suggest that Aβ aggregation occurs within the mitochondria and both found evidence of metabolic dysfunction in the form of oxidative damage, increased hydrogen peroxide (H_2O_2) and decreases in enzymes of the respiratory complexes (e.g. Cytochrome *c* oxidase (COX)) as a result of Aβ presence (Caspersen et al., 2005, Manczak et al., 2006). Alongside these studies, Aβ was found to co-localise with complex II of the electron transport chain (ETC) further suggesting that Aβ accumulates and possibly interacts in the mitochondria (Tillement et al., 2006, Tillement et al., 2011).

Due to the orientation of APP it has been deemed unlikely that cleavage of APP occurs to release Aβ within the mitochondria and therefore, Aβ must gain entry into the mitochondria via other routes (Lin and Beal, 2006). Evidence for direct entry into the mitochondria provides various theories for access. Aβ has been found to permeabilize through lipid bilayers in its oligomeric form and as such has the ability to pass across the mitochondrial membrane by exerting effects on conductance of the lipid membrane (Kayed et al., 2004, Glabe, 2006). This relates to previous findings that Aβ is most toxic in the oligomeric form.

Further investigation into how Aβ enters the mitochondria indicates that Aβ uses the inherent import machinery of the mitochondria. A neuroblastoma cell line (SH-SY5Y) was used to detect the mitochondrial internalisation of cytosolic Aβ, initially confirming that Aβ did enter the mitochondria from the cytosol (Hansson Petersen et al., 2008). Additional experiments showed that Aβ was dependent on the TOM/TIM machinery to gain access to the cristae of the mitochondria (Hansson Petersen et al., 2008). This is now the most widely accepted theory for Aβ entry into the mitochondria.

1.3.2 MITOCHONDRIAL DYSFUNCTIONS

Mitochondrial dysfunction has long been implicated in neurodegenerative diseases including Alzheimer's disease (reviewed in Borger et al., 2011). Mitochondria are the main source of energy for the brain and as such there are very high numbers present in neurons (Pagani and Eckert, 2011). Neurons are very particular in the type of energy substrates they use, only utilizing glucose and ketone bodies to produce ATP (Di Paolo and Kim, 2011) .

During normal cellular metabolism the final step of energy respiration, the ETC, in the mitochondria produces small amounts of reactive oxygen species (ROS), which over time accumulate and can generate oxidative stress (Richter et al., 1988, Parker et al., 1994). As neurons are densely packed with mitochondria they are more likely to have naturally higher levels of ROS thereby increasing their susceptibility to oxidative stress and consequently increased lipid peroxidation and DNA damage.

Indeed plasma from AD patients post-mortem, have shown elevated levels of the toxic aldehyde, 4-hydroxynoneal (4-HNE), a marker for lipid peroxidation (McGrath et al., 2001). Living AD sufferers' blood samples have also shown a significant increase in another toxic aldehyde, malondialdehyde (MDA), and a decrease in superoxide dismutase (SOD) activity, which is an important anti-oxidant enzyme (Padurariu et al., 2010). These findings signify a disruption between the delicate balance of anti-oxidants and pro-oxidants which result in the protection against the effects of increased oxidative stress and lipid peroxidation.

Oxidative stress is thought to influence the morphology and dynamics of mitochondria. Hirai (2001) described several abnormalities in mitochondria from AD patients linked with increases in oxidative markers. In particular, it was reported that there were significant decreases in the number of intact mitochondria, and in addition there were significant incidences of abnormal mitochondrial DNA from the pyramidal neurons of the hippocampus . These findings have been mirrored in cybrid cell lines from AD patients or controls of late

passage, that additionally show a disruption in their mitochondrial membrane potential, indicating that the cells are compromised (Trimmer et al., 2004).

As well as the oxidative stress and mitochondrial morphology abnormalities seen in AD patients there are also changes in energy production, mitochondrial protein expression and key mitochondrial enzyme activities. Alterations in brain energy metabolism, in particular hypometabolism are seen to occur asymptomatically early on in the brains of AD patients (Cunnane et al., 2011). Investigating changes in glucose metabolism, PET scans from high risk AD individuals have been analysed and show significant areas of hypometabolism particularly in the parietal, temporal and frontal cortices (Kennedy et al., 1995). There are many theories behind this decrease in metabolic rate ranging from a reduction in the numbers of glucose transporters (GLUT) traversing the blood brain barrier, through to alterations in glycolysis (Arias et al., 2002, Yurko-Mauro et al., 2010).

Key metabolic enzymes that are linked to mitochondrial dysfunction in AD are α-ketoglutarate dehydrogenase complex (KGDHC), pyruvate dehydrogenase complex (PDHC) and COX activity (Gibson et al., 1999, Bubber et al., 2005, Fukui et al., 2007). The function of KGDHC in the citric acid cycle is crucial for ATP production, its close proximity to the ETC has produced theories that the ROS that are produced, could affect the functioning of this enzyme. However, studies into other neurological diseases have found that deficiencies in this enzyme could in fact cause oxidative stress (Albers et al., 2000, Blass, 2000).

Mitochondria isolated from triple transgenic mice (encoding mutations in APP, PSEN and Tau) have been analysed using two dimensional-difference gel electrophoresis (2D-DIGE) and tandem mass spectrometry to profile differences in mitochondrial protein expression (Chou et al., 2011). The findings from this study showed the down-regulation in specific enzymes involved in the ETC, such as NADH dehydrogenase which acts within the first complex of ETC, signifying defects in ATP production (Chou et al., 2011). One of the three components of the enzyme KGDHC (dihydrolipoamide succinyltransferase component) was also

shown to be up-regulated in comparison to controls, implying a demand for this enzyme (Chou et al., 2011). Additionally, many studies have reported a decrease in levels of KGDHC, hypothesising that the effect of this complex within the citric acid cycle are consequently reduced which results in a decrease in metabolic activity (Chou et al., 2011). Studies into why specific regions of the brain degenerate in AD have used a computer simulation of neuronal networks to show that by disrupting the KGDHC, the glucose metabolic rate drops but only in excitatory neurons (Lewis et al., 2010). The theory that this enzyme may cause a reduction in function in excitatory neurons is noteworthy as the areas which degenerate in AD are packed with primarily excitatory pyramidal neurons. However, in *in vitro* experiments where KGDHC was decreased in cell lines, these cells showed increased vulnerability to metabolic insults and apoptosis (Huang et al., 2003).

As well as the reported changes to the ETC within the mitochondria, Aβ has been reported to exert its toxicity by associating with other components within the mitochondria, in particular two mitochondrial proteins; amyloid binding alcohol dehydrogenase (ABAD) and Cyclophilin D (CypD). These proteins appear to be able to mediate and amplify the toxicity of the Aβ peptide. Binding of both proteins to $A\beta_{40}$ and $A\beta_{42}$ has been demonstrated at nM Aβ concentrations, and Aβ accumulation within cells is known to result in an increase in expression of both of these proteins (Yan et al., 1997, Du et al., 2008, Du et al., 2009).

1.3.3 AMYLOID- β BINDING ALCOHOL DEHYDROGENASE

Initially ABAD was purified from bovine liver and was described as having activity reflecting that of 3-hydroxyacyl-CoA dehydrogenase (HADH), an enzyme found in the third step of β-oxidation of fatty acids in human mitochondria (Kobayashi et al., 1996). ABAD was later purified from rat liver and classed as short chain L-3-hydroxy-2-methylacyl-CoA dehydrogenase (SC-HMAD) (Luo et al., 1995). This change in nomenclature has occurred several times for ABAD as it has been discovered from different mitochondrial sources and utilising different substrates (see table 1.1 for full list of ABAD identities).

The 27kDa protein, ABAD is a unique nicotinamide adenine dinucleotide (NAD^+) dependent enzyme, as it has a broad range of substrates including steroids such as 17β-estradiol, estrone and dihydroandrosterone and in particular secondary alcohols (e.g. 2-propanol) were found to be better substrates over primary alcohols (He et al., 1999, Powell et al., 2000, He et al., 2001). In the mitochondria, ABAD reversibly oxidises alcohols into aldehydes and ketone (Figure 1.2). The rat ABAD has been crystallised with NAD^+ bound as these reactions are dependent on the co-factor NAD^+(Powell et al., 2000, Yan et al., 2000).

Table 1-1: In literature, ABAD is referred to by many different names indicated here.

Alias	Author
SC-HMAD: short chain L-3-hydroxy-2-methylacyl-CoA dehydrogenase	(Luo et al., 1995)
ERAB: Endoplasmic reticulum amyloid-β binding protein	(Yan et al., 1997)
HADH II: L-3-hydroxyacyl-CoA dehydrogenase type II	(He et al., 1998)
SCHAD: short chain L-3-hydroxyacyl-CoA dehydrogenase	(He et al., 1999)
ABAD: amyloid-β binding alcohol dehydrogenase	(Yan et al., 2000)
HSD10: 17β-hydroxysteroid dehydrogenase type 10	(He et al., 2001)

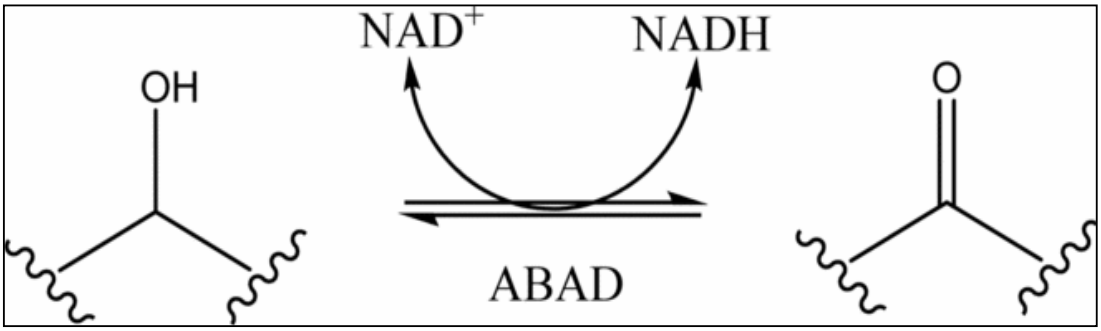

Figure 1-2: This schematic diagram represents the oxidation/reduction reaction that ABAD catalyses (Muirhead et al., 2010a).

1.3.3.1 Aβ AND ABAD INTERACTION

ABAD, was initially found to bind to Aβ using a yeast two hybrid screen by Yan et al. (1997). In the same study it was seen that by mutating ABAD the toxic effects of Aβ were prevented, and by over-expressing ABAD, Aβ toxicity was increased. Following this initial discovery Lustbader et al. (2004) confirmed that Aβ directly interacts with ABAD and furthermore Aβ binds at residues 1-158 of ABAD (Lustbader et al., 2004). The Aβ-ABAD interaction was crystallised to reveal that Aβ binding does not occur with the presence of the co-factor NAD and in fact the binding of Aβ to ABAD distorts the NAD binding site, and thereby may explain the reported inhibition of ABAD activity (Lustbader et al., 2004). The crystal structure of ABAD shows three secondary protein structures, L_F, L_E and L_D loops (Figure 1.3), a particular insertion occurs within the L_D loop of ABAD which is lacking in other short chain dehydrogenase/reductase enzymes (Lustbader et al., 2004). As well as the presence of the unique region of the L_D loop, it was reported that mutations at residues 95-113 which contain the L_D loop prevent the interaction of Aβ with ABAD, the L_D loop region was therefore predicted to be the binding site for Aβ (Lustbader et al., 2004).

Lustbader et al. (2004) further investigated the prediction that L_D loop of ABAD bound to Aβ, by creating a peptide containing the 28 amino acids of L_D loop, called ABAD-decoy peptide (ABAD-DP), and this decoy peptide was subsequently shown by surface plasmon resonance (SPR) to bind preferentially to Aβ (Lustbader et al., 2004). In addition, when this peptide was fused to the cell membrane permeabilising TAT peptide then this prevented Aβ induced cytochrome c release in primary neurons and therefore was proposed to protect the Aβ induced disruption of ABAD enzyme activity(Lustbader et al., 2004).

In summary these studies showed that Aβ binds to ABAD preventing its enzymatic function by distorting the binding pocket for NAD. Stopping this co-factor's binding halted its oxidation and reduction reactions consequently potentially affecting metabolism, fatty acid oxidation and ketone body production within the mitochondria.

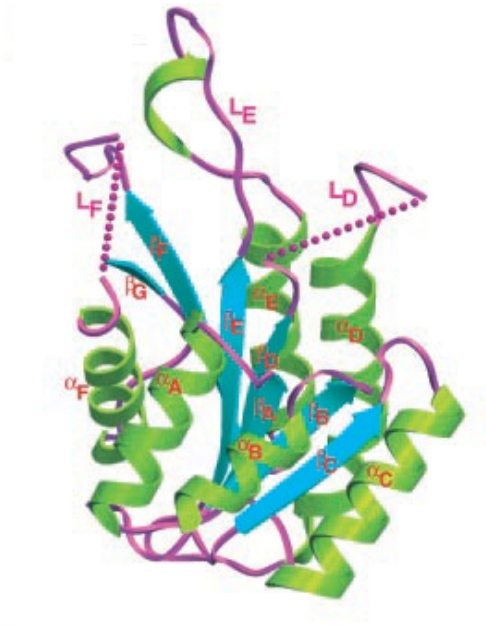

Figure 1-3: Human ABAD showing three secondary protein structures L_F, L_E and L_D loops(Lustbader et al., 2004).

1.3.3.2 CONSEQUENCES OF Aβ-ABAD INTERACTION

As well as inhibiting the enzyme function of ABAD the Aβ-ABAD complex was also predicted to cause other toxic effects within the mitochondria. The release of ROS was investigated in double transgenic (mAPP/ABAD) mice. The reported findings show significantly increased levels of H_2O_2 and superoxide anions when ABAD is over-expressed in the presence of Aβ, in comparison to controls (Takuma et al., 2005).

ROS increases the levels of oxidative stress in the mitochondria and consequently increases the oxidative breakdown of lipids, previously shown (section 1.3.1) products of lipid peroxidation are increased in AD, in particular the

toxic aldehydes 4-HNE and MDA. The over-expression of wild type- ABAD (wtABAD) and mutated APP (mAPP) within COS-1 cell lines showed a significant increase in both 4-HNE and MDA generation implying that Aβ over-expression with ABAD is a cause of toxicity (Yan et al., 1999). Interestingly when ABAD activity is inhibited by two substitution mutations made between residues 168-172 (mutABAD) and expressed with elevated levels of Aβ, the increase in toxic aldehydes did not occur, and the cells were subsequently protected from Aβ toxicity (Yan et al., 1999). These results along with the knowledge that Aβ binds to ABAD suggest that an accumulation of toxic aldehydes enhances mitochondrial dysfunction and that the reduction in the metabolic function of ABAD consequently causes lipid peroxidation. Furthermore ABAD has been implicated in the reduction of these toxic aldehydes into alcohols suggesting that the reduction capacity of ABAD is inhibited when Aβ is bound to ABAD (Murakami et al., 2009).

An indication that the Aβ-ABAD complex affects energy production has also been reported by analysis of neurons from double transgenic mice overexpressing ABAD and Aβ. Takuma *et al* (2005) report significant decreases in ATP content and COX activity within mitochondria of these neurons compared to single transgenic controls (mAPP or ABAD alone) (Takuma et al., 2005). COX activity within the ETC is a vital step in the production of ATP and Takuma *et al* (2005) suggested that the Aβ-ABAD complex could affect the activity of this enzyme consequently decreasing ATP levels (Takuma et al., 2005).

Consequences of the Aβ-ABAD interaction also appear as changes in protein levels within AD brains. Proteomic analysis of brains from transgenic mice overexpressing ABAD and Aβ (Tg mAPP/ABAD) discovered an increase in the anti-oxidant protein, Peroxiredoxin 2 (Prdx-2)(Yao et al., 2007). Prdx-2 was reported by western blot analysis and immunocytochemistry to be present in cerebral cortex from both the double transgenic mice and AD patients (Yao et al., 2007). The increased expression of Prdx-2 in the presence of Aβ–ABAD complex was suggested to be a protective mechanism in response to increased ROS and oxidative stress. Survival assays conducted on primary cortical neurons expressing a plasmid containing Prdx-2 were found to be protected from toxic levels of Aβ

(Yao et al., 2007). Increased anti-oxidant, Prdx-2, levels in response to Aβ binding to ABAD is understood to attenuate the effects of elevated oxidative stress. To support this, reported findings from hippocampal tissue from Prdx-2 $^{-/-}$ mice showed significant increases in MDA production and the marker for oxidative damage, 8-hydroxyguanosine (8-OHG)(Kim et al., 2011).

Further proteomic analysis of transgenic mice overexpressing ABAD and Aβ found increased expression of Endophilin 1 (Ep-1), a key pre-synaptic protein which acts to mediate invagination of synaptic vesicles and it is also associated with c-Jun N-terminal kinase (JNK) activity (Schmidt et al., 1999, Ren et al., 2008). The activation of JNK is linked to tumour necrosis factor (TNFα) induced apoptotic signalling pathway (Liu and Lin, 2005). Increased expression of Ep-1 in Tg mAPP/ABAD mice was confirmed by immunocytochemistry and further established in brain tissue from AD patients by western blot analysis and immunocytochemistry (Ren et al., 2008). Investigations into the prediction that Ep-1 contributes to JNK activation were carried out in HEK 293 cells and primary cortical neurons by western blot analyses; when Ep-1 expression is increased JNK activity increases, furthermore when Ep-1 is truncated the activation of JNK is inhibited (Ren et al., 2008).

Therefore the increased levels of Prdx-2 and Ep-1 are good indicators of the Aβ-ABAD interaction. Interestingly when the Aβ-ABAD complex is interrupted levels of these elevated proteins decrease to endogenous levels signifying the cytotoxic consequences of this interaction (See below).

1.3.3.3 PREVENTING Aβ BINDING TO ABAD

The binding of Aβ to ABAD can have a number of consequences ranging from the molecular through to the cellular and to the brain as a whole. It is generally believed that by inhibiting the Aβ-ABAD complex, this will reduce toxicity with the cells and decrease mitochondrial dysfunctions.

Creation of the ABAD-DP fused to the 11 amino acid transduction domain from human immunodeficiency virus 1-transactivator (HIV-1 Tat) protein allowed the decoy peptide to be used in primary neuronal culture therefore producing a novel inhibitor for the Aβ-ABAD complex *in vitro* and *in vivo* (Lustbader et al., 2004, Yao et al., 2011).

The activation of JNK by Ep-1 is reported to significantly reduce neuronal survival but interestingly by interrupting the interaction between Aβ and ABAD with the HIV-1 TAT- ABAD-DP, Ep-1 levels are decreased back to endogenous levels (Ren et al., 2008). Additionally, the increased levels of Prdx-2 seen as a consequence of Aβ-ABAD interaction were also reversed to normal levels in Tg mAPP/ABAD animals in the presence of the HIV-1 TAT- ABAD-DP (Yao et al., 2007).

The benefits of introducing this decoy-peptide into Tg mAPP mice were also seen as an intracellular reduction of oxidative stress in the form of a decreases in 4-HNE and increasing the formation of ABAD-DP–Aβ complex signifying a inhibition in the ABAD-Aβ interaction (Yao et al., 2011). Encouragingly the *in vivo* effects of intraperitoneal addition of ABAD-DP HIV-1 Tat protein into Tg mAPP mice showed an improvement in spatial memory when tested with radial water arm maze. Furthermore Aβ accumulation within the mitochondria was decreased and the activity of the Aβ degradation enzyme, PreP, was increased when compared with ABAD-DP null Tg mAPP mice (Yao et al., 2011).

Other inhibitors of the ABAD-Aβ complex have been identified such as the small molecule inhibitor classes of benzothiazole ureas e.g. ThioflavinT which is used in Aβ imaging (Xie et al., 2006). As well as these potential inhibitors, the crystal structure of ABAD with NAD allowed for the creation of the inhibitor AG18051, a specific inhibitor for ABAD as it binds co-valently with NAD^+ in the binding pocket of ABAD (Kissinger et al., 2004, Marques et al., 2008). This inhibitor has been used *in vitro* in a neuroblastoma cell line (SK-N-SH) to show inhibition of ABAD (Muirhead et al., 2010b). However the inhibition of ABAD by blocking its active site

would not be predicted to be a realistic protocol *in vivo*, because as already described, the disruption of ABAD functioning has significant consequences.

1.3.3.4 MODULATION OF ABAD ACTIVITY

The consequence of Aβ binding to ABAD is commonly reported as a complete inhibition of the enzyme activity. Within the majority studies this is shown by increased production of ROS, products of lipid peroxidation and apoptosis (see above), however *in vivo* this complete inactivation of ABAD may not be the case. As ABAD has multiple substrates it could be suggested that the presence of Aβ could alter substrate specificity.

The flexibility of ABAD has been demonstrated with the substrate 17β estradiol. The estrogen receptor alpha (ERα) was found to co-localise and further interact with ABAD in rat cardiac myocytes (Jazbutyte et al., 2009). An important finding was discovered by co-immunoprecipitation of ERα with ABAD from HELA cells, as this interaction would only occur when intracellular estrogen levels were low signifying that high quantities of 17β estradiol were present (Figure 1.4) (Jazbutyte et al., 2009, Yang et al., 2011). This reversible binding appears to be influenced by the levels of substrate present within the cell, the binding of ERα to ABAD occurs when 17β estradiol is low and when increased binds to ERα allowing ABAD to metabolise 17β estradiol into esterone. The binding of ERα to ABAD could allow for a different substrate to be metabolised, preferentially when 17β estradiol levels are low.

The finding that ABAD is involved in adapting its activity under changing substrate levels provides the concept that ABAD can modulate its' substrate specificity. Initial investigations by Shi Du Yan et al (1999) reported that ABAD was essential for the toxic effects of Aβ to occur within COS cells, in comparison to expressing ABAD or Aβ alone and as such Aβ affected the enzyme function of ABAD (Yan et al., 1999). The effect of increasing the nM concentration of Aβ on ABAD activity was reported to suppress oxidation of 17β-estradiol and octanol and further suppress the reduction of *S*-acetoacetyl-CoA (Yan et al., 1999).

The reduction of ABAD activity in the presence of Aβ is not reported as a complete inhibition of ABAD activity but a slow reduction in correlation with the increase of Aβ concentration. These results suggest that Aβ could be modulating the substrates the ABAD uses in a similar way that low levels of 17β-estradiol modulates the binding of ERα to ABAD. It could be proposed in the early stages of AD, when Aβ levels are low, Aβ acts to modulate substrate specificity and the increasing levels of Aβ eventually overwhelm ABAD activity causing oxidative stress and lipid peroxidation.

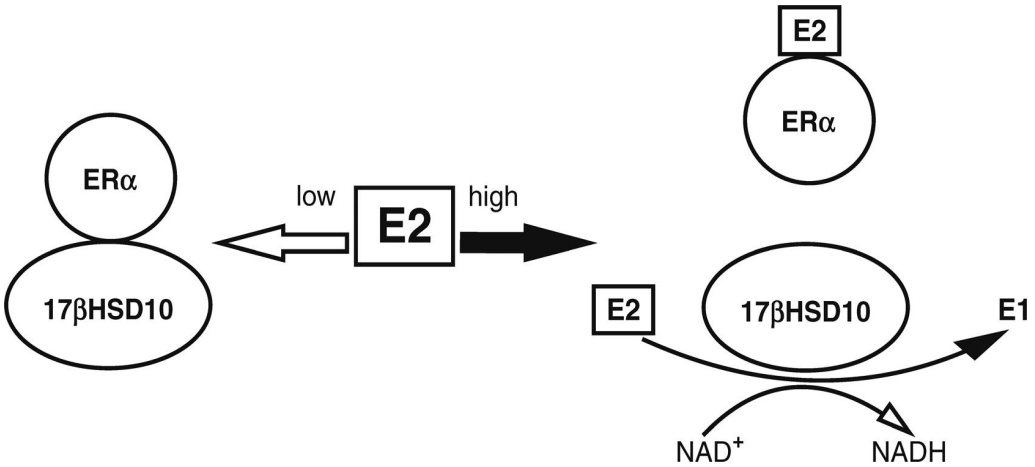

Figure 1-4: A schematic diagram of the modulation of ABAD (17βHSD10) under varying estrogen levels. When E2 (17β estradiol) levels are low the ERα binds to ABAD, when E2 levels increase the ERα is disassociated from ABAD and binds to 17β estradiol allowing the ABAD activity to be restored (shown by the oxidation of E2 to E1 (estron)) (Jazbutyte et al., 2009)

1.3.4 CYCLOPHILIN D

The family of proteins called Cyclophilin were originally identified as the intracellular binding proteins for the immunosuppressive drug cyclosporine A (CsA) (Handschumacher et al., 1984). Cyclophilins are peptidylprolyl isomerases and as such they have the capability to catalyse the isomeration between *cis-trans* isomers in amino bonds containing proline in order to aid chaperone protein folding (Tapparo et al., 1999, Giorgio, 2010). Different isoforms of Cyclophilin were characterised and found to localise with the ER, the cytosol and in particular the mitochondria (Tapparo et al., 1999). The mitochondrial isoform of Cyclophilin is

called CypD and has a mitochondrial pre-sequence at the N-terminal (Connern and Halestrap, 1992). Within the mitochondria immunohistological staining of CypD shows co-localising with cytochrome oxidase in the mitochondrial matrix (Hazelton et al., 2009). CypD has also been found to interact with the inner mitochondrial membrane (IMM) under periods of cellular stress (Connern and Halestrap, 1994). CypD from rat liver mitochondria was shown to be involved in the formation of the mitochondrial permeability transition pore (mPTP) which opens under cellular stress, in this case oxidative stress induced by thiol agents (Connern and Halestrap, 1994).

1.3.4.1 THE MITOCHONDRIAL PERMEABILITY TRANSITION PORE

The mPTP is reported to mediate necrosis, spontaneous cell death and have some involvement in apoptosis, cell death. Spontaneous cell death occurs in response to oxidative stress whereas apoptosis is a suicidal process requiring ATP, which occurs in normal cell turnover (Majno and Joris, 1995). Initial reports of the mPTP describe heart mitochondria, as open and leaky under conditions of high calcium levels and oxidative stress (Crompton, 1987). Further investigations showed that in periods of cellular stress and high intracellular Ca^{2+} levels mPTP formation occurs and subsequently opens. Pore opening allows small molecules to pass across the outer and inner membranes of the mitochondria and into the mitochondrial matrix (Halestrap, 2005). This flux causes a depolarization of the membrane (altering the membrane potential), increasing the permeability of the inner membrane and disrupting ion homeostasis (Schinzel et al., 2005). Consequently the mitochondria swell and the membranes eventually rupture. It is hypothesised that with prolonged opening of the mPTP necrosis occurs as ATP is depleted but if the mPTP closes cytochrome c is released which initiates apoptosis of the cell (Schinzel et al., 2005, Halestrap, 2005).

1.3.4.1.1 mPTP COMPOSITION

The mPTP has been hypothesised to contain 3 main components: CypD, the adenine nucleotide translocase (ANT) and the voltage dependent anion channel (VDAC) (Figure 1.5).

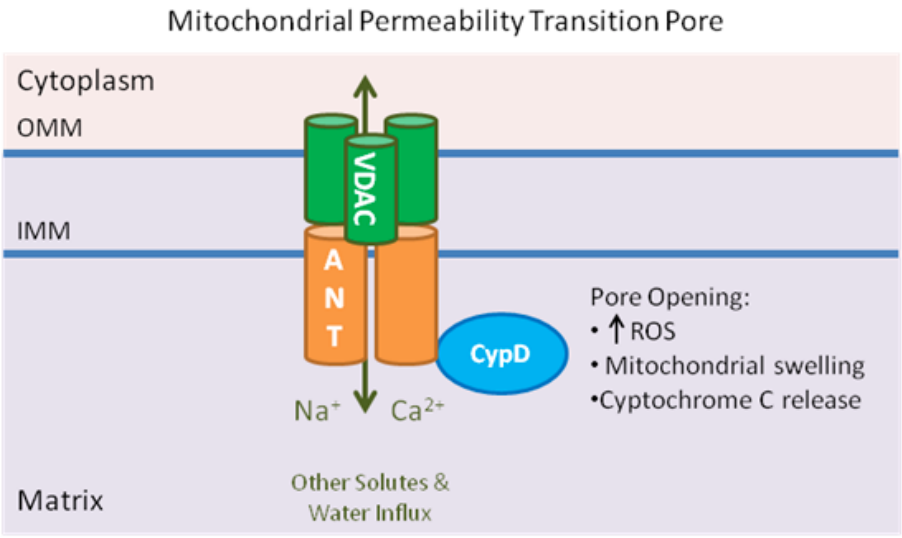

Figure 1-5: Mitochondrial permeability transition pore, when open allows solutes and water to flux into the mitochondria initially giving rise to an increase in ROS then mitochondrial swelling and cytochrome c release(Halestrap et al., 2002).

The transmembrane protein, ANT, spans the IMM and its endogenous function is to drive transportation of ATP and ADP (Machida et al., 2002). The importance of ANT within the mPTP is reviewed thoroughly by Halestrap and Brenner (2003); in summary, increased oxidative stress present in neurons is reported to alter ANT by glutathione-mediated cross-linking of two cysteine residues which consequently inhibits endogenous activity of ADP binding and increases CypD binding (Halestrap and Brenner, 2003). The binding of CypD to ANT is supported by the observation that when external oxidative stress was applied to cells, then CypD translocated to the IMM where it was initially suggested to bind to an integral membrane protein (Connern and Halestrap, 1994). It is now known that CypD interacts with ANT in the IMM, as CypD was purified from rat liver mitochondria and found bound to the IMM (Woodfield, 1998). The significance of CypD translocation and binding by exerting isomeration of cis-trans isomers at a proline residue to ANT is reported to mediate the high levels of Ca^{2+} which results

in a conformational change of ANT to a non-specific 'open' pore (Halestrap and Brenner, 2003, Halestrap, 2005).

Along with the interaction of ANT with CypD, Crompton *et al* (1998) purified CypD, and found that VDAC and ANT were bound to CypD(Crompton et al., 1998). VDAC is a voltage dependent transmembrane pore that spans across the outer mitochondrial membrane (OMM). The importance of VDAC as part of the mPTP is still in debate, as it has been reported to have a superfluous role but has also been shown to interact with ANT allowing pore formation and opening (Krauskopf et al., 2006). VDAC was determined to not be the site for mPTP inhibition but could still play a role as an OMM component of the mPTP. Recent studies have reported further OMM components that could regulate the IMM pore, such as the translocator protein (TSPO) and the phosphate carrier (PiC) (Halestrap and Brenner, 2003, Krauskopf et al., 2006, Sileikyte et al., 2011). It could be suggested that different OMM proteins could regulate permeability transition but that the crucial factor of transition is CypD.

Analyses of the three main components reported to form the mPTP, has determined that CypD is an essential component of the mPTP, facilitating necrosis. CypD has previously been suggested to mediate necrosis as a component of the mPTP, by binding to ANT and accelerating the Ca^{2+} induced conformational change of ANT (Halestrap and Brenner, 2003). To investigate the role of CypD and consequently the mPTP in apoptosis and necrosis, CypD deficiency was studied.

In the absence of CypD, murine embryonic fibroblast (MEF) cells (cultured from CypD deficient (*CypD*$^{-/-}$) mice) were still reported to undergo apoptosis after insults from TNFα and staurosporin (Nakagawa et al., 2005). However, when pore opening was initiated by the addition of H_2O_2, causing ROS production, no adverse effects on the MEF cells were reported (Nakagawa et al., 2005). Additionally the membrane potential of these CypD deficient cells was resistant to excess Ca^{2+} (Nakagawa et al., 2005). These results suggest that CypD is absent from the apoptotic pathway but is essential in mediating the necrotic consequences of oxidative stress and increased calcium levels. Apoptotic stimulation failed to

induce apoptosis in CypD deficient MEF cells suggesting that the mPTP does not play an important role in apoptosis but it appears to be necessary for necrosis to occur (Nakagawa et al., 2005, Halestrap, 2005). The hypothesis that CypD is essential in mPTP formation and specifically in facilitating necrosis over apoptosis is supported by the finding that transgenic mice over-expressing CypD were particularly sensitive to mitochondrial swelling and remarkably showed spontaneous cell death (Baines et al., 2005).

1.3.4.2 Aβ AND CYCLOPHILIN D

As was found with ABAD the expression of CypD is altered in AD patient brains, specifically CypD is elevated in mitochondria from the hippocampus and temporal cortex (Chen and Yan, 2010). CypD was also found to be increased in the mitochondria from the hippocampus of transgenic mouse models for AD over-expressing Aβ (Tg mAPP) (Du et al., 2008, Chen and Yan, 2010). Following this, the binding of Aβ to CypD was investigated, and results from SPR revealed that indeed Aβ did bind to CypD and especially with higher affinity to $A\beta_{42}$ and Aβ oligomers (Du et al., 2008). CypD and Aβ were also seen to co-localise and immunoprecipitation studies carried out showed that the CypD-Aβ complex occurred in mitochondria from AD brains (Du et al., 2008). It is also interesting to note that simulations of protein-protein interactions hypothesised that Aβ could bind to CypD and, interestingly, also to ANT with a higher affinity suggesting that binding is energetically favourable (Singh et al., 2009).

The main consequence of CypD binding to Aβ is an increase in ROS production, which in turn initiates mPTP opening and subsequently necrosis. However, the effects of this interaction have been reported when CypD is absent. Specifically, transgenic mice overexpressing Aβ (Tg mAPP) and CypD deficient were seen to mitigate the effects of mitochondrial swelling, increased membrane permeability and Cytochrome C release, all reported when Aβ is present with CypD (Du et al., 2008). The consequence of Aβ interacting with CypD to instigate mPTP opening can be evaluated by the mitochondrial calcium retention capacity (CRC), which determines the likelihood of mPTP formation. Non-transgenic mice are seen to

have a high CRC and the ability to uptake calcium normally whereas with Tg mAPP mice the CRC is low and signifies that the threshold for mPTP formation is increased (Du et al., 2009). However, Tg mAPP mice deficient in CypD had an increased CRC and therefore a higher threshold for mPTP formation (Du et al., 2009). The absence of CypD in Tg mAPP mice appeared to protect them from necrosis, which suggests that it is caused by the interaction between CypD and Aβ, or that CypD facilitates the process of necrosis as previously mentioned. To further support these hypotheses the introduction of the CypD inhibitor, CsA, to Tg mAPP mouse mitochondria caused an increase in the CRC, implying that any interaction between Aβ and CypD has been prevented (Du et al., 2009). These results suggest that CypD in the presence of Aβ instigate mPTP formation and that by inhibiting CypD calcium retention can be restored.

The benefits of deleting CypD were also examined in the behaviour of mice. Tg mAPP mice deficient in CypD were assessed using the radial arm water maze test. In comparison to Tg mAPP mice, CypD deficient Tg mAPP mice showed significant improvement in spatial learning and memory tasks (Du et al., 2008). Indicating that CypD is responsible for initiating pathways that lead to neuronal degeneration.

In summary, the binding of Aβ to CypD has been shown to initiate and enhance mPTP formation and consequently, through mitochondrial swelling and disruption of the mitochondrial membrane potential, instigate necrosis. The translocation of CypD to the IMM is induced by the presence of oxidative stress in AD, largely caused by the prevalence of Aβ accumulating in the mitochondria. Normally, CypD is found in the matrix of the mitochondria and the question remains what are the mechanisms that control its translocation from the matrix to the IMM?

One such possibility has come from unpublished results that indicate that ABAD may also influence CypD's location. For example, ABAD and CypD have been reported to exist as a protein complex in normal aged humans, and this binding occurs at nM interaction (Yan, personal communication)(Yan and Stern, 2005).

Also previous observations from förster resonance energy transfer (FRET) studies have indicated that ABAD and CypD are close enough to interact (Ren, 2008).

1.4 METABOLOMICS AND LIPIDOMICS IN ALZHEIMER'S DISEASE BRAIN

The consequences of Aβ accumulation within the mitochondria can provide an explanation for the well noted problems associated with metabolism in AD patients. The mitochondria are essential in regulating energy within cells and as previously mentioned consequences of their dysfunction appear as oxidative stress, increased ROS production and lipid peroxidation. In addition to the cellular stress caused by mitochondrial dysfunction in AD, decreased energy metabolism is also very prevalent (Atamna and Frey, 2007). It is important to note that decreases in energy metabolism are also seen in aging brains, but hypometabolism is much more pronounced in AD (Bentourkia et al., 2000). The reason for hypometabolism in the AD brain are largely unknown, though some events are known such as alterations in the respiratory chain enzymes, changes in glucose transport, the presence of Aβ within the mitochondria and changes in lipid membrane composition are all known to be involved.

1.4.1 GLUCOSE METABOLISM

Glucose enters the brain via glucose transporters (GLUTs), and in this way GLUTs are very valuable for providing the correct levels of glucose and consequently the energy levels in neurons. The three main GLUTs that regulate glucose entry into the brain are GLUT1 which facilitates glucose across the blood brain barrier, GLUT2 which is present in astrocytes and allows for glucose storage via slow glucagon release, and finally GLUT3 which transports glucose into neurons for the first step of ATP production (Marty et al., 2005, Cunnane et al., 2011). The three stages of energy production are glycolysis, citric acid cycle and the electron transport chain. Glycolysis is where glucose is converted to pyruvate

and acetyl CoA which feeds into the citric acid cycle (Stryer, 1995). In the citric acid cycle fatty acids, amino acids and carbohydrates undergo oxidative degradation and are fed into the electron transport chain is where electrons are transferred in order to synthesis ATP (Stryer, 1995).

Metabolic changes in glucose have long been associated with aging and AD. Initially, age related changes in glucose metabolism were noted in aged rat models. It was reported that specific regions of the brain such as the hippocampus (CA1 and CA3) and prefrontal cortex, showed significant decline in glucose metabolism (Gage et al., 1984). In addition, difficulties in learning and memory were seen to correlate with the decline of glucose metabolism in these aged rats (Gage et al., 1984). This finding implied that a reduction of glucose utilisation can occur in the aged brain.

In conjunction with the reduction of glucose metabolism, aged rats subjected to hypertension were reported to show reduced cerebral glucose utilization in the hippocampus and cerebral cortex along with impairments in learning, highlighting the importance of a healthy diet and exercise in old age (Mori et al., 1995). This could suggest that hypertension in AD patients could exacerbate the reduction of glucose utilisation. The metabolic rate for glucose was measured in young and old participants and a significant decrease was reported in the elderly participants (Bentourkia et al., 2000). It was reported that in normal aging a decrease of 13.3% in glucose utilisation occurs along with a degeneration of 12% of hippocampal neurons, in comparison AD sufferers are reported to lose 57% of hippocampal neurons (Bentourkia et al., 2000, Sakamoto et al., 2002).

MEASURING HYPOMETABOLISM IN THE AD BRAIN

Oxygen metabolism, glucose utilization and cerebral blood flow have all been seen to decrease in AD brains (Ishii et al., 1996). In order to observe these changes, in particular, the reduction of glucose utilisation in AD brains, positron emission tomography (PET) imaging is used. PET detects biologically active materials within the brain; (^{18}F) Fluorodeoxyglucose (FDG) is primarily used as the

radioactive tracer in glucose investigations as it is a derivative of glucose and is up taken by the brain in a similar manner (Muehllehner and Karp, 2006).

PET scans uniformly describe hypometabolism in the AD brain, localising specifically in regions known to degenerate in AD e.g. the temporal lobe (Desgranges et al., 1998, Li et al., 2008). Within the temporal lobe, the hippocampus is reported to show reduced cerebral metabolic rate of glucose (CMRg) early on in AD disease and following this other regions of the temporal lobe such as the medial temporal lobe show decreases in CMRg too (Ishii et al., 1996, Cunnane et al., 2011). These areas are particularly involved in the processing of memory. Understandably, low CMRg in these regions would lead to difficulties in storing and retrieving memories, the key problem associated with AD.

The temporal lobe shows hypometabolism before the parietal and frontal lobes in AD brains, why this is, is unclear. However, studies into the effects of Aβ on CMRg in AD have been investigated. To facilitate the imaging of Aβ a unique type of PET can be used; Pittsburgh compound B (PIB) is a fluorescent derivative of the dye benzothiazole thioflavin T and is used for its binding capability with Aβ and its ability to cross the blood brain barrier (Klunk et al., 2004). It can be imaged using PET and so PIB-PET measures aggregated Aβ fibrillar deposition in the living brain. In contrast to regions of brain degeneration and hypometabolism, PIB detects the areas of late stage Aβ plaque accumulation. When comparing PET and PIB-PET scans from the Hippocampus of AD sufferers, there are unexpected findings. Only small deposits of Aβ are seen, whereas the CMRg is reduced, thus implying that there is no link between Aβ deposition and decreases in glucose utilisation. PIB-PET also showed retention in the middle frontal gyrus, posterior cingulate cortex and inferior parietal lobe while FDG-PET detected hypometabolism in very different areas of the brain (Li et al., 2008). These results were confirmed in further PET and PIB-PET investigations of AD patients where it was concluded that amyloid plaques and the loss of glucose metabolism do not correlate (Furst et al., 2010). The dye used in PIB-PET scanning could provide an explanation as thioflavinT will only bind to specific Aβ fibrils and therefore not all Aβ forms will show in this type of analysis, rendering it somewhat misleading.

EFFECT OF Aβ ON HYPOMETABOLISM

Studies have shown that accumulation of Aβ within neurons could have an effect on energy metabolism specifically on the transportation of glucose to neurons for ATP generation. The presence of Aβ in hippocampal and cortical neuronal cultures has been observed to impair glucose transport. Furthermore, it was seen that the decrease in glucose was enough to cause reductions in cellular ATP levels (Mark et al., 1997). Additional studies in mice over-expressing Aβ, showed that early changes in metabolism occur in regions of the brain such as the parietal cortex and thalamus whereas older mice show further hypometabolism in the hippocampal region CA3 (Dodart et al., 1999). *In vivo* investigations of cerebrospinal fluid (CSF) from AD patients also showed a significant correlation with decreased metabolic glucose rate in the brain and decreased levels of $A\beta_{42}$ compared to non-AD control patients (Okamura et al., 1999). These results provide a connection between the reduction of $A\beta_{42}$ in CSF with decreased glucose utilisation in the AD brain, implying that as decreased CMRg indicates neuronal loss the decreased levels of $A\beta_{42}$ will reflect this loss.

As previously noted the accumulation of Aβ has been observed to induce oxidative stress within AD neurons and products of this oxidative stress have been reported to be involved in the reduction of CMRg. 4-HNE is produced as a consequence of oxidative stress and Mark et al. (1997) found that 4-HNE acts as a direct instigator of hypometabolism more than other lipid peroxidation products (Mark et al., 1997). Evidence from immunoprecipitation investigations from hippocampal neuronal cultures implied that Aβ initiates 4-HNE conjugation to GLUT3, and consequently it was described as a possible route for hypometabolism via oxidative stress caused by Aβ (Mark et al., 1997). Astrocytes have also been seen to be affected by the presence of Aβ as glutamate and glucose uptake were significantly reduced, and so it was suggested that the reduction of glucose uptake in astrocytes could lead to a decrease in the storage of glucose and consequently affect long term usage of glycogen stores (Parpura-Gill et al., 1997).

The GLUTs are very important for regulating the levels of glucose available within the brain and decreases in glucose metabolism could therefore be due to a reduction in glucose presence. Research supporting this shows a reduction in GLUT1 expression in the hippocampus of Tg mAPP mice (Lauderback et al., 2001). In addition to the previous finding that lipid peroxidation in astrocytes blocks GLUT3, another study has found that GLUT1 is inhibited by an interaction with 4-HNE (Lauderback et al. 2001). Hence the presence of Aβ induces lipid peroxidation and as such reduces the intake of glucose into neurons via GLUT1.

As well as the effect of Aβ on glucose transportation, Aβ induced oxidative stress has been reported to affect ATP via alterations in glycolysis. Pereira et al. (1999) investigated pyruvate levels in PC12 cells to find that in the presence of Aβ levels of pyruvate were significantly decreased . Reduced levels of pyruvate suggest that the conversion of glucose to pyruvate in glycolysis is compromised by the presence of Aβ. In addition, Aβ was observed to inhibited complexes I, II-III and IV of the electron transport chain as a decrease in each complex's activity was observed (Pereira et al., 1999). Interestingly the activity of each complex was substantially recovered by the addition of antioxidants signifying that the decline in activity was a consequence of oxidative stress.

Collectively these findings suggest that Aβ is involved in the decreased CMRg observed in AD. When the levels of glucose start to decrease in neurons another energy source is required, as neurons cannot utilise fatty acids directly, they must be metabolised to ketones for use in the citric acid cycle and subsequently ATP production (Di Paolo and Kim, 2011) .

1.4.2 LIPID METABOLISM

Lipid metabolism includes cholesterol production, steroid generation and specifically the breakdown of fatty acids, to be used as an alternative fuel to glucose. Under periods of starvation, hypoglycaemia can occur and the brain must use other sources for energy production (Di Paolo and Kim, 2011). The brain cannot use fatty acids themselves only ketone bodies and glucose (Di Paolo and

Kim, 2011). Therefore, fatty acids are released from adipose tissue and oxidised in three steps, the last of which is controlled by the 3-hydroxyacyl-CoA-dehydrogenase enzyme ABAD. Ketone bodies such as D-β-hydroxybutyrate and acetoacetate are produced as by-products of these reactions. Derivatives from ketone bodies feed into the citric acid cycle at different points in order to produce ATP (Kashiwaya et al., 2000). This alternative source of fuel is essential in AD due to the reduction in glucose uptake. It is interesting to note that ABAD is up regulated in AD and therefore could be under high demand if ketones are the main source of fuel in AD (Lustbader et al., 2004). Therefore, Aβ could be hypothesised to have a two-pronged attack on energy metabolism by initially reducing CMRg and compromising the alternative energy source by impairing ABAD activity.

USE OF KETONE BODIES AS AN ALTERNATIVE ENERGY SOURCE

Products of fatty acid metabolism, ketone bodies, such as D-β-hydroxybutyrate and acetoacetate have been seen to attenuate the effects of hypometabolism and are thought to protect neurons in AD by providing an alternative route to ATP production.

The use of ketones in the brain could have therapeutic properties as they may be sufficient to buffer the effects of Aβ in AD as the following studies have seen the addition of ketones to AD models have beneficial effects. For example, hippocampal neurons treated with $A\beta_{42}$ were rescued from toxicity by the addition of D-β-hydroxybutyrate. This beneficial effect of ketones was explained by the bypassing of glycolysis or by the activation of a pathway that leads to the phosphorylation of PDHC (Kashiwaya et al., 2000). The finding that high levels of ketones protect cells suggests that a diet high in ketones could be used as a therapeutic measure to prevent hypometabolism in neurons. Following this, Tg mice expressing $A\beta_{40}$ and $A\beta_{42}$ that were put on a ketogenic diet, consisting of low carbohydrates and high fat induced a ketogenic state, and resulted in a significant reduction of $A\beta_{40}$ and $A\beta_{42}$ levels (Van der Auwera et al., 2005). The effects of introducing excess ketones into the body to counteract glucose deficiency, has proven to be successful even in clinical trials (Reger et al., 2004, Henderson, 2008).

The addition of the medium chain triglyceride, D-β-hydroxybutyrate, into the diet of 20 participants with AD showed a significant improvement in memory (Reger et al., 2004). D-β-hydroxybutyrate allows the initial steps of the citric acid cycle to be bypassed along with avoiding the oxidation of free fatty acids in the body. Furthermore, recent clinical trials in the USA have induced a ketogenic state within AD patients to try and reverse the effects of hypometabolism. By introducing an oral ketogenic compound, AC-1202, into their diet the levels of D-β-hydroxybutyrate increased in their serum and significant cognitive improvements were observed (Henderson, 2008). The use of ketone bodies is therefore now being seen as a potential suitable therapy in AD; however, the effects of inducing ketogenesis on Aβ, hyperphosphoyrlated tau production and lipid granule accumulation in AD are yet to be studied.

Collectively these findings could propose a route for declining metabolism in AD, because Aβ may exert effects within the early reactions of the citric acid cycle and the external addition of ketones can feed into the cycle and so attenuate hypometabolism. Alternatively the knowledge that ABAD works in the β-oxidation of fatty acids to produce ketone bodies, infers that the inhibition of this enzyme by Aβ, could consequently reduce both ATP from fat stores and the essential supply of ketone bodies.

Other areas of lipid metabolism seem to be effected in AD such as decreases in omega-3 fatty acids reported post mortem in AD brains and additionally with the knowledge that hypometabolism occurs in AD, fatty acid metabolism must be affected too (Freemantle et al., 2006, Cole et al., 2009).

Reduction in the omega-3 fatty acid, docosahexaenoic acid (DHA), has been linked to regulations of GLUT1 expression and consequently glucose uptake in rat endothelial brain cells (Pifferi et al., 2010). Investigation into rat models of AD given DHA significantly found that in addition with improved memory and learning, a reduction in oxidative stress and lipid peroxidation was observed (Hashimoto et al., 2002). DHA has been reported to increase the fluidity of membranes, and from previous research it can be concluded that this will reduce

the generation of Aβ via the amyloidogenic processing of APP (Florent-Bechard et al., 2009). It can be deduced from these results that membrane fluidity and consequently lipid composition of neurons is of extreme importance in the production of Aβ.

In summary, the decreasing glucose metabolism in AD is attributed to the interference of GLUTs and glycolysis by oxidative stress, which is caused by Aβ accumulation. The low levels of glucose have a knock-on effect on the utilisation of alternative energy sources used by the brain by demanding high levels of ketone bodies. Inhibition of the ketone production pathway will result in the brain not receiving enough fuel and consequently cause cells to die. Reductions in the brain of essential fatty acids such as DHA induce Aβ production and in turn reduce the availability of an alternative brain fuel.

KEY ISSUES TO BE ADDRESSED IN THIS THESIS

Research will be focussed on the prediction that CypD will have a strong interaction to ABAD. It is hypothesised that this interaction will allow CypD to be sequestered away from the mitochondrial membrane and consequently inhibit the formation of the mPTP and necrosis.

In AD patients, it is known that protein levels of ABAD are increased, suggesting a demand for this enzyme in the metabolism of fatty acids and lipids. It is unknown whether the well-established decrease in glucose metabolism in AD patients affects ABAD activity. By specifically investigating ABAD activity, it is hypothesised that decreases in glucose levels will induce an increase in the activity of this enzyme, further indicating an increase in fatty acid and lipid catabolism.

In addition to the predicted increase of ABAD activity, an initial lipid scan in the presence of ABAD and Aβ will determine if there are any changes in the lipid content of cells, occurring in AD.

Chapter 2: MATERIALS AND METHODS

2.1 MOLECULAR BIOLOGICAL AND CLONING METHODS

2.1.1 POLYMERASE CHAIN REACTION (PCR)

PCR was performed to clone three constructs, in a 25µl reaction volume containing PfuTurbo DNA polymerase (Agilent Technologies, Berkshire) with appropriate 10x cloned Pfu buffer (supplied by Aigilent), 200µM dNTPS (Roche)(for PfuTurbo reactions or ReadyMix Taq PCR reaction mix with $MgCl_2$ (Sigma-Aldrich) 10µM of forward and reverse primers (Invitrogen) and 25-100ng template DNA. PCR reactions were carried out in a Bio-Rad Gradient Thermal Cycler (Bio-Rad, UK) thermal PCR cycle is described in table 2.1.

Table 2-1: PCR cycle temperatures and corresponding times. Denaturing of DNA occurs at 94°C, annealing of primers is dependent on the primer composition and Tm and varies with each PCR (occurring at χ°C) and elongation of DNA occurs at 72°C.

Temperature	Time (sec)
94°C	180
94°C	40
χ°C	50
72°C	90
72°C	600
4°C	∞

2.1.2 AGAROSE GEL ELECTROPHORESIS

DNA fragments were run and separated on 1% (w/v), 1.5% (w/v) or 2%(w/v) agarose gel, depending on fragment size. DNA smaller than 1kb was run on a 1% gel, for DNA fragments between 1-2kb were run on a 1.5% gel and fragments larger than 2kb were run on a 2% gel. The appropriate agarose was melted in TBE

buffer (0.45M Tris-borate 10mM EDTA, pH 8.3, Sigma) and once cool ethidium bromide (Sigma) was added to a final concentration of 0.5µg/ml. Agarose plus ethidium bromide was poured in a rig and left at room temperature for 20 minutes to set. DNA samples were prepared by adding 5x loading buffer, blue (Bioline) and once the gel was set added into the gel wells. HyperLadder I (Bioline) was run concurrently in order to analyse DNA band size. The agarose gel was run at 65V for 45 minutes and detected.

2.1.3 PURIFICATION OF DNA FRAGMENTS FROM AGAROSE GEL

DNA was visualized using a UV transilluminator (Herolab) and bands were excised from agarose gel using a clean, sharp scalpel. DNA was cleaned up and purified from agarose gel using QIAEX II gel extraction kit (Qiagen) following the manufacturer's protocol.

2.1.4 RESTRICTION ENZYME DIGEST

1-5µg of DNA were cut in reaction volume of 10-50µl per µg of DNA. Restriction digests were prepared on ice and components added to a sterile 0.6 ml microtube. The DNA was digested following the manufacturer's protocol using 1-5 units of restriction enzyme (Promega) and the appropriate 10x buffer (Promega). The enzyme was then heat inactivated at 65^{o}C for 15 minutes. For double restriction digests, an initial digest was performed, heat activated and cleaned up from solution using the QIAEX II - gel extraction kit (Qiagen) (See section 2.1.3.). Subsequently the second digest was performed and then heat inactivated. Restriction digest product was run on an agarose gel (see section 2.1.2) for analysis and extraction (see section 2.1.3).

2.1.5 DNA LIGATION

Ligation of DNA insert into a restriction digested plasmid vector was performed in a 10µl reaction (see table 2.2) using T4 DNA ligase (Promega) and the appropriate 10x ligase buffer (Promega), following the manufacturers protocol.

Table 2-2: Ligation reaction volumes using T4 DNA ligase (Promega), assembled in a sterile 0.6ml microtube.

Ligation Reaction	Volume
Vector DNA	100ng
Inset DNA	17ng
Ligase 10x Buffer	1 µl
T4 DNA Ligase	1 µl
Nuclease-free water to final volume of	10µl

2.1.6 FORMATION OF $CaCl_2$-COMPETENT DH5α CELLS

Competent *Escherichia.Coli* (*E.Coli*) DH5α cells were generated from a glycerol scrape of *E.Coli* DH5α which was grown in 5ml Luria Bertani (LB) medium (Sigma). The bacterial cells were incubated for 16-18 hours rocking at 210rpm, 37°C in an orbital incubator. After incubation 0.5ml of the DH5α culture was then diluted in 50ml of LB medium and rocked at 210rpm until an absorbance of 0.3-0.4 was read at 600nm (Uv Spectrophotometer, Shimadzu). DH5α cells were harvested by centrifugation, 3500xg for 10 minutes at 4°C using a 4.2 rotar Beckman Coulter J6-MI (Beckman). The cells were placed on ice, the supernatant was carefully removed and the cell pellet was gently resuspended in 20ml of ice-cold 100mM calcium chloride ($CaCl_2$). The cells were then incubated on ice for 30 minutes, following this the cells were centrifuged at 1000xg. Supernatant was again removed gently and the cell pellet was resuspended in 1ml of 100mM $CaCl_2$ and incubated on ice for a further 30 minutes before transformation (see section 2.1.7). For future use, aliquots of DH5α cells were stored at -80 in 20% glycerol.

2.1.7 TRANSFORMATION

To a 200µl aliquot of competent DH5α cells in a 1.5ml microtube, 10 µl of ligation product (see 2.1.5) was added and incubated on ice for 30 minutes. The bacterial cells plus ligation product was then heat shocked at 42°C for 45 seconds and placed on ice for a further minute. 800 µl of SOC medium (2% tryptone, 0.5% yeast extract, NaCl 10mM, $MgCl_2$ 2mM, $MgSO_4$ 10mM, 2.5mM KCl, glucose 20mM) was added to the transformation mix which was then incubated at 37°C in a pre-warmed orbital incubator at 210rpm for 45-60 minutes. LB-Agar plates were prepared with the appropriate antibiotic resistance for the DNA plasmid (100 µg/ml ampicillin or 50 µg/ml kanamycin). 100 µl of the incubated transformation culture was spread onto the relevant agar plates and incubated at 37°C upside down for 16-18 hours. When ligating into a pGEMT easy plasmids, DH5α transformed cells were spread on to LB/ampicillin/IPTG/X-Gal plates (LB-agar, 100 µg/ml ampicillin, 0.1mM IPTG and 2% X-Gal).

2.1.8 PLASMID DNA PURIFICATION FROM TRANSFORMED DH5α CELLS

Bacteria (either a single colony or a scrape from a glycerol stock) was added to 5ml LB-medium containing the correct antibiotic resistance (100µg/ml ampicillin or 50µg/ml kanamycin) and cultured overnight (16 hours) at 37°C rocking at 210rpm in an incubator. Small scale plasmid purification was carried out using the Qiagen spin Miniprep kit (Qiagen), according to manufacturer's protocol. DNA purifications of a larger scale were performed according to manufacturer's protocol using the Qiagen EndoFree plasmid maxi kit (Qiagen). DNA concentrations were measured (NanoVue, GE Healthcare) and DNA was stored at -20°C until needed.

2.1.9 GLYCEROL STOCKS

For long term storage transformed DH5α cultures were frozen at -80°C in a mix of 600µl transformed DH5α cultures with 400µl 50% glycerol.

2.2 CELL CULTURE

2.2.1 CELL CULTURE

All cells were cultured in Nunc T-75 or T-25 plastic flasks, at 37°C in a humid incubator in the presence of 5% CO_2. Human embryonic kidney 293 (HEK 293) cells were cultured in minimum essential medium eagle (MEM) (Invitrogen) with added 10% foetal calf serum (FCS) (Seralab), 100 units Penicillin 0.1mg/ml Streptomycin, and 2mM L-Glutamine. Human neuroblstoma cell lines (SK-N-SH) were cultured in Dulbecco's Modified Eagle's Medium (DMEM) with additional 10% FCS, 100 units Penicillin 0.1mg/ml Streptomycin, and 2mM L-Glutamine (P/S/G).

2.2.2 PASSAGE OF CELLS

All cells were passaged when reached a 70-80% confluent layer in the culture dish. When confluent, culture medium was aspirated and cells were washed with pre-warmed (37°C) 1 x phosphate buffered saline (PBS). Cells were then trypsinised from the culture dish by adding 0.05% trypsin/ 0.02% EDTA solution (Sigma), either 500µl (T25 flask) or up to 3ml (T75 flask), and incubated at 37°C, 5% CO_2 for 1-5 minutes depending on adherence of cells. Once cells are detached from culture dish, they are taken up in 5-10 ml of fresh medium and transferred to a 15ml tube. Cells were then pelleted in a centrifuge for 5 minutes at 1000xg and resuspended in fresh medium. Cells were then plated out into an appropriate dish.

2.2.3 DNA TRANSFECTION OF MAMMALIAN CELL LINES WITH LIPOFECTAMINE 2000 TRANSFECTION REAGENT

SK-N-SH cells and were 90-95% confluent within the culture dish when they were transfected with Lipofectamine 2000 reagent (Invitrogen) according to the manufacturer's protocol (volumes for transfection see table 2.3). SK-N-SH cells were plated one day before transfection either with glass coverslips or not. Cells on coverslips were used for fluorescence microscopy and FRET whereas cells

transfected on the dish alone were collected for western blotting, immunoprecipitation studies, initial ABAD activity assays or lipid extraction.

Table 2-3: Reaction volumes used for differing culture dishes

Size of dish	Lipofectamine 2000 reagent (µl/dish)	DNA (µg/dish)	Opti-MEM (µl/dish)	Medium (ml/dish)
35mm	2.5/5	½	500	2
T-25 flask	10	4	500	8

2.2.4 DNA TRANSFECTION OF MAMMALIAN CELL LINES WITH GENEJAMMER TRANSFECTION REAGENT

HEK 293 cells were cultured in a similar manner except a different transfection reagent was used. GeneJammer (Stratagene) was used according to manufacturer's protocol (see table 2.4 for reaction volumes). HEK 293 cells were plated either with or without coverslips on the culture dish one day before transfection.

Table 2-4: Reaction volumes used with GeneJammer transfection reagent

Size of dish	GeneJammer reagent (µl/dish)	DNA (µg/dish)	Opti-MEM (µl/dish)	Medium (ml/dish)
96 well plate	0.15	0.05	5	0.1
35mm	3/6	1/2	100	2
T-25 flask	9	2	150	8

2.2.5 STORAGE OF CELL LINES

Cells are stored long term in liquid nitrogen. Cells for storage were trypsinised (see section 2.2.2) and pelleted in a centrifuge for 5 minutes at 1000xg. Cell pellet was resuspended in 900µl of fresh cold medium and cooled down on ice. 900µl of medium containing 20% Dimethyl sulfoxide (DMSO) was added to the pre-cooled cell/medium mix to a total volume of 1.8ml and transferred to a Cryotube (Nunc). Cryotubes were placed in an isopropanol container and cooled to -80^{o}C before placing in liquid nitrogen.

2.2.6 RESCUE OF FROZEN CELL LINES

Cells were rescued from liquid nitrogen stores by quickly thawing and transferred to culture dish containing appropriate medium. The medium was changed after 24 hours to remove any residual DMSO.

2.3 CELL ASSAYS AND TECHNIQUES

2.3.1 FIXING CELLS

35mm plastic dishes (Nunc) with glass coverslips were used to culture cell lines for fixing. After 48 hours of transfection medium was aspirated from culture dishes and the cells were washed very gently with 1xPBS, three times at 5 minute intervals. Once washed cells were fixed with 4% paraformaldehyde (PFA) and left for 20 minutes at room temperature in the dark. Remaining 4% PFA was removed after 20 minutes and the cells were again washed with 1xPBS, four times at 5 minute intervals. The coverslips were then mounted onto glass slides using mowiol (Sigma) with or without 4',6-diamidino-2-phenylindole (DAPI). Slides were imaged using multiphoton confocal laser scanning microscope (Leica).

2.3.2 MITOTRACKER STAINING

Cells were cultured (see sections 2.2.1 - 2.2.4) in 35mm dishes (Nunc) on glass slides. MitoTracker Deep red probe was used to selectively dye the mitochondria. The MitoTracker was diluted to a concentration of 100nM (for cell lines) in the appropriate medium; medium from the cell culture dish was aspirated and replaced with 1-2ml of the diluted MitoTracker. The cells were then incubated for 20-40 minutes at 37^{o}C, 5% CO_2. After incubation with the mitochondrial dye, the cells were washed with pre-warmed medium and then fixed for imaging (see 2.3.1). MitoTracker staining was visualized by excitation at 633nm and emission collected at 640-670nm using a multiphoton confocal laser scanning microscope (Leica).

2.3.3 IMMUNOPRECIPITATION

Immunoprecipitation was carried out using GFP-Trap A (Chromotek) which is a green fluorescent protein (GFP) binding protein already coupled to cross-linked agarose. GFP-Trap A was used to pull down yellow fluorescent protein (YFP) and cyan fluorescent protein (CFP) tagged proteins.

2.3.3.1 WHOLE CELL EXTRACTION

Cells were cultured and transfected (see sections 2.2.1 - 2.2.4) and the cell lysates were harvested after 48 hours of transfection. Cell culture dishes were placed on ice, the medium was aspirated and the cells were washed twice with ice cold 1xPBS. Cells were harvested using 60µl of a non-denaturing lysis buffer: 20mM Tris-HCL pH8, 137mM NaCl, 2mM EDTA, 10% glycerol, 1% NP-40, 1mM Phenylmethulsuflonylfluoride (PMSF) and 1% protease inhibitor complex mix (Roche). Cell lysates were collected and sonicated for 30 seconds and placed on ice for 15minutes. They were then spun at 13,000xg for 5minutes at 4^{o}C. The cell pellets were resuspended with 500-1000 µl of dilution buffer: 20mM Tris-HCL pH8, 137mM NaCl, 2mM EDTA, 1mM PMSF and 1% protease inhibitor complex mix (Roche).

GFP Trap A Chromotek protocol was followed for immunoprecipitation and the eluted products were kept for SDS-PAGE and western blot analysis.

2.3.4 ABAD ENZYME ACTIVITY ASSAY

2.3.4.1 CELL CULTURE

HEK 293 and SK-N-SH cells were cultured in a black walled clear bottom 96 well plates (Thermo Scientific Nunc) and HEK 293 cells were transfected after 24 hours whereas SK-N-SH cells were not transfected (see section 2.2.4).

2.3.4.2 GLUCOSE DEPLETION

48 hours after plating, cell medium was substituted, for a phenol red free medium supplemented with altered glucose concentrations (see table 2.5).

HEK 293 medium: Low glucose (1g/l), phenol red free and no glutamine MEM (Invitrogen): 1% FCS (charcoal filtered), Penicillin 0.1mg/ml Streptomycin (P/S) and 10mM HEPES.

SK-N-SH medium: No glucose, phenol red free and no glutamine DMEM powder (Sigma) (made up according to the manufacturer's instructions): 1% FCS (charcoal filtered), Penicillin 0.1mg/ml Streptomycin (P/S) and 10mM HEPES.

Table 2-5: The varying glucose concentrations of the medium used in the ABAD activity assay.

Name	Glucose concentration g/l
Normal Glucose	4.5
Medium Glucose	3
Low Glucose	2
Very Low Glucose	1

2.3.4.3 FLUORESCENT MEASURMENT ASSAY

24 hours after the glucose concentration has been reduced in the medium, it is removed and replaced with glucose depleted, phenol red free medium containing 20µM of the fluorogenic probe, (-)- CHANA. The black walled 96 well plates are then analysed in a 96 well plate reader (FLUOstar Optima microplate reader) for 8 hours (see table 2.6).

Further analysis of fluorescent measurements included calculating average and standard error of the fluorescent signal and rate of CHANK production per minute with an unpaired T-Test as the statistical analyisis.

Table 2-6: FLUOstar Optima microplate reader set up, excitation and emission of fluorogenic probe and length of measurements.

Parameters for fluorescent measurement	
Bottom Optic	
Excitation	380nm
Emission	520nm
Orbital averaging	3mm
Number of flashes	10
Cycle time	300 seconds
Number of cycles	97

2.3.5 MTT ASSAY

Cells cultured in a 96-well plate in a total volume of 100µl, when ready for analysis cell medium was removed and 3-(4,5-Dimethylthiazol-2-yl)-2,5-diphenyltetrazolium bromide (MTT) added to make a final concentration of 1mg/ml. The cells were then incubated for 5 hours in a sterile incubator at 37^{o}C, 5% CO_2. Once incubation complete, cell medium was removed and 100µl of DMSO was added to each well. The plate was agitated and then the absorbance was measured at 570nm (FLUOstar Optima microplate reader).

2.4 FLUORESCENCE MICROSCOPY TECHNIQUES

2.4.1 FLUORESCENCE RESONANCE ENERGY TRANSFER (FRET) ANALYSIS

To detect a protein-protein interaction, FRET analysis can be used. FRET is the energy transfer between fluorphores with overlapping spectra when they are within a 1-10nm range of each other. In this study initial FRET analysis was conducted on fixed cells and latterly on live cells.

2.4.2 FIXED CELL FRET EXPERIMENTS

HEK 293 cells and SK-N-SH cells were cultured in 35mm dishes on coverslips and transfected following the protocol outlined in sections 2.2.4 & 2.2.3 respectively. The cells were transfected with DNA plasmids containing expression for the proteins of interest and corresponding fluorophores (ECFP-enhanced cyan fluorescent protein or EYFP- enhanced yellow fluorescent protein). 48 hours after transfection the cells were immobilized on the coverslips (see section 2.3.1) and mounted onto glass slides with mowiol, these slides were then imaged using a Leica TCS multiphoton confocal laser scanning microscope. Subsequently the fluorophores ECFP and EYFP were excited with argon laser set at 458nm or 514nm respectively and emission was collected between 468-498nm for ECFP and 550-582 nm for EYFP.

To detect the occurrence of FRET, Leica software for the analysis of photobleaching was used. Specific regions of interest (ROI) were highlighted using the software and the following steps of photobleaching were conducted. Initially, emission images of the donor fluorophore (ECFP) and acceptor fluorophore (EYFP) were captured before photobleaching excited at 458nm (laser power set at 55% of total power) and 514nm (laser power set at 21% of total power) respectively. The next step is the photobleaching of the acceptor fluorophore, which consists of repeated excitation at 514nm laser at full power. Finally, images were taken of the fluorophores post bleaching and the fluorescent intensities from these images (Dpost – donor post bleaching; Dpre – Donor pre bleaching) were

used to calculate the FRET efficiency using the following formula FRET eff = (Dpost-Dpre)/Dpost.

$$FRET_{eff} = (D_{post} - D_{pre}) / D_{post}$$

2.4.3 LIVE CELL FRET ANALYSIS

HEK 293 cells were cultured in 35mm dishes and transfected with the same plasmid DNA expressing the fluorescently tagged proteins of interest (see section 2.2.4). After 48 hours the HEK 293 cells were trypsinised and centrifuged for 5minutes at 800xg, the medium was aspirated and the cell pellet washed with 1xPBS. Cells were centrifuged again at 800xg for 5minutes and the final cell pellet was resuspended in 500µl of cold 1xPBS.

150µl of the cell suspension was transferred into a quartz cuvette and the fluorescent signal was measured using a Varian Cary Eclipse Spectrophotometer. ECFP was excited at 436nm, fluorescence was subsequently collected between 460-800nm, EYFP was excited at 517nm and collect between 525-800nm. Measurement of excitation and emission occurred through a slit width of 5mm. Specific measurements were taken: excitation of the donor fluorophore (ECFP) alone, excitation of the donor fluorophore in the presence of the acceptor fluorophore (EYFP) and excitation at the donor excitation wavelength in the presence of the acceptor fluorophore alone.

The spectra gained from the spectrophotometer was analysed to determine the likelihood of FRET. The FRET ratio was calculated using Origin 8 software initially, by plotting the emission spectra from the donor (alone) and the emission spectra from the donor (in the presence of the acceptor – experimental), the data was normalised, and the experimental acceptor emission spectra was calculated by subtracting the donor spectra. Following this the experimental acceptor emission was divided by the emission obtained when the acceptor (alone) was excited at the donor wavelength in order to gain ratio A which in turn establishes the probability of FRET.

2.5 PROTEIN ANALYSIS

2.5.1 WESTERN BLOTTING

2.5.1.1 BRADFORD REAGENT

Protein quantification was carried out by using Bradford reagent. A standard calibration curve was formed using known concentrations of BSA protein, 500µl distilled H_2O and 500µl Bradford reagent. Form this curve protein samples could be determined: 5µl sample, 495µl distilled H_2O and 500µl Bradford reagent. Absorbance was measured at 595nm with MRX plate reader (DYNEX Technology).

2.5.1.2 CELL LYSATES FOR SODIUM DODECYL SULPHATE–POLYACRYLAMIDE GEL ELECTROPHORESIS (SDS-PAGE)

Cells were cultured and transfected (see sections 2.2.1 - 2.2.4) and the cell lysates were harvested after 48 hours of transfection. Cell culture dishes were placed on ice, the medium was aspirated off and the cells were washed twice with ice-cold 1xPBS. Cells were harvested using 3-[(3-cholamidopropyl) dimethylammonio]-1-propanesulfonate (CHAPS) lysis buffer: 8.27M Urea, 4.7% (w/v) CHAPS, 1% (w/v) DTT, 1mM PMSF and 1% protease inhibitor complex mix (Roche). Cell lysates were collected and sonicated for 30 seconds and placed on ice for 15minutes. They were then spun at 13,000xg for 5minutes at 4^{o}C, aliquots of the supernatant were made either stored at -20^{o}C or used straight away for SDS-PAGE. Samples for SDS-PAGE were prepared by adding 4 x protein sample buffer (PSB): 106mM Tris-HCL, 141mM Tris-Base, 8% SDS, 51mM EDTA, 40% (w/v) glycerol, 400mM DTT and 0.08% Bromphenol Blue. Once 4 x PSB was added, samples were heated to 100^{o}C for 5 minutes, followed by centrifugation at 13000xg for 30-60 seconds.

2.5.1.3 SDS-PAGE

Bio-Rad casting equipment was used to make 10% Polyacrylamide gels made up to the specifications in table 2.7. Once the gels were set they were placed in an electrophoresis chamber (Bio-Rad) and surrounded by 1 x electrophoresis buffer: 25mM Tris, 192mM Glycine and 0.1% SDS. Protein samples were loaded into the gels and separated by electrophoresis at 85 volts (v) for 90minutes.

2.5.1.4 TRANSFER OF PROTEIN TO NITROCELLULOSE MEMBRANE

SDS-PAGE gels were transferred onto nitrocellulose membrane (Whatman) by wet transfer, whereby the gel is placed between sponges, blotting paper (Whatman) and the membrane all soaked in transfer buffer: 25mM Tris-Base, 192mM Glycine and 20% methanol. Electroblotting of the transfer was carried out in an *X* cell II chamber (Invitrogen) at 30V for 70 minutes.

2.5.1.5 WESTERN BLOTTING

Full transfer of proteins onto the nitrocellulose membrane was verified by passing membrane through Ponceau S solution (0.1% Ponceau (w/v) in 5% acetic acid). To remove excess Ponceau S solution, the membrane was washed with Tris Buffered Saline (TBS): 50mM Tris, 138mM NaCl and 2.7mM KCl with 0.1% tween 20 (TBS-T). Following this the membrane was blocked with 5% (w/v) dried non-fat milk (Marvel) in TBS-T for 45 – 60 minutes, rocking at room temperature. The blots were then washed with TBS-T and the primary antibody (in either 5% (w/v) dried non-fat milk (Marvel) or 5% (w/v) BSA) added to the blot. The blots were incubated at 4^{o}C, rocking overnight.

After incubation blots were washed three times with TBS-T at 10 minute intervals, the HRP-conjugated secondary antibody was added and the blot was incubated at room temperature, rocking for 1hour. The blot was further washed (three times with TBS-T at 10 minute intervals), Enhanced chemiluminescence reagent was applied to the blot following manufacturer's instructions and the immunoreactive bands were imaged using LAS-3000 image reader (Fuji).

Table 2-7: Polyacrylamide gel composition. PAGE gels were made up to the specific quantities below to allow for efficient electrophoresis

Separating Gel	**10%**
Distilled H_2O	4.8 ml
1.5 M Tris-HCl, pH 8.8	2.5 ml
10% SDS	100 µl
40% Acrylamide	2.5 ml
10% APS	100 µl
TEMED	4 µl
Stacking Gel	**1-fold**
Distilled H_2O	3.14 ml
0.5 M Tris-HCl, pH 6.8	1.25 ml
10% SDS	50 µl
40 % Acrylamide	0.5 ml
10% APS	50 µl
TEMED	10 µl

2.5.2 LIPIDOMICS

2.5.2.1 LIPID EXTRACTION

Cells cultured in T-25 flasks, when 90% confluent, were trypsinised and centrifuged for 5minutes at 1000xg, the medium was aspirated and the cell pellet washed with 1xPBS. Cells were centrifuged again at 1000xg for 5minutes and the final cell pellet was resuspended in 100µl 1xPBS and transferred to a glass vial.

1:2 (v/v) $CHCl_3$:MeOH was added to the cell suspension and vortexed. Cells were agitated for 10-15 minutes at room temperature. After agitation $CHCl_3$ was added, the cells vortexed and then H_2O added and further vortexed. Finally cells were centrifuged for 5 minutes, 1000xg at room temperature. The cells are now biphasic with aqueous solution at the top and organic material in the bottom. The lower phase was collected and dried under nitrogen and stored at 4^oC.

2.5.2.2 ELECTROSPRAY IONISATION (ESI) MASS SPECTROMETRY

Nitrogen dried lipids extracts from HEK 293 and SK-N-SH cells were re-dissolved in chloroform/methanol (1/2 v/v). The samples were loaded into thin-wall nanoflow capillary tips (Waters) and electrospray mass spectrometry (ES-MS) both in positive and negative ion modes were used to analyse the lipid extracts. The MS used was Micromass LCT mass spectrometer with a nanoelectrospray source using a capillary voltage of 0.9 kV and cone voltages of 50 V to gain lipid spectra. To identify product ion spectrum, *m/z* fragmentation scan was conducted using Micromass Quattro Ultima triple quadrupole with argon collision gas or a ABSCIEX 4000 Q-Trap mass spectrometer with a nanoelectrospray source using nitrogen as a collision gas, collision energies between 35-70V depending upon lipid class. Each product ion spectrum incorporates a minimum of 50 repetitive scans.

Chapter 3: INTERACTION BETWEEN AMYLOID β BINDING ALCOHOL DEHYDROGENASE & CYCLOPHILIN D

3.1 INTRODUCTION

3.1.1 ABAD INTERACTS WITH CYPD

ABAD has been reported to have protective functions within neurons, in particular the catalytic ability of ABAD allows for the attenuation of the accumulations of toxic aldehydes within neurons (Murakami et al., 2009). I propose that ABAD interacts with CypD in order to induce further protective roles within the cell by preventing the formation of the mPTP and consequently cell death.

Evidence to suggest that ABAD interacts with CypD originates from unpublished results in two different studies. Initially Yan and Stern (2005) observed binding of ABAD to CypD and it was suggested that this binding could be either a measure for maintaining homeostasis or a protective mechanism in response to stress (Yan and Stern, 2005). ABAD binding to CypD could prevent the translocation of CypD to the IMM seen in response to oxidative stress (Connern and Halestrap, 1994). Implying that sequestration of CypD by ABAD would therefore prevent the formation of the mPTP and furthermore reduce mitochondrial dysfunction and cell death.

CypD and ABAD have both been established as mitochondrial proteins and further unpublished observations witness the co-localization of CypD and ABAD (Ren, 2008). Following these results, acceptor photo-bleaching FRET analysis was carried out with fluorescently tagged ABAD and CypD proteins. Strongly positive FRET signals were noted an thus signifying an interaction between these proteins (Ren, 2008).

To further investigate the possible binding of ABAD with CypD in the mitochondria three different methods were used; acceptor photo-bleaching FRET analysis on immobilised cells, spectroscopic FRET analysis with live cells and immunoprecipitation.

3.1.2 FRET ANALYSIS

The process of FRET is used to detect protein-protein interactions by the distances between fluorophores tagged to the proteins of interest. Different fluorophores with over-lapping excitation and emission wavelengths are used in order to observe FRET interactions. The over-lapping spectrum is crucial as when the fluorophore tags are within a 1-10nm range of each other and the donor fluorphore has been excited, the emission from the donor will excite the acceptor fluorophore (Wallrabe and Periasamy, 2005). Only when the fluorophores are within this specific range will FRET occur, this is important as proteins will only be close enough to cause FRET if they are interacting with each other.

Confocal microscopy is primarily used to record FRET however other methods that can be used include spectral imaging using a spectrophotometer, which measures the fluorescent emission spectra. The intensity of emission spectra is then used to determine the intensity of FRET (Clegg, 1992).

Measuring FRET with a confocal microscope can either be done by acceptor photo-bleaching, sensitised emission or via fluorescence lifetime imaging microscopy (FLIM).

FLIM-FRET

The principle of FLIM-FRET is based on the lifetime of fluorophores. Standard FLIM measures the rate of decay of fluorescence emission, which is altered by changes in pH, ions and importantly FRET (Wallrabe and Periasamy, 2005). This technique can therefore be used to investigate protein-protein interactions by measuring the increase in the decay of emission. Initially the lifetime of the donor fluorophore must be measured along with the life-time of the donor when the acceptor fluorophore is present to allow for FRET efficiency to be calculated.

SENSITISED EMISSION

Sensitised emission of the acceptor fluorophore is a simple method using a confocal microscope. The donor fluorophore is excited and due to the overlapping fluorescence spectra, the emission from the donor should excite the acceptor if they are within the 10nm range. Therefore, to analyse the occurrence of FRET, only the emission from the acceptor fluorophore is recorded. However, sensitised emission is prone to inaccuracies due to the neighbouring fluorescence spectras and must have strict controls in order to reduce spectral bleed-through (cross-talk) emission. Spectral bleed-through can occur as a consequence of the excitation of the donor wavelength exciting the acceptor and so a control where the donor fluorophore is absent is essential to allow for reduction of the background fluorescence in this method of FRET (Wallrabe and Periasamy, 2005).

ACCEPTOR PHOTO-BLEACHING

The method behind acceptor photo-bleaching is based on the repeated excitation of the acceptor fluorophore which prevents excitation by the donor fluorophore (Swift, 2004). In this instance FRET is measured by the increased fluorescence intensity emitted by the donor fluorophore caused by the inability to excite the bleached acceptor by 'donating' its fluorescence. This method for analysing FRET removes the likelihood of spectral bleed-through due to the removal of one fluorophore. Acceptor photo-bleaching is ideal for fixed cell imaging as fully photo-bleaching live cell is problematic due to cellular movement, morphology and focal plane, these problems also occur in time lapse experiments (Zal and Gascoigne, 2004). Acceptor photo-bleaching was the method of FRET initially used to discover the positive interaction between ABAD and CypD and therefore this method was attempted in order to replicate the study.

FRET was determined by tagging the two proteins with fluorophore pairs, ABAD was tagged with the acceptor fluorophore EYFP (enhanced yellow fluorescent protein) and CypD was tagged with the donor fluorophore ECFP (enhanced cyan fluorescent protein). Both of these fluorescent spectra overlap allowing for FRET to occur (Figure 3.1). Excitation wavelength for the donor, CFP, has two major

excitation peaks at 434nm and 453nm whereas the excitation of the acceptor, YFP, ranges between 450–565nm and only has one major excitation peak at 514nm. Emission from CFP spans between 460–520nm with main peaks at 475nm and 501nm therefore allowing excitation of YFP.

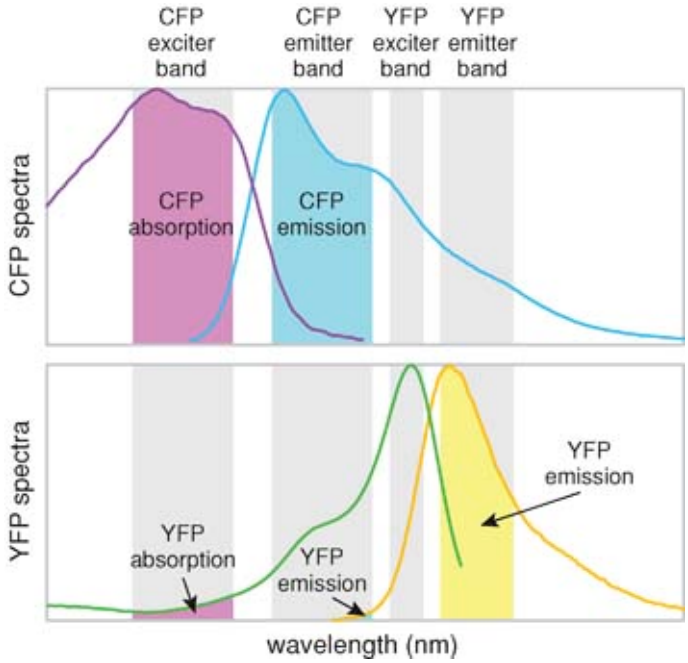

Figure 3-1.: CFP and YFP excitation and emission spectrum (Erdogan, 2011)

SPECTROSCOPIC METHOD OF FRET ANALYSIS

In addition to the use of confocal microscopy to identify FRET signals, steady state fluorescent spectrophotometry can be used. This allows for the live cell imaging of a protein-protein interaction via FRET. The spectrophotometer is used to excite fluorophores within a quartz cuvette and the fluorescence intensity is subsequently measured. In order to determine if energy transfer has occurred between proteins there are three measurements that are required to be taken:

A. Excitation of the pure donor (ECFP at 436nm) alone.
B. Excitation of the experimental donor in the presence of the acceptor (at 436nm) alone.
C. Excitation of the pure acceptor (EYFP at 517nm) alone.

These three measurements allow for the calculation of the ratio A value. Ratio A is proportional to the FRET efficiency and signifies the intensity of the FRET interaction (Clegg, 1992).

Ratio A **=** Area under **(D)/** Area under **(E)**

To calculate ratio A the intensity emitted from step A and B must be normalised at peak 488nm (the emission peak observed for ECFP), this permits the subtraction of the pure donor intensity from the experimental donor intensity **(B-A)**. The remaining fluorescence intensity therefore is a consequence of FRET whereby, the donor emission has excited the acceptor to emit fluorescence and therefore this is a good indicator of FRET. Furthermore, to gain Ratio A, the remaining emitted intensity from the experimental acceptor (D) is divided by the acceptor emission when excited at 517nm (obtaining the acceptor emission intensity). This division will give the ratio A value and signify the intensity of the FRET interaction.

3.1.3 IMMUNOPRECIPITATION

To further investigate the interaction between ABAD and CypD immunoprecipitation was used. The process of immunoprecipitation uses specific antibodies to identify proteins within a sample of whole cell lysates. Immunoprecipitation can be used to detect singular proteins or bound protein complexes.

The principle behind immunoprecipitation originates from an immunoadsorbent property possessed by protein A and G found in bacterial walls of *Staphylococcus aureus* and *Streptococci* strains C and G, respectively (Firestone and Winguth, 1990, Sjobring et al., 1991). Protein A and G bind to the fragment crystallizable (Fc) regions of antibodies, and these proteins are used to coat a solid state matrix such as Sepharose (Separation Pharmacia agarose)/agarose beads.

The standard methods for immunoprecipitation are either direct or indirect. The direct method uses coated agarose beads whereby the specific antibody required is coupled before the addition of cell lysates. The indirect method allows the specific antibody to bind within the cell lysates first, and then protein coated agarose is added to the lysates which binds to the antibody. The indirect method of immunoprecipitation is preferentially used as the antibody is able to bind to the protein of interest naturally without hindrance from the coupled agarose beads (Thompson, 2004).

In order to detect if ABAD binds to CypD, GFP-Trap A binding proteins were used. GFP-Trap A beads have a GFP binding protein (an antibody) coupled to agarose which encompass a high affinity for epitopes on GFP and YFP. In this instance the antibody for GFP is used to pull down the EYFP-tagged ABAD protein and it is hypothesised that an interaction between ABAD and CypD will result in the presence of CypD in the final pull down precipitate.

Over-expression of ABAD and CypD within cell lines increased the potential for witnessing an interaction between the pair. Using GFP-Trap A beads, the EYFP tag on ABAD was initially employed to pull down the overexpressed ECFP fused CypD protein. However, CFP was found to interfere with the immunoprecipitation and a myc-tagged CypD was created in order to counteract this interference. Additionally, as CFP was found to bind to the GFP-Trap A beads the ECFP-fused CypD was overexpressed in cell lysates with a mitochondrial targeted ABAD protein. This allowed for the prevention of any interference from the large protein tags affecting the regions of interaction.

3.2 AIMS OF CHAPTER

In the presence of Aβ and oxidative stress, CypD translocates from the matrix of the mitochondria to the IMM where it associates with the ANT and the VDAC forming the mPTP across the IMM and the OMM (Singh et al., 2009). This pore facilitates mitochondrial dysfunction and cell death, the translocation of CypD to

the IMM and the presence of Aβ are the triggers for these consequences, Aβ could be the disruptive factor behind the translocation of CypD.

Considering that Aβ has been shown to bind to ABAD and prevent enzyme functioning, this interaction could also cause a disruption of potential protective activity of ABAD whereby ABAD sequesters CypD away from the IMM. The ability of ABAD to retain CypD away from the IMM would reduce the likelihood of mPTP formation and consequently prevent cell death.

In order to ascertain if ABAD binds to CypD three methods used to detect protein-protein interactions were used, acceptor photo-bleaching FRET, spectroscopic FRET analysis and immunoprecipitation.

3.3 RESULTS: FÖRSTER RESONANCE ENERGY TRANSFER ANALYSIS OF THE ABAD –CypD INTERACTION

To determine a FRET interaction between CypD and ABAD, both proteins needed to be tagged with pairing fluorophores. A plasmid containing a mitochondrial targeting sequence, ABAD and a EYFP (pMTS-ABAD-EYFP) had been previously produced in our laboratory by Dr Yimin Ren and a plasmid with CypD and ECFP (pCypD-ECFP) was gifted to us by Dr Anne Murphy (Department of Pharmacology, University of California, San Diego).

3.3.1 CO-LOCALISATION OF MTS-ABAD-EYFP AND CYPD-ECFP

To confirm the co-localization of MTS-ABAD-EYFP and CypD-ECFP within the mitochondria, HEK 293 cells were grown on glass coverslips in 35mm dishes and transfected with either both plasmids or on their own. Cells were immobilised on the coverslips with 4% PFA (as in section 2.3.1) and mounted to glass slides with Mowiol+Dapi solution (Cells transfected with pCypD-ECFP were mounted with Mowiol without Dapi). MitoTracker was used to verify mitochondrial localisation

of pMTS-ABAD-EYFP. MitoTracker was added to the cell culture dish (following the method described in section 2.3.2) and incubated at 37^{o}C, 5% CO_2 for 20-30 minutes, this was then removed and the cells were fixed and mounted onto slides. MitoTracker is a fluorescent probe which can cross the plasma membrane of cells and upon oxidation within mitochondria it will fluoresce. Using a multiphoton confocal laser scanning microscope (Leica TCS-SP) equipped with x40 and x63 oil emersion objectives, fluorescence from the cells were recorded (Figure 3.2A-G).

MTS-ABAD-EYFP showed strong mitochondrial localisation (Figure 3.2 B & D), co-localising with MitoTracker shown in the merged image (Figure 3.2 G), whereas CypD-ECFP appeared to localise within the nucleus of these cells (Figure 3.2 A & C). In order to be able to measure FRET the constructs must co-localise, therefore a mitochondrial targeting sequence was attached to the CypD-ECFP sequence.

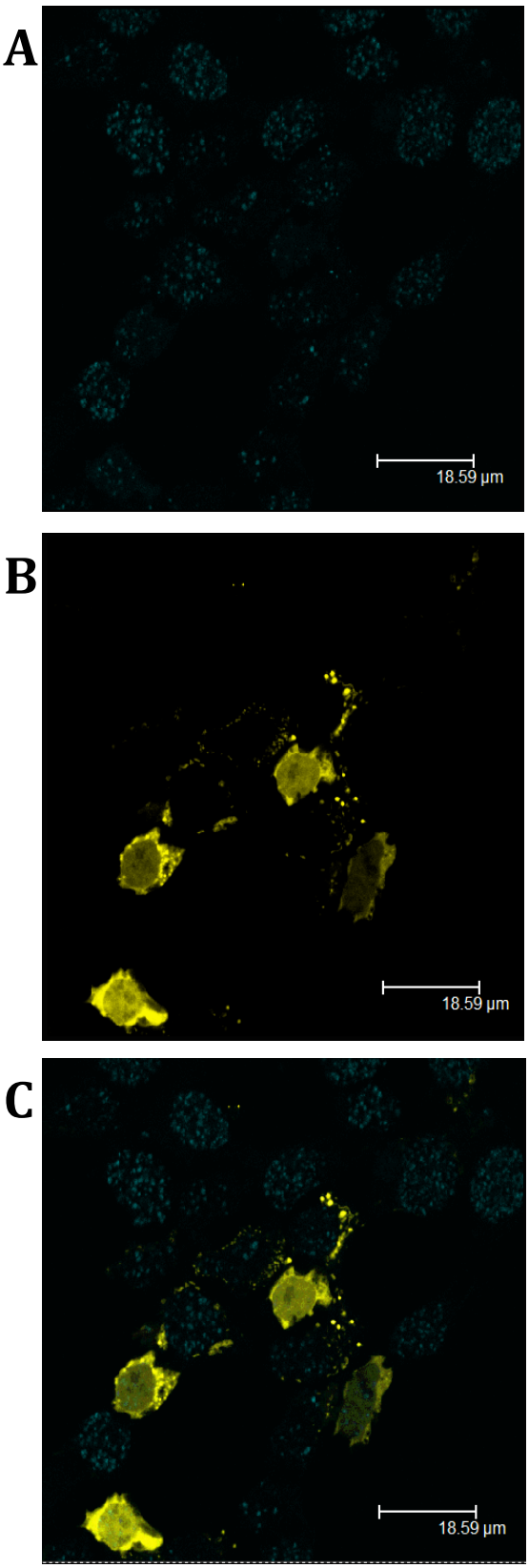
A
18.59 µm
B
18.59 µm
C
18.59 µm

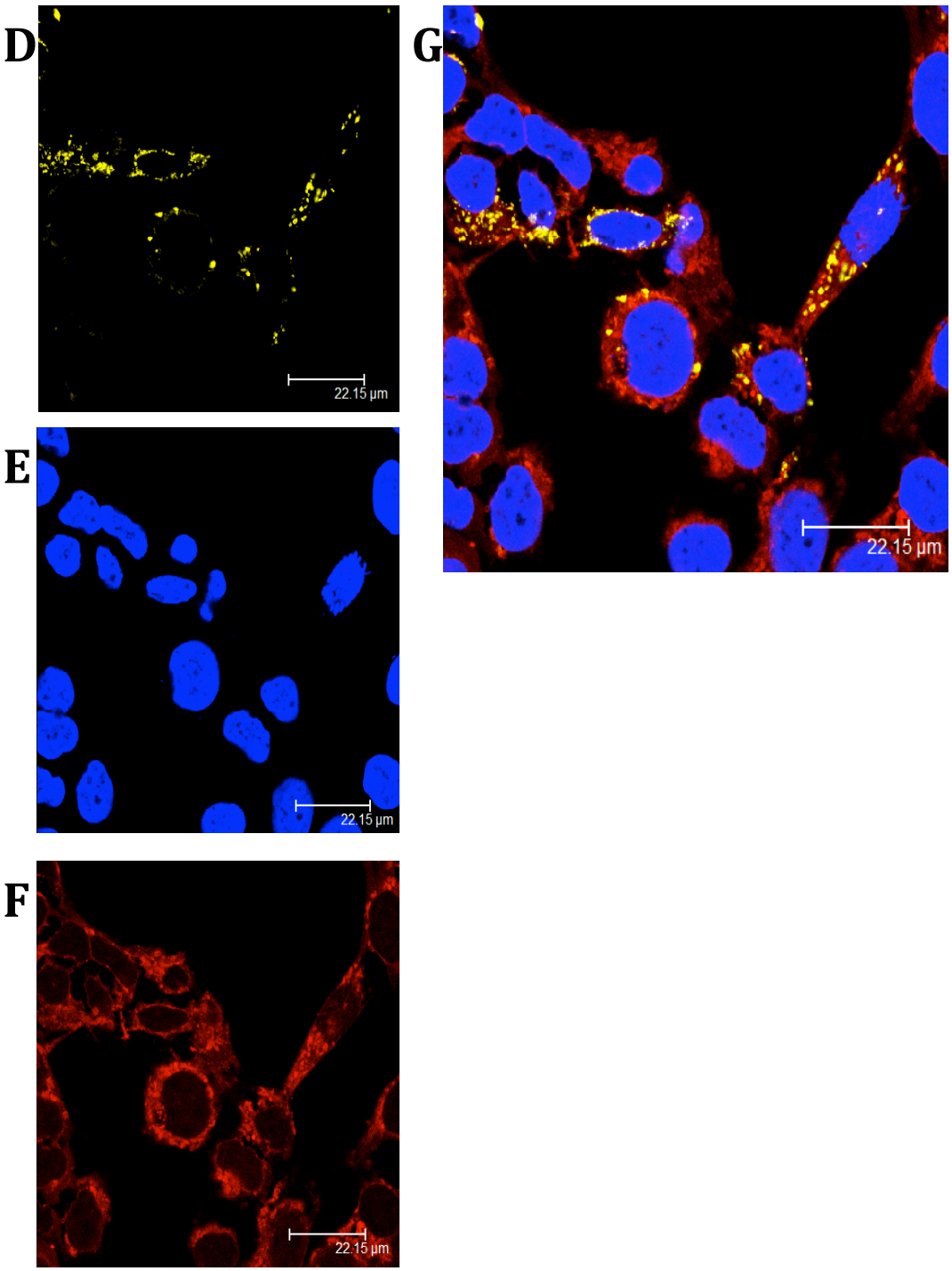

Figure 3-2: A)HEK 293 cells expressing MTS-ABAD-EYFP(yellow) in the mitochondria and B) HEK 293 cells expressing CypD-ECFP(light blue) appearing in the nucleus.C) overlapping image of A and B. D) HEK 293 cells expressing MTS-ABAD-EYFP, E) stained with Dapi (dark blue)and F) MitoTracker deep red (red). G) Overlapping image of D-F.

3.3.2 CONSTRUCTION OF pMTS-CypD-ECFP

To create a mitochondrial-directed pMTS-CypD-ECFP plasmid, the DNA sequence for CypD-ECFP was ligated into pDsRed2-Mito plasmid (Clontech), therefore using the mitochondrial targeting sequence from this plasmid, cloning strategy is outlined in figure 3.3. The mitochondrial targeting sequence is from subunit VIII of human COX and has been expressed in a mammalian expression vector along with red fluorescent protein isolated from *Discosoma sp* (Matz et al., 1999, Clontech, 2003).

Initially, a restriction digest of the target plasmid the pDsRed2-Mito using *BamHI* and *NotI* was carried out to remove the fluorescent DsRed sequence and to enable ligation of CypD-ECFP flanked with restriction sites for *BglII* and *NotI*. The digested plasmid was run on an agarose gel and purified from the gel (see section 2.1.2-2.1.4)

CypD-ECFP was cloned by PCR, using pCypD-ECFP as the template DNA (Figure 3.3 and section 2.1.1). In order to conduct PCR the following primers were created: the forward primer **5'** GGAAGATCTATGCTGGCGCTGCGC **3'**, encodes (underlined) the restriction site for *BglII* and the reverse primer **5'** TGCGGCCGCCTTGTACAGCTCGTC **3'**, encodes the restriction site for *NotI* (underlined). Products from PCR were digested with *BglII* and *NotI* and run on an agarose gel to confirm successful PCR (see section 2.1.4). The resulting 1383bp fragment was cleaned up from the agarose gel and ligated into the final plasmid. The ligation mixture was transformed into competent *E.coli* (DH5α), following successful transformation the plasmid DNA was purified from the bacteria using the method described in section 2.1.8. The plasmid DNA was sequenced and presence of pMTS-CypD-ECFP verified.

The localisation of pMTS-CypD-ECFP within the mitochondria and co-localisation with pMTS-ABAD-EYFP was confirmed in transfected HEK 293 cells by multiphoton confocal laser scanning microscope (Leica TCS-SP) (Figure 3.4 A-F).

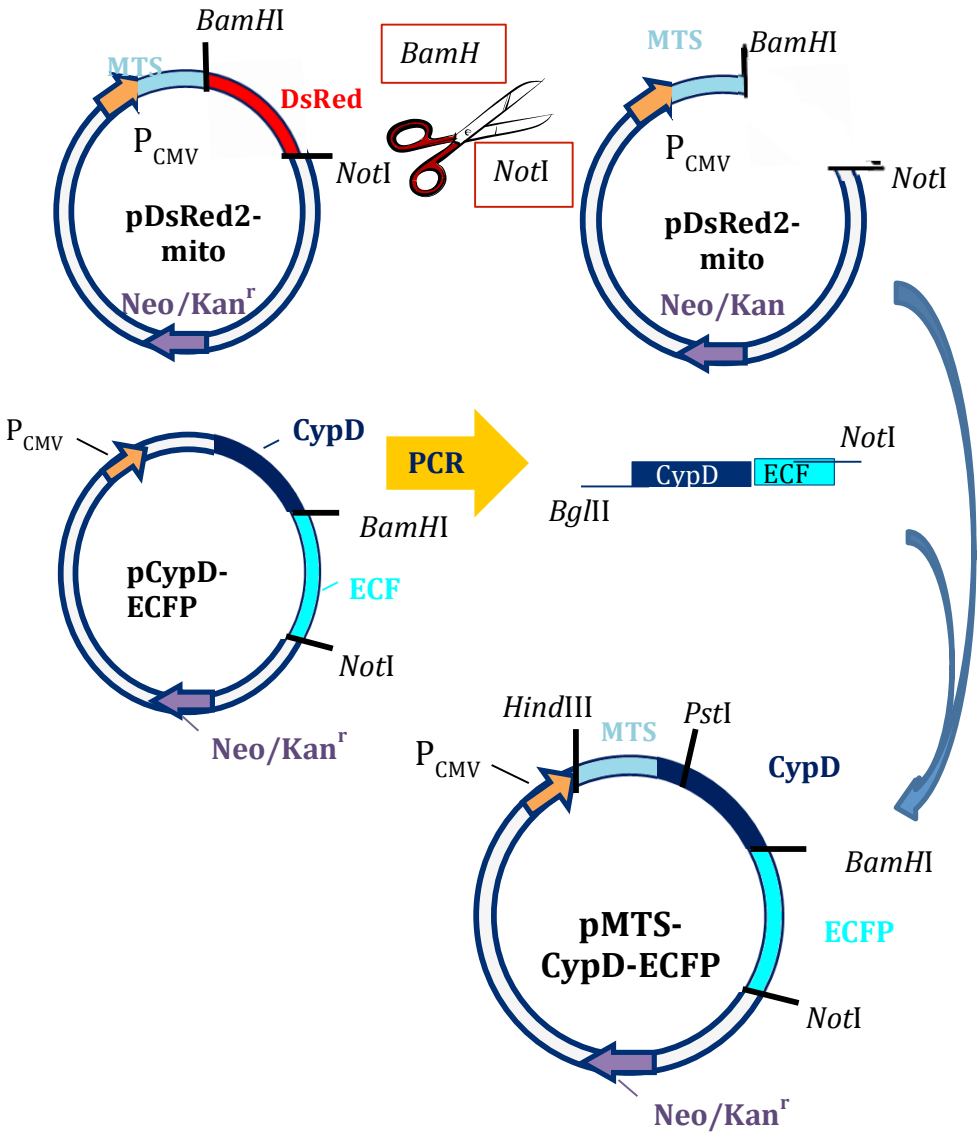

Figure 3-3: One step cloning strategy: pDsRed2-mito was digested with *BamH*I and *Not*I to allow for insertion of the PCR fragment. PCR was conducted following protocol outlined in section 2.1.1 with annealing temperature at 61.9°C using 100ng of the template DNA, pCypD-ECFP. The PCR fragment containing CypD-ECFP was ligated into the digested DsRed2-mito DNA plasmid.

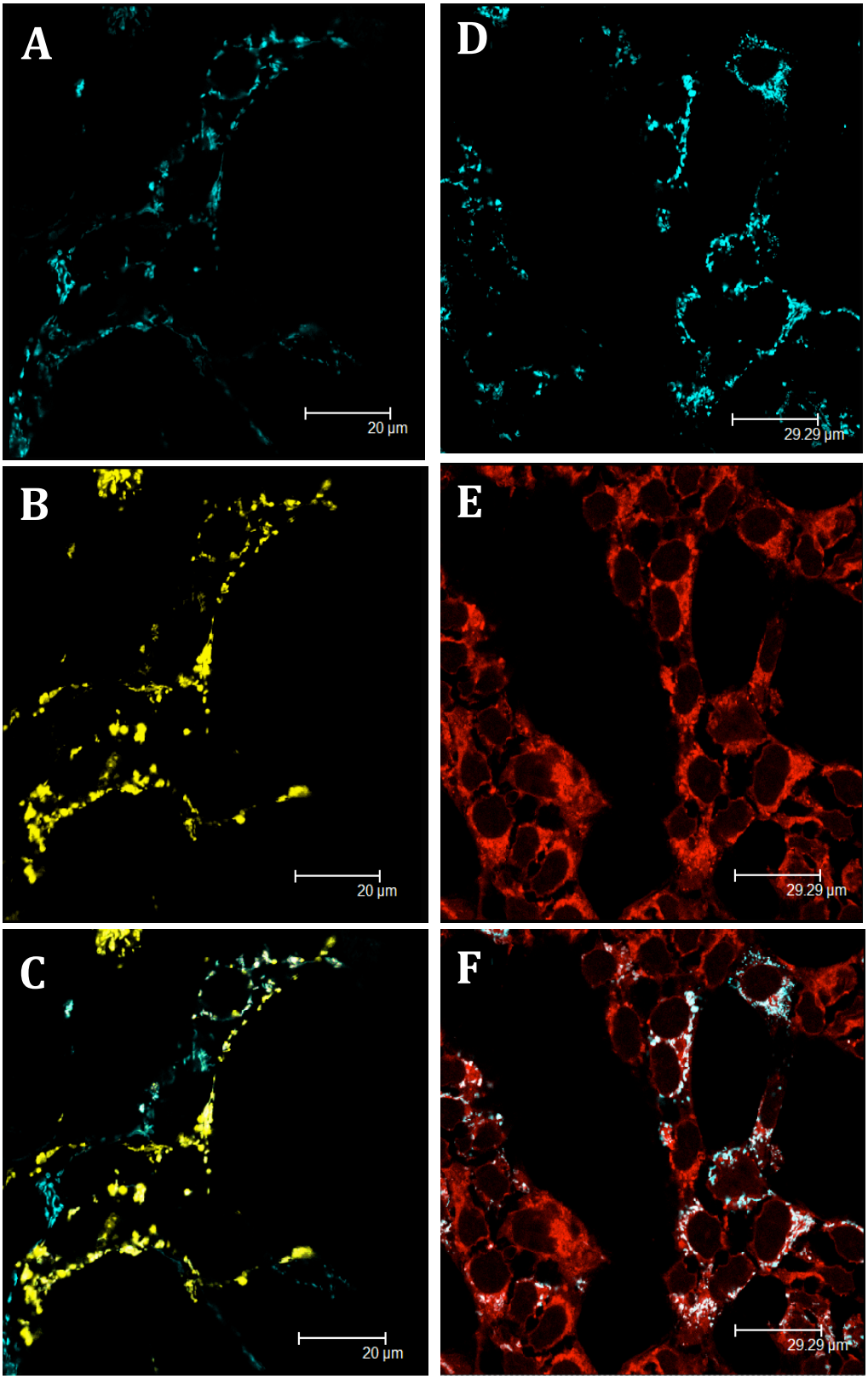

Figure 3-4: A) HEK 293 cells expressing MTS-CypD-ECFP (blue) and B) MTS-ABAD-EYFP (yellow), C) overlapping image of A and B. D) HEK 293 cells expressing MTS-CypD-ECFP (light blue) and E) MitoTracker Deep red (red) F) Overlapping image of D and E..

3.3.3 INVESTIGATION OF ABAD-CypD INTERACTION BY FRET ANALYSIS USING ACCEPTOR PHOTO-BLEACHING

Once co-localization of the fluorescently-tagged proteins was established, the hypothesised interaction between ABAD and CypD could be investigated. The fluorophores YFP and CFP are an ideal pair of fluorescent proteins that allow for the occurrence of FRET due to their overlapping emission and excitation spectra. The method of FRET analysis that was used was acceptor photo-bleaching, as previous studies using this method had hinted at an interaction between ABAD and CypD (Ren, 2008). The acceptor fluorophore, EYFP, is excited by the donor fluorophore ECFP, in this instance when MTS-CypD-ECFP is within a 1-10nm range of MTS ABAD-EYFP transmission of energy should occur from ECFP to EYFP (Figure 3.5). However, the photo-bleaching of EYFP, by applying intense repeated excitation to the EYFP fluorophore, prevents energy transfer from ECFP to EYFP and consequently ECFP emission will increase. In order to calculate the energy transfer occurring during FRET, the intensity of fluorescence from the donor (D) is measured before (D_{pre}) and after (D_{post}) excitation, subsequently the difference is used to determine the FRET efficiency. D_{post} must be greater than D_{pre} to determine a positive FRET interaction.

$$\mathbf{FRET}_{eff} = (\mathbf{D}_{post} - \mathbf{D}_{pre}) / \mathbf{D}_{post}$$

Two cell lines were used in this series of FRET experiments, HEK 293 and SK-N-SH cells were transfected with pMTS-CypD-ECFP and pMTS ABAD-EYFP, in a 3:1 ratio respectively. Due to the low fluorescence of ECFP and the further decrease in the presence of EYFP Zal et al. (2002) determined that donation of energy was most sensitive at a ratio of 3:1 (ECFP to EYFP) . Furthermore, previous acceptor photo-bleaching FRET experiments using pCypD-ECFP and pMTS ABAD-EYFP were successful using the same 3:1 ratio (Ren, 2008). Consequently, pMTS-CypD-ECFP and pMTS ABAD-EYFP were transfected at 3μg:1.5μg and 1.5μg:0.5μg

respectively. The same approach was applied when transfecting cells with control DNA. There were two negative controls: HEK 293 cells transfected with pMTS-CypD-ECFP alone and HEK 293 cells transfected with pMTS-CypD-ECFP and pEYFP plasmid (Clontech). The positive control was a fusion protein given as a gift from Professor J. Tavaré (Department of Biochemistry, University of Bristol). This fusion protein expressing ECFP and EYFP is connected by the 18 amino acid sequence from the caspase 3 cleavage site DEVD (pECFP-DEVD-EYFP) (Tyas et al., 2000).

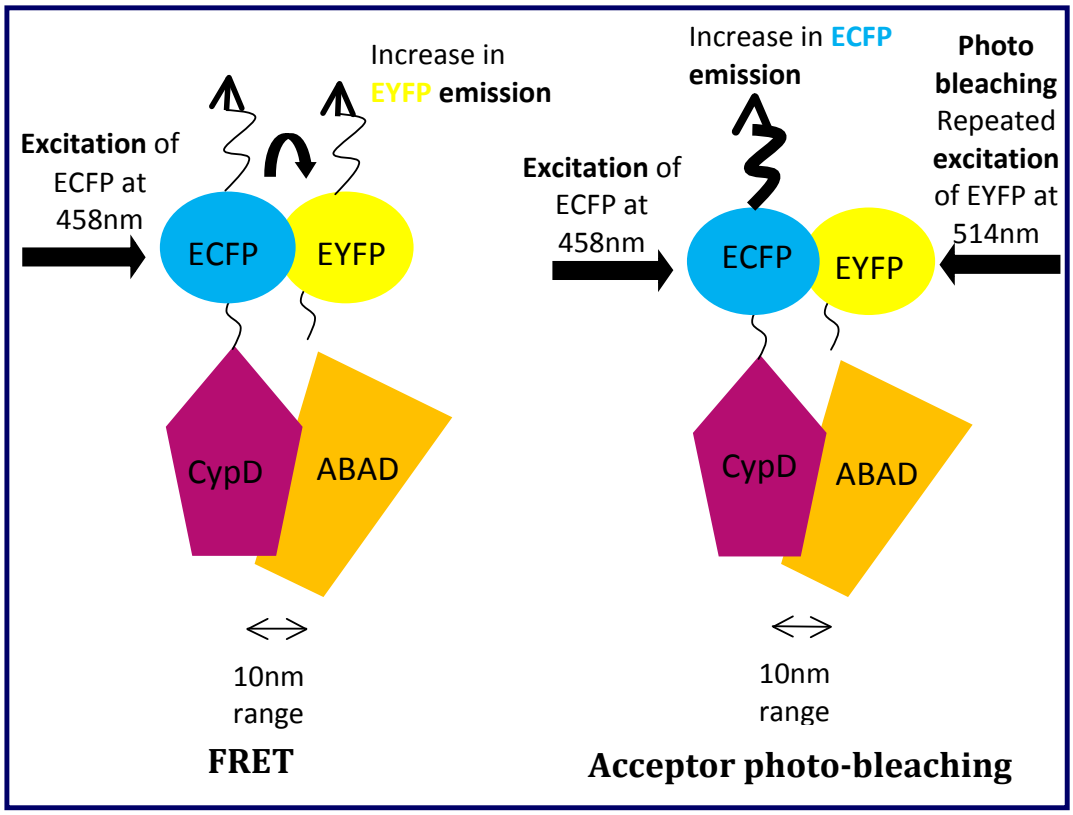

Figure 3-5: Schematic diagram describing the process of FRET and acceptor photo-bleaching FRET with the two fluorescently tagged proteins, ABAD and CypD. FRET: The donor fluorophore (ECFP) is excited and an increase in acceptor flourophore (EYFP) emission is recorded. Acceptor photo-bleaching: Initially, the acceptor flourophore is repeatedly excited to cause photo-bleaching of the acceptor flourophore. Next the donor fluorophore is excited, which causes an increase in donor fluorophore emission as the fluorescences cannot be donated to the bleached acceptor flourophore.

Previous FRET analysis of the pECFP-DEVD-EYFP construct expressed in COS-7 cells has shown that in the presence of caspase 3, FRET is disturbed as the fluorophores are cleaved apart, therefore the distance between the fluorophores is such that FRET will occur under normal cellular activity (Brophy et al., 2002).

Initially, HEK 293 and SK-N-SH cells were seeded onto coverslips in 35mm dishes and once confluent, transfected with varying plasmid DNA (see section 2.2). After 48 hours cells were immobilised on the coverslips and fixed with 4% PFA onto glass slides (see section 2.3.1). The glass slides were imaged using a Leica TCS multiphoton confocal laser scanning microscope with argon lasers set at 458nm and 514nm which excite ECFP and EYFP respectively. For the excitation of ECFP the 458nm laser intensity was set at 55% and emission was collected between 468-498nm. EYFP was excited at 514nm and emission collected between 550-582nm, laser intensity of the 514nm laser was set at 21% of total power.

To verify the presence of FRET using acceptor photo-bleaching the positive control was examined first. After several attempts no FRET was observed. Suggestions for why this occurred may be derived from the immobilisation of the cells, as the fluorophores may not be able to interact if they were not in the correct orientation. Furthermore, the reliability of other FRET interactions that could occur is reduced due to immobilising the cells. Previously studies using this construct have been carried out in live cell experiments and after personal communication with Professor Tavaré it was recommended that FRET investigations using this construct would be best conducted with live cells.

Following this advice further FRET investigations were carried out by measuring the emission spectra of the fluorophores using a spectrophotometer and calculating the ratio A value. Ratio A is the difference between the emission produced from the acceptor when the donor is excited over the emission produced when the acceptor is excited (Clegg, 1992). This ratio can signify if FRET is occurring by comparing the emission spectra given off from the acceptor fluorophore.

3.3.4 INVESTIGATION OF THE ABAD-CypD INTERACTION BY SPECTROSCOPIC FRET ANALYSIS

FRET interactions between MTS-ABAD-EYFP and MTS-CypD-ECFP can be deduced by measuring their fluorescent spectra under differing conditions. Examining live cells for a FRET interaction is a much more robust method as cells reside in a physiologically similar environment allowing clearer detection of potential protein-protein interactions.

HEK 293 and SK-N-SH cells were grown in 35mm dishes and transfected with plasmids expressing a combination of the following proteins: pMTS-CypD-ECFP, pMTS-ABAD-EYFP, pEYFP-DEVD-ECFP, pEYFP (see sections 2.2.1, 2.2.3, 2.2.4, 2.4.3). After 48 hours the cells were collected, resuspended in 1xPBS and held on ice. The first measurement taken was from the cells transfected with pMTS-CypD-ECFP, the pure donor fluorophore. The cell suspension was added to a quartz cuvette and excited with the laser line at 436nm, the fluorescent emission spectrum recorded from the pure donor (A) was used to calculate the experimental emission from the acceptor fluorophore. Secondly the emission spectrum from the experimental condition was measured, here pMTS-CypD-ECFP and pMTS-ABAD-EYFP were transfected together and excited at 436nm, the donor emission from the experimental condition (B) was also used to calculate the emission from the acceptor when excited at 436nm.

Once the emission spectra for the pure donor and the experimental donor were recorded, the intensity of the emissions spectra were normalised at 488nm (donor emission peak). The resulting normalised emission data was used to determine the experimental acceptor emission spectra by subtracting the spectra (B-A) to leave the residing emission from the acceptor fluorophore when excited by the donor emission (D). Finally the cell suspension from the experimental condition was excited at the acceptor excitation wavelength of 517nm. The subsequent emission spectra between 526-700nm (E) was used to calculate ratio A (Figure 3.6).

$$\textit{Ratio A} = \text{Area under } \mathbf{(D)} / \text{ Area under } \mathbf{(E)}$$

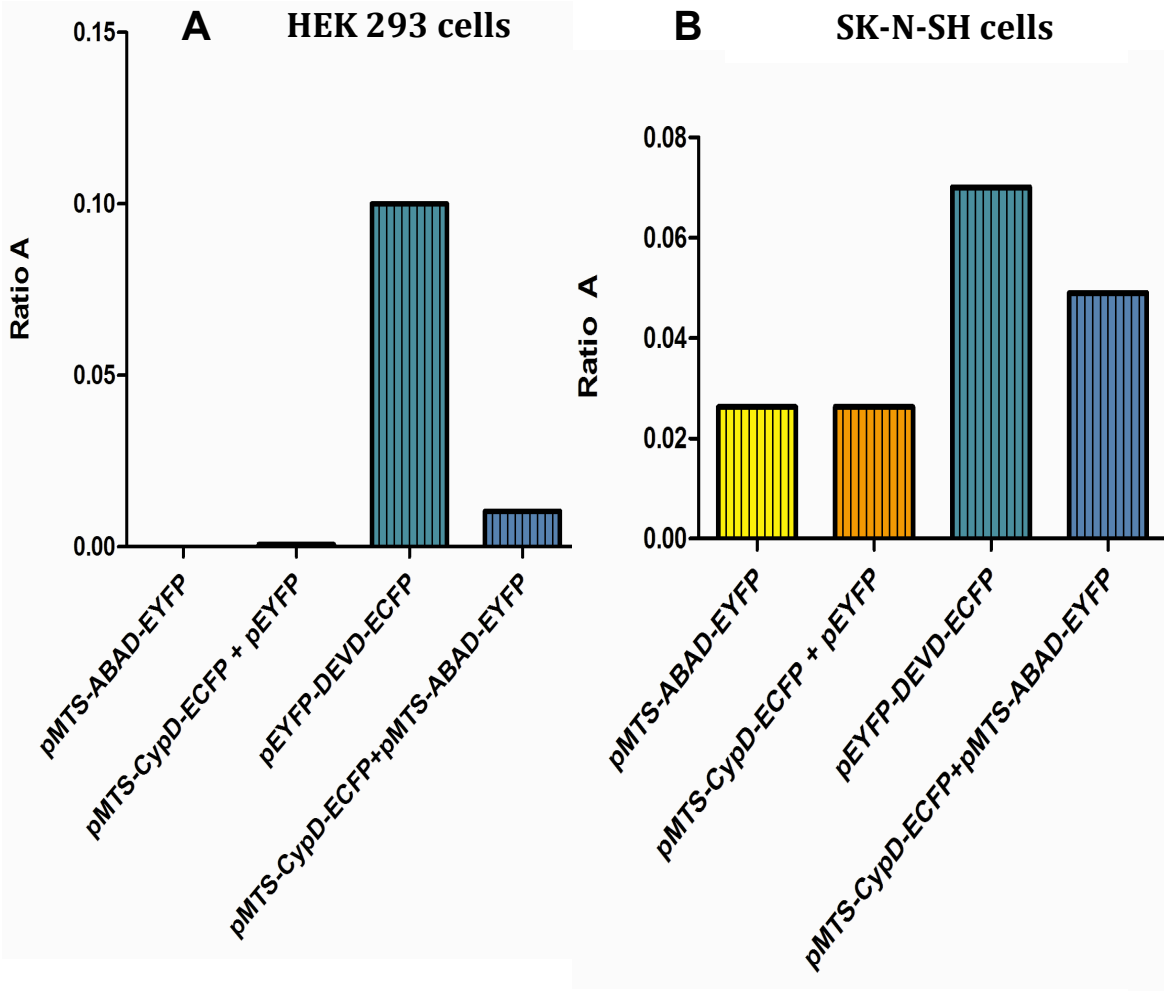

Figure 3-6: Ratio A values for each condition; cells transfected with experimental pMTS-CypD-ECFP + pMTS-ABAD-EYFP, negative control pMTS-CypD-ECFP + pEYFP, positive control pEYFP-DEVD-ECFP and to obtain the baseline the acceptor alone, pMTS-ABAD-EYFP was used. A) HEK 293 cells (N=1/condition) B) SK-N-SH cells (N=1/condition).

The spectroscopic FRET analysis of the ABAD-CypD interaction in HEK 293 cells revealed a weak FRET interaction. The ratio A value is proportional to the FRET efficiency and from the results, shown in figure 3.6, it can be determined that in HEK 293 cells, ratio A for a potential ABAD-CypD interaction is 10% of the ratio A observed in the positive control. This is a good indicator that FRET and consequently and interaction between ABAD and CypD is occurring.

Furthermore, in comparison to HEK 293 cells, SK-N-SH cells expressing ABAD and CypD, the ratio A value is higher proportional to the ratio A determined for the positive control, at 25%. The results from the SK-N-SH cells further indicate a weak FRET interaction.

3.4 RESULTS: IMMUNOPRECIPITATION

The positive but weak FRET interaction between ABAD and CypD observed in live cell experiments was investigated further by immunoprecipitation. The pull-down assay was carried out to explore if the interaction was strong enough to allow precipitation from solution of ABAD bound to CypD. In these experiments GFP trap beads were used to bind to the EYFP tag of MTS-ABAD-EYFP, and it was predicted that MTS-ABAD-EYFP would bind to MTS-CypD-ECFP co-transfected in HEK 293 cells. In order to ascertain if the large ECFP protein tag attached to CypD affected the hypothesised ABAD-CypD interaction, a plasmid expressing CypD without ECFP but with a myc tag was created. This CypD-myc fusion protein was predicted to be pulled from solution with ABAD using the EYFP tag.

3.4.1 CONSTRUCTION OF pCypD-MYC

A one step cloning strategy was used to create pCypD-myc, the DNA sequence for CypD was cloned into a pcDNA$_4$ plasmid expressing myc (Figure 3.7). The target plasmid (pcDNA4/TO/myc-His 5 A) was digested with *EcoRI* and *XhoI* to allow for insertion of CypD. A pGEX4T-1 vector expressing CypD was used as the template DNA for PCR (see section 2.1.1.) and the following primers were used: forward primer **5'** CGGAATTCATGCTGGCGCTGCGCTGC **3'** encoding for *EcoRI* (underlined) and reverse primer **5'** CAACTCGAGGCTCAACTGGCCACAG **3'** which encodes the restriction site *XhoI* (underlined). PCR products were digested with restriction enzymes *EcoRI* and *XhoI* and products run on an agarose gel to verify successful PCR (see section 2.1.2). The 624bp fragment (CypD) was purified from the agarose gel and ligated into the pre-prepared plasmid (see sections 2.1.3 and 2.1.5). Once ligated the plasmid was transformed into *E.coli* (DH5α), finally the

from the bacteria and sequenced to confirm DNA sequenced (see section 2.1.7 and 2.1.8).

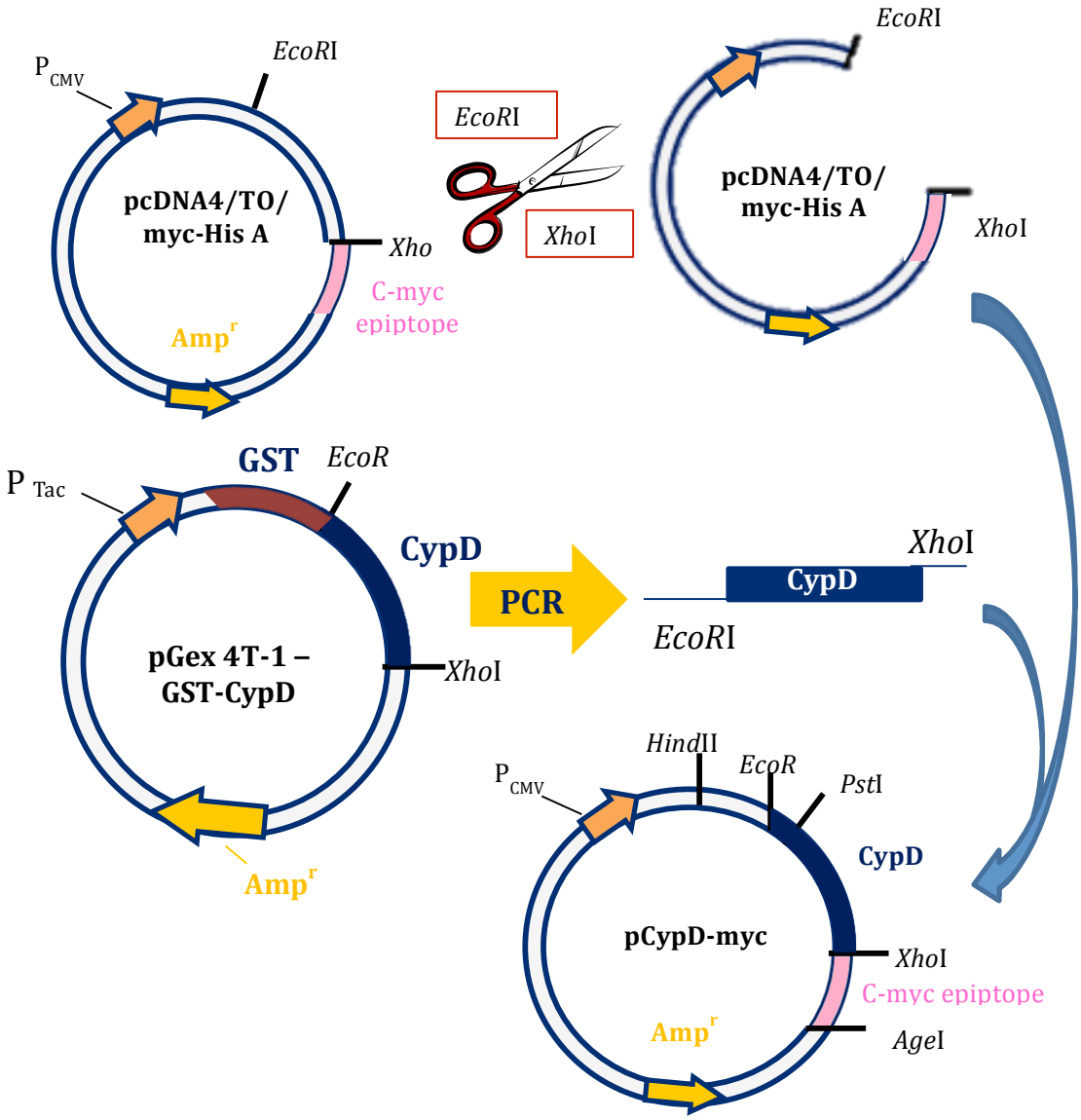

Figure 3-7: one step cloning strategy: pcDNA4/TO/myc-His A vector was digested with *EcoR*I and *Xho*I to allow for insertion of the PCR fragment. PCR was conducted following protocol outlined in section 2.1.1 with annealing temperature at 59.2°C using 200ng of the template DNA, pGex 4T1-CypD. The PCR fragment-containing CypD was ligated into the digested pcDNA4/TO/myc-His A DNA plasmid.

3.4.2 IMMUNOPRECIPITATION OF MTS-ABAD-EYFP USING GFP BINDING PROTEINS

HEK 293 cells were seeded in 35mm dishes, after 24 hours, they were transfected (section 2.2.4) with a combination of DNA plasmid expressing the following different proteins: pMTS-ABAD-EYFP, pMTS-ABAD (a kind gift from Dr Kirsty E A Muirhead), pMTS-CypD-ECFP, pCypD-ECFP, pEYFP (Clontech), pECFP (Clontech), pCyp-myc, pcDNA3.; of which one plasmid would contain the required EYFP, to enable binding to the GFP binding protein. Whole cell lysates were collected 48 hours after transfection, following the manufacturer's protocol (see section 2.3.3) cell lysates were incubated with pre-washed GFP binding proteins and the resultant protein samples were analysed by SDS-PAGE gel and western blot (see section 2.5.1).

Initially, using the GFP Trap A, MTS-ABAD-EYFP was seen to bind to the GFP binding protein, this is shown in figure 3.8 in the bound fractions containing MTS-ABAD-EYFP (Figure 3.8). Western blot analysis with CypD antibody indicates that MTS-CypD-ECFP has either been pulled down with MTS-ABAD-EYFP or that the ECFP has bound to the GFP binding protein. Interestingly MTS-CypD-ECFP also appeared in the bound fraction when only pEYFP was present. Additionally, CypD-myc was not seen to be precipitated with MTS-ABAD-EYFP. These results suggest that the ECFP present binds to the GFP-binding protein despite the manufacturer's claims that CFP cannot bind due to amino acid differences (Chromotek).

To explore whether ECFP could bind to the GFP Trap A beads and potentially be used to immunoprecipitate MTS-ABAD, pMTS-CypD-ECFP was transfected with pMTS-ABAD. Investigating immunoprecipitation with differently tagged constructs of ABAD and CypD reduces interference from the large fluorescence proteins, myc or MTS with the hypothesised ABAD-CypD interaction. HEK 293 cells were transfected with a combination of the aforementioned DNA plasmids and their cell lysates harvested immunoprecipitated with GFP Trap A and analysed by SDS-PAGE gel and western blot (see sections 2.2.4, 2.3.3 and 2.5.1). From the western blot

analysis in Figure 3.9b using CypD antibody it can be determined that the CypD constructs with ECFP (CypD-ECFP and MTS-CypD-ECFP present at ~40kDa and ~45kDa respectively) can be precipitated using GFP trap A binding protein. Whereas endogenous CypD present in the input and unbound fractions were not precipitated, signifying that ECFP is the binding factor.

Western blot analysis with an ABAD antibody indicated that MTS-ABAD was not bound to CypD-ECFP, MTS-CypD-ECFP or ECFP. Additionally no change in size of the immunoreactive band expressed in figure 3.9a, when MTS-CypD-ECFP or CypD-ECFP was present with pMTS-ABAD suggests that ABAD has not bound to CypD.

In order to ensure that any protein present in the bound fractions of the pull-down assay, a control immunoprecipitation was conducted using only Sepharose A beads without the presence of GFP Trap A. Western blot analysis of the immunoprecipitation fractions are shown in figure 3.10 where only immunoreactive bands were seen when the CypD antibody was used (data from ABAD antibody not shown as nothing reacted on the blot). There were four incidences where reactive bands were seen in the bound fractions (Figure 3.10a & b). In figure 3.10a, the bound fraction from HEK 293 cell lysates expressing pCypD-ECFP showed a faint binding at 40kDa. As this protein was not expressed in the bound fractions of HEK 293 cell lysates expressing pECFP alone or pMTS-CypD-ECFP and the appearance of β-actin in the bound fraction this non-specific band could be explained by contamination of the sample. Additionally, the three non-specific bands expressed in the bound fractions from HEK 293 cell lysates expressing pMTS-ABAD-EYFP, pMTS-CypD-myc and pCypD-myc could be explained as a non-specific band as it appears in the unbound and input samples too. Overall, as there was no overlay with the non-specific protein binding and the proteins expressed during the GFP Trap A immunprecipitation, it could be suggested that protein present in the bound fractions (figure 3.8-3.9) have indeed been pulled down by GFP Trap A and not by binding to the sepharose A beads.

ABAD antibody (AbCam) (1:5000)
Secondary αRb-HRP (AbCam) (1:60000)

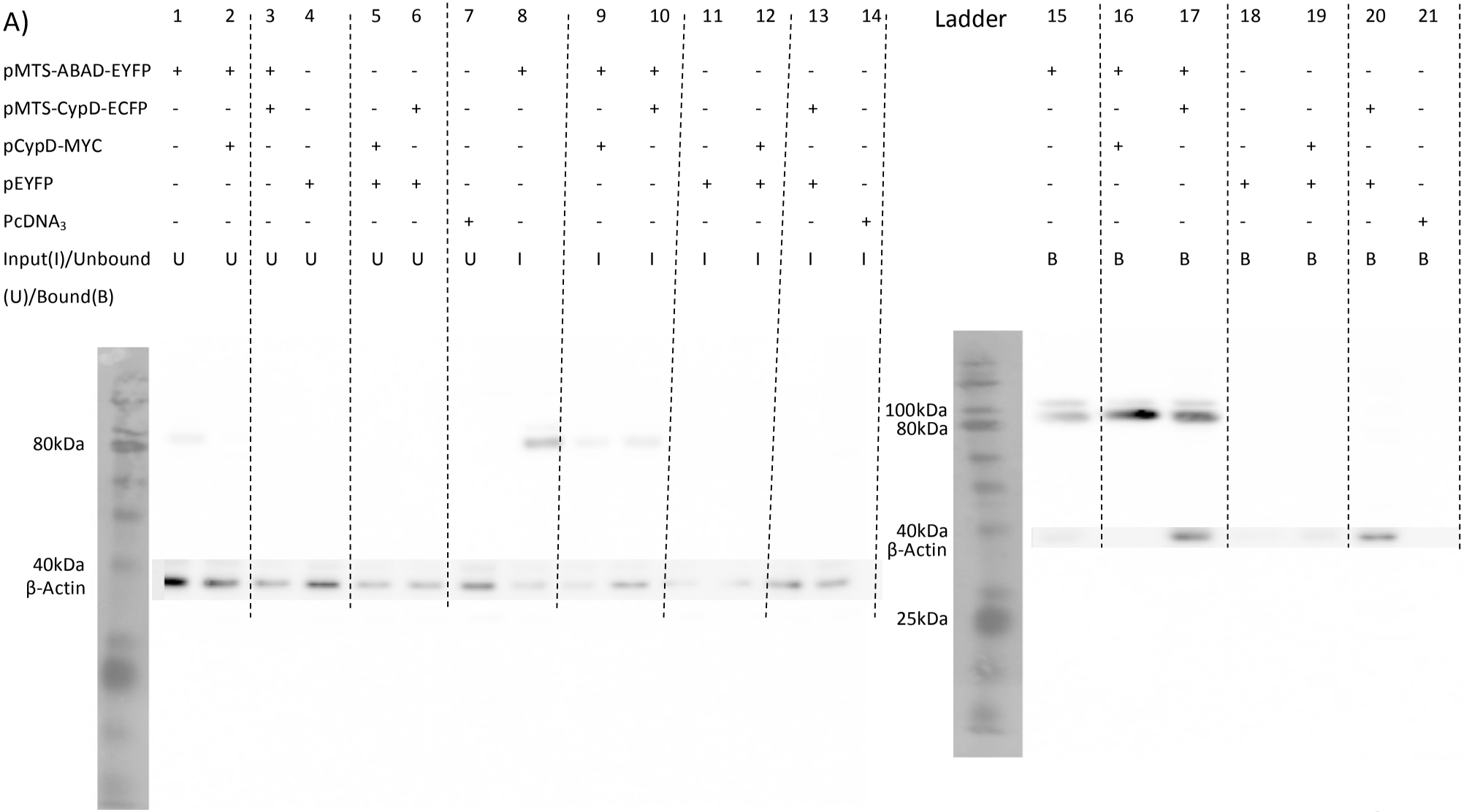

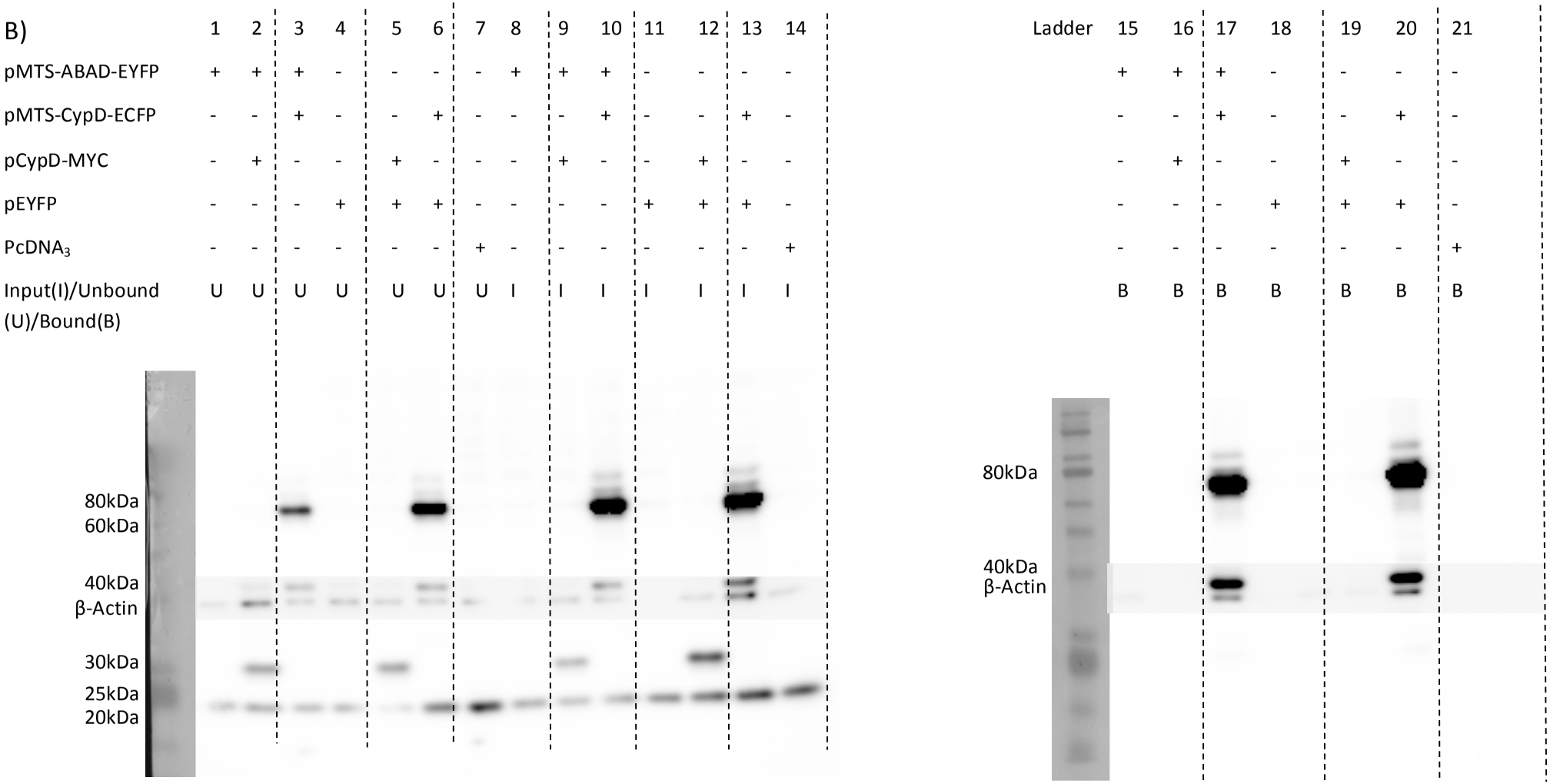

CypD antibody (AbCam) (1:20000)

Secondary αM-HRP (AbCam) (1:20000)

Figure 3-8: Immunoprecipitation with GFP Trap A, Western blot with ABAD and CypD antibody. Each lane contains either 1) the input (I), whole cell lysate from HEK293 cells transfected with a combination of different DNA plasmids (lanes 8-14) 2) the unbound (U) fraction of the immunoprecipitation (lanes 1-7) 3) the bound (B) fraction, which is the final immunoprecipitate sample (lanes 15-21).

A) IP with GFP Trap, Western blot with anti-ABAD. *Lane 1, 8 & 15*: pMTS-ABAD-EYFP plasmid alone. *Lane 2, 9 & 16*: pMTS-ABAD-EYFP and pCypD-MYC. *Lane 3, 10 & 17*: pMTS-ABAD-EYFP and pMTS-CypD-ECFP. *Lane 4, 11 & 18*: pEYFP plasmid alone. *Lane 5, 12 & 19*: pEYFP and pCypD-MYC. *Lane 6, 13 & 20*: pEYFP and pMTS-CypD-.ECFP. *Lane 7, 14 & 21*: Control empty $PcDNA_3$ vector. Lanes 15-21 show the proteins that have bound to the GFP Trap A beads, on this blot MTS-ABAD-EYFP appears to have bound (lanes 15-17).

B) IP with GFP Trap, Western blot with anti-CypD. *Lane 1, 8 & 15*: pMTS-ABAD-EYFP plasmid alone. *Lane 2,9 & 16*: pMTS-ABAD-EYFP and pCypD-MYC. *Lane 3, 10 & 17*: pMTS-ABAD-EYFP and pMTS-CypD-ECFP. *Lane 4, 11 & 18*: pEYFP plasmid alone. *Lane 5, 12 & 19*: pEYFP and pCypD-MYC. *Lane 6, 13 & 20*: pEYFP and pMTS-CypD-.ECFP. *Lane7, 14 & 21*: Control empty $PcDNA_3$ vector. Lanes 15-21 show the proteins that have bound to the GFP Trap A beads. On this blot MTS-CypD-ECFP (~40kDa) appears to be bound to the GFP Trap A beads and a further protein fraction has bound at ~80kDa indicating that MTS-CypD-ECFP bound to MTS-ABAD-EYFP by the increase in molecular weight (lane 17 & 20).

A)

	1	2	3	4	5	6	7	8	9	10	11	12	13	14	15	16	17	18	19	20	21	22	23	24
pMTS-ABAD	-	-	-	-	-	-	-	-	-	-	-	-	+	+	+	+	+	+	+	+	+	+	+	+
pECFP	+	+	+	-	-	-	-	-	-	-	-	-	-	-	-	+	+	+	-	-	-	-	-	-
pCypD-ECFP	-	-	-	+	+	+	-	-	-	-	-	-	-	-	-	-	-	-	+	+	+	-	-	-
pMTS-CypD-ECFP	-	-	-	-	-	-	+	+	+	-	-	-	-	-	-	-	-	-	-	-	-	+	+	+
$PcDNA_3$	-	-	-	-	-	-	-	-	-	+	+	+	-	-	-	-	-	-	-	-	-	-	-	-
Input(I)/Unbound (U)/Bound(B)	I	U	B	I	U	B	I	U	B	I	U	B	I	U	B	I	U	B	I	U	B	I	U	B

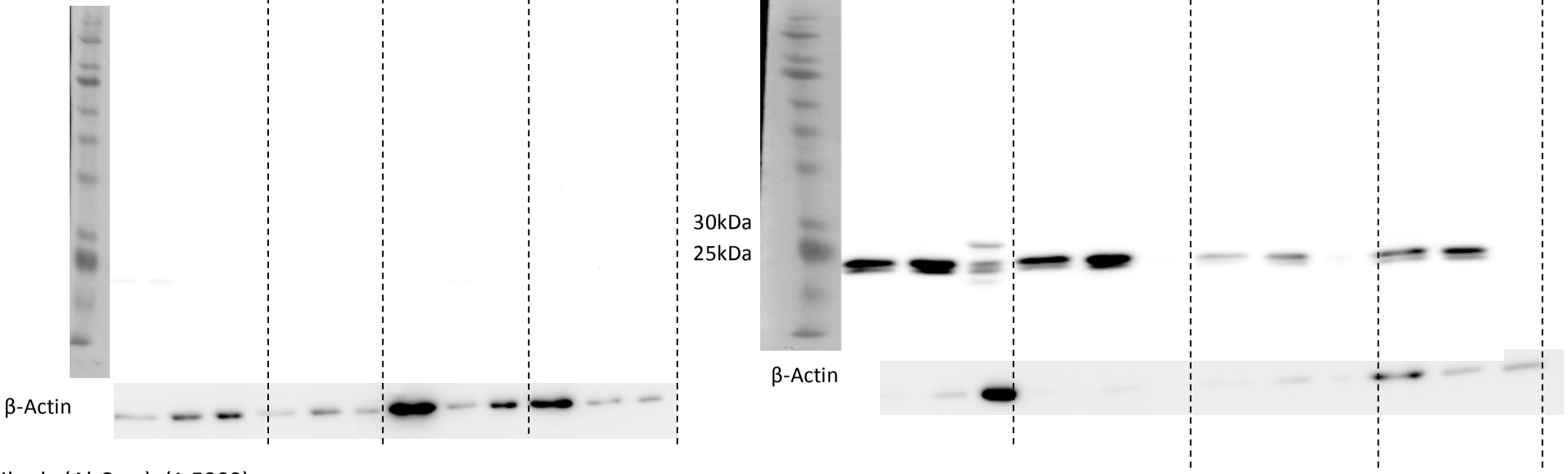

ABAD antibody (AbCam) (1:5000)
Secondary αRb-HRP (AbCam) (1:60000)

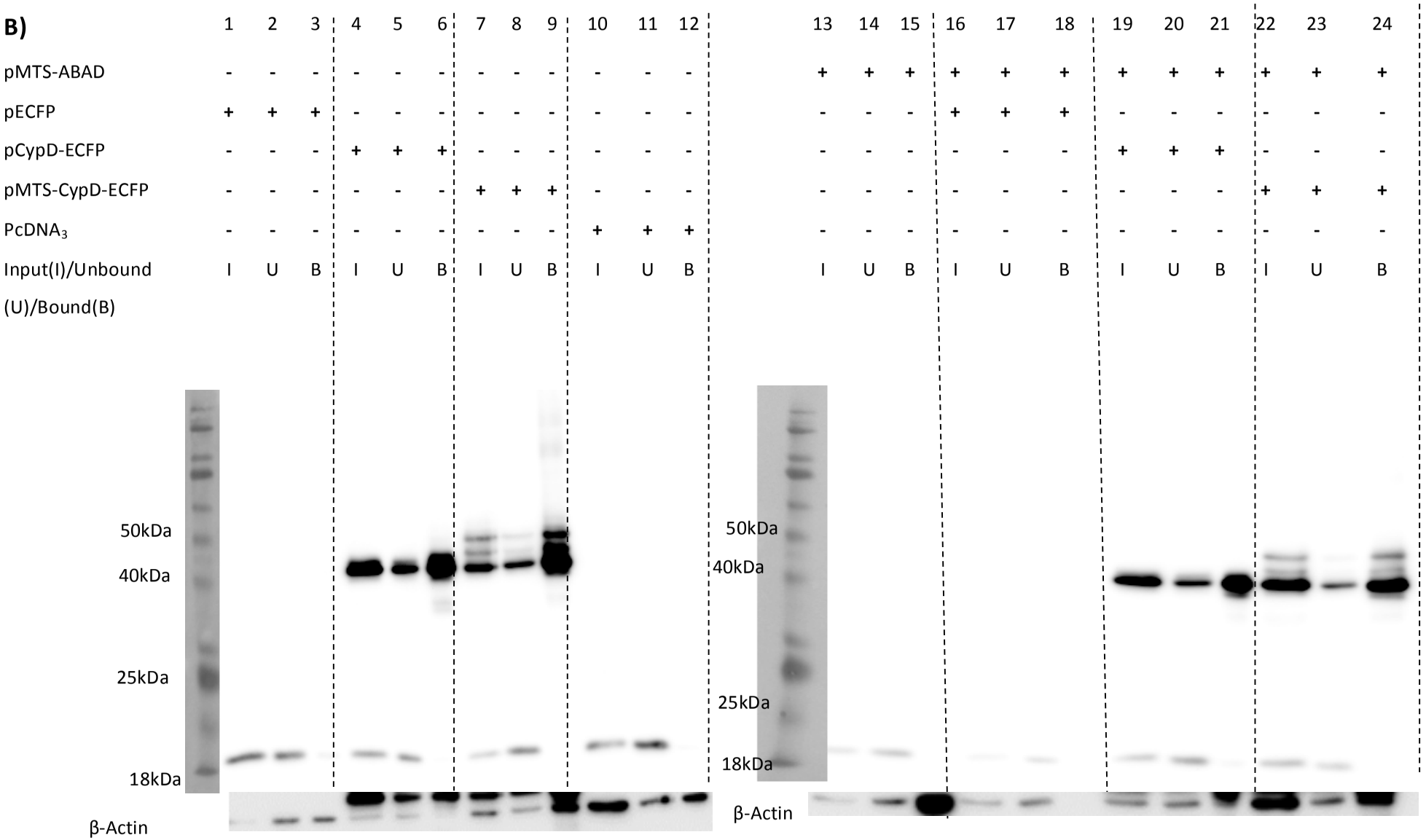

CypD antibody (AbCam) (1:20000)

Secondary αM-HRP (AbCam) (1:20000)

Figure 3-9: Immunoprecipitation with GFP Trap A, Western blot with ABAD and CypD antibody. Each lane contains either 1) the input (I), whole cell lysate from HEK293 cells transfected with a combination of different DNA plasmids 2) the unbound (U) fraction of the immunoprecipitation 3) the bound (B) fraction, which is the final immunoprecipitate sample.

A) IP with GFP Trap, Western blot with anti-ABAD. *Lane 1-3*: pECFP plasmid alone. *Lane 4-6*: pCypD- ECFP alone. *Lane 7-9*: pMTS-CypD-ECFP. *Lane 10-12*: Control empty $PcDNA_3$ vector. *Lane 13-15*: pMTS-ABAD alone. *Lane 16-18*: pMTS-ABAD and pECFP. *Lane 19-21*: pMTS-ABAD and pCypD-ECFP. *Lane 22-24*: pMTS-ABAD and pMTS-CypD-ECFP.

B) IP with GFP Trap, Western blot with anti-CypD. *Lane 1-3*: pECFP plasmid alone. *Lane 4-6*: pCypD- ECFP alone. *Lane 7-9*: pMTS-CypD-ECFP. *Lane 10-12*: Control empty $PcDNA_3$ vector. *Lane 13-15*: pMTS-ABAD alone. *Lane 16-18*: pMTS-ABAD and pECFP. *Lane 19-21*: pMTS-ABAD and pCypD-ECFP. *Lane 22-24*: pMTS-ABAD and pMTS-CypD-ECFP.

CypD antibody (AbCam) (1:20000)
Secondary αM-HRP (AbCam) (1:20000)

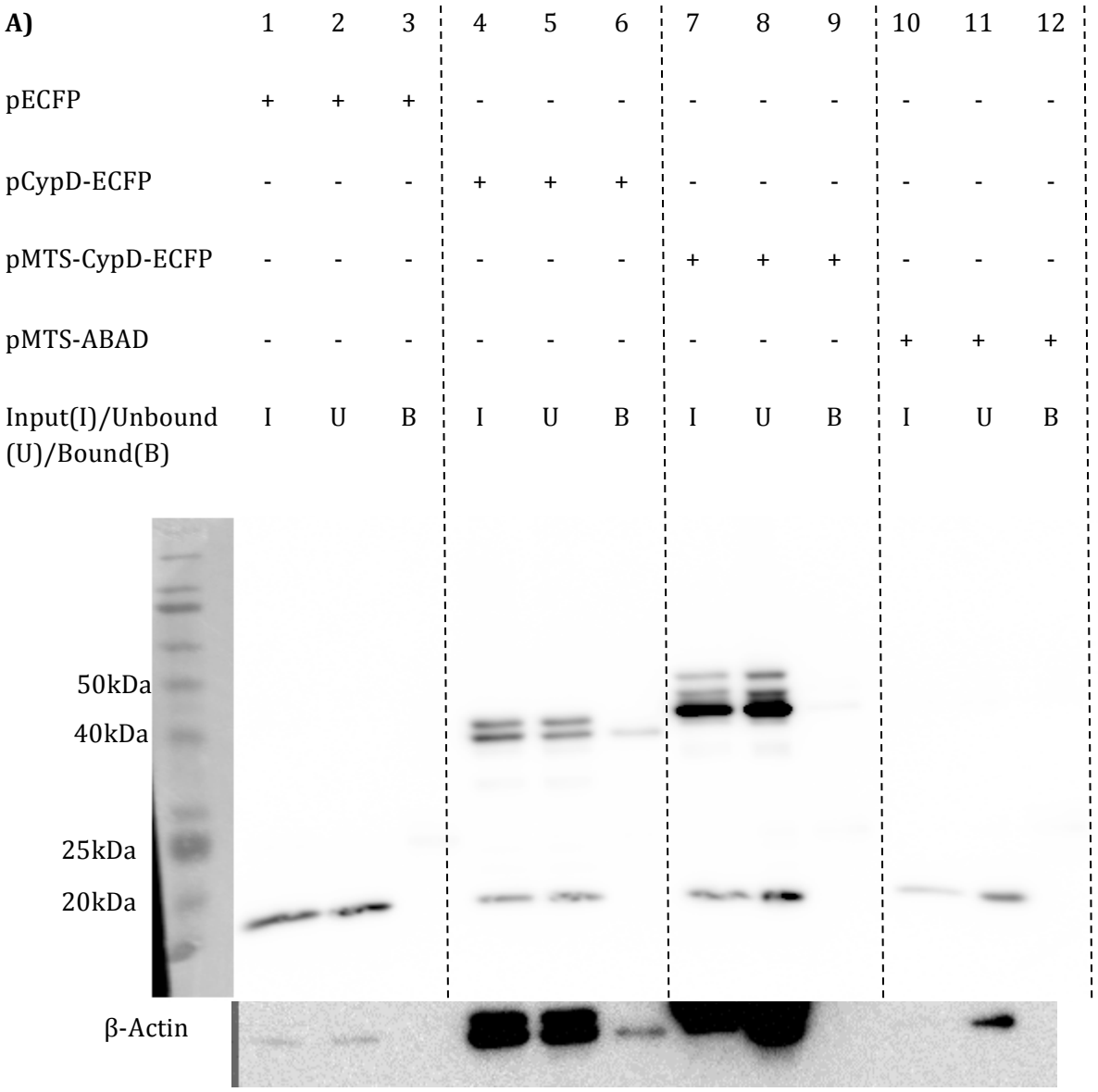

CypD antibody (AbCam) (1:20000)
Secondary αM-HRP (AbCam) (1:20000)

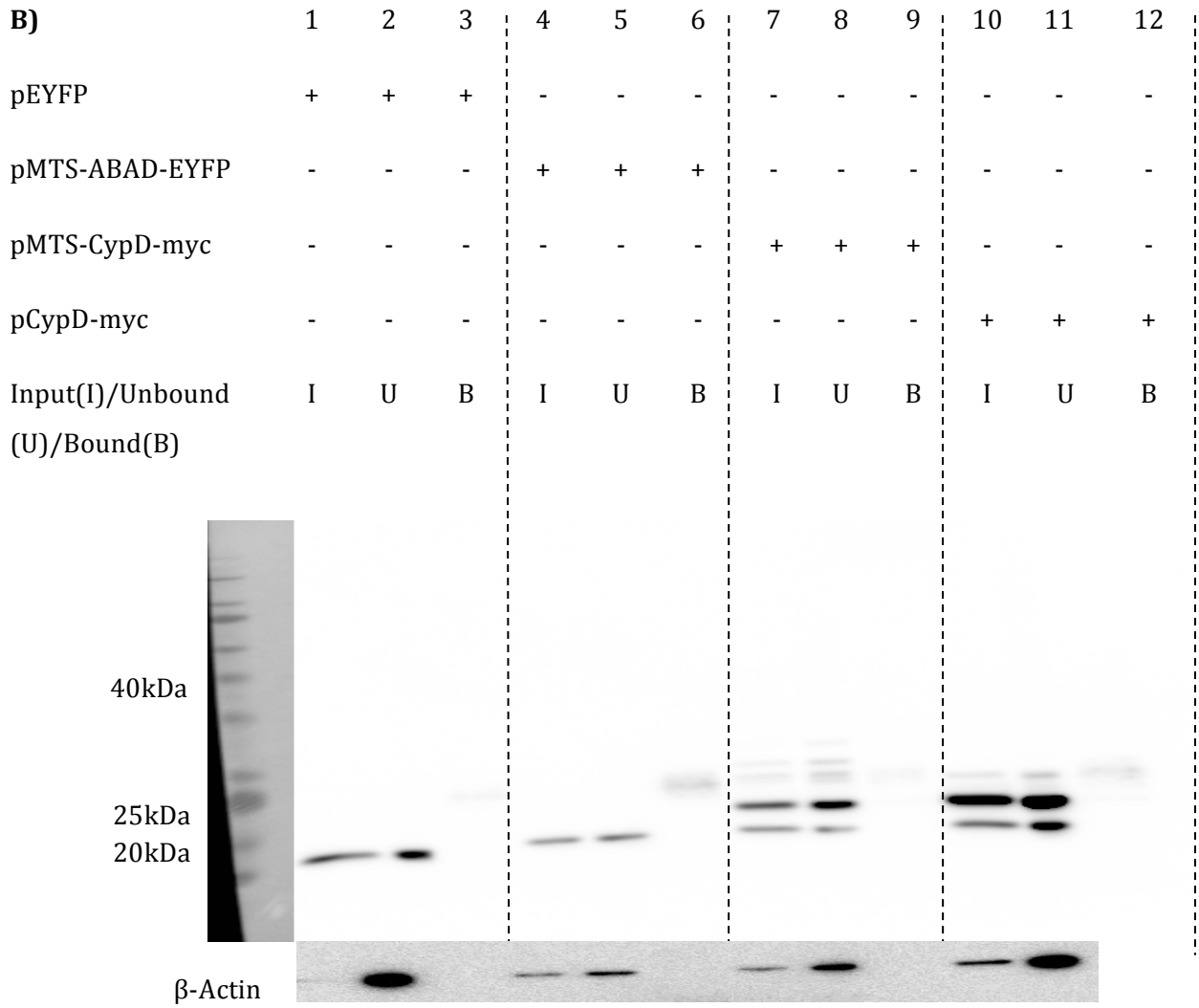

Figure 3-10: Immunoprecipitation with Sepharose A beads alone, to determine non-specfic binding, Western blot with CypD antibody. Each lane contains either 1) the input (I), whole cell lysate from HEK293 cells transfected with a combination of different DNA plasmids 2) the unbound (U) fraction of the immunoprecipitation 3) the bound (B) fraction, which is the final immunoprecipitated sample.

A) IP with Sepharose A, Western blot with anti-CypD. *Lane 1-3*: pECFP plasmid alone. *Lane 4-6*: pCypD- ECFP alone. *Lane 7-9*: pMTS-CypD-ECFP. *Lane 10-12*: pMTS-ABAD alone. There appears to be slight non-specific binding in lane 6 at 40kDa.

B) IP with Sepharose A, Western blot with anti-CypD. *Lane 1-3*: pEYFP plasmid alone. *Lane 4-6*: pMTS-ABAD-EYFP alone. *Lane 7-9*: pMTS-CypD-myc. *Lane 10-12*: pCypD-myc alone. There appears to be further non-specific binding in the bound fraction of lane 6, 9 and 12 at 30kDa.

3.5 DISCUSSION OF THE ABAD-CypD INTERACTION

Neuronal death and mitochondrial dysfunction in AD originates from the necrosis and apoptotic pathways leading from mitochondria. In AD, the presence of Aβ in the mitochondria has been observed to bind to a key enzyme, ABAD, which is involved in fatty acid metabolism (Powell et al., 2000, Lustbader et al., 2004). Furthermore, the occurrence of Aβ in the mitochondria has been reported to induce the production of oxidative stress which in turn is noted to initiate the translocation of CypD to the IMM. Further investigations of the action of CypD at the IMM have noted the formation of the mPTP and the subsequent leaky mitochondria and the initiation of energy independent process, necrosis (Connern and Halestrap, 1992, Halestrap and Brenner, 2003, Nakagawa et al., 2005). It would not be prudent to suggest that as a consequence of Aβ's presence within the mitochondria, CypD would be prompted to translocate to the IMM due to the oxidative stress caused by Aβ. Additionally, unpublished observations have implied that ABAD binds to CypD, and so from this it can be suggested that the presence of Aβ and its binding to ABAD could displace the endogenous binding of CypD to ABAD in the matrix of the mitochondria (Yan and Stern, 2005). However, the evidence obtained from the presented series of experiments suggests that there is a weak, transient interaction between ABAD and CypD signifying that the initial hypothesis that, ABAD sequesters, with a strong interaction, CypD in the mitochondrial matrix preventing translocation to the IMM, is not as clear cut as originally believed.

The initial results obtained from acceptor photo-bleaching the fixed cells (see section 3.3.3), showed no signs of FRET in comparison to previous studies where strong FRET signals were detected using this method (Ren, 2008). Further investigation used intensity-based FRET analysis to determine that a brief interaction appeared to occur between MTS-ABAD-EYFP and MTS-CypD-ECFP. The ratio A value gained from both cell types (HEK 293 and SK-N-SH cells) is a good indicator that FRET occurs between these two proteins. The ratio A value was

notably higher in SK-N-SH cells in comparison to HEK 293 cells which may suggest that the interaction between ABAD and CypD is not a global effect and that it may be required more in neuronal type cells.

ABAD did not appear to pull down CypD or vice versa in the immunoprecipitation experiments, insinuating that the interaction between these proteins is not strong and that the extraction of proteins from whole cells is a non-physiological action resulting in interference with the interaction (Voss et al., 2005). This theory could also be applied to the reason why FRET was not seen when the cells were fixed on coverslips, if the interaction is weak and transient this biological surround could be crucial. Additionally, the ABAD-CypD interaction may occur in the initial stages of cellular stress as a protective response mechanism whereby ABAD sequesters CypD to prevent translocation to the IMM. The accumulation of excessive oxidative stress could still induce the translocation but before this ABAD could slow the initiation of spontaneous necrosis.

The significance of the finding that ABAD interacts weakly with CypD indicates that the original hypothesis that CypD scaffolds to ABAD in the mitochondrial matrix, is not correct (Yan and Stern, 2005). Strong binding between these proteins may still occur but only in response to developing cellular stress. This could be further investigated by attempting to stimulate strong binding by inducing oxidative stress or increasing calcium levels in transfected cell lines and further monitoring FRET intensities.

CypD could however, play a very different role in the dynamic relationship with ABAD. The principal function of ABAD is the β-oxidation of fatty acids, which is crucial in the production of ketones and subsequently the production of reserve energy, which is especially required when glucose levels in the brain start to decrease. The significant FRET intensity recorded when CypD interacts with ABAD therefore could indicate that CypD could be involved in a metabolic process in the mitochondrial matrix. The notion that CypD could be interacting with ABAD to aid a step in the metabolic pathway or another oxidation/reduction reaction is not implausible as the highly similar (83%) Cyclophilin protein, AtCyP20-3 present in

plants, acts to enable the full functioning of serine acetyltransferase (SAT) in plant mitochondria, which is involved in redox reactions (Dominguez-Solis et al., 2008, Haas et al., 2008). Further investigations suggest that CypD does have an effect on the metabolic activity of ABAD (see section 4.3.2).

The translocation of the CypD to the IMM in the presence of oxidative stress has previously been investigated and in particular it has been shown that CypD is redox sensitive (Linard et al., 2009). Of particular interest a specific cysteine residue on CypD (Cys^{203}) was observed to be especially sensitive when exposed to an oxidating agent. This was noted to induce a conformational change in CypD (Linard et al., 2009). To verify this conformational change alterations in fluorescence emission were noted and reported to be caused by the increased exposure of tryptophan residues present in CypD (Linard et al., 2009). This conformational change induced by oxidative stress could be the key factor in causing the translocation of CypD to the IMM, renouncing the interaction with ABAD and further signifying that the presence of Aβ could initiate the translocation of CypD but not via the displacement from ABAD. In this instance it would be interesting to measure the FRET intensity in the presence of Aβ.

It is important to note that the positive FRET interactions do not directly determine an interaction between the tagged proteins but that it is a good indicator that the proteins of interest are within a close enough range (1-10nm) to be interacting. Further analytical techniques need to be used to fully explore the interaction of ABAD to CypD, expressly additional immunoprecipitation studies investigating different cross-linking agents. More biochemical techniques could also be trialled such as SPR and thermal shift analysis could be used to identify this protein-protein interaction.

Chapter 4: THE INVOLVEMENT OF AMYLOID β BINDING ALCOHOL DEHYDROGENASE IN METABOLISM IN ALZHEIMER'S DISEASE

4.1 INTRODUCTION

4.1.1 PROBLEMS WITH METABOLISM IN ALZHEIMER'S DISEASE

It is well established that changes in brain metabolism occur in AD patients; in particular decreased glucose utilisation has been recorded using PET. This reduction in the use of glucose has been suggested by Cunnane et al. (2011) to signify that there is either a) reductions in the levels of glucose present in the brain and furthermore that the glucose present may be less accessible to neurons or b) that the reduction and degeneration of neurons, observed in AD brains, requires less glucose and therefore the measurement of hypometabolism in AD patients is a result of this. It seems that the reduction in glucose utilisation is a consequence of processes occurring much earlier before AD symptoms appear, and so identifying this change as a contributing factor in neuronal death in AD (Mark et al., 1997). In response to reduced glucose levels in the brain and in order to maintain metabolic homeostasis, specialized neurons called glucosensing neurons, spaced throughout the brain, detect changes in metabolites especially glucose (Levin et al., 2006). Once declining glucose levels are detected, neurons must act to generate energy via a different source, and this is where the β-oxidation of free fatty acids is crucial. In oxidising fatty acids, ketone bodies are produced and subsequently feed into the citric acid cycle allowing for energy production to continue. The key enzyme in the third stage of β-oxidation of free fatty acids is ABAD (Yang et al., 2005, Muirhead et al., 2010a). A previous study conducted by Yan et al. (2000) investigated different substrates of ABAD, particularly β-hydroxybutyrate, by removing all external energy sources from cells. Interestingly, this study found that when β-hydroxybutyrate was provided as the sole energy source, and ABAD protein levels were increased in COS cells, the COS cells maintained normal cellular function without the presence of glucose. Even more interesting was the comparative finding that when ABAD was mutated, then the COS cells showed a reduction in MTT assay activity indicating that the mitochondrial activity was compromised and that ABAD was essential in the survival of cells by supplying energy through the substrate β-hydroxybutyrate. Additionally, they explored ABAD protein

expression in wild type mice, under ischemic conditions (transient middle cerebral occlusion: reduced glucose) and found that there was an increased expression of ABAD in those mice that underwent cerebral ischemia. In addition, transgenic mice that over-expressed ABAD were protected from cerebral ischaemia and had lower levels of β-hydroxybutyrate. These findings signify that ABAD protein levels are increased when neurons are under stress and suggest a protective mechanism of ABAD in the absence of Aβ peptide.

Following on from this, I investigated specifically the activity of ABAD when glucose levels were reduced in the presence of a synthetic alcohol substrate. Following on from Yan et al. (2000) where levels of ABAD expression were investigated under cellular stress (ischemia), we hypothesised that the removal of glucose could directly stimulate an increase in ABAD activity in order to compensate for the loss of glucose. I therefore investigated the potential changes in ABAD activity under differing glucose concentrations in different cell lines. Furthermore, from the previous finding that CypD interacts with ABAD, I also explored the potential effect CypD expression could have on ABAD activity.

4.1.2 FLUORESCENT ASSAY

In order to investigate the activity of ABAD, I used a fluorgenic substrate for ABAD developed by our collaborator Drs Dalibor Sames and Mary Froemming (Department of Chemistry, Columbia University, New York)(Froemming and Sames, 2007). The fluorescent probe, cyclohexenyl amino naphthalene alcohol ((-)-CHANA) when oxidised by ABAD produces cyclohexenyl amino naphthalene ketone (CHANK) which emits a yellow fluorescence at 510nm (Figure 4.1)(Muirhead et al., 2010b). This fluorogenic probe allows for the measurement of ABAD activity in cells by mimicking the structure of the steroid 17β-estradiol. Most importantly, when (-)-CHANA is oxidised the product, a cyclic ketone, will only fluoresce in an hydrophobic environment such as chloroform or cell membranes, this is suggested to derive from polar sensitive emission shown by CHANK which in turn fluoresces brighter in non-polar environments (Froemming and Sames, 2007, Muirhead et al., 2010b). This fluorogenic probe is therefore ideal for

indirectly determining the activity of ABAD by measuring the intensity of the fluorescence emitted.

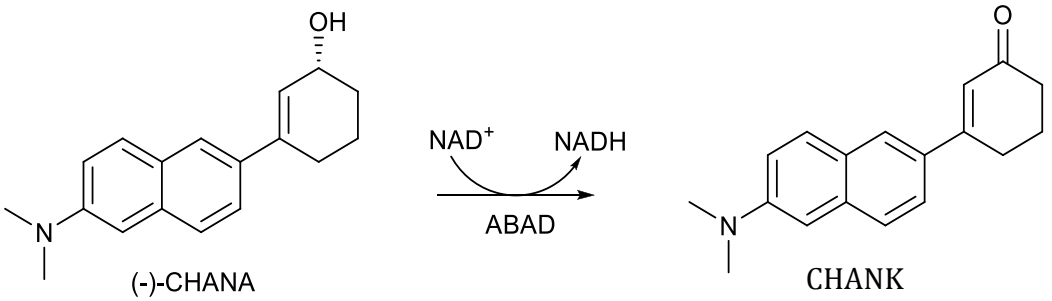

Figure 4-1: Oxidation of (-)-CHANA by ABAD. Schematic diagram of cyclic alcohol, (-)-CHANA oxidised by ABAD with co-factor NAD^+ to CHANK

4.2 AIMS OF CHAPTER

The primary aim of this first part of the chapter was to explore the activity of ABAD when the glucose concentration was decreased. The specifically constructed fluorogenic probe, (-)-CHANA, was used to determine any changes in ABAD activity by measuring the intensity of the emitted fluorescent light from CHANK.

Additionally, lipidomic investigations were carried out to investigate the potential changes in lipid content of cells expressing ABAD to detect if ABAD is potentially using other substrates. *In vitro* conditions of AD were established by expressing ABAD and/or mAPP separately and together in cell lines, with the lipid extracts obtained from these cell lysates analysed by lipid extraction and electronspray ionisation mass spectrophotometry (ESI-MS).

4.3 RESULTS: ACTIVITY OF ABAD WHEN ENERGY SOURCES ARE DEPLETED

4.3.1 THE INTRACELLULAR MEASUREMENT OF ABAD ACTIVITY

4.3.1.1 INITIAL FLUOROMETRIC ASSAY

Previous investigations into the intracellular activity of ABAD were carried out in live HEK 293 and SK-N-SH cells, over-expressing MTS-ABAD (Muirhead et al., 2010b, Muirhead, 2011). These experiments were carried out using a Leica SP multiphoton confocal laser scanning microscope by measuring the fluorescence emitted at 15 minute intervals over a one hour time period, and subsequently analysing the images taken for their fluorescence intensity (Muirhead, 2011). This preliminary assay was further developed into a 96 well format to allow for multiple replications and longer analysis (unpublished Muirhead, 2011).

HEK 293 cells were seeded into a black-walled 96 well plate and after 24 hours the HEK 293 cells were transfected with 0.05μg plasmid DNA encoding for MTS-ABAD or the control empty vector, pcDNA3. 24 hours after transfection, the normal MEM medium was removed and replaced with phenol-red and glutamine free MEM medium containing 10mM HEPES pH7.4, 1% FCS (charcoal-filtered), penicillin/streptomycin and one of the following concentrations of glucose: 4.5g/l, 3g/l, 2g/l or 1g/l. The cells were incubated with medium containing the various concentrations of glucose for a further 24 hours. Following this 20μM (-)- CHANA, (prepared from a 5mM stock in DMSO) was added to each well. The black walled 96 well plate was then transferred to the FLUOstar optima microplate reader which was set to measure fluorescence, exciting at 380nm and collecting the emission spectra at 520nm for 60 minutes, measuring each well at cycle intervals of 300 seconds with the temperature at 37^{o}C (See Figure 4.2).

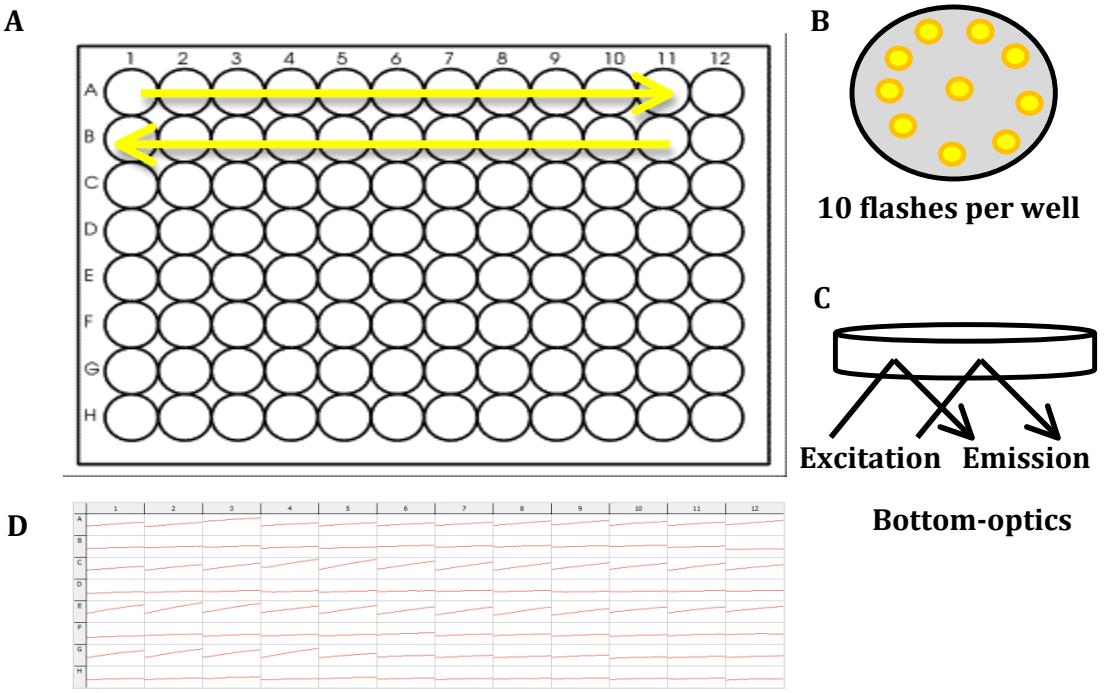

Figure 4-2: Schematic diagram of protocol and set up for fluorescence measurement using FLUOstar Optima plate reader. A) Reading direction of fluorescence from a black walled 96 well plate. B) Excitation of the well occurred in 10 flashes per well at 380nm. C) Fluorescent emission was collected at 520nm from bottom optics. D) an example of the readout gained from the FLUOstar Optima microplate reader.

In the initial experiments, the emitted fluorescence signal (at 520nm) from the HEK 293 cells was measured over a period of 8 hours. Figure 4.3 shows that over this time period there was an initial difference in those cells expressing ABAD as compared to the control cells. In those cells expressing ABAD, the amount of fluorescence emitted slowed with time, thus signifying that the enzyme activity of ABAD had reached maximal activity within the first 60 minutes and/or the (-)-CHANA substrate was becoming limiting. Consequently, further experiments focussed on the first 60 minutes of the reaction to determine the activity of ABAD.

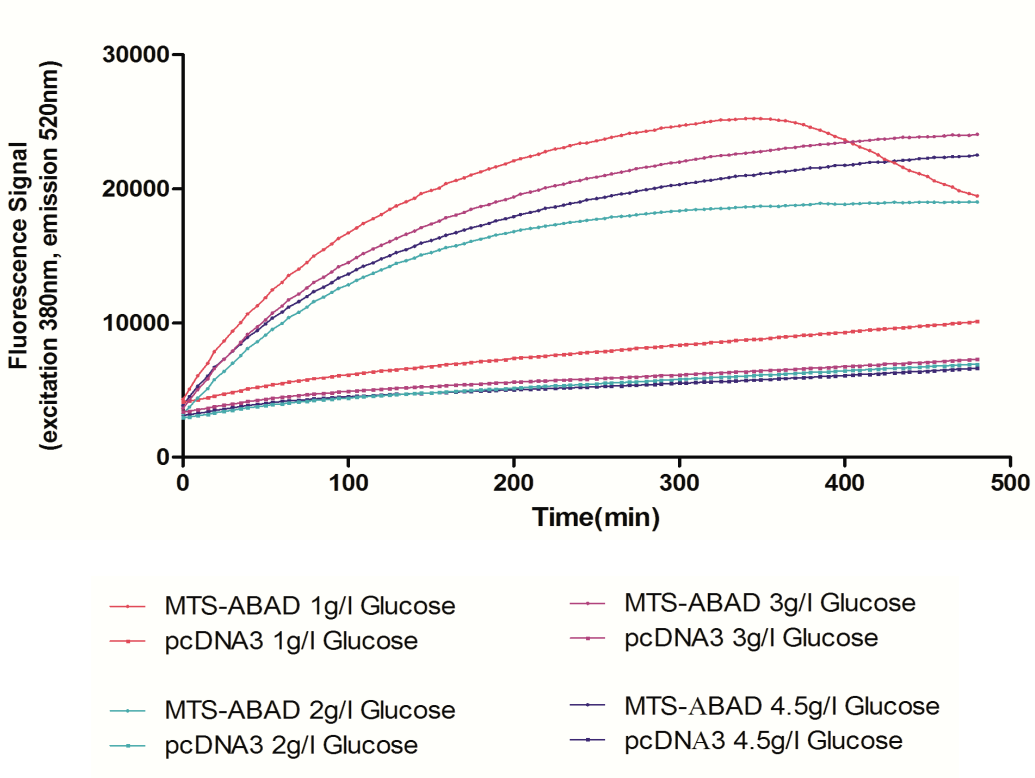

Figure 4-3: Fluorescent signal emitted over 8 hours (measured at 520nm) illustrating the slowing of the rate of ABAD activity by the saturation of fluorescent production. The top four traces were recorded from HEK 293 cells transfected with DNA plasmid expressing MTS-ABAD showing that the largest reduction of glucose in the presence of expressed ABAD produces the largest fluorescent signal. The bottom four traces are from HEK 293 cells transfected with the control vector, pcDNA3. The trace equals the measures of mean fluorescence emitted from 12 wells under equal conditions at each time point. N=97 per trace.

Therefore the same experiment was performed as described above but measured now over a 60 minute time period. The total fluorescence signals over 60 minutes are shown in the appendix and the average mean is shown in Figure 4.4. The data in figure 4.4 displays an initial significant difference between the HEK 293 cells expressing ABAD compared to the empty vector (PcDNA3) (confirmed by a two-way ANOVA). More interestingly are the significant differences when comparing within conditions where ABAD was expressed i.e. under conditions when the glucose concentration was reduced from 4.5g/l to 1g/l and 2g/l there was a significant contrast in the amount of fluorescence emitted.

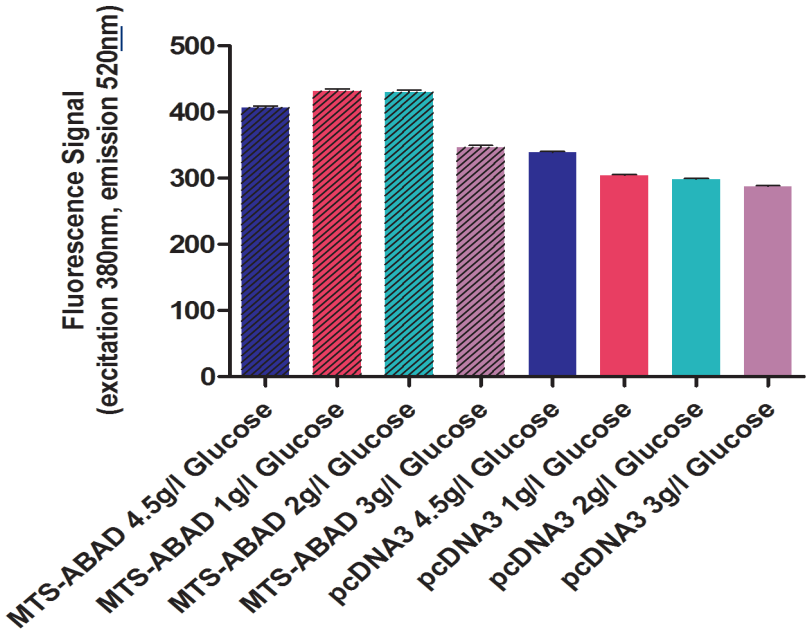

Figure 4-4: The mean of the total fluorescence signal detected at 520nm over 60 minutes. A two-way ANOVA was used to determine differences between the presence of ABAD versus the presence of a control vector, comparing the overall fluorescence emitted from pMTS-ABAD transfected and PcDNA3 transfected HEK 293 cells with respective glucose concentrations. Planned contrasts revealed, in the presence of ABAD, that decreasing glucose from 4.5g/l to 1g/l or 2g/l increased fluorescent emission, t=-2.453, p<0.05 (one tailed) (one-way ANOVA comparing each variable (presence of ABAD or not)). When ABAD was not present (control vector, PcDNA3) planned contrasts showed that decreasing glucose concentration from 4.5g/l decreased fluorescence emission, t=4.009, p<0.01(one tailed) N=13/condition.

To confirm that these changes observed were not due to changes in protein levels, a western blot was conducted of cells treated under these conditions (Figure 4.5). Western blot analysis of the cell extracts collected from the pMTS-ABAD transfected HEK 293 cells revealed no alterations in expression of ABAD when the concentrations of glucose were altered (Figure 4.5). Therefore, the increased fluorescence signal emitted when the glucose concentration was decreased was due to changes in ABAD activity and not protein levels of expression.

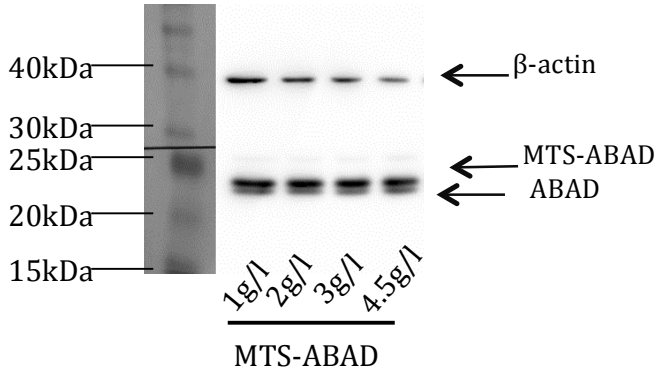

Figure 4-5: Expression of ABAD in HEK 293 cells. HEK 293 cells were transfected with pMTS-ABAD and their cell lysates collected and used for western blot analysis. Immunoreactive bands were detected with anti-ABAD (Abcam) (mouse, 1:1000) and anti-mouse HRP (Abcam) (mouse, 1:20000). Bands were expressed at ~24kDa (MTS-ABAD) and ~22kDa (endogenous ABAD). As a loading control anti-β-actin (mouse, 1:10000) with anti-mouse HRP (mouse 1:20000) were used to detect actin, revealing a band at ~ 40kDa.

Following this, the rate of ABAD activity was also calculated to establish if decreasing glucose concentration altered the rate of ABAD activity in addition to the total increase of fluorescence emitted. As the graphs were linear within the first 60 minutes, the rate of CHANK production was calculated by measuring the slope of the fluorescent signal over this time period (Figure 4.6). Again, the rate of CHANK production was observed to increase when glucose levels were reduced to 1g/l or 2g/l; signifying that the rate of ABAD activity was also significantly increased when glucose levels were reduced. As HEK 293 cells do not contain high levels of endogenous ABAD, this could explain the lack of increase in fluorescence observed in the control HEK 293 cells (PcDNA3 transfected) when glucose concentrations were varied (Figure 4.4, Figure 4.6, Muirhead et al 2010b).

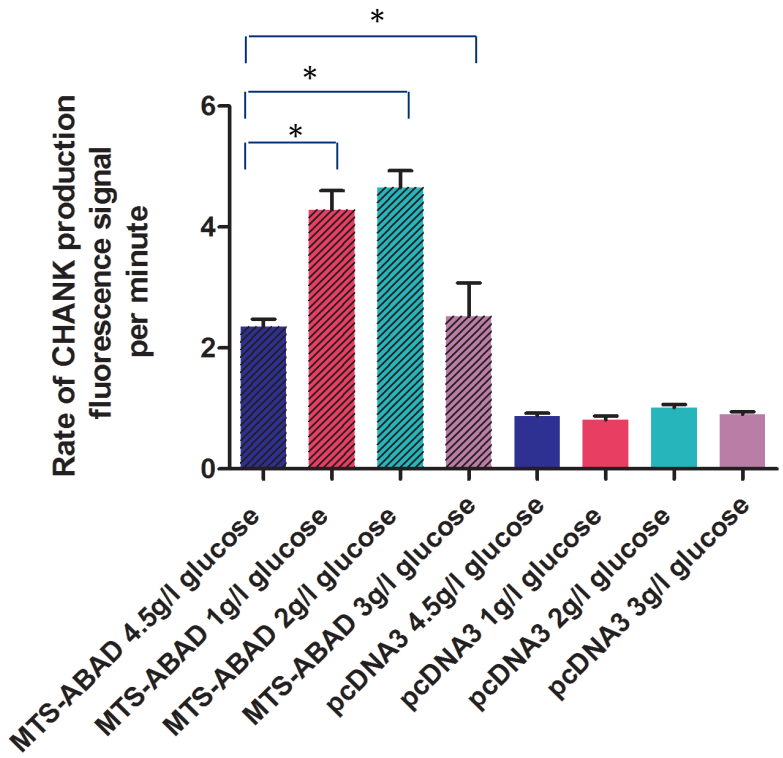

Figure 4-6: The mean rate of CHANK production over 60 minutes. Statistical analysis shows that there is a significant effect when ABAD is present (two-way ANOVA, $p<0.001$). Analysis to determine significance when glucose levels are decreased in each condition (ABAD or PcDNA3) revealed that when ABAD was present there was a significant increase in the rate of CHANK production when glucose was decreased (one-way ANOVA, *post hoc* Bonferroni's multiple comparison's test $F(2,12)=11.4$, $p<0.05$*). There was no significance observed when ABAD was absent (PcDNA3 control vector present)(one-way ANOVA, *post hoc* Bonferroni's multiple comparison's test $F(3,44)=2.85$, p=non significant). N=12/condition.

In order to verify that the results obtained were due to the varied glucose concentrations and not as a result of increase or decrease in cell numbers a MTT assay was carried out under the same conditions (see section 2.3.5 for protocol). HEK 293 cells were cultured in the same manner as if they were to be used in the fluorescence assay, in a 96 well plate. They were subsequently transfected with either 0.05µg of pMTS-ABAD or pcDNA3, 24 hours later the medium was replaced with phenol-red and glutamine free MEM medium containing 10mM HEPES pH7.4, 1% FCS (charcoal-filtered), penicillin/streptomycin and one of the following concentrations of glucose: 4.5g/l, 3g/l, 2g/l or 1g/l. After a further 24 hours MTT

reagent was added to 100 µl of the respective medium to make a final concentration of 1mg/ml.

The HEK 293 cells were incubated for 5-6 hours, the MTT removed and DMSO added to each well. The absorbance of the cells was measured and the results are shown in Figure 4.7. The MTT assay indicated that the varying concentrations of glucose did not significantly affect the mitochondrial ability to reduce MTT to formazan, thus indicating that the differences observed between altering the glucose concentration from 4.5g/l to 1g/l is a result of decreasing this energy substrate and not due to increases or decreases in general mitochondrial activity.

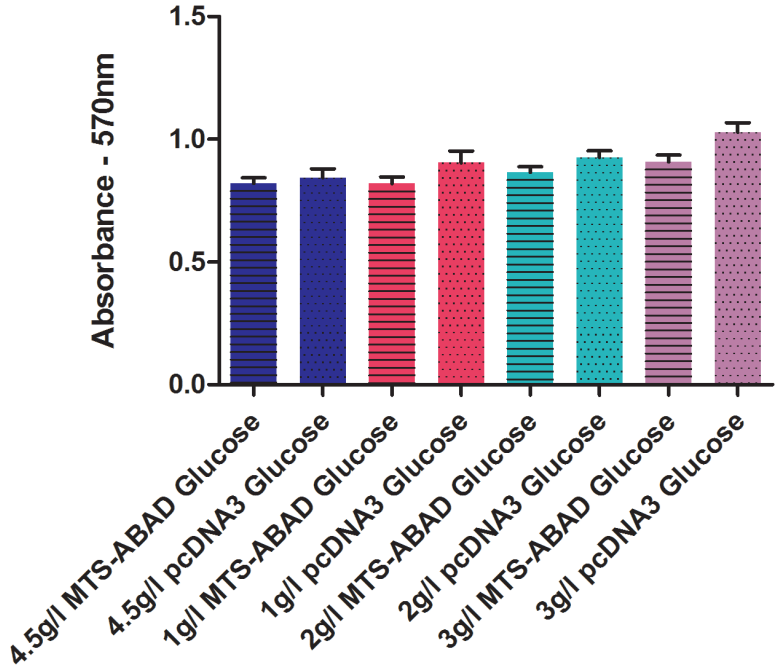

Figure 4-7: Cell viability assay. Absorbance results from an MTT assay conducted on HEK 293 cells, absorbance was measured at 570nm. Statistical analysis revealed that there was no significant interaction but that the presence of ABAD was significant (two-way ANOVA $F(3,44)=4.151$ $p=<0.05$*). Further analysis determined that reducing glucose from 4.5g/l to 3g/l, 2g/l, or 1g/l had no significance (one-way ANOVA, *post hoc* Bonferroni's multiple comparison's test on individual variables (ABAD, $F(3,44)=3.0$, no significance, or PcDNA3, $F(3,44)=4.15$, no significance)). N=12/condition.

4.3.3 ABAD ACTIVITY IN A NEUROBLASTOMA CELL LINE, SK-N-SH CELLS

The experiments above indicated that decreasing the glucose concentrations could directly induce ABAD activity without affecting its expression levels. Therefore, to explore if this effect also occurs in other cell lines and in particular neuronal like cell lines, SK-N-SH cells were next investigated.

SK-N-SH cells are derived from a neuroblastoma and so have neuronal-like qualities, and as such they have been extensively utilised in the investigation of AD. In addition, endogenous levels of ABAD in SK-N-SH cells are high, and so there was no need to transfect the SK-N-SH cells, allowing for an enquiry of the direct effect of altering glucose concentration on endogenous ABAD activity in this cell-type (Muirhead, 2011). As the greatest effects were seen when glucose was decreased to 1g/l in these studies, I investigated the comparison between normal glucose levels and a reduction to 1g/l. Therefore, SK-N-SH cells were seeded in a black-walled 96 well plate and incubated for 48 hours at a humidity of 5% CO_2, at 37^{0}C. After 48 hours, the cellular medium was replaced with a base medium of varying concentrations of glucose, glutamine and phenol red free DMEM with additional FCS (1%, charcoal filtered), penicillin/streptomycin and HEPES (10mM, pH7.4), and either 1 or 4.5g/l, final concentrations of glucose was added to the cells. After the cells were incubated for a further 24 hours, 20μM (-)-CHANA was added to each well and the plate was placed in the FLUOstar Optima microplate reader to enable analysis of the fluorescence emitted.

The total fluorescence emitted at 520nm was initially examined to determine if there were changes when the glucose concentration was decreased. A significant increase in the total mean fluorescence emitted (over the 60 minutes) was observed when glucose concentrations were decreased (1g/l) in comparison to the normal concentrations of glucose (4.5g/l) (Figure 4.8). The significant increase in fluorescence indicates that more CHANK had been produced over this set time period. Analysis of the rate of CHANK production under the decreased glucose concentration also indicated a significant increase in the overall rate of CHANK production in comparison to the control (Figure 4.9).

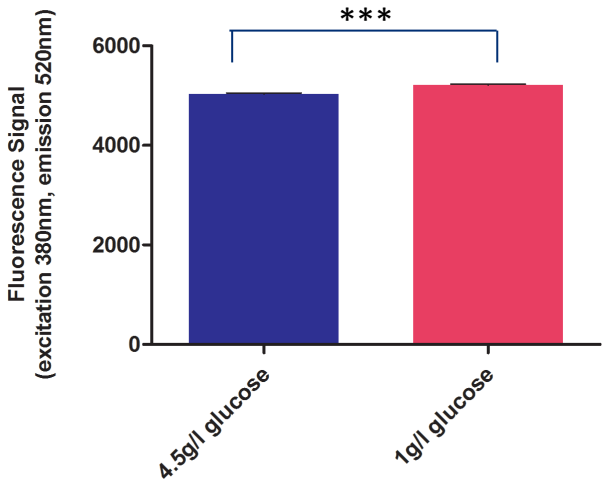

Figure 4-8: Total mean fluorescence emitted over 60 minutes. Fluorescent signals emitted from the activity of endogenous ABAD in SK-N-SH cells. Statistical analysis using a dependent T-Test determined a significant increase in fluorescent emission when glucose concentrations were reduced. ($t(12)=-160.9$ $p<0.001$*** (one-tailed) $r=0.7$) N=13

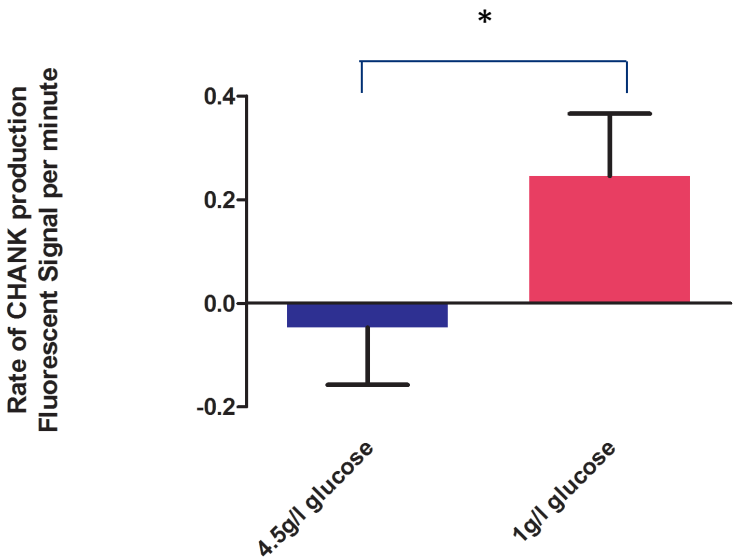

Figure 4-9: The mean rate of CHANK production by endogenous ABAD under varying concentrations of glucose in SK-N-SH cells. A dependent T-Test revealed a significant difference between the reduced glucose conditions in comparison to 4.5g/l glucose. T (23) = -1.852 p<0.05*(one-tailed) r=0.1 N=24/condition.

In order to confirm that cell viability and mitochondrial activity were not influencing the results, a MTT assay was performed under the same conditions (Figure 4.10). Interestingly, the assay showed a slight but significant decrease in absorbance when glucose concentrations were reduced to 1g/l. The decrease in absorbance implies that the reduction in glucose in SK-N-SH cells impacts on general mitochondrial activity, but even with a decrease in mitochondrial activity result, ABAD activity was significantly increased.

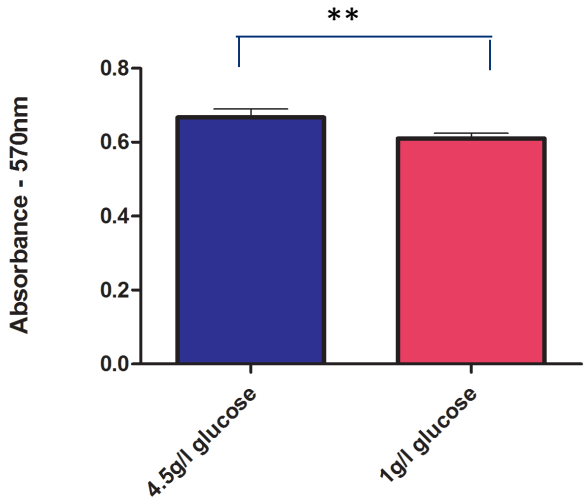

Figure 4-10: Cell viability assay. MTT assay illustrating mitochondrial activity in SK-N-SH cells, under varying glucose concentrations. A significant decrease was observed when the glucose concentration was decreased to 1g/l (Dependent T-Test, $t(23)=2.544$ $p<0.01$**, $r=0.2$ N=24/condition)

In summary, differences were observed when the glucose concentration was decreased in the cellular environment of both HEK 293 cells expressing ABAD, but also endogenously ABAD expressing SK-N-SH cells.

4.3.2 DOES CypD AFFECT ABAD ACTIVITY

The results obtained from the previous chapter (see section 3.3) using live FRET analysis, indicated that there was a potential transient interaction between CypD and ABAD. Therefore, I decided to use the fluorometric assay to determine if CypD expression could have an effect on ABAD activity, and thus indicate that this interaction has a potential functional role.

4.3.2.1 CONSTRUCTION OF DNA PLASMID EXPRESSING MTS-CYPD-MYC

In order to investigate the metabolic effect of CypD on ABAD, a mitochondrial targeted non-fluorescent tagged CypD protein needed to be developed. From the previously created DNA plasmid encoding for CypD-myc and the plasmid expressing MTS-CypD-ECFP, a cloning strategy was developed whereby the mitochondrial targeting sequence (MTS) and CypD were cloned and ligated with a myc tag (Figure 4.11).

Initially, the target plasmid, pCypD-myc, was digested with *Hind*III and *Pst*I and cleaned up to allow for insertion of the PCR product containing the MTS and a section of CypD. PCR was carried out using pMTS-CypD-ECFP as the template DNA (see section 2.1.1) and the following primers were used: forward primer **5'** CCAAGCTTATGTCCGTCCTGACGCCGCT **3'** encoding for *Hind*III (underlined) and reverse primer **5'** ACGTCCAGGTACACGAGCGG **3'**. PCR products were digested with restriction enzymes *Hind*III and *Pst*I and products run on an agarose gel to verify successful PCR (see section 2.1.2). The PCR product (MTS-CypD) was purified from the agarose gel and ligated into the pre-prepared plasmid (see sections 2.1.3 and 2.1.5). Once ligated the plasmid was transformed into *E.coli* (DH5α), and finally the plasmid DNA was purified from the bacteria and sequenced to confirm the correct DNA construct had been made (see section 2.1.7 and 2.1.8).

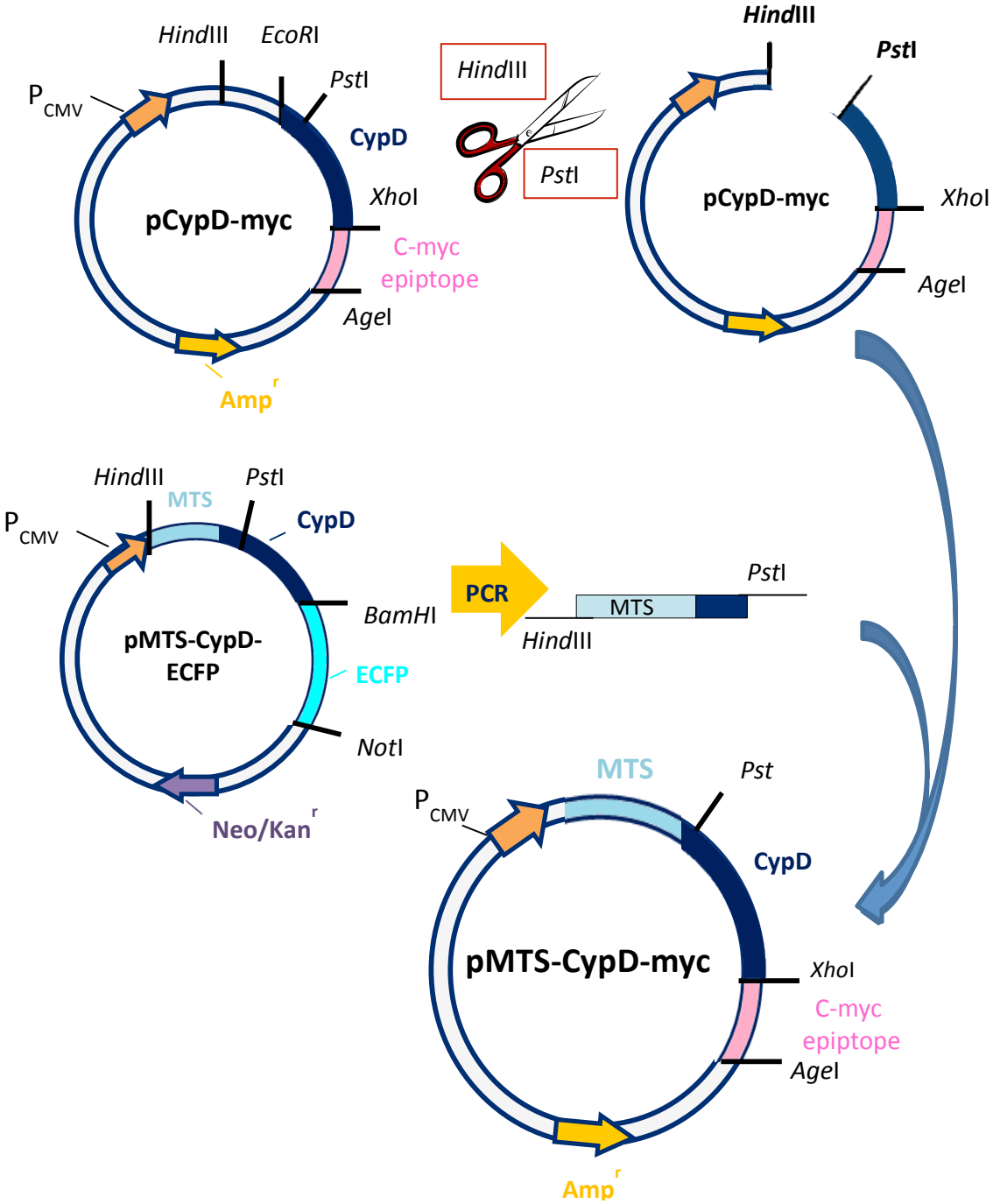

Figure 4-11: Outline of cloning steps. pCypD-myc was digested with *Hind*III and *Pst*I to allow for insertion of the PCR fragment. PCR was conducted following protocol outlined in section 2.1.1 with annealing temperature at 48.3°C using 100ng of the template DNA, pMTS-CypD-ECFP. The PCR fragment containing MTS-CypD was ligated into the digested CypD-myc plasmid.

4.3.2.2 FLUOROMETRIC ASSAY DETERMINING THE METABOLIC EFFECT OF CypD ON ABAD

To investigate the effect CypD could have on the activity of ABAD, HEK 293 cells were seeded in a black walled 96 well plate and after 24 hours they were double transfected with: either 0.025µg of pMTS-ABAD and 0.025µg of pMTS-CypD-myc or 0.025µg of pMTS-ABAD and 0.025µg of an empty control vector (pcDNA3). The medium of the HEK 293 cells, after a further 24 hours, was changed for phenol-red and glutamine free MEM medium (with added 10mM HEPES pH7.4, 1% FCS (charcoal-filtered), penicillin/streptomycin) containing 4.5g/l of glucose. Following a 24 hour incubation period 20µM (-)-CHANA was added to the cells and the black walled plate was then transferred to the microplate reader.

The rate of CHANK production recorded over 60 minutes was significantly decreased in HEK 293 cells transfected with both ABAD and CypD (Figure 4.12). Under normal glucose concentrations this significant decrease of ABAD activity, suggests that CypD could have an effect on ABAD activity in normal cellular functioning. To determine if the effects discovered were a consequence of the expression of CypD, western blot analysis was conducted along with an MTT assay (Figure 14 & 15 respectively). Western blot analysis determined that levels of ABAD expression in HEK 293 cells were not altered when transfected with pMTS-ABAD and pMTS-CypD-myc or control, pcDNA3 (Figure 4.13). In addition the MTT assay (Figure 4.14) revealed that there were also no significant differences when CypD was expressed with ABAD in HEK 293 cells in comparison to ABAD expressed with a control vector (pcDNA3).

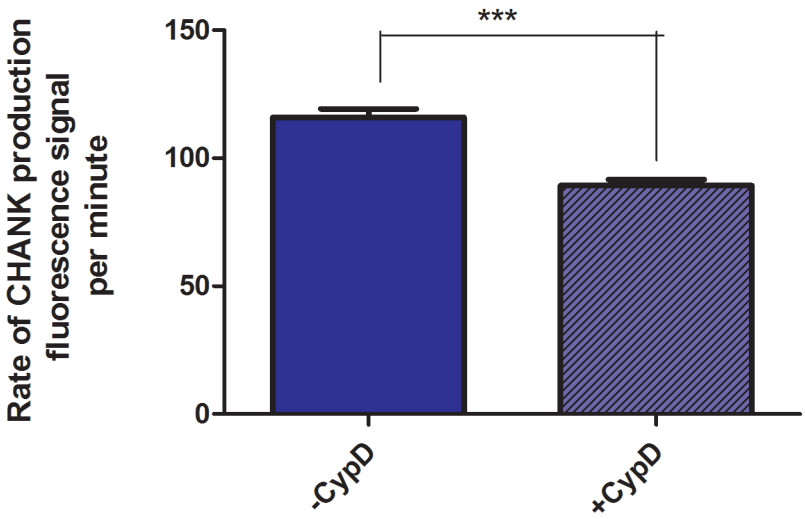

Figure 4-12: The mean rate of CHANK production over 60 minutes. CHANK production in transfected HEK 293 cells expressing ABAD and CypD or control, pcDNA3. Statistical analysis shows a significant decrease in the rate of CHANK production when CypD is present (dependent T–test, $t(11) = -13.582$, $p<0.001$***, $r=0.9$). N=12/condition.

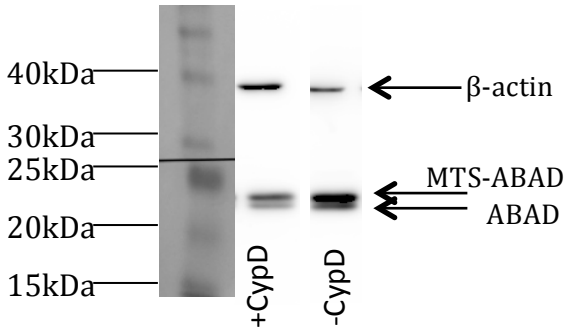

Figure 4-13: Expression of ABAD in HEK 293 cells. HEK 293 cells were transfected with pMTS-ABAD and pMTS-CypD-myc (+CypD) or pcDNA3 (-CypD), their cell lysates collected and used for western blot analysis. Immunoreactive bands were detected with anti-ABAD (Abcam) (mouse, 1:1000) and anti-mouse HRP (Abcam) (mouse, 1:20000). Bands were expressed at ~24kDa (MTS-ABAD) and ~22kDa (endogenous ABAD). As a loading control anti-β-actin (mouse, 1:10000) with anti-mouse HRP (mouse 1:20000) were used to detect actin, revealing a band at ~ 40kDa.

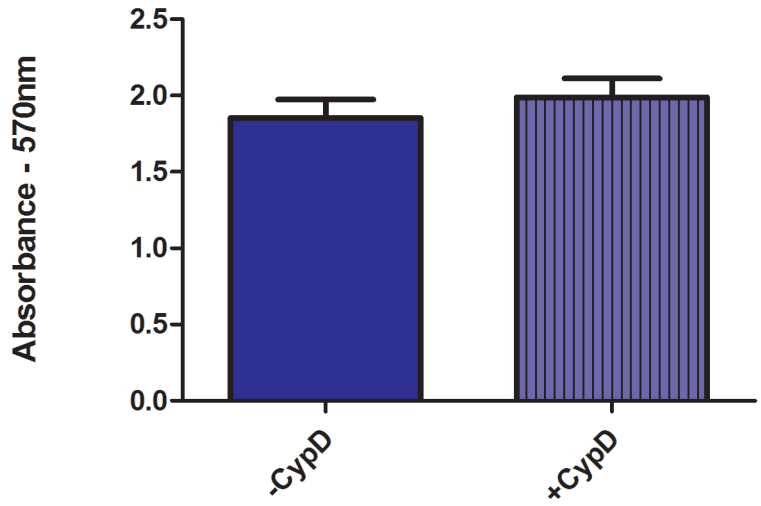

Figure 4-14: Cell viability of HEK 293 cells. MTT assay showed no significant difference in HEK 293 cells expressing ABAD and CypD or ABAD and pcDNA3. (dependent T–test, $t(11)=0.791$, $Ns= 0.446$, N=12/condition).

In summary, from the results obtained from expressing CypD with ABAD in HEK 293 cells, they show that there was a significant decrease in the rate of CHANK production in the presence of elevated levels of CypD, indicating that levels of CypD expression can influence ABAD activity.

4.4 RESULTS: LIPIDS IN ALZHEIMER'S DISEASE

There are 5 main classes of lipids: Fatty acyl, glycerolipids, glycerophospholipids, sterol lipids and sphingolipids (Figure 4.15). Each class of lipid has different biological importance and specific responsibilities, for example the glycerolphospholipid, phosphatidylcholine (PC), is the main component of cell membranes and ceramide is a crucial second messenger in both cell growth and death (Mulder et al., 2003). The major components of these lipids are fatty acids, which are a crucial energy source, and when cleaved from their head group, by phospholipases, they have been reported to be a substrate for ABAD (Muirhead et al., 2010a, Stryer, 1995). The metabolism of fatty acids functions to maintain homeostasis of energy within cells, furthermore the cleavage of phospholipids generates neuronal signalling lipids and other cell regulating factors (Scorrano et al., 2001, Grossfield et al., 2006, Astarita and Piomelli, 2011, Di Paolo and Kim, 2011).

In AD, lipids are reported to be involved in several aspects such as Aβ production via APP metabolism, neuronal inflammation, oxidative stress and neurotoxicity (Di Paolo and Kim, 2011, Scorrano et al., 2001). Specifically lipid metabolizing enzymes such as phospholipase A2 (PLA_2), phospholipase C (PLC), CLU and ApoE ε4 have been reported to be involved in affecting cellular functioning in AD(Florent-Bechard et al., 2009, Di Paolo and Kim, 2011, Cunnane et al., 2011). PLC has been described to stimulate the non-amyloidogenic pathway of APP cleavage via protein kinase C (PKC) activation, implying that inhibition of PLC would cause a shift to the amyloidgenic pathway (Di Paolo and Kim, 2011, Rossner, 2004). This pathway, where PC is hydrolysed to produce Phosphatidic acid (PA) (figure 4.16), further initiates the production of other lipid products and consequently variations between normal neuronal functions and any inhibition of PLC in AD neurons would be observed when investigating lipid profiles.

Fatty Acyl:
- Octadecanoids
- Eicosanoids
- Docosanoids
- Fatty alcohol
- Fatty aldehydes
- Fatty esters

Glycerolipids:
- Monoacylglycerols
- Diacylglcerols
- Triacylglycerols

Glycerophospholipids:
- Phosphatidic acids
- Phosphtidylcholine
- Phosphtidylserines
- Phosphtidylglycerols
- Phosphtidylethanolamines
- Phosphtidylinositols
- Phosphtidylinositides
- cardiolipins

Sterol lipids:
- Sterols
- Steroids
- Secosteroids
- Bile acids and derivatives

Sphingolipids:
- Sphingold bases
- Ceramides
- Phophosphingolipids
- Phosphonosphingolipids
- Acidic glycosphingolipids
- Neutral glycosphingolipids

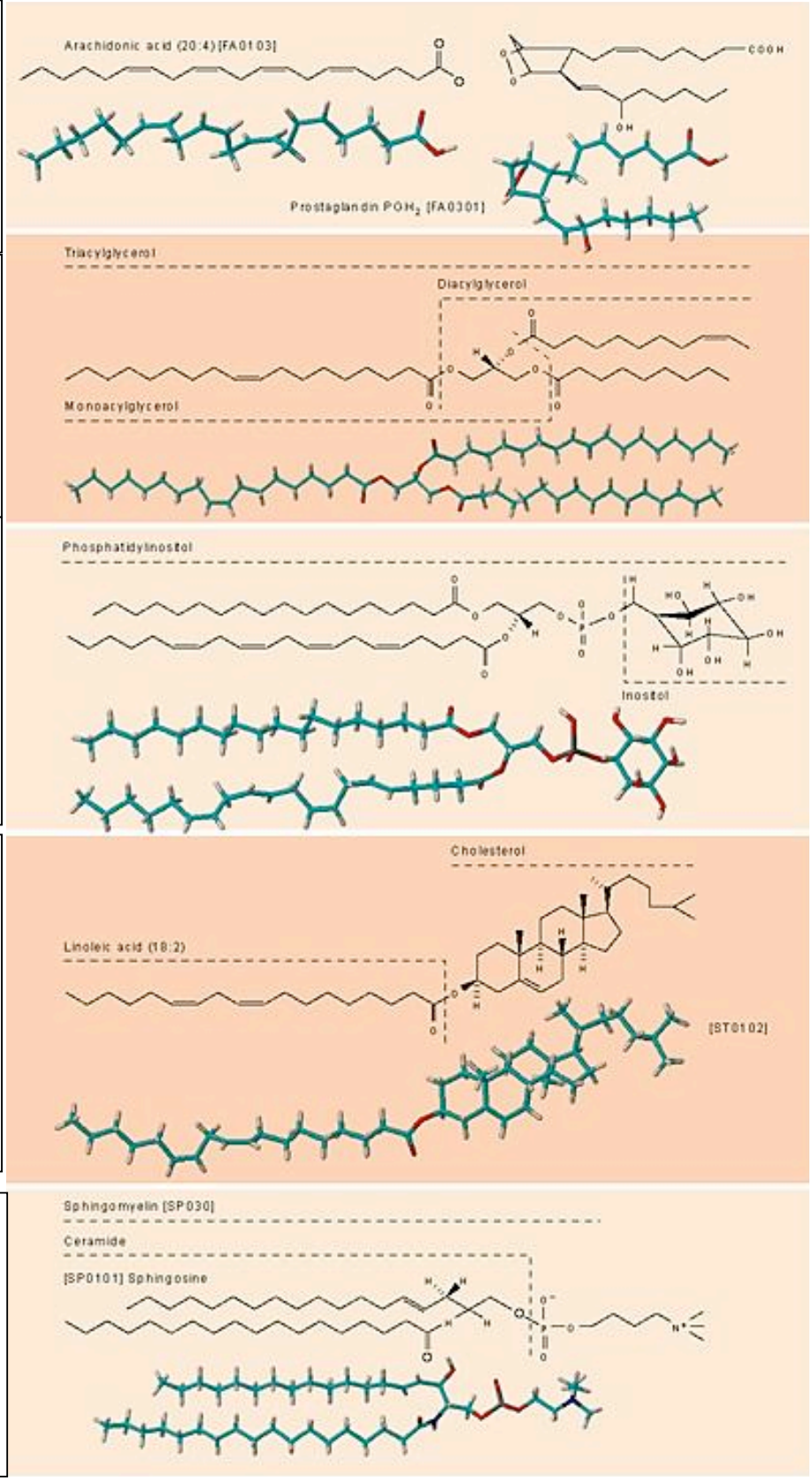

Figure 4-15: Five main lipid classes and lipid members. Figure adapted from Wenk (2005).

ABAD is another lipid metabolising enzyme which features prevalently in AD; however, it has previously only been reported to utilise fatty acids as substrates (Muirhead et al., 2010a). Furthermore with the reported findings that Aβ inhibits ABAD enzyme function, it could be suggested that this inhibition hinders fatty acid oxidation and subsequently alter the lipid composition of neurons (Lustbader et al., 2004). Consequently, this inhibition of ABAD could prevent the production of energy through this back-up system. However, as previously mentioned (see section 1.3.3.4) the activity of ABAD could be modulated by the presence of Aβ by influencing substrate changes to various lipids and not cause a digital on/off response, as suggested in previous studies.

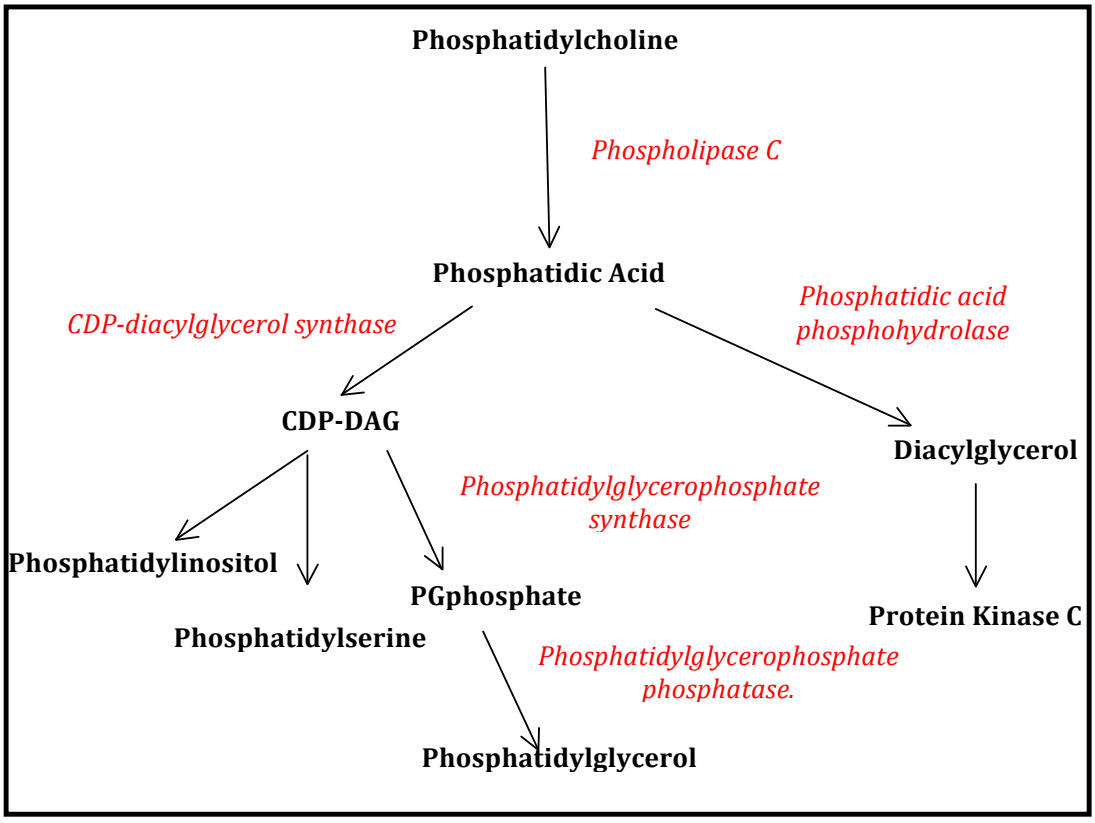

Figure 4-16: Biosynthesis pathway of phosphatidylinositol (PI), phosphatidylserine (PS) and phosphatidylglycerol (PG) from the breakdown of phosphatidylcholine. (Delhaize et al., 1999, Wright and McMaster, 2002)

Therefore, in this part of the chapter, I investigated the effect of expressing ABAD and Aβ on lipid metabolism in living cells, in particular the effects of ABAD in the absence and presence of elevated levels of Aβ. To do this I explored the lipid composition of cells expressing ABAD and Aβ, using a method called lipidomics.

4.4.1 ELECTROSPRAY IONISATION-MASS SPECTROMETRY BASED LIPIDOMICS

The method of lipidomics allows for the analysis of lipids within tissue and cell samples (outlined in Figure 4.17). Once the lipids have been extracted from the samples, they are analysed by ESI-MS. Initially, lipids are carefully extracted following the protocol defined by Bligh and Dyer (1959). Early studies used thin-layer chromatography (TLC) as the method of choice for lipid separation which has been superseded by the development of mass spectrometry which in comparison to TLC provides a higher resolution and sensitivity with larger complex lipid samples. However, TLC is still used in conjunction with mass spectrometry in order to provide a fuller set of data. In this investigation, the mass spectrometry technique used was electrospray ionisation, as it detects polar lipids and subsequently is suitable for ascertaining the presence of glycophospholipids (Wenk, 2005).

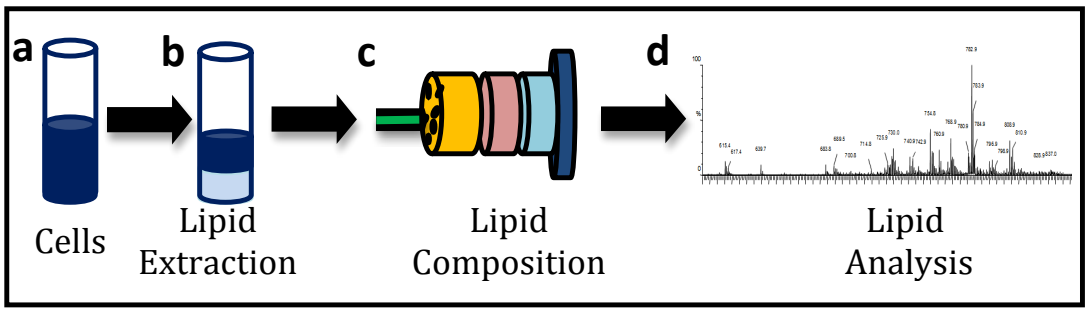

Figure 4-17: Process of lipidomics and lipid analysis a) culture of cells/ tissue of interest b) the extraction of lipids from cultured samples following the rapid lipid extraction protocol determined by (Bligh and Dyer, 1959). c) Lipid profiling by ESI-MS d) Analysis of lipid spectrum.

For ESI-MS analysis, lipid extracts are re-dissolved in solvent, in this case chloroform/methanol (1/2 v/v), to obtain a liquid to pass through the fine needle Figure 4.18a. Once the sample is loaded into the fine needle, a large voltage is applied across the sample causing it to become charged. While the sample is travelling through the needle the passing voltage increases the charge until it reaches a maximum at the tip of the needle, at this point the sample droplets burst apart into smaller droplets due to electrostatic repulsion (Coulomb's law of repulsion). Subsequently, the solvent evaporates and the charge is deposited on the analytes within the sample, now the particles are charged and can be analysed by mass spectrometry. Mass to charge ratio (m/z) can be determined by using a Micromass Quattro Ultima triple quadrupole (depicted in Figure 4.18b); quadropole 1 (Q1) detects all charged analytes within the sample whereas in Q2 (collision chamber) either argon or nitrogen collision gas can be used to examine product ions by inducing collision of particles. The particles from the collision chamber are then collected and filtered in Q3 and results detected in the final stage.

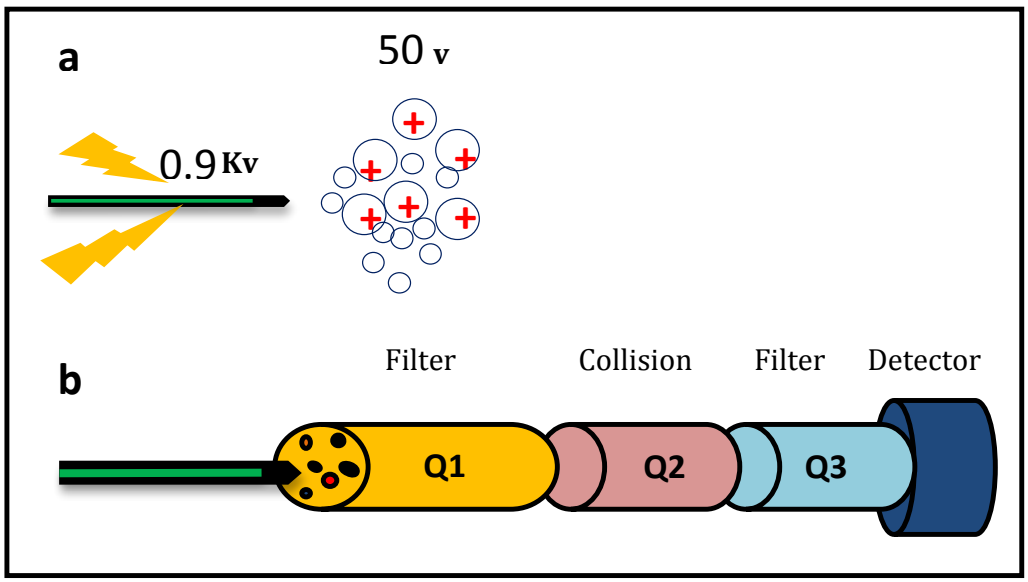

Figure 4-18: Schematic diagram of ESI-MS. a) diagram of the entry of lipid extraction through a fine needle, large voltage applied to needle to charge analytes, b) simplified diagram of the steps involved in ESI-MS. b) At quadropole 1 (Q1) the filtration by mass of parent ions occurs, at Q2, collision of analytes occurs to produce product/daughter ions and Q3, the filtration of the product ions occurs, and then finally the detection of the lipids.

4.5 RESULTS: LIPIDOMIC INVESTIGATIONS

Preliminary investigations into a possible link between ABAD and lipid metabolism was carried out in transfected HEK 293 cells. Initially, the composition of glycophospholipids was analysed and in order to identify any variations, lipid extracts from specifically transfected HEK 293 cells, were examined using ESI-MS.

To investigate the effects of ABAD and a mutant form of mAPP bearing a mutation associated with FAD, (a Val(642Phe) substitution, which is similar to the mutation carried in the mAPP/ABAD mouse studied by Ren et al. (2008)) on the cellular lipid content of HEK 293 cells were plated in T25 flask (Nunc) and incubated for 24 hours. Following incubation the cells were then transfected, using the GeneJammer transfection reagent (see section 2.2.4), with 2µg (total amount) of either one or a combination of the following DNA plasmids expressing: MTS-ABAD, mAPP or pcDNA3. Following 48 hours after transfection, HEK 293 cells were harvested by trypsinising the cells, resuspending them in medium and then gently pelleting the cells by centrifugation (1000xg, 5min). The resultant pellet was washed in 1 x PBS and further centrifuged (1000xg, 5min). Finally, with the supernatant removed, the cell pellet was resuspended in 100µl of 1 x PBS, transferred to a glass vile and placed on ice.

To extract the lipid content from the transfected HEK 293 cells, a chloroform-methanol mix ($CHCl_3$:MeOH, 1:2 v/v) was added to the 100µl cell suspension and vortexed. Following this, the cell suspension was further agitated and $CHCl_3$ was added, subsequently vortexing of the cells was carried out with the addition of H_2O. The cells were then centrifuged (1000xg, 5min) to divide the solution: the lower phase containing lipids were collected and dried under nitrogen. These nitrogen-dried lipid-extracts from the transfected HEK293 cells were analysed by ESI-MS by resuspension of the dried extracts with a chloroform/methanol mix (1:2 v/v). In order to disperse the resuspended lipid extraction samples, small volumes were loaded into thin-walled nanoflow capillary tips (Waters). The thin-walled capillary tips allow for the sample to be dispersed in an 'aerosol' like fashion into

the ionisation chamber where, depending on the lipids being analysed, either a hydrogen ion is added or removed/ left as neutral via a high voltage.

The lipid extract samples were analysed using Micromass LCT mass spectrometer with a nanoelectrospray source (capillary voltage of 0.9 kV and cone voltages of 50 V) in order to gain the lipid spectra. Further analysis, to determine the product ion spectrum (which produces the different fragments of glycophospholipids from the original lipid extract) was carried out by a m/z fragmentation scan following the protocol outlined in section 2.5.2.2.

Once ESI-MS was performed the lipid spectra were analysed to explore the variations in the lipid content (figures 4.19 & 4.20). Initially, the positive ion mode shown in Figure 4.19 does not appear to show major differences in the PC species across the conditions as the overall lipid levels are unchanged. However, on closer inspection of these positive ion mode results, where ABAD is expressed in HEK 293 cells, indicated an increase in sphingomyelin (SM) (730.0 m/z). Notably NMR analysis of AD brain samples have reported a similar finding whereby SM levels were increased in comparison to non-demented age matched controls (Pettegrew et al., 2001). An increase in SM has also been shown to increase rigidity of the cellular membranes which in turn promotes Aβ production (Wolozin, 2001). This suggests that the increased expression of ABAD in AD could indirectly stimulate Aβ production possibly through changes in lipid metabolism. Examination of the negative ion spectra revealed an overall suppression of the lipid species PI, PG and PC when mAPP was present in the HEK 293 cells; the dominant lipid species was phosphatidylethanolamine (PE) (744.8 m/z). The decrease of PI, PG and PC suggests a reduction in their synthesis or even an increase in metabolism of these particular lipids. In order to synthesise these particular phospholipids, cytidine diphosphate-diacylglycerol (CDP-DAG) is required, consequently the results imply that this lipid could also be suppressed causing a reduction in the production of PI, PG and PC. As the brain ages, neurons have been reported to show reduced content of the inner mitochondrial membrane lipid, cardiolipin, which is particularly important in the regulation of mitochondria membranes (Ruggiero et al., 1992, Chicco and Sparagna, 2007).

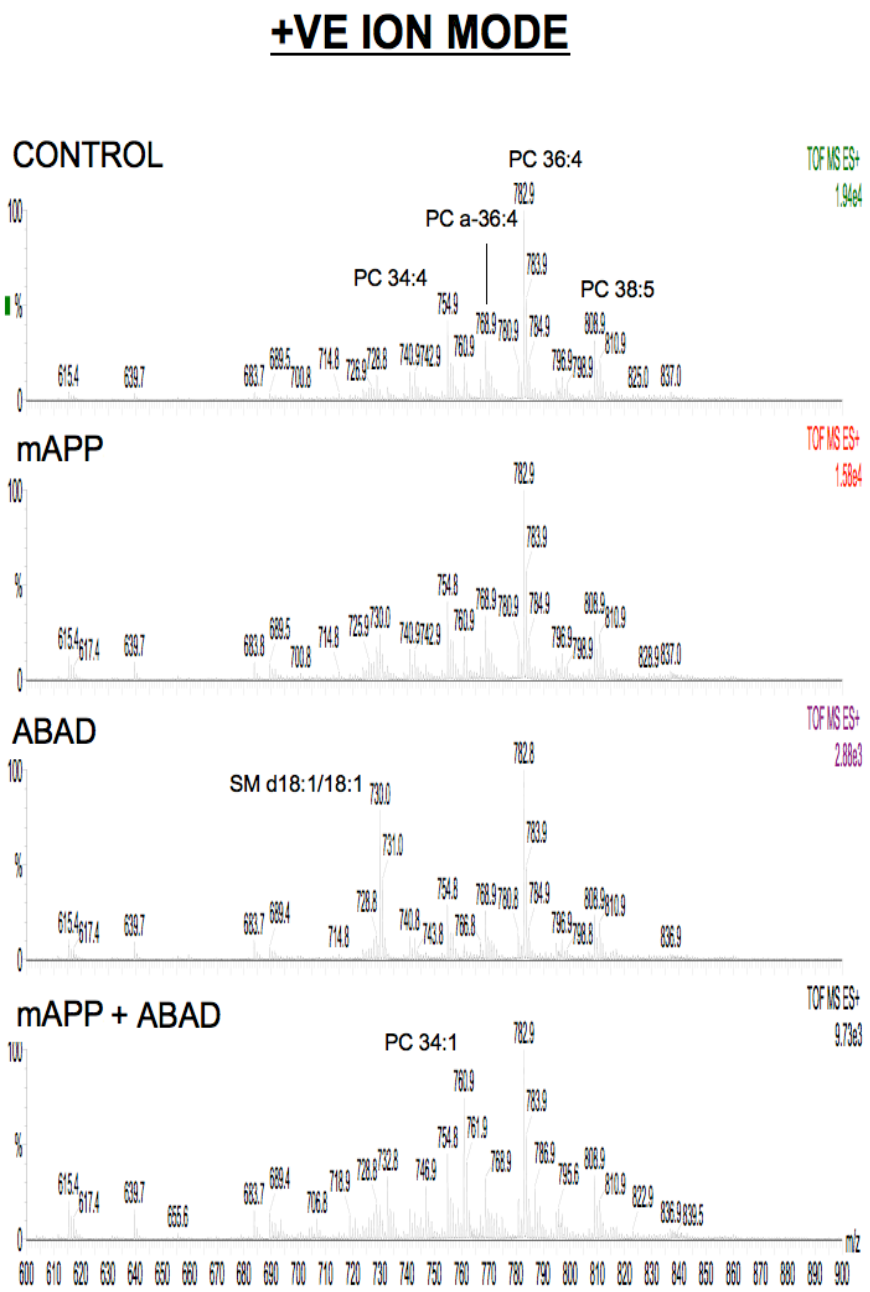

Figure 4-19: ESI-MS analysis of lipid content in HEK293 cells in positive ion mode. Analyses of positively charged lipids (e.g PC & SM) determined from lipid extracts from HEK293 cells transfected with DNA plasmids expressing; pcDNA3 (Control), mAPP, MTS-ABAD or mAPP with MTS-ABAD. Labelled are the key changes seen; SM – sphingomyelin and PC-phosphatidylcholine. The main changes were observed in the spectra from the lipids extracted from HEK 293 cells expressing ABAD and both mAPP and ABAD. In the presence of ABAD there is an increase in SM and in mAPP and ABAD there is an increase PC.

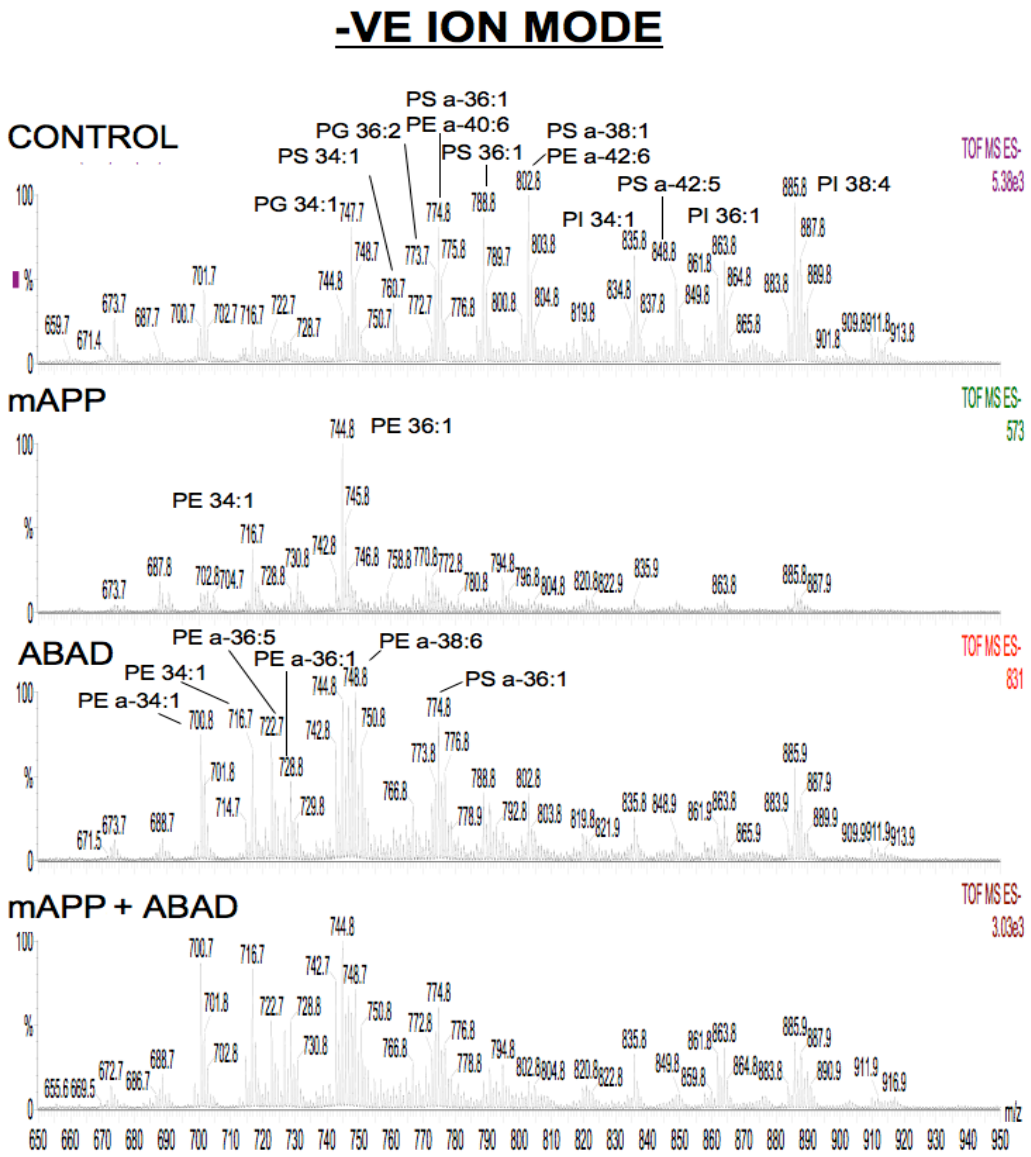

Figure 4-20: ESI-MS spectra of lipid content in HEK 293 cells negavtive ion mode, analysis of negatively charged glycophospholipids (e.g PS & PI) determined from lipid extracts from HEK 293 cells transfected with DNA plasmids expressing; pcDNA3 (Control), mAPP, MTS-ABAD or mAPP with MTS-ABAD. Labelled are the key changes seen, such as a shift to PE and PS species when ABAD was expressed. This shift is also observed when mAPP and ABAD were expressed together. Additionally, there was a depression of lipid species observed when mAPP was expressed in HEK 293 cells.

Importantly, cardiolipin is synthesised from PG and CDP-DAG and subsequently a reduction in these lipids could be causing impairments in this biosynthetic pathway (Chicco and Sparagna, 2007). Again, explorations from the negative ion mode showed that lipids extracted from HEK 293 cells expressing ABAD, indicated further increases in the PE species along with decreases in diacyl containing phospholipids, in particular the PI and PS species. In comparison to the controls, the expression of ABAD appears to induce a shift to the production of PE and PS species containing shorter diacyl and acyl-alkyl lipids. The lipid shift to PE and PS species is noteworthy as decarboxylation of PS produces PE, and significantly the PS decarboxylase used to synthesise this PE when its function is disrupted, has been reported to cause mitochondrial dysfunction and abnormalities in mice null for PS decarboxylase (Steenbergen et al., 2005). This study implied that the changes and disruptions in the tightly regulated synthesis of PE from PS could contribute to mitochondrial abnormalities in AD.

Overall, this preliminary exploration into the effects of ABAD and mAPP on lipid content has revealed interesting changes in the lipid composition within HEK 293 cells expressing ABAD and mAPP.

4.6 DISCUSSION OF THE EFFECT CHANGING GLUCOSE CONCENTRATION HAS ON ABAD ACTIVITY

Metabolism in AD has long been noted as a significant problem, deficits in glucose utilisation and lipid metabolism have been increasingly reported in AD (Astarita and Piomelli, 2011, Cunnane et al., 2011, Di Paolo and Kim, 2011). The production of energy from free fatty acids within the mitochondria is reliant on the enzyme ABAD (Yang et al., 2005) and during times of starvation when glucose levels are low, the β-oxidation of fatty acids is crucial in maintaining energy homeostasis(Cunnane et al., 2011). Indeed elevated levels of ABAD have been shown to compensate under conditions of low glucose (Yan et al., 2000). ABAD has also been well established to be involved in AD, particularly in instigating toxicity by interacting with Aβ (Lustbader et al., 2004, Yan et al., 1997, Yan et al., 1999). Additionally, from investigations reported in chapter 3, ABAD has now been observed to interact weakly with CypD. This is another key protein involved, in AD, with a functional role in the necrosis of neurons (Connern and Halestrap, 1994, Crompton et al., 1998, Du, 2010, Li et al., 2004b). The role of this observed interaction between ABAD and CypD is unknown but this chapter also investigated whether it played a functional role in the activity of ABAD.

Initial investigations into ABAD activity, under conditions when glucose concentrations were reduced, showed significant increases in this enzyme's activity. The significant increase of ABAD activity, measured via the rate of CHANK production, suggests that there is requirement from the HEK 293 cells for an alternative source of energy. As expected the SK-N-SH cells also showed a similar response to when glucose levels were decreased.

ABAD has previously investigated in conditions where the ketone, β-hydroxybutyrate, was the principle energy substrate. The oxidation of this ketone by ABAD was reported to maintain cellular functioning without any other energy source (Yan et al., 2000). I have shown that, specifically, ABAD activity is increased when energy sources are removed, suggesting that ABAD is a crucial enzyme in

conditions of starvation. This fits with the data of Yan et al. (2000) where they reported an increase in ABAD expression in response to cerebral ischaemia in wild-type mice . From this study it was suggested that the increased expression of ABAD could be increasing the metabolism of the ketone, β-hydroxybutyrate . This is an interesting finding as I found that protein expression was not changed but it was the actual activity of the enzyme that was enhanced, this implies that in response to energy depletion then the activity of ABAD is enhanced to increase fatty acid metabolism. The increased metabolism of fatty acid would buffer the effects of starvation and as shown by Yan et al. (2000) maintain cellular integrity, preventing cell death.

CypD has a well-established role in the formation of the mPTP and as a chaperone protein in protein folding (Connern and Halestrap, 1992, Schinzel et al., 2005, Muirhead et al., 2010a). CypD, which is known to induce cell death via mPTP formation, has been hypothesised to bind to ABAD before being displaced by the binding of Aβ peptide and so leaving CypD to translocate to the IMM to form the mPTP (Yan and Stern, 2005). However, my live cell FRET analysis revealed that CypD only appeared to transiently interact with ABAD, and so a very different role of the interaction between CypD and ABAD must exist.

The expression of CypD with ABAD in HEK 293 cells revealed that ABAD activity was supressed in the increased presence of CypD in comparison to controls. This finding suggests that when CypD interacts with ABAD, CypD induces a reduction in the β-oxidation of fatty acids which in turn would decrease the levels of energy produced via fatty acid metabolism. This could be significant in times of low glucose levels as CypD may hinder the production of reserve energy. However in AD, in the presence of Aβ, glucose levels and utilisation are reported to be decreased and oxidative stress is known to occur, under which conditions CypD has been reported to translocate to the IMM and form the mPTP (Connern and Halestrap, 1994, Bentourkia et al., 2000). With this in mind, CypD may therefore not reduce the activity of ABAD in AD but in fact, purely by the translocation of CypD, consequentially increase ABAD activity. Therefore, the presence of Aβ and oxidative stress does indeed induce an increase in ABAD activity by perhaps

causing the prevention of an interaction between CypD and ABAD. My findings, therefore, suggest a functional role for CypD in the maintenance of metabolism within mitochondrial matrix, by the transient interaction with ABAD. This functional role of CypD could be the contributing factor to the increase of fatty acid metabolism observed when glucose is reduced.

The presence of lipids within the cells is essential for membrane composition, signal transduction and metabolism. Crucially, many key lipid-metabolising enzymes have been noted to be involved in AD, such as increased activity cytosolic PLA2, sphingomyelinase and phospholipase D (Oliveira and Di Paolo, 2010, Di Paolo and Kim, 2011). Additionally, fatty acids, in particular the omega 3 fatty acid, DHA, has been repeatedly reported to be lower in the brains of AD patients (Soderberg et al., 1991). The intake of this essential fatty acid has been noted to reduce levels of the fatty acid, arachidonic acid (AA) which is involved in initiating the inflammatory response (Wenk, 2005, Cole et al., 2009, Astarita and Piomelli, 2011, Di Paolo and Kim, 2011). Consequently in AD lower levels of DHA will increase AA and induce inflammation, a further pathology found in AD (Akiyama et al., 2000). These changes in lipids and fatty acid composition noted in AD are thought to be a consequence of changes in metabolism and as observed in section 4.5 the activity of the metabolising enzyme ABAD increases when fatty acid metabolism is required.

My preliminary investigations into the consequence of expressing ABAD and mAPP in HEK 293 cells showed an overall suppression of the majority of lipid species (in the negative ion mode – figure 4.20). When mAPP was expressed in the HEK 293 cells, PE was the major phospholipid. This could suggest that the other lipids were broken down to form PE implying that PE is an important lipid in the functioning of this cell line, for example in signifying cellular stress (Stryer, 1995). However, a reduction in the overall suppression of lipids was observed when mAPP was expressed in the presence of ABAD (figure 4.20). The expression of ABAD alone revealed a shift in phospholipids to shorter diacyl and acyl-alkyl PE and PS species; this suggests that when ABAD is expressed, the long chain polyunsaturated fatty acids are being catabolised in order to produce energy via β-

oxidation. A similar lipid profile was observed when mAPP was expressed with ABAD further signifying energy production via β-oxidation. This is a significant finding as ABAD expression is being shown to affect lipid metabolism, and on particular lipids.

In addition to the depletion of specific lipids and an increase in PE in the negative ion mode, when ABAD was separately expressed, there was an increase in SM species observed in the positive ion mode (Figure 4.19). In AD, SM species have been noted to be down-regulated as a consequence of the increased activity of sphingomyelinase (the enzyme that converts SM to ceramide) (Grimm et al., 2005, Di Paolo and Kim, 2011). The increased activity of sphingomyelinase and the subsequent increase in ceramide favours the amyloidogenic processing of APP, due to the presence of SM and ceramide in membranes increasing rigidity (Wolozin, 2001, Kojro et al., 2001, Grimm et al., 2005, Di Paolo and Kim, 2011). Therefore, it is interesting to note that when ABAD is heterologously expressed in HEK 293 cells, an increase in SM production was observed. This increase in SM suggested that sphingomyelinase activity is decreased and in turn ceramide levels would be decreased (figure 4.21). The reduction of ceramide when ABAD is expressed could imply that ABAD has a protective effect by reducing cell death (Di Paolo and Kim, 2011). However, the prolonged expression of ABAD causing an irregular increase of SM species could induce rigidity of many membranes stimulating the amyloidogenic cleavage of APP. Therefore, the initial protective response, of the increased expression of ABAD reported in AD, consequently could cause further production of Aβ. Additionally, when ABAD was expressed with mAPP a reduction in increased SM species was observed. Aβ has previously been noted to cause activation of sphingomyelinase and therefore my findings could signify an increase in sphingomyelinase activity inducing cell death (Lee et al., 2004).

On the whole, my findings suggest that there are depletions of only specific lipids, perhaps caused by an increase in the degradation of lipids in response to the expression of ABAD and mAPP. Furthermore, the expression of ABAD alone appeared to affect the composition of lipids in cells, thus indicating that, the increase of ABAD as noted in AD, can indeed affect lipid metabolism.

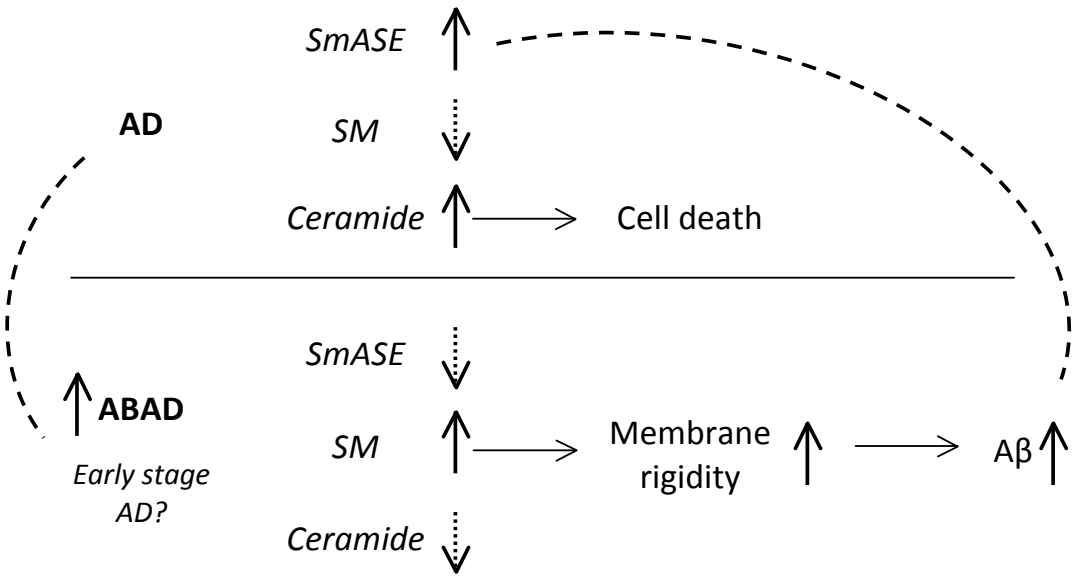

Figure 4-21: Hypothesised explanation for the increased levels of SM when ABAD was expressed in HEK 293 cells.

Chapter 5: CONCLUSION AND FUTURE STUDIES

ABAD INTERACTION WITH CypD

From previous unpublished research, an interaction between ABAD and CypD had been noted and hypothesised to be a protective mechanism where CypD was sequestered by ABAD within the mitochondrial matrix (Yan and Stern, 2005). This sequestering of CypD by ABAD was suggested to prevent the reported translocation of CypD to the IMM, where CypD has been observed to be part of the mPTP (Connern and Halestrap, 1992, Connern and Halestrap, 1994, Yan and Stern, 2005). The mPTP has been reported to open under conditions of cellular stress, resulting in necrosis and cell death; therefore, indicating that this interaction between ABAD and CypD, could be a potential controlling mechanism to prevent cell death (Li et al., 2004b). Consequently, any disruption of this interaction could promote cell death, and so as Aβ binds to both ABAD and CypD, it could change the conformation of both ABAD and CypD resulting in the disruption of their interaction. This would mean that the binding of Aβ to both ABAD and CypD could have multiple effects with ABAD's activity being distorted (potentially changing the substrates it can now use: see below) resulting in the production of toxic products, whilst CypD translocates to the IMM opening the mPTP (Lustbader et al., 2004, Du et al., 2008).

To investigate this potential interaction, I performed both immunoprecipitation and live cell FRET experiments. The immunoprecipitation studies did not show any interaction between ABAD and CypD; however, as this interaction could be transient (see below) further studies could be performed to specifically look for such weak interactions. This would involve the addition of cross-linkers to these immunoprecipitation studies in order to retain the weaker binding between the proteins (Kluger and Alagic, 2004). Interestingly, previous experiments in the laboratory had indicated that it was possible to achieve FRET signals between fluorescently labelled ABAD and CypD from fixed cell samples (Ren, 2008), and indeed I did find an interaction occurring between ABAD and CypD when live cell FRET analysis was carried out. Specifically a small Ratio A value was calculated

which corresponds to a low FRET efficiency of ~10% of the positive control (which is set to 100%). This implies that despite the immunoprecipitation experiments, there is a potential interaction between ABAD and CypD. This suggests that the original hypothesis of Yan and Stern (2005) concerning the sequestration of CypD by ABAD is not completely correct, as their prediction was of a strong binding between CypD to ABAD. As such the observed weak/transient interaction could explain why nothing was seen with the immunoprecipitation studies and hence, as indicated above it would not be easily observed without the use of chemical cross-linkers to sustain the interaction. As well as these modified immunoprecipitation studies further investigations into the ABAD-CypD interaction using live cell FRET analysis could also include an exploration into the conditions which control this interaction. Indeed as these FRET experiments were performed on live cells, it will be possible to perform experiments with the addition of Aβ or other oxidative stresses and measure the subsequent FRET efficiency. Additionally, it would be interesting to investigate whether this interaction can be seen using other biophysical methods such as thermal shift analysis and/or surface plasmon resonance or isothermal calorimetry using purified proteins.

ABAD ACTIVITY AND REDUCED GLUCOSE

It has already been established in AD, that there are problems with glucose utilisation, consequently this causes a starvation of energy for neurons and so they must resort to utilising alternative energy sources. When glucose is not available neurons use ketone bodies to produce energy from the metabolism of fatty acids, importantly this metabolism uses ABAD. Starvation conditions increase the requirement for ketones as an energy source, which may provide a reason for the reported high levels of ABAD in AD but also under conditions of ischaemia (Yan et al., 1999, Yan et al., 2000).

I investigated the effects of reducing glucose levels in the medium surrounding cells and exploring its effect directly on the activity of ABAD. It is interesting to note that Cunnane et al. (2011) reported that within the brain, levels of ketone-metabolising enzymes are not altered by changes in glucose, and I too have shown

this is also true when investigating the protein expression of ABAD, as under decreased levels of glucose I did not see any changes of proteins expression (figure 4.5). However, this suggests that any changes in expression of ketone-metabolising enzymes such as ABAD is a consequence of another factor. In this case the instigating factor(s) could be changes in the available substrates or even the presence of Aβ modulating substrate specificity. Yan et al. (1999) previously proposed that Aβ induces cytotoxicity through ABAD by modifying ABAD's substrate specificity to using linear alcohols and that this reaction consequently causes an accumulation of toxic aldehydes (e.g. 4-HNE and MDA) . My results indicate that the suggestion that Aβ can alter the substrates that ABAD can use, this could be investigated using the (-)-CHANA assay by repeating the reduced glucose assays but now in the presence of Aβ. Previous work has shown that the addition of Aβ to cells expressing ABAD has an overall inhibitory effect on ABAD activity (Muirhead et al., 2010a), but the question remains does it change ABAD's substrate specificity? The substrate preference of ABAD could be explored under conditions either where Aβ is increased or glucose levels are depleted by the addition of other known substrates of ABAD to the CHANA assay and observing the changes in the fluorescence emitted i.e. if a substrate is still utilised then it will replace the CHANA substrate with a subsequent reduction in fluorescence.

In the absence of Aβ, I have managed to show that decreased glucose within HEK 293 and SK-N-SH cells causes an increase in the activity of the enzyme ABAD. This agrees with the findings from Yan et al. (2000), where wild type mice were reported to up-regulate ABAD protein levels under cellular stress (ischemia) with subsequent reduction in the levels of the ABAD substrate, β-hydroxybutyrate. However, I have found that the actual activity of ABAD is enhanced when energy sources are depleted whereas it was previously only inferred as the protein levels are increased. Future work will look further into the mechanisms of regulation of this ABAD activity but at the post-translational modification level. At present nothing is known about this with regard to ABAD activity, but it is possible that that the drop in glucose levels leads to, for example, changes in the phosphorylation state of this protein which are commonly used to modify

metabolic enzyme activity. As such my experience in mass spectrometry (see below) could be utilised to look into this.

The finding that ketonegenesis in AD patients aids the survival of neurons through increasing energy production when neurons are lacking glucose, signifies that the addition of a more specific energy substrate would increase these benefits further. Also with the knowledge that the introduction of higher levels of fatty acids into the diet of AD patients results in these patients displaying cognitive improvement, perhaps suggests that the inhibition of ABAD by Aβ is not an on/off encounter but a graded response (Lustbader et al., 2004, Freemantle et al., 2006, Lim et al., 2005, Henderson, 2008). By determining the preferred substrates for ABAD in the presence of Aβ then this knowledge could be translated and used as therapeutic treatments for increasing energy production in neurons.

ABAD ACTIVITY IN THE PRESENCE OF CypD

Following the findings that ABAD activity increases under reduced glucose conditions in chapter 4, and that the FRET studies in chapter 3 indicated a close association of ABAD and CypD, an investigation was conducted to see whether CypD plays a functional role through its potential interaction with ABAD by altering its metabolic activity. Under normal glucose conditions, an increase in CypD expression was observed to suppress significantly the activity of ABAD, whilst not affecting the general mitochondrial activity. This suggests that the interaction between CypD and ABAD could also be used to regulate the enzymatic function of ABAD. Therefore this interaction of ABAD and CypD may be a control point not just for CypD translocation to the mPTP but it also controls ABAD activity. Again it is unknown at present, whether this inhibition of ABAD activity is a general inhibition of its activity or whether it can also change the preferred substrates that ABAD can utilise. This warrants further exploration into the action of CypD on ABAD activity under AD like conditions. These would involve the investigation of ABAD activity in the presence of Aβ and CypD but also under reduced glucose concentrations allowing for examination of ABAD activity. In particular, it would be interesting to observe if ABAD activity is increased upon

removal of CypD activity. Cyclosporine A is an inhibitor of CypD and has been shown to protect against some of the toxicities induced by Aβ (Du et al., 2008); however it is not suitable as a drug as it has immunosuppressive side-effects and is also not specific to CypD. Therefore a more specific inhibitor such as antamanide could be used (Azzolin et al., 2011).

ABAD ACTIVITY AND LIPID COMPOSITION

The effect of ABAD on lipid metabolism was also investigated to explore if the presence of Aβ and ABAD altered the lipid composition of cells. It was found that Aβ and ABAD, when their levels of expression were increased in HEK 293 cells either singularly or together, did indeed affect the composition of lipids. Lipids are crucial for membrane structure and signalling. Their composition within membranes has been reported to influence Aβ production, for example the presence of cholesterol in membranes increases the rigidity of the membrane and as such induces the amyloidogenic cleavage of APP (Wolozin, 2001).

The change in cellular lipid composition when ABAD was expressed in HEK 293 cells revealed an increase in SM species, which affects rigidity of lipid membranes, and a shift in PE and PS lipid species, which implies a breakdown in large fatty acids. In particular the reduction of larger lipids from the lipid profile and the shift to PE and PS species when ABAD is expressed alone implies that the long chain polyunsaturated fatty acids are being metabolised to generate an alternative energy source, other than glycolysis. ABAD expression consequently increases β-oxidation and additionally, when Aβ and ABAD were expressed together, there was an overall suppression of larger lipid species. This further signifies a catabolism of fatty acids by β-oxidation in the presence of ABAD. Therefore, I have shown that expression of ABAD in HEK 293 cells does influence specific changes in lipid metabolism. This preliminary work opens up the possibility for a further more detailed investigation into the lipid and fatty acid composition when ABAD is expressed but also when Aβ is present and when glucose levels are reduced. Additionally, analysis should include exploration of the lipid composition and fatty acid content from brain material using transgenic animals that have previously

shown novel proteomic changes when ABAD is expressed with Aβ (Yao et al., 2007, Ren et al., 2008).

In this thesis, I set out to investigate the potential interaction between ABAD and CypD, the metabolic changes in ABAD activity induced by lowering glucose concentration and also the effect of ABAD expression on lipid metabolism. In summary (Figure 5.1), ABAD appears to affect many areas of metabolism in the AD brain and as such further investigations into metabolism and ABAD activity need to be explored. I have shown that under nutritional stress where glucose was depleted the activity of ABAD is in increased probably as a method to produce alternative energy sources for neurons. Additionally, I showed that CypD transiently/weakly interacts with ABAD and in so doing potentially controls ABAD activity. Lipid metabolism in AD has also been shown to be affected by the presence of Aβ and ABAD suggesting a disruption of the crucial regulatory function of lipids in AD. Most importantly is the combined finding that ABAD activity increased when glucose levels were reduced along with the shift to shorter lipids (diacyl and acyl-alkyl) when ABAD and mAPP were expressed in HEK 293 cells. An overall change in metabolism can be seen from these results. Initially an increase in ABAD activity was shown implying an increase in β-oxidation of fatty acids, when glucose levels were reduced. Additionally, when Aβ and ABAD were expressed changes in lipid catabolism were shown. These findings reveal an overall shift in energy source, connecting ABAD the crucial energy production in AD.

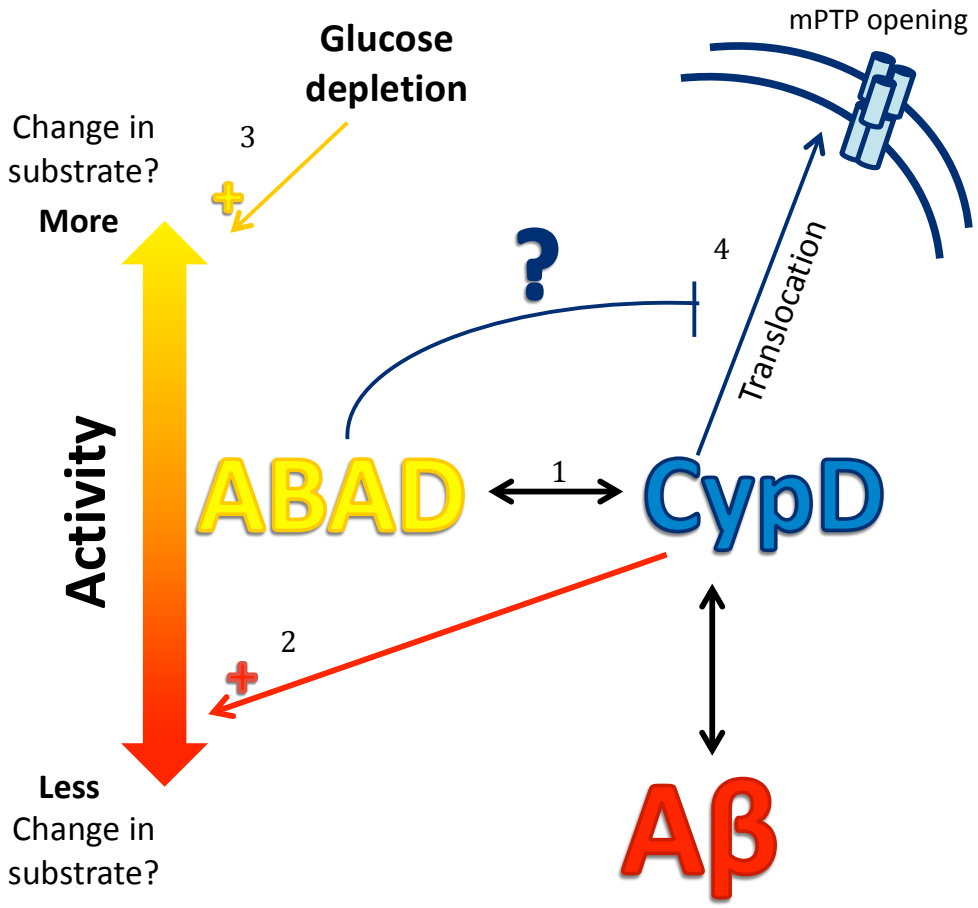

Figure 5-1: **Summarising the findings of this thesis** (1) CypD was found to interact weakly with ABAD, (2) the presence of CypD was observed to decrease the activity of ABAD in HEK 293 cells. Implying a functional role of the interaction between CypD and ABAD, CypD may endogenously regulate the activity of ABAD. 3) In conditions of Alzheimer's disease, glucose levels are depleted and as such I have shown that ABAD activity is increased. 4) The presence of Aβ in AD has been shown to cause oxidative stress and the translocation of CypD, the weak interaction between ABAD and CypD is thought to prevent the translocation of CypD to the IMM and inhibit the formation of the mPTP.

REFERENCES

AHMED, M., DAVIS, J., AUCOIN, D., SATO, T., AHUJA, S., AIMOTO, S., ELLIOTT, J. I., VAN NOSTRAND, W. E. & SMITH, S. O. 2010. Structural conversion of neurotoxic amyloid-beta(1-42) oligomers to fibrils. *Nat Struct Mol Biol,* 17**,** 561-7.

AKIYAMA, H., BARGER, S., BARNUM, S., BRADT, B., BAUER, J., COLE, G. M., COOPER, N. R., EIKELENBOOM, P., EMMERLING, M., FIEBICH, B. L., FINCH, C. E., FRAUTSCHY, S., GRIFFIN, W. S., HAMPEL, H., HULL, M., LANDRETH, G., LUE, L., MRAK, R., MACKENZIE, I. R., MCGEER, P. L., O'BANION, M. K., PACHTER, J., PASINETTI, G., PLATA-SALAMAN, C., ROGERS, J., RYDEL, R., SHEN, Y., STREIT, W., STROHMEYER, R., TOOYOMA, I., VAN MUISWINKEL, F. L., VEERHUIS, R., WALKER, D., WEBSTER, S., WEGRZYNIAK, B., WENK, G. & WYSS-CORAY, T. 2000. Inflammation and Alzheimer's disease. *Neurobiol Aging,* 21**,** 383-421.

ALBERS, D. S., AUGOOD, S. J., PARK, L. C., BROWNE, S. E., MARTIN, D. M., ADAMSON, J., HUTTON, M., STANDAERT, D. G., VONSATTEL, J. P., GIBSON, G. E. & BEAL, M. F. 2000. Frontal lobe dysfunction in progressive supranuclear palsy: evidence for oxidative stress and mitochondrial impairment. *J Neurochem,* 74**,** 878-81.

ALMEIDA, C. G., TAKAHASHI, R. H. & GOURAS, G. K. 2006. Beta-amyloid accumulation impairs multivesicular body sorting by inhibiting the ubiquitin-proteasome system. *J Neurosci,* 26**,** 4277-88.

ALZHEIMER'S RESEARCH TRUST. 2010. *Dementia 2010 executive summary* [Online]. Available: http://www.dementia2010.org/reports/Dementia2010ExecSummary.pdf [Accessed 04.01.11.

ANANDATHEERTHAVARADA, H. K., BISWAS, G., ROBIN, M. A. & AVADHANI, N. G. 2003. Mitochondrial targeting and a novel transmembrane arrest of Alzheimer's amyloid precursor protein impairs mitochondrial function in neuronal cells. *J Cell Biol,* 161**,** 41-54.

ARIAS, C., MONTIEL, T., QUIROZ-BAEZ, R. & MASSIEU, L. 2002. beta-Amyloid neurotoxicity is exacerbated during glycolysis inhibition and mitochondrial impairment in the rat hippocampus in vivo and in isolated nerve terminals: implications for Alzheimer's disease. *Exp Neurol,* 176**,** 163-74.

ASTARITA, G. & PIOMELLI, D. 2011. Towards a whole-body systems [multi-organ] lipidomics in Alzheimer's disease. *Prostaglandins Leukot Essent Fatty Acids,* 85**,** 197-203.

ATAMNA, H. & FREY, W. H., 2ND 2007. Mechanisms of mitochondrial dysfunction and energy deficiency in Alzheimer's disease. *Mitochondrion,* 7**,** 297-310.

AVILA, J. 2006. Tau phosphorylation and aggregation in Alzheimer's disease pathology. *FEBS Lett,* 580**,** 2922-7.

AZZOLIN, L., ANTOLINI, N., CALDERAN, A., RUZZA, P., SCIACOVELLI, M., MARIN, O., MAMMI, S., BERNARDI, P. & RASOLA, A. 2011. Antamanide, a derivative of Amanita phalloides, is a novel inhibitor of the mitochondrial permeability transition pore. *PLoS ONE,* 6**,** e16280.

BAINES, C. P., KAISER, R. A., PURCELL, N. H., BLAIR, N. S., OSINSKA, H., HAMBLETON, M. A., BRUNSKILL, E. W., SAYEN, M. R., GOTTLIEB, R. A., DORN, G. W., ROBBINS, J. & MOLKENTIN, J. D. 2005. Loss of cyclophilin D reveals a critical role for mitochondrial permeability transition in cell death. *Nature,* 434**,** 658-62.

BENTOURKIA, M., BOL, A., IVANOIU, A., LABAR, D., SIBOMANA, M., COPPENS, A., MICHEL, C., COSNARD, G. & DE VOLDER, A. G. 2000. Comparison of regional cerebral blood flow and glucose metabolism in the normal brain: effect of aging. *J Neurol Sci,* 181**,** 19-28.

BLASS, J. P. 2000. The mitochondrial spiral. An adequate cause of dementia in the Alzheimer's syndrome. *Ann N Y Acad Sci,* 924**,** 170-83.

BLENNOW, K., HAMPEL, H., WEINER, M. & ZETTERBERG, H. 2010. Cerebrospinal fluid and plasma biomarkers in Alzheimer disease. *Nature Reviews Neurology,* 6**,** 131-144.

BLENNOW, K., J DE LEON, M., ZETTERBERG,H. 2006. Alzheimer's disease. *Lancet,* 368**,** 387-403.

BLIGH, E. G. & DYER, W. J. 1959. A rapid method of total lipid extraction and purification. *Can J Biochem Physiol,* 37**,** 911-7.

BORGER, E., AITKEN, L., MUIRHEAD, K. E. A., ALLEN, E. Z., AINGE, J. A., CONWAY, S. J. & GUNN MOORE, F. J. 2011. Mitochondrial beta-amyloid in Alzheimer's disease. *Biochemical Society Transactions,* 39**,** 868-873.

BOROVECKI, F., KLEPAC, N., MUCK-SELER, D., HAJNSEK, S., MUBRIN, Z. & PIVAC, N. 2011. Unraveling the biological mechanisms in Alzheimer's disease — Lessons from genomics. *Progress in Neuro-Psychopharmacology and Biological Psychiatry,* 35**,** 340-347.

BROPHY, V. A., TAVARE, J. M. & RIVETT, A. J. 2002. Treatment of COS-7 cells with proteasome inhibitors or gamma-interferon reduces the increase in caspase 3 activity associated with staurosporine-induced apoptosis. *Arch Biochem Biophys,* 397**,** 199-205.

BUBBER, P., HAROUTUNIAN, V., FISCH, G., BLASS, J. P. & GIBSON, G. E. 2005. Mitochondrial abnormalities in Alzheimer brain: mechanistic implications. *Ann Neurol,* 57**,** 695-703.

BUCKIG, A., TIKKANEN, R., HERZOG, V. & SCHMITZ, A. 2002. Cytosolic and nuclear aggregation of the amyloid beta-peptide following its expression in the endoplasmic reticulum. *Histochem Cell Biol,* 118**,** 353-60.

CASPERSEN, C., WANG, N., YAO, J., SOSUNOV, A., CHEN, X., LUSTBADER, J. W., WEI XU, H., STERN, D., MCKHANN, G. & YAN, S. D. 2005. Mitochondrial Aβ: a potential focal point for neuronal metabolic dysfunction in Alzheimer's disease. *FASEB J.***,** 05-3735fje.

CHEN, J. X. & YAN, S. D. 2007. Amyloid-beta-induced mitochondrial dysfunction. *J Alzheimers Dis,* 12**,** 177-84.

CHEN, J. X. & YAN, S. S. 2010. Role of Mitochondrial Amyloid-β in Alzheimer's Disease *Journal of Alzheimer's Disease.* Wednesday, May 12, 2010 ed.

CHICCO, A. J. & SPARAGNA, G. C. 2007. Role of cardiolipin alterations in mitochondrial dysfunction and disease. *Am J Physiol Cell Physiol,* 292**,** C33-44.

CHOU, J. L., SHENOY, D. V., THOMAS, N., CHOUDHARY, P. K., LAFERLA, F. M., GOODMAN, S. R. & BREEN, G. A. 2011. Early dysregulation of the mitochondrial proteome in a mouse model of Alzheimer's disease. *J Proteomics,* 74**,** 466-79.

CITRON, M., TEPLOW, D. B. & SELKOE, D. J. 1995. Generation of amyloid beta protein from its precursor is sequence specific. *Neuron,* 14**,** 661-70.

CLEGG, R. M. 1992. Fluorescence resonance energy transfer and nucleic acids. *Methods Enzymol,* 211**,** 353-88.

CLONTECH. 2003. Living Colors: User Manual Volume II. Available: http://www.molecularinfo.com/MTM/K/K2/K2-1/RedManual.pdf [Accessed 22.11.11].

COLE, G. M., MA, Q. L. & FRAUTSCHY, S. A. 2009. Omega-3 fatty acids and dementia. *Prostaglandins Leukot Essent Fatty Acids,* 81**,** 213-21.

CONNERN, C. P. & HALESTRAP, A. P. 1992. Purification and N-terminal sequencing of peptidyl-prolyl cis-trans-isomerase from rat liver mitochondrial matrix reveals the existence of a distinct mitochondrial cyclophilin. *Biochem J,* 284 (Pt 2)**,** 381-5.

CONNERN, C. P. & HALESTRAP, A. P. 1994. Recruitment of mitochondrial cyclophilin to the mitochondrial inner membrane under conditions of oxidative stress that enhance the opening of a calcium-sensitive non-specific channel. *Biochem. J.,* 302**,** 321-324.

COOK, D. G., FORMAN, M. S., SUNG, J. C., LEIGHT, S., KOLSON, D. L., IWATSUBO, T., LEE, V. M. & DOMS, R. W. 1997. Alzheimer's A beta(1-42) is generated in the endoplasmic reticulum/intermediate compartment of NT2N cells. *Nat Med,* 3**,** 1021-3.

CORDY, J. M., HUSSAIN, I., DINGWALL, C., HOOPER, N. M. & TURNER, A. J. 2003. Exclusively targeting beta-secretase to lipid rafts by GPI-anchor addition up-regulates beta-site processing of the amyloid precursor protein. *Proc Natl Acad Sci U S A,* 100**,** 11735-40.

CROMPTON, M., COSTI, A., HAYAT, L. 1987. Evidence for the presence of a reversible Ca2+-dependent pore activated by oxidative stress in heart mitochondria. *The journal of Biochemistry,* 245**,** 915-918.

CROMPTON, M., VIRJI, S. & WARD, J. M. 1998. Cyclophilin-D binds strongly to complexes of the voltage-dependent anion channel and the adenine nucleotide translocase to form the permeability transition pore. *Eur J Biochem,* 258**,** 729-35.

CRUTS, M., DERMAUT, B., RADEMAKERS, R., ROKS, G., VAN DEN BROECK, M., MUNTEANU, G., VAN DUIJN, C. M. & VAN BROECKHOVEN, C. 2001. Amyloid beta secretase gene (BACE) is neither mutated in nor associated with early-onset Alzheimer's disease. *Neurosci Lett,* 313**,** 105-7.

CULVENOR, J. G., MAHER, F., EVIN, G., MALCHIODI-ALBEDI, F., CAPPAI, R., UNDERWOOD, J. R., DAVIS, J. B., KARRAN, E. H., ROBERTS, G. W., BEYREUTHER, K. & MASTERS, C. L. 1997. Alzheimer's disease-associated presenilin 1 in neuronal cells: evidence for localization to the endoplasmic reticulum-Golgi intermediate compartment. *J Neurosci Res,* 49**,** 719-31.

CUNNANE, S., NUGENT, S., ROY, M., COURCHESNE-LOYER, A., CROTEAU, E., TREMBLAY, S., CASTELLANO, A., PIFFERI, F., BOCTI, C., PAQUET, N.,

BEGDOURI, H., BENTOURKIA, M., TURCOTTE, E., ALLARD, M., BARBERGER-GATEAU, P., FULOP, T. & RAPOPORT, S. I. 2011. Brain fuel metabolism, aging, and Alzheimer's disease. *Nutrition,* 27**,** 3-20.

D'ANDREA, M. R., NAGELE, R. G., GUMULA, N. A., REISER, P. A., POLKOVITCH, D. A., HERTZOG, B. M. & ANDRADE-GORDON, P. 2002. Lipofuscin and Abeta42 exhibit distinct distribution patterns in normal and Alzheimer's disease brains. *Neurosci Lett,* 323**,** 45-9.

DAJANI, S. 2011. *The Mini Mental State Examination (MMSE)* [Online]. Available: http://www.alzheimers.org.uk/site/scripts/documents_info.php?documentID=121 [Accessed 26 September 2011 2011].

DE STROOPER, B. 2007. Loss-of-function presenilin mutations in Alzheimer disease. Talking Point on the role of presenilin mutations in Alzheimer disease. *EMBO Rep,* 8**,** 141-6.

DELHAIZE, E., HEBB, D. M., RICHARDS, K. D., LIN, J. M., RYAN, P. R. & GARDNER, R. C. 1999. Cloning and expression of a wheat (Triticum aestivum L.) phosphatidylserine synthase cDNA. Overexpression in plants alters the composition of phospholipids. *J Biol Chem,* 274**,** 7082-8.

DESGRANGES, B., BARON, J. C., DE LA SAYETTE, V., PETIT-TABOUE, M. C., BENALI, K., LANDEAU, B., LECHEVALIER, B. & EUSTACHE, F. 1998. The neural substrates of memory systems impairment in Alzheimer's disease. A PET study of resting brain glucose utilization. *Brain,* 121 (Pt 4)**,** 611-31.

DI PAOLO, G. & KIM, T. W. 2011. Linking lipids to Alzheimer's disease: cholesterol and beyond. *Nat Rev Neurosci,* 12**,** 284-96.

DODART, J. C., MATHIS, C., BALES, K. R., PAUL, S. M. & UNGERER, A. 1999. Early regional cerebral glucose hypometabolism in transgenic mice overexpressing the V717F beta-amyloid precursor protein. *Neurosci Lett,* 277**,** 49-52.

DOMINGUEZ-SOLIS, J. R., HE, Z., LIMA, A., TING, J., BUCHANAN, B. B. & LUAN, S. 2008. A cyclophilin links redox and light signals to cysteine biosynthesis and stress responses in chloroplasts. *Proc Natl Acad Sci U S A,* 105**,** 16386-91.

DU, H., GUO, L., FANG, F., CHEN, D., SOSUNOV, A. A., MCKHANN, G. M., YAN, Y., WANG, C., ZHANG, H., MOLKENTIN, J. D., GUNN-MOORE, F. J., VONSATTEL, J. P., ARANCIO, O., CHEN, J. X. & YAN, S. D. 2008. Cyclophilin D deficiency attenuates mitochondrial and neuronal perturbation and ameliorates learning and memory in Alzheimer's disease. *Nat Med,* 14**,** 1097-105.

DU, H., GUO, L., ZHANG, W., RYDZEWSKA, M. & YAN, S. 2009. Cyclophilin D deficiency improves mitochondrial function and learning/memory in aging Alzheimer disease mouse model. *Neurobiol Aging*.

DU, H., YAN, S. 2010. Mitochondrial permeability transition pore in Alzheimer's disease: Cyclophilin D and amyloid beta. *Biochimica et Biophysica Acta,* 1802**,** 198-204.

EHEHALT, R., KELLER, P., HAASS, C., THIELE, C. & SIMONS, K. 2003. Amyloidogenic processing of the Alzheimer beta-amyloid precursor protein depends on lipid rafts. *J Cell Biol,* 160**,** 113-23.

ERDOGAN, T. 2011. Optical filters for wavelength selection in fluorescence instrumentation. *In:* CROSSTALK, F. (ed.) *Curr Protoc Cytom.* 2011/04/02 ed.

ERTEKIN-TANER, N. 2007. Genetics of Alzheimer's disease: a centennial review. *Neurologic Clinics,* 25**,** 611-667.

FALKEVALL, A., ALIKHANI, N., BHUSHAN, S., PAVLOV, P. F., BUSCH, K., JOHNSON, K. A., ENEQVIST, T., TJERNBERG, L., ANKARCRONA, M. & GLASER, E. 2006. Degradation of the Amyloid beta-Protein by the Novel Mitochondrial Peptidasome, PreP. *J. Biol. Chem.,* 281**,** 29096-29104.

FASSBENDER, K., SIMONS, M., BERGMANN, C., STROICK, M., LUTJOHANN, D., KELLER, P., RUNZ, H., KUHL, S., BERTSCH, T., VON BERGMANN, K., HENNERICI, M., BEYREUTHER, K. & HARTMANN, T. 2001. Simvastatin strongly reduces levels of Alzheimer's disease beta -amyloid peptides Abeta 42 and Abeta 40 in vitro and in vivo. *Proc Natl Acad Sci U S A,* 98**,** 5856-61.

FIRESTONE, G. L. & WINGUTH, S. D. 1990. Immunoprecipitation of proteins. *Methods Enzymol,* 182**,** 688-700.

FLORENT-BECHARD, S., DESBENE, C., GARCIA, P., ALLOUCHE, A., YOUSSEF, I., ESCANYE, M. C., KOZIEL, V., HANSE, M., MALAPLATE-ARMAND, C., STENGER, C., KRIEM, B., YEN-POTIN, F. T., OLIVIER, J. L., PILLOT, T. & OSTER, T. 2009. The essential role of lipids in Alzheimer's disease. *Biochimie,* 91**,** 804-9.

FOLEY, P. 2010. Lipids in Alzheimer's disease: A century-old story. *Biochim Biophys Acta,* 1801**,** 750-3.

FREEMANTLE, E., VANDAL, M., TREMBLAY-MERCIER, J., TREMBLAY, S., BLACHERE, J. C., BEGIN, M. E., BRENNA, J. T., WINDUST, A. & CUNNANE, S. C. 2006. Omega-3 fatty acids, energy substrates, and brain function during aging. *Prostaglandins Leukot Essent Fatty Acids,* 75**,** 213-20.

FROEMMING, M. K. & SAMES, D. 2007. Harnessing Functional Plasticity of Enzymes: A Fluorogenic Probe for Imaging 17β-HSD10 Dehydrogenase, an Enzyme Involved in Alzheimer's and Parkinson's Diseases. *Journal of the American Chemical Society,* 129**,** 14518-14522.

FUKUI, H., DIAZ, F., GARCIA, S. & MORAES, C. T. 2007. Cytochrome c oxidase deficiency in neurons decreases both oxidative stress and amyloid formation in a mouse model of Alzheimer's disease. *Proc Natl Acad Sci U S A,* 104**,** 14163-8.

FURST, A. J., RABINOVICI, G. D., ROSTOMIAN, A. H., STEED, T., ALKALAY, A., RACINE, C., MILLER, B. L. & JAGUST, W. J. 2010. Cognition, glucose metabolism and amyloid burden in Alzheimer's disease. *Neurobiol Aging*.

GAGE, F. H., KELLY, P. A. & BJORKLUND, A. 1984. Regional changes in brain glucose metabolism reflect cognitive impairments in aged rats. *J Neurosci,* 4**,** 2856-65.

GIBSON, G. E., PARK, L. C., ZHANG, H., SORBI, S. & CALINGASAN, N. Y. 1999. Oxidative stress and a key metabolic enzyme in Alzheimer brains, cultured cells, and an animal model of chronic oxidative deficits. *Ann N Y Acad Sci,* 893**,** 79-94.

GIORGIO, V., SORIANO, M.E., BASSO, E., BISETTO, E., LIPPE, G., FORTE, M.A., BERNARDI, P. 2010. Cyclophilin D in mitochondrial pathophysiology. *Biochimica et Biophysica Acta,* 1797.

GLABE, C. G. 2006. Common mechanisms of amyloid oligomer pathogenesis in degenerative disease. *Neurobiol Aging,* 27**,** 570-5.

GOEDERT, M., WISCHIK, C. M., CROWTHER, R. A., WALKER, J. E. & KLUG, A. 1988. Cloning and sequencing of the cDNA encoding a core protein of the paired helical filament of Alzheimer disease: Identification as the microtubule-associated protein tau. *Proc. Nati. Acad. Sci. USA,* 85**,** 4051-4055.

GOLDE, T. E., ESTUS, S., YOUNKIN, L. H., SELKOE, D. J. & YOUNKIN, S. G. 1992. Processing of the amyloid protein precursor to potentially amyloidogenic derivatives. *Science,* 255**,** 728-30.

GOURAS, G. K., ALMEIDA, C. G. & TAKAHASHI, R. H. 2005. Intraneuronal Abeta accumulation and origin of plaques in Alzheimer's disease. *Neurobiol Aging,* 26**,** 1235-44.

GOURAS, G. K., TSAI, J., NASLUND, J., VINCENT, B., EDGAR, M., CHECLER, F., GREENFIELD, J. P., HAROUTUNIAN, V., BUXBAUM, J. D., XU, H., GREENGARD, P. & RELKIN, N. R. 2000. Intraneuronal Abeta42 accumulation in human brain. *Am J Pathol,* 156**,** 15-20.

GRIMM, M. O., GRIMM, H. S., PATZOLD, A. J., ZINSER, E. G., HALONEN, R., DUERING, M., TSCHAPE, J. A., DE STROOPER, B., MULLER, U., SHEN, J. & HARTMANN, T. 2005. Regulation of cholesterol and sphingomyelin metabolism by amyloid-beta and presenilin. *Nat Cell Biol,* 7**,** 1118-23.

GROSSFIELD, A., FELLER, S. E. & PITMAN, M. C. 2006. A role for direct interactions in the modulation of rhodopsin by omega-3 polyunsaturated lipids. *Proc Natl Acad Sci U S A,* 103**,** 4888-93.

HAAS, F. H., HEEG, C., QUEIROZ, R., BAUER, A., WIRTZ, M. & HELL, R. 2008. Mitochondrial serine acetyltransferase functions as a pacemaker of cysteine synthesis in plant cells. *Plant Physiol,* 148**,** 1055-67.

HAASS, C., HUNG, A. Y., SCHLOSSMACHER, M. G., TEPLOW, D. B. & SELKOE, D. J. 1993. beta-Amyloid peptide and a 3-kDa fragment are derived by distinct cellular mechanisms. *J Biol Chem,* 268**,** 3021-4.

HAASS, C., SCHLOSSMACHER, M. G., HUNG, A. Y., VIGO-PELFREY, C., MELLON, A., OSTASZEWSKI, B. L., LIEBERBURG, I., KOO, E. H., SCHENK, D., TEPLOW, D. B. & ET AL. 1992. Amyloid beta-peptide is produced by cultured cells during normal metabolism. *Nature,* 359**,** 322-5.

HALESTRAP, A. 2005. Biochemistry: a pore way to die. *Nature,* 434**,** 578-9.

HALESTRAP, A. P. & BRENNER, C. 2003. The adenine nucleotide translocase: a central component of the mitochondrial permeability transition pore and key player in cell death. *Curr Med Chem,* 10**,** 1507-25.

HALESTRAP, A. P., MCSTAY, G. P. & CLARKE, S. J. 2002. The permeability transition pore complex: another view. *Biochimie,* 84**,** 153-66.

HAN, X., ROZEN, S., BOYLE, S. H., HELLEGERS, C., CHENG, H., BURKE, J. R., WELSH-BOHMER, K. A., DPRAISWAMY, P. M. & KADDURAH-DAOUK, R. 2011. Metabolomics in Early Alzheimer's Disease: Identification of Altered Plasma Sphingolipidome Using Shotgun Lipidomics. *PLoS ONE,* 6**,** e21643.

HANDSCHUMACHER, R. E., HARDING, M. W., RICE, J., DRUGGE, R. J. & SPEICHER, D. W. 1984. Cyclophilin: a specific cytosolic binding protein for cyclosporin A. *Science,* 226**,** 544-7.

HANSSON PETERSEN, C. A., ALIKHANI, N., BEHBAHANI, H., WIEHAGER, B., PAVLOV, P. F., ALAFUZOFF, I., LEINONEN, V., ITO, A., WINBLAD, B., GLASER, E. & ANKARCRONA, M. 2008. The amyloid beta-peptide is imported into mitochondria via the TOM import machinery and localized to mitochondrial cristae. *Proc Natl Acad Sci U S A,* 105**,** 13145-50.

HAROLD, D., ABRAHAM, R., HOLLINGWORTH, P., SIMS, R., GERRISH, A., HAMSHERE, M. L., PAHWA, J. S., MOSKVINA, V., DOWZELL, K., WILLIAMS, A., JONES, N., THOMAS, C., STRETTON, A., MORGAN, A. R., LOVESTONE, S., POWELL, J., PROITSI, P., LUPTON, M. K., BRAYNE, C., RUBINSZTEIN, D. C., GILL, M., LAWLOR, B., LYNCH, A., MORGAN, K., BROWN, K. S., PASSMORE, P. A., CRAIG, D., MCGUINNESS, B., TODD, S., HOLMES, C., MANN, D., SMITH, A. D., LOVE, S., KEHOE, P. G., HARDY, J., MEAD, S., FOX, N., ROSSOR, M., COLLINGE, J., MAIER, W., JESSEN, F., SCHURMANN, B., VAN DEN BUSSCHE, H., HEUSER, I., KORNHUBER, J., WILTFANG, J., DICHGANS, M., FROLICH, L., HAMPEL, H., HULL, M., RUJESCU, D., GOATE, A. M., KAUWE, J. S., CRUCHAGA, C., NOWOTNY, P., MORRIS, J. C., MAYO, K., SLEEGERS, K., BETTENS, K., ENGELBORGHS, S., DE DEYN, P. P., VAN BROECKHOVEN, C., LIVINGSTON, G., BASS, N. J., GURLING, H., MCQUILLIN, A., GWILLIAM, R., DELOUKAS, P., AL-CHALABI, A., SHAW, C. E., TSOLAKI, M., SINGLETON, A. B., GUERREIRO, R., MUHLEISEN, T. W., NOTHEN, M. M., MOEBUS, S., JOCKEL, K. H., KLOPP, N., WICHMANN, H. E., CARRASQUILLO, M. M., PANKRATZ, V. S., YOUNKIN, S. G., HOLMANS, P. A., O'DONOVAN, M., OWEN, M. J. & WILLIAMS, J. 2009. Genome-wide association study identifies variants at CLU and PICALM associated with Alzheimer's disease. *Nat. Genet.,* 41**,** 1088-93.

HARRIS, J. R. 2008. Cholesterol binding to amyloid-beta fibrils: a TEM study. *Micron,* 39**,** 1192-6.

HASHIMOTO, M., HOSSAIN, S., SHIMADA, T., SUGIOKA, K., YAMASAKI, H., FUJII, Y., ISHIBASHI, Y., OKA, J. & SHIDO, O. 2002. Docosahexaenoic acid provides protection from impairment of learning ability in Alzheimer's disease model rats. *J Neurochem,* 81**,** 1084-91.

HAZELTON, J. L., PETRASHEUSKAYA, M., FISKUM, G. & KRISTIAN, T. 2009. Cyclophilin D is expressed predominantly in mitochondria of gamma-aminobutyric acidergic interneurons. *J Neurosci Res,* 87**,** 1250-9.

HE, X.-Y., MERZ, G., MEHTA, P., SCHULZ, H. & YANG, S.-Y. 1999. Human Brain Short Chain L-3-Hydroxyacyl Coenzyme A Dehydrogenase Is a Single-domain Multifunctional Enzyme. Characterization of a novel 17-ß-hydroxysteroid dehydrogenase. *J. Biol. Chem.,* 274**,** 15014-15019.

HE, X.-Y., SCHULZ, H. & YANG, S.-Y. 1998. A Human Brain L-3-Hydroxyacyl-coenzyme A Dehydrogenase Is Identical to an Amyloid ß -Peptide-binding Protein Involved in Alzheimer's Disease. *J. Biol. Chem.,* 273**,** 10741-10746.

HE, X. Y., MERZ, G., YANG, Y. Z., MEHTA, P., SCHULZ, H. & YANG, S. Y. 2001. Characterization and localization of human type10 17beta-hydroxysteroid dehydrogenase. *Eur J Biochem,* 268**,** 4899-907.

HENDERSON, S. T. 2008. Ketone bodies as a therapeutic for Alzheimer's disease. *Neurotherapeutics,* 5**,** 470-480.

HIRAI, K., ALLEV, G., NUNOMURE, A., FUJLOKA, H., RUSSELL, R.L., ATWOOD, C.S., JOHNSON, A.B., KRESS, Y., VINTERS, H.V., TABATON, M., SHIMOHAMA, S., CASH, A.D., SLEDLAK, S.L., HARRIS, P.L.R., JONES, P.K., PETERSEN, R.B., PERRY, G., SMITH, M.A. 2001. Mitochondrial Abnormalities in Alzheimer's Disease. *The journal of Neuroscience,* 21**,** 3017-3023.

HUANG, H. M., ZHANG, H., XU, H. & GIBSON, G. E. 2003. Inhibition of the alpha-ketoglutarate dehydrogenase complex alters mitochondrial function and cellular calcium regulation. *Biochim Biophys Acta,* 1637**,** 119-26.

IQBAL, K., ALONSO ADEL, C., CHEN, S., CHOHAN, M. O., EL-AKKAD, E., GONG, C. X., KHATOON, S., LI, B., LIU, F., RAHMAN, A., TANIMUKAI, H. & GRUNDKE-IQBAL, I. 2005. Tau pathology in Alzheimer disease and other tauopathies. *Biochim Biophys Acta,* 1739**,** 198-210.

ISHII, K., KITAGAKI, H., KONO, M. & MORI, E. 1996. Decreased medial temporal oxygen metabolism in Alzheimer's disease shown by PET. *J Nucl Med,* 37**,** 1159-65.

JACK, C., R, JR., , BERNSTEIN, M., A., , FOX, N. C., THOMPSON, P., ALEXANDER, G., HARVEY, D., BOROWSKI, B., BRITSON, P. J., WHITWELL, J. L., WARD, C., DALE, A. M., FELMLEE, J. P., GUNTER, J. L., HILL, D. L. G., KILLIANY, R., SCHUFF, N., FOX-BOSETTI, S., LIN, C., STUDHOLME, C., DECARLI, C. S., KRUEGER, G., WARD, H. A., METZGER, G. J., SCOTT, K. T., MALLOZZI, R., BLEZEK, D., LEVY, J., DEBBINS, J. P., FLEISHER, A. S., ALBERT, M., GREEN, R., BARTZOIKS, G., MUGLER, J. & WEINER, M. 2008. The Alzheimer's Disease Neuroimaging Initiative (ADNI): MRI methods. *Journal of Magnetic Resonance Imaging: JMRI,* 27**,** 685-691.

JAZBUTYTE, V., KEHL, F., NEYSES, L. & PELZER, T. 2009. Estrogen receptor alpha interacts with 17beta-hydroxysteroid dehydrogenase type 10 in mitochondria. *Biochem Biophys Res Commun,* 384**,** 450-4.

JUDD, N. 2011. *Am I at risk of developing dementia?* [Online]. Alzheimer's Society. Available: http://www.alzheimers.org.uk/site/scripts/documents_info.php?documentID=102 [Accessed 26 September 2011 2011].

KAMBOH, M. I., MINSTER, R. L., DEMIRICI, F. Y., GANGULI, M., DEKOSY, S. T., LOPEZ, O. L. & BARMADA, M. M. *in press*. Association of CLU and PICALM variants with Alzheimer's disease. *Neurobiology of Aging*.

KASHIWAYA, Y., TAKESHIMA, T., MORI, N., NAKASHIMA, K., CLARKE, K. & VEECH, R. L. 2000. D-beta-hydroxybutyrate protects neurons in models of Alzheimer's and Parkinson's disease. *Proc Natl Acad Sci U S A,* 97**,** 5440-4.

KAWARABAYASHI, T., SHOJI, M., YOUNKIN, L. H., WEN-LANG, L., DICKSON, D. W., MURAKAMI, T., MATSUBARA, E., ABE, K., ASHE, K. H. & YOUNKIN, S. G. 2004. Dimeric amyloid beta protein rapidly accumulates in lipid rafts followed by apolipoprotein E and phosphorylated tau accumulation in the Tg2576 mouse model of Alzheimer's disease. *J Neurosci,* 24**,** 3801-9.

KAYED, R., SOKOLOV, Y., EDMONDS, B., MCINTIRE, T. M., MILTON, S. C., HALL, J. E. & GLABE, C. G. 2004. Permeabilization of lipid bilayers is a common

conformation-dependent activity of soluble amyloid oligomers in protein misfolding diseases. *J Biol Chem,* 279**,** 46363-6.

KENNEDY, A. M., FRACKOWIAK, R. S., NEWMAN, S. K., BLOOMFIELD, P. M., SEAWARD, J., ROQUES, P., LEWINGTON, G., CUNNINGHAM, V. J. & ROSSOR, M. N. 1995. Deficits in cerebral glucose metabolism demonstrated by positron emission tomography in individuals at risk of familial Alzheimer's disease. *Neurosci Lett,* 186**,** 17-20.

KIM, S. U., JIN, M. H., KIM, Y. S., LEE, S. H., CHO, Y. S., CHO, K. J., LEE, K. S., KIM, Y. I., KIM, G. W., KIM, J. M., LEE, T. H., LEE, Y. H., SHONG, M., KIM, H. C., CHANG, K. T., YU, D. Y. & LEE, D. S. 2011. Peroxiredoxin II preserves cognitive function against age-linked hippocampal oxidative damage. *Neurobiol Aging,* 32**,** 1054-68.

KISSINGER, C. R., REJTO, P. A., PELLETIER, L. A., THOMSON, J. A., SHOWALTER, R. E., ABREO, M. A., AGREE, C. S., MARGOSIAK, S., MENG, J. J., AUST, R. M., VANDERPOOL, D., LI, B., TEMPCZYK-RUSSELL, A. & VILLAFRANCA, J. E. 2004. Crystal Structure of Human ABAD/HSD10 with a Bound Inhibitor: Implications for Design of Alzheimer's Disease Therapeutics. *Journal of Molecular Biology,* 342**,** 943-952.

KLUGER, R. & ALAGIC, A. 2004. Chemical cross-linking and protein-protein interactions-a review with illustrative protocols. *Bioorg Chem,* 32**,** 451-72.

KLUNK, W. E., ENGLER, H., NORDBERG, A., WANG, Y., BLOMQVIST, G., HOLT, D. P., BERGSTROM, M., SAVITCHEVA, I., HUANG, G. F., ESTRADA, S., AUSEN, B., DEBNATH, M. L., BARLETTA, J., PRICE, J. C., SANDELL, J., LOPRESTI, B. J., WALL, A., KOIVISTO, P., ANTONI, G., MATHIS, C. A. & LANGSTROM, B. 2004. Imaging brain amyloid in Alzheimer's disease with Pittsburgh Compound-B. *Ann Neurol,* 55**,** 306-19.

KOBAYASHI, A., JIANG, L. L. & HASHIMOTO, T. 1996. Two mitochondrial 3-hydroxyacyl-CoA dehydrogenases in bovine liver. *J Biochem,* 119**,** 775-82.

KOJRO, E., GIMPL, G., LAMMICH, S., MARZ, W. & FAHRENHOLZ, F. 2001. Low cholesterol stimulates the nonamyloidogenic pathway by its effect on the alpha -secretase ADAM 10. *Proc Natl Acad Sci U S A,* 98**,** 5815-20.

KRAUSKOPF, A., ERIKSSON, O., CRAIGEN, W. J., FORTE, M. A. & BERNARDI, P. 2006. Properties of the permeability transition in VDAC1(-/-) mitochondria. *Biochim Biophys Acta,* 1757**,** 590-5.

LANNFELT, L., BASUN, H., WAHLUND, L. O., ROWE, B. A. & WAGNER, S. L. 1995. Decreased alpha-secretase-cleaved amyloid precursor protein as a diagnostic marker for Alzheimer's disease. *Nat Med,* 1**,** 829-32.

LAUDERBACK, C. M., HACKETT, J. M., HUANG, F. F., KELLER, J. N., SZWEDA, L. I., MARKESBERY, W. R. & BUTTERFIELD, D. A. 2001. The glial glutamate transporter, GLT-1, is oxidatively modified by 4-hydroxy-2-nonenal in the Alzheimer's disease brain: the role of Abeta1-42. *J Neurochem,* 78**,** 413-6.

LEE, J. T., XU, J., LEE, J. M., KU, G., HAN, X., YANG, D. I., CHEN, S. & HSU, C. Y. 2004. Amyloid-beta peptide induces oligodendrocyte death by activating the neutral sphingomyelinase-ceramide pathway. *J Cell Biol,* 164**,** 123-31.

LEVIN, E., B., KANG, L., SANDERS, N. M. & DUNN-MEYNELL, A. A. 2006. Role of neuronal glucosensing in the regulation of energy homestasis. *American Diabetes Association,* 55**,** s122.

LEWIS, N. E., SCHRAMM, G., BORDBAR, A., SCHELLENBERGER, J., ANDERSEN, M. P., CHENG, J. K., PATEL, N., YEE, A., LEWIS, R. A., EILS, R., KONIG, R. & PALSSON, B. O. 2010. Large-scale in silico modeling of metabolic interactions between cell types in the human brain. *Nat Biotechnol,* 28**,** 1279-85.

LI, L., CAO, D., KIM, H., LESTER, R. & FUKUCHI, K. 2006. Simvastatin enhances learning and memory independent of amyloid load in mice. *Ann Neurol,* 60**,** 729-39.

LI, R., LINDHOLM, K., YANG, L. B., YUE, X., CITRON, M., YAN, R., BEACH, T., SUE, L., SABBAGH, M., CAI, H., WONG, P., PRICE, D. & SHEN, Y. 2004a. Amyloid beta peptide load is correlated with increased beta-secretase activity in sporadic Alzheimer's disease patients. *Proc Natl Acad Sci U S A,* 101**,** 3632-7.

LI, Y., JOHNSON, N., CAPANO, M., EDWARDS, M. & CROMPTON, M. 2004b. Cyclophilin-D promotes the mitochondrial permeability transition but has opposite effects on apoptosis and necrosis. *Biochem. J.,* 383**,** 101-109.

LI, Y., RINNE, J. O., MOSCONI, L., PIRRAGLIA, E., RUSINEK, H., DESANTI, S., KEMPPAINEN, N., NAGREN, K., KIM, B. C., TSUI, W. & DE LEON, M. J. 2008. Regional analysis of FDG and PIB-PET images in normal aging, mild cognitive impairment, and Alzheimer's disease. *Eur J Nucl Med Mol Imaging,* 35**,** 2169-81.

LIM, G. P., CALON, F., MORIHARA, T., YANG, F., TETER, B., UBEDA, O., SALEM, N., JR., FRAUTSCHY, S. A. & COLE, G. M. 2005. A diet enriched with the omega-3 fatty acid docosahexaenoic acid reduces amyloid burden in an aged Alzheimer mouse model. *J Neurosci,* 25**,** 3032-40.

LIN, M. T. & BEAL, M. F. 2006. Alzheimer's APP mangles mitochondria. *Nat Med,* 12**,** 1241-3.

LINARD, D., KANDLBINDER, A., DEGAND, H., MORSOMME, P., DIETZ, K. J. & KNOOPS, B. 2009. Redox characterization of human cyclophilin D: identification of a new mammalian mitochondrial redox sensor? *Arch Biochem Biophys,* 491**,** 39-45.

LIU, J. & LIN, A. 2005. Role of JNK activation in apoptosis: a double-edged sword. *Cell Res,* 15**,** 36-42.

LUO, M. J., MAO, L. F. & SCHULZ, H. 1995. Short-chain 3-hydroxy-2-methylacyl-CoA dehydrogenase from rat liver: purification and characterization of a novel enzyme of isoleucine metabolism. *Arch Biochem Biophys,* 321**,** 214-20.

LUSTBADER, J. W., CIRILLI, M., LIN, C., XU, H. W., TAKUMA, K., WANG, N., CASPERSEN, C., CHEN, X., POLLAK, S., CHANEY, M., TRINCHESE, F., LIU, S., GUNN-MOORE, F., LUE, L. F., WALKER, D. G., KUPPUSAMY, P., ZEWIER, Z. L., ARANCIO, O., STERN, D., YAN, S. S. & WU, H. 2004. ABAD directly links Abeta to mitochondrial toxicity in Alzheimer's disease. *Science,* 304**,** 448-52.

MACHIDA, K., HAYASHI, Y. & OSADA, H. 2002. A novel adenine nucleotide translocase inhibitor, MT-21, induces cytochrome c release by a mitochondrial permeability transition-independent mechanism. *J Biol Chem,* 277**,** 31243-8.

MAJNO, G. & JORIS, I. 1995. Apoptosis, oncosis, and necrosis. An overview of cell death. *Am J Pathol,* 146**,** 3-15.

MANCZAK, M., ANEKONDA, T. S., HENSON, E., PARK, B. S., QUINN, J. & REDDY, P. H. 2006. Mitochondria are a direct site of A beta accumulation in Alzheimer's

disease neurons: implications for free radical generation and oxidative damage in disease progression. *Hum Mol Genet,* 15**,** 1437-49.

MANDELKOW, E. M., STAMER, K., VOGEL, R., THIES, E. & MANDELKOW, E. 2003. Clogging of axons by tau, inhibition of axonal traffic and starvation of synapses. *Neurobiol Aging,* 24**,** 1079-85.

MARK, R. J., PANG, Z., GEDDES, J. W., UCHIDA, K. & MATTSON, M. P. 1997. Amyloid beta-peptide impairs glucose transport in hippocampal and cortical neurons: involvement of membrane lipid peroxidation. *J Neurosci,* 17**,** 1046-54.

MARQUES, A. T., FERNANDES, P. A. & RAMOS, M. J. 2008. Molecular dynamics simulations of the amyloid-beta binding alcohol dehydrogenase (ABAD) enzyme. *Bioorg Med Chem,* 16**,** 9511-8.

MARTY, N., DALLAPORTA, M., FORETZ, M., EMERY, M., TARUSSIO, D., BADY, I., BINNERT, C., BEERMANN, F. & THORENS, B. 2005. Regulation of glucagon secretion by glucose transporter type 2 (glut2) and astrocyte-dependent glucose sensors. *J Clin Invest,* 115**,** 3545-53.

MATTSON, M. P. 2004a. Pathways towards and away from Alzheimer's disease. *Nature,* 430**,** 631-9.

MATTSON, M. P. 2004b. Pathways towards and away from Alzheimer's disease: APP cut down to size. Nature.

MATZ, M. V., FRADKOV, A. F., LABAS, Y. A., SAVITSKY, A. P., ZARAISKY, A. G., MARKELOV, M. L. & LUKYANOV, S. A. 1999. Fluorescent proteins from nonbioluminescent Anthozoa species. *Nat Biotechnol,* 17**,** 969-73.

MCGRATH, L. T., MCGLEENON, B. M., BRENNAN, S., MCCOLL, D., MC, I. S. & PASSMORE, A. P. 2001. Increased oxidative stress in Alzheimer's disease as assessed with 4-hydroxynonenal but not malondialdehyde. *QJM,* 94**,** 485-90.

MORI, S., KATO, M. & FUJISHIMA, M. 1995. Impaired maze learning and cerebral glucose utilization in aged hypertensive rats. *Hypertension,* 25**,** 545-53.

MUEHLLEHNER, G. & KARP, J. S. 2006. Positron emission tomography. *Phys Med Biol,* 51**,** R117-37.

MUIRHEAD, K. E., BORGER, E., AITKEN, L., CONWAY, S. J. & GUNN-MOORE, F. J. 2010a. The consequences of mitochondrial amyloid beta-peptide in Alzheimer's disease. *Biochem J,* 426**,** 255-70.

MUIRHEAD, K. E., FROEMMING, M., LI, X., MUSILEK, K., CONWAY, S. J., SAMES, D. & GUNN-MOORE, F. J. 2010b. (-)-CHANA, a fluorogenic probe for detecting amyloid binding alcohol dehydrogenase HSD10 activity in living cells. *ACS Chem Biol,* 5**,** 1105-14.

MUIRHEAD, K. E. A. 2011. *An investigation of the ABAD-Aβ interaction as a potential therapeutic target for the treatment of Alzheimer's disease.* Ph.D Ph.D, University of St Andrews.

MULDER, C., WAHLUND, L. O., TEERLINK, T., BLOMBERG, M., VEERHUIS, R., VAN KAMP, G. J., SCHELTENS, P. & SCHEFFER, P. G. 2003. Decreased lysophosphatidylcholine/phosphatidylcholine ratio in cerebrospinal fluid in Alzheimer's disease. *J Neural Transm,* 110**,** 949-55.

MURAKAMI, Y., OHSAWA, I., KASAHARA, T. & OHTA, S. 2009. Cytoprotective role of mitochondrial amyloid [beta] peptide-binding alcohol dehydrogenase against a cytotoxic aldehyde. *Neurobiol. Aging,* 30**,** 325-329.

NAKAGAWA, T., SHIMIZU, S., WATANABE, T., YAMAGUCHI, O., OTSU, K., YAMAGATA, H., INOHARA, H., KUBO, T. & TSUJIMOTO, Y. 2005. Cyclophilin D-dependent mitochondrial permeability transition regulates some necrotic but not apoptotic cell death. *Nature,* 434**,** 652-8.

NITSCH, R. M., BLUSZTAJN, J. K., PITTAS, A. G., SLACK, B. E., GROWDON, J. H. & WURTMAN, R. J. 1992. Evidence for a membrane defect in Alzheimer disease brain. *Proc Natl Acad Sci U S A,* 89**,** 1671-5.

OKAMURA, N., ARAI, H., HIGUCHI, M., TASHIRO, M., MATSUI, T., ITOH, M., IWATSUBO, T., TOMITA, T. & SASAKI, H. 1999. Cerebrospinal fluid levels of amyloid beta-peptide1-42, but not tau have positive correlation with brain glucose metabolism in humans. *Neurosci Lett,* 273**,** 203-7.

OLIVEIRA, T. G. & DI PAOLO, G. 2010. Phospholipase D in brain function and Alzheimer's disease. *Biochim Biophys Acta,* 1801**,** 799-805.

PADURARIU, M., CIOBICA, A., HRITCU, L., STOICA, B., BILD, W. & STEFANESCU, C. 2010. Changes of some oxidative stress markers in the serum of patients with mild cognitive impairment and Alzheimer's disease. *Neurosci Lett,* 469**,** 6-10.

PAGANI, L. & ECKERT, A. 2011. Amyloid-Beta interaction with mitochondria. *International Journal of Alzheimer's Disease***,** 12.

PARK, H. J., SEONG, Y. M., CHOI, J. Y., KANG, S. & RHIM, H. 2004. Alzheimer's disease-associated amyloid beta interacts with the human serine protease HtrA2/Omi. *Neurosci Lett,* 357**,** 63-7.

PARKER, W. D., JR., PARKS, J., FILLEY, C. M. & KLEINSCHMIDT-DEMASTERS, B. K. 1994. Electron transport chain defects in Alzheimer's disease brain. *Neurology,* 44**,** 1090-6.

PARPURA-GILL, A., BEITZ, D. & UEMURA, E. 1997. The inhibitory effects of beta-amyloid on glutamate and glucose uptakes by cultured astrocytes. *Brain Res,* 754**,** 65-71.

PEREIRA, C., SANTOS, M. S. & OLIVEIRA, C. 1999. Involvement of oxidative stress on the impairment of energy metabolism induced by A beta peptides on PC12 cells: protection by antioxidants. *Neurobiol Dis,* 6**,** 209-19.

PETTEGREW, J. W., PANCHALINGAM, K., HAMILTON, R. L. & MCCLURE, R. J. 2001. Brain membrane phospholipid alterations in Alzheimer's disease. *Neurochem Res,* 26**,** 771-82.

PIFFERI, F., JOUIN, M., ALESSANDRI, J. M., ROUX, F., PERRIERE, N., LANGELIER, B., LAVIALLE, M., CUNNANE, S. & GUESNET, P. 2010. n-3 long-chain fatty acids and regulation of glucose transport in two models of rat brain endothelial cells. *Neurochem Int,* 56**,** 703-10.

PIGINO, G., MORFINI, G., PELSMAN, A., MATTSON, M. P., BRADY, S. T. & BUSCIGLIO, J. 2003. Alzheimer's presenilin 1 mutations impair kinesin-based axonal transport. *J Neurosci,* 23**,** 4499-508.

POOLER, A. M., USARDI, A., EVANS, C. J., PHILPOTT, K. L., NOBLE, W. & HANGER, D. P. 2011. Dynamic association of tau with neuronal membranes is regulated by phosphorylation. *Neurobiol Aging*.

POWELL, A. J., READ, J. A., BANFIELD, M. J., GUNN-MOORE, F., YAN, S. D., LUSTBADER, J., STERN, A. R., STERN, D. M. & BRADY, R. L. 2000. Recognition of structurally diverse substrates by type II 3-hydroxyacyl-CoA

dehydrogenase (HADH II)/amyloid-beta binding alcohol dehydrogenase (ABAD). *J Mol Biol,* 303**,** 311-27.

REBECK, G. W., REITER, J. S., STRICKLAND, D. K. & HYMAN, B. T. 1993. Apolipoprotein E in sporadic Alzheimer's disease: allelic variation and receptor interactions. *Neuron,* 11**,** 575-580.

REGER, M. A., HENDERSON, S. T., HALE, C., CHOLERTON, B., BAKER, L. D., WATSON, G. S., HYDE, K., CHAPMAN, D. & CRAFT, S. 2004. Effects of beta-hydroxybutyrate on cognition in memory-impaired adults. *Neurobiol Aging,* 25**,** 311-4.

REN, Y. 2008. *Consequences of the interaction of Amyloid Beta with Amyloid Binding Alcohol Dehydrogenase and the Receptor for Advanced Glycation End products.* Ph.D, University of St Andrews.

REN, Y., XU, H. W., DAVEY, F., TAYLOR, M., AITON, J., COOTE, P., FANG, F., YAO, J., CHEN, D., CHEN, J. X., YAN, S. D. & GUNN-MOORE, F. J. 2008. Endophilin I expression is increased in the brains of Alzheimer disease patients. *J Biol Chem,* 283**,** 5685-91.

RICHTER, C., PARK, J. W. & AMES, B. N. 1988. Normal oxidative damage to mitochondrial and nuclear DNA is extensive. *Proceedings of the National Academy of Sciences of the United States of America,* 85**,** 6465-6467.

ROSSNER, S. 2004. New players in old amyloid precursor protein-processing pathways. *Int J Dev Neurosci,* 22**,** 467-74.

ROVELET-LECRUX, A., HANNEQUIN, D., RAUX, G., LE MEUR, N., LAQUERRIERE, A., VITAL, A., DUMANCHIN, C., FEUILLETTE, S., BRICE, A., VERCELLETTO, M., DUBAS, F., FREBOURG, T. & CAMPION, D. 2006. APP locus duplication causes autosomal dominant early-onset Alzheimer disease with cerebral amyloid angiopathy. *Nat Genet,* 38**,** 24-6.

RUGGIERO, F. M., CAFAGNA, F., PETRUZZELLA, V., GADALETA, M. N. & QUAGLIARIELLO, E. 1992. Lipid composition in synaptic and nonsynaptic mitochondria from rat brains and effect of aging. *J Neurochem,* 59**,** 487-91.

SAKAMOTO, S., ISHII, K., SASAKI, M., HOSAKA, K., MORI, T., MATSUI, M., HIRONO, N. & MORI, E. 2002. Differences in cerebral metabolic impairment between early and late onset types of Alzheimer's disease. *J Neurol Sci,* 200**,** 27-32.

SALMINEN, A., KAUPPINEN, A., SUURONEN, T., KAARNIRANTA, K. & OJALA, J. 2009. ER stress in Alzheimer's disease: a novel neuronal trigger for inflammation and Alzheimer's pathology. *J Neuroinflammation,* 6**,** 41.

SASTRE, M., STEINER, H., FUCHS, K., CAPELL, A., MULTHAUP, G., CONDRON, M. M., TEPLOW, D. B. & HAASS, C. 2001. Presenilin-dependent gamma-secretase processing of beta-amyloid precursor protein at a site corresponding to the S3 cleavage of Notch. *EMBO Rep,* 2**,** 835-41.

SCHINZEL, A. C., TAKEUCHI, O., HUANG, Z., FISHER, J. K., ZHOU, Z., RUBENS, J., HETZ, C., DANIAL, N. N., MOSKOWITZ, M. A. & KORSMEYER, S. J. 2005. Cyclophilin D is a component of mitochondrial permeability transition and mediates neuronal cell death after focal cerebral ischemia. *Proc Natl Acad Sci U S A,* 102**,** 12005-10.

SCHMIDT, A., WOLDE, M., THIELE, C., FEST, W., KRATZIN, H., PODTELEJNIKOV, A. V., WITKE, W., HUTTNER, W. B. & SOLING, H. D. 1999. Endophilin I mediates

synaptic vesicle formation by transfer of arachidonate to lysophosphatidic acid. *Nature,* 401**,** 133-41.

SCORRANO, L., PENZO, D., PETRONILLI, V., PAGANO, F. & BERNARDI, P. 2001. Arachidonic acid causes cell death through the mitochondrial permeability transition. Implications for tumor necrosis factor-alpha aopototic signaling. *J Biol Chem,* 276**,** 12035-40.

SILEIKYTE, J., PETRONILLI, V., ZULIAN, A., DABBENI-SALA, F., TOGNON, G., NIKOLOV, P., BERNARDI, P. & RICCHELLI, F. 2011. Regulation of the inner membrane mitochondrial permeability transition by the outer membrane translocator protein (peripheral benzodiazepine receptor). *J Biol Chem,* 286**,** 1046-53.

SINGH, P., SUMAN, S., CHANDNA, S. & DAS, T. K. 2009. Possible role of amyloid-beta, adenine nucleotide translocase and cyclophilin-D interaction in mitochondrial dysfunction of Alzheimer's disease. *Bioinformation,* 3**,** 440-5.

SJOBRING, U., BJORCK, L. & KASTERN, W. 1991. Streptococcal protein G. Gene structure and protein binding properties. *J Biol Chem,* 266**,** 399-405.

SODERBERG, M., EDLUND, C., KRISTENSSON, K. & DALLNER, G. 1991. Fatty acid composition of brain phospholipids in aging and in Alzheimer's disease. *Lipids,* 26**,** 421-5.

STEENBERGEN, R., NANOWSKI, T. S., BEIGNEUX, A., KULINSKI, A., YOUNG, S. G. & VANCE, J. E. 2005. Disruption of the phosphatidylserine decarboxylase gene in mice causes embryonic lethality and mitochondrial defects. *J Biol Chem,* 280**,** 40032-40.

STOOTHOFF, W. H. & JOHNSON, G. V. 2005. Tau phosphorylation: physiological and pathological consequences. *Biochim Biophys Acta,* 1739**,** 280-97.

STRYER, L. 1995. *Biochemistry,* New York, W.H. Freeman.

SWIFT, S. R. T.-M., L. 2004. Basic principles of FRAP, FLIM and FRET. *Proc. Royal. Mic. Soc,* 39**,** 3-10.

TAKAHASHI, R. H., MILNER, T. A., LI, F., NAM, E. E., EDGAR, M. A., YAMAGUCHI, H., BEAL, M. F., XU, H., GREENGARD, P. & GOURAS, G. K. 2002. Intraneuronal Alzheimer abeta42 accumulates in multivesicular bodies and is associated with synaptic pathology. *Am J Pathol,* 161**,** 1869-79.

TAKUMA, K., YAO, J., HUANG, J., XU, H., CHEN, X., LUDDY, J., TRILLAT, A. C., STERN, D. M., ARANCIO, O. & YAN, S. S. 2005. ABAD enhances Abeta-induced cell stress via mitochondrial dysfunction. *Faseb J,* 19**,** 597-8.

TAPPARO, A., KIEFFER, S., CRETIN, F., SATRE, M. & KLEIN, G. 1999. The multigene immunophilin family of Dictyostelium discoideum. Characterization of microsomal and mitochondrial cyclophilin isoforms. *Biochimie,* 81**,** 943-54.

THOMPSON, S. 2004. Immunoprecipitation and blotting: the visualization of small amounts of antigens using antibodies and lectins. *Methods Mol Med,* 94**,** 33-45.

TILLEMENT, L., LECANU, L. & PAPADOPOULOS, V. 2011. Alzheimer's disease: effects of beta-amyloid on mitochondria. *Mitochondrion,* 11**,** 13-21.

TILLEMENT, L., LECANU, L., YAO, W., GREESON, J. & PAPADOPOULOS, V. 2006. The spirostenol (22R, 25R)-20alpha-spirost-5-en-3beta-yl hexanoate blocks mitochondrial uptake of Abeta in neuronal cells and prevents Abeta-induced impairment of mitochondrial function. *Steroids,* 71**,** 725-35.

TRIMMER, P. A., KEENEY, P. M., BORLAND, M. K., SIMON, F. A., ALMEIDA, J., SWERDLOW, R. H., PARKS, J. P., PARKER, W. D., JR. & BENNETT, J. P., JR. 2004. Mitochondrial abnormalities in cybrid cell models of sporadic Alzheimer's disease worsen with passage in culture. *Neurobiol Dis,* 15**,** 29-39.

TSAI, M. S., TANGALOS, E. G., PETERSEN, R. C., SMITH, G. E., SCHAID, D. J., KOKMEN, E., IVNIK, R. J. & THIBODEAU, S. N. 1994. Apolipoprotein E: risk factor for Alzheimer disease. *American Journal of Human Genetics,* 54**,** 643-649.

TYAS, L., BROPHY, V. A., POPE, A., RIVETT, A. J. & TAVARE, J. M. 2000. Rapid caspase-3 activation during apoptosis revealed using fluorescence-resonance energy transfer. *EMBO Rep,* 1**,** 266-70.

VAN DER AUWERA, I., WERA, S., VAN LEUVEN, F. & HENDERSON, S. T. 2005. A ketogenic diet reduces amyloid beta 40 and 42 in a mouse model of Alzheimer's disease. *Nutr Metab (Lond),* 2**,** 28.

VESTERGAARD, M., HAMADA, T. & TAKAGI, M. 2008. Using model membranes for the study of amyloid beta:lipid interactions and neurotoxicity. *Biotechnol Bioeng,* 99**,** 753-63.

VOSS, T. C., DEMARCO, I. A. & DAY, R. N. 2005. Quantitative imaging of protein interactions in the cell nucleus. *Biotechniques,* 38**,** 413-24.

WALLRABE, H. & PERIASAMY, A. 2005. Imaging protein molecules using FRET and FLIM microscopy. *Curr Opin Biotechnol,* 16**,** 19-27.

WENK, M. R. 2005. The emerging field of lipidomics. *Nat Rev Drug Discov,* 4**,** 594-610.

WIRTHS, O., MULTHAUP, G., CZECH, C.,BLANCHARD, V., MOUSSAOUI, S., TREMP, G., PRADIER, L., BEYREUTHER, K., & BAYER, T.A., 2001. Intraneuronal Aβ accumulation precedes plaques formation in β-amyloid precursor protein and in presenilin-1 double-transgenic mice. . *Neuroscience Letters,* 306**,** 116-120.

WISNIEWSKI, T. & SIGURDSSON, E. M. 2010. Murine models of Alzheimer's disease and their use in developing immunotherapies. *Biochim Biophys Acta,* 1802**,** 847-59.

WOLOZIN, B. 2001. A fluid connection: cholesterol and Abeta. *Proc Natl Acad Sci U S A,* 98**,** 5371-3.

WOODFIELD, K., RUCK, A., BRDICZKA, D., HALESTRAP, A.P. 1998. Direct demonstration of a specific interaction between cyclophilin-D and the adenine nucleotide translocase confirms their role in the mitochondrial permeability transition. *The journal of Biochemistry,* 336.

WRIGHT, M. M. & MCMASTER, C. R. 2002. Phospholipid synthesis, diacylglycerol compartmentation, and apoptosis. *Biol Res,* 35**,** 223-9.

XIE, Y., DENG, S., CHEN, Z., YAN, S. & LANDRY, D. W. 2006. Identification of small-molecule inhibitors of the A-ß-ABAD interaction. *Bioorg. Med. Chem. Lett.,* 16**,** 4657-4660.

YAMAGUCHI, H., YAMAZAKI, T., ISHIGURO, K., SHOJI, M., NAKAZATO, Y. & HIRAI, S. 1992. Ultrastructural localization of Alzheimer amyloid beta/A4 protein precursor in the cytoplasm of neurons and senile plaque-associated astrocytes. *Acta Neuropathol,* 85**,** 15-22.

YAN, S. D., FU, J., SOTO, C., CHEN, X., ZHU, H., AL-MOHANNA, F., COLLISON, K., ZHU, A., STERN, E., SAIDO, T., TOHYAMA, M., OGAWA, S., ROHER, A. & STERN, D. 1997. An intracellular protein that binds amyloid-beta peptide and mediates neurotoxicity in Alzheimer's disease. *Nature,* 389**,** 689-95.

YAN, S. D., SHI, Y., ZHU, A., FU, J., ZHU, H., ZHU, Y., GIBSON, L., STERN, E., COLLISON, K., AL-MOHANNA, F., OGAWA, S., ROHER, A., CLARKE, S. G. & STERN, D. M. 1999. Role of ERAB/L-3-Hydroxyacyl-coenzyme A Dehydrogenase Type II Activity in Aß-induced Cytotoxicity. *J. Biol. Chem.,* 274**,** 2145-2156.

YAN, S. D. & STERN, D. M. 2005. Mitochondrial dysfunction and Alzheimer's disease: role of amyloid-beta peptide alcohol dehydrogenase (ABAD). *Int J Exp Pathol,* 86**,** 161-71.

YAN, S. D., ZHU, Y., STERN, E. D., HWANG, Y. C., HORI, O., OGAWA, S., FROSCH, M. P., CONNOLLY, E. S., JR., MCTAGGERT, R., PINSKY, D. J., CLARKE, S., STERN, D. M. & RAMASAMY, R. 2000. Amyloid beta -Peptide-binding Alcohol Dehydrogenase Is a Component of the Cellular Response to Nutritional Stress. *J. Biol. Chem.,* 275**,** 27100-27109.

YANG, A. J., CHANDSWANGBHUVANA, D., SHU, T., HENSCHEN, A. & GLABE, C. G. 1999. Intracellular accumulation of insoluble, newly synthesized abetan-42 in amyloid precursor protein-transfected cells that have been treated with Abeta1-42. *J Biol Chem,* 274**,** 20650-6.

YANG, S. Y., HE, X. Y. & MILLER, D. 2011. Hydroxysteroid (17beta) dehydrogenase X in human health and disease. *Mol Cell Endocrinol,* 343**,** 1-6.

YANG, S. Y., HE, X. Y. & SCHULZ, H. 2005. 3-Hydroxyacyl-CoA dehydrogenase and short chain 3-hydroxyacyl-CoA dehydrogenase in human health and disease. *FEBS J,* 272**,** 4874-83.

YAO, J., DU, H., YAN, S., FANG, F., WANG, C., LUE, L. F., GUO, L., CHEN, D., STERN, D. M., GUNN MOORE, F. J., XI CHEN, J., ARANCIO, O. & YAN, S. S. 2011. Inhibition of amyloid-beta (Abeta) peptide-binding alcohol dehydrogenase-Abeta interaction reduces Abeta accumulation and improves mitochondrial function in a mouse model of Alzheimer's disease. *J Neurosci,* 31**,** 2313-20.

YAO, J., TAYLOR, M., DAVEY, F., REN, Y., AITON, J., COOTE, P., FANG, F., CHEN, J. X., YAN, S. D. & GUNN-MOORE, F. J. 2007. Interaction of amyloid binding alcohol dehydrogenase/Abeta mediates up-regulation of peroxiredoxin II in the brains of Alzheimer's disease patients and a transgenic Alzheimer's disease mouse model. *Mol Cell Neurosci,* 35**,** 377-82.

YURKO-MAURO, K., MCCARTHY, D., ROM, D., NELSON, E. B., RYAN, A. S., BLACKWELL, A., SALEM, N., JR. & STEDMAN, M. 2010. Beneficial effects of docosahexaenoic acid on cognition in age-related cognitive decline. *Alzheimers Dement,* 6**,** 456-64.

ZAL, T. & GASCOIGNE, N. R. 2004. Photobleaching-corrected FRET efficiency imaging of live cells. *Biophys J,* 86**,** 3923-39.

ZAL, T., ZAL, M. A. & GASCOIGNE, N. R. 2002. Inhibition of T cell receptor-coreceptor interactions by antagonist ligands visualized by live FRET imaging of the T-hybridoma immunological synapse. *Immunity,* 16**,** 521-34.

ZHANG, Y., MCLAUGHLIN, R., GOODYER, C. & LEBLANC, A. 2002. Selective cytotoxicity of intracellular amyloid beta peptide1-42 through p53 and Bax in cultured primary human neurons. *J Cell Biol,* 156**,** 519-29.

ZHONG, Z., HIGAKI, J., MURAKAMI, K., WANG, Y., CATALANO, R., QUON, D. & CORDELL, B. 1994. Secretion of beta-amyloid precursor protein involves multiple cleavage sites. *J Biol Chem,* 269**,** 627-32.

APPENDIX

APPENDIX A: DNA PLASMIDS

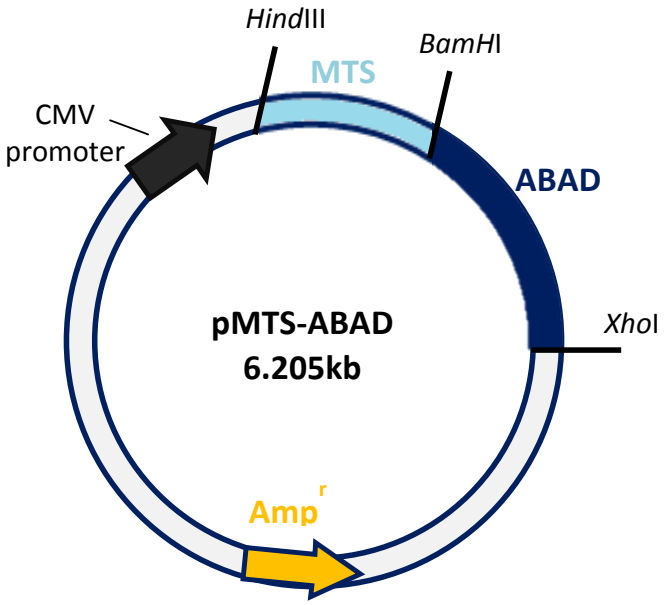

DNA plasmid pMTS-ABAD, Mitochondrial targeting sequence expressed with ABAD.

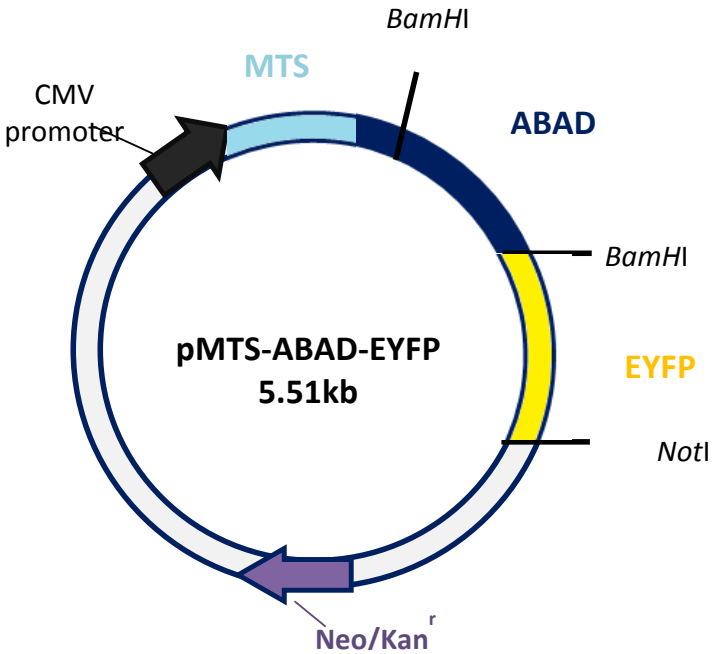

DNA plasmid pMTS-ABAD-EYFP, mitochondrial targeting sequence expressed with ABAD and fluorescent EYFP.

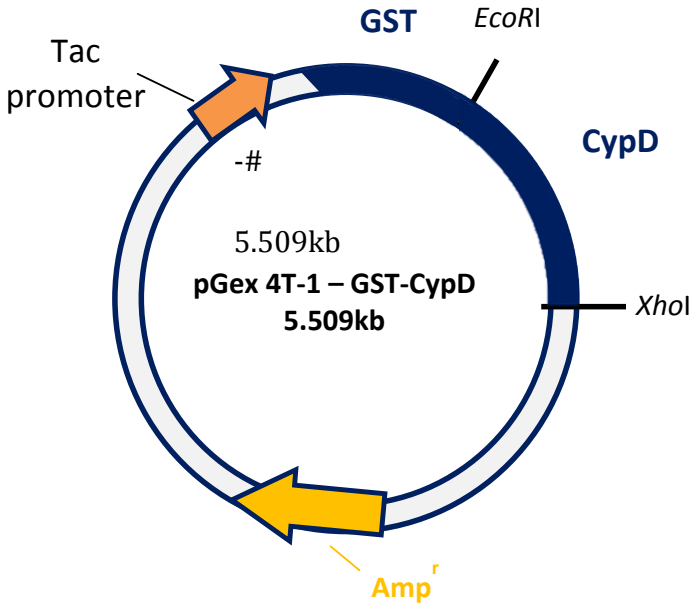

DNA Plasmid: pGex 4T-1-GST-CypD, used for cloning of pCypD-myc and MTS-CypD-myc.

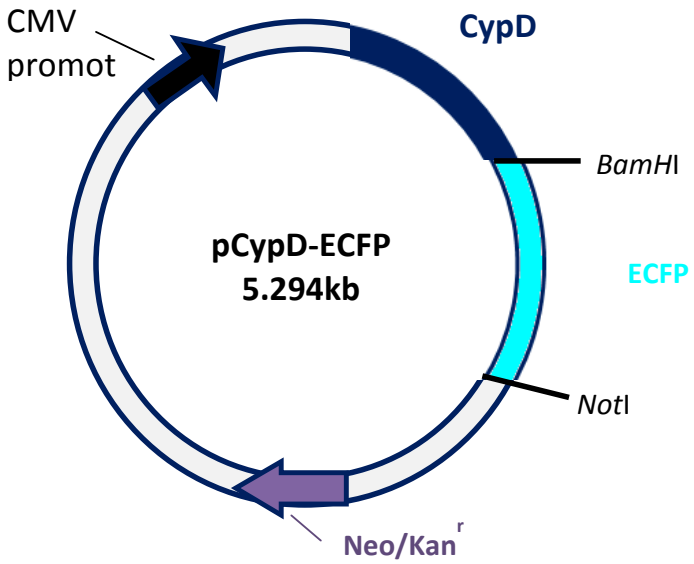

DNA plasmid pCypD-ECFP, CypD expressed with fluorescent ECFP.

APPENDIX B: CHAPTER 3: LIVE CELL FRET SPECTRA

(D)=B-A

***Ratio A* =** Area under **(D)/** Area under **(E)**

FLUOROPHORE EMISSION SPECTRA

B-1

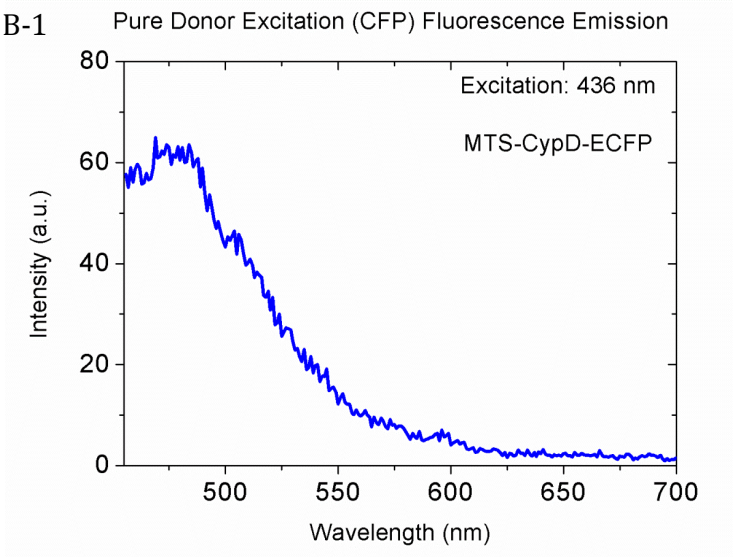

HEK cells expressing MTS-CypD-ECFP, emission spectra when excited donor fluorophore ECFP at 436nm. Values for (A) the ratio A equation.

B-2

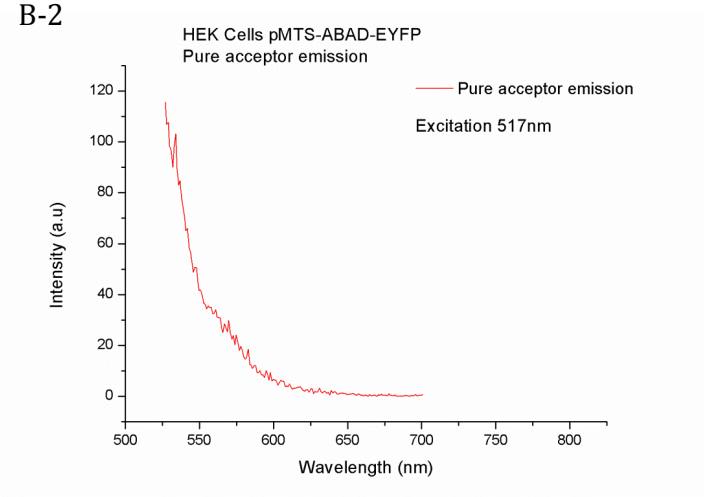

HEK cells expressing MTS-ABAD-EYFP, emission spectra when acceptor fluorophore, EYFP, is excitted at 517nm. Values for (E) the ratio A equation.

EXPERIMENTAL SPECTRA

B-3

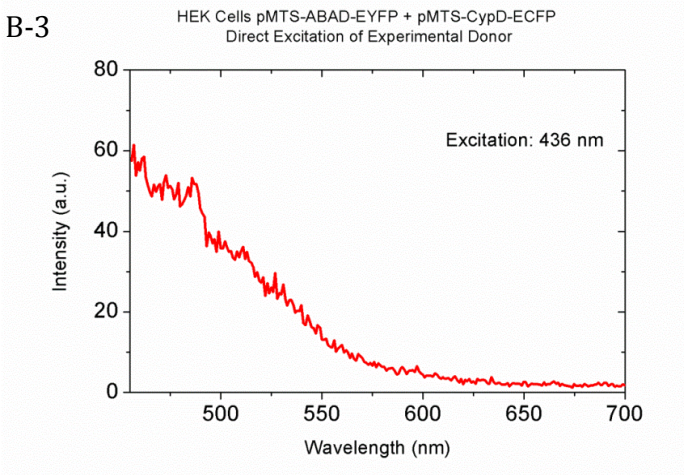

B-4

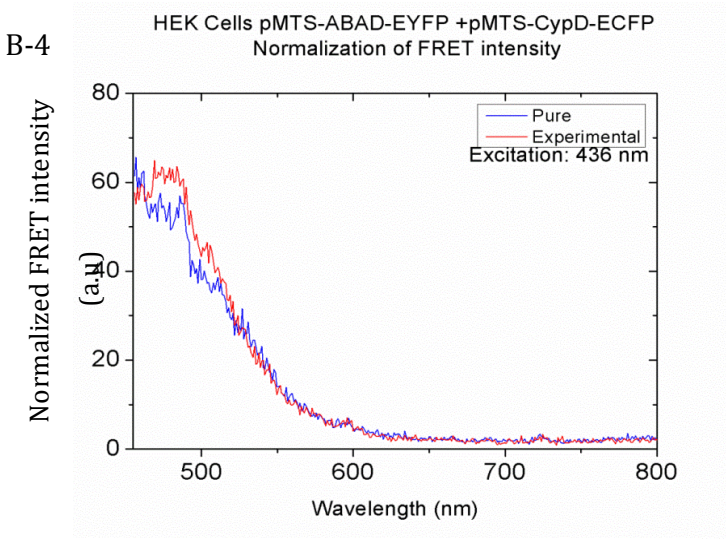

B-5

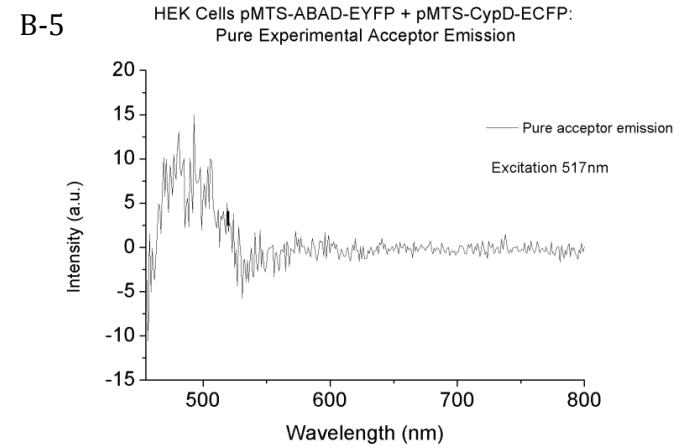

HEK cells expressing MTS-ABAD-EYFP and MTS-CypD-ECFP: **B-3)** emission spectra when donor fluorophore is excited in the presence of an acceptor EYFP. **B-4)** Normalisation of emission spectra from figure B-1 & B-3 to allow for determination of (D) ratio A. **B-5)** Excitation of acceptor fluorophore (517nm) emission spectra to obtain values (E) for ratio A.

NEGATIVE CONTROL SPECTRA

B-6

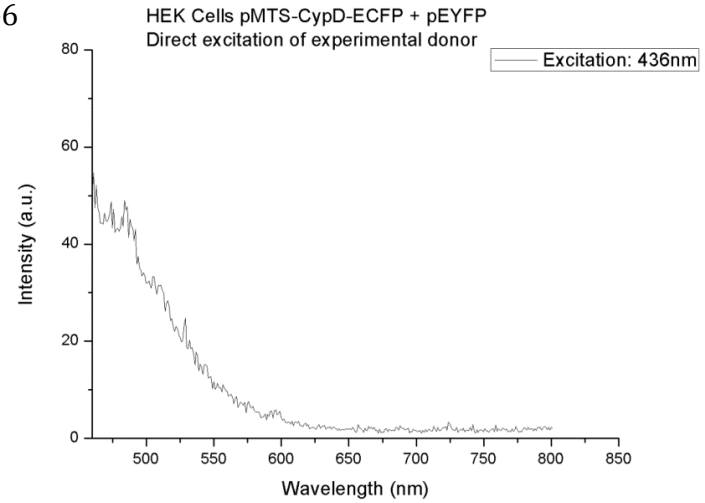

B-7

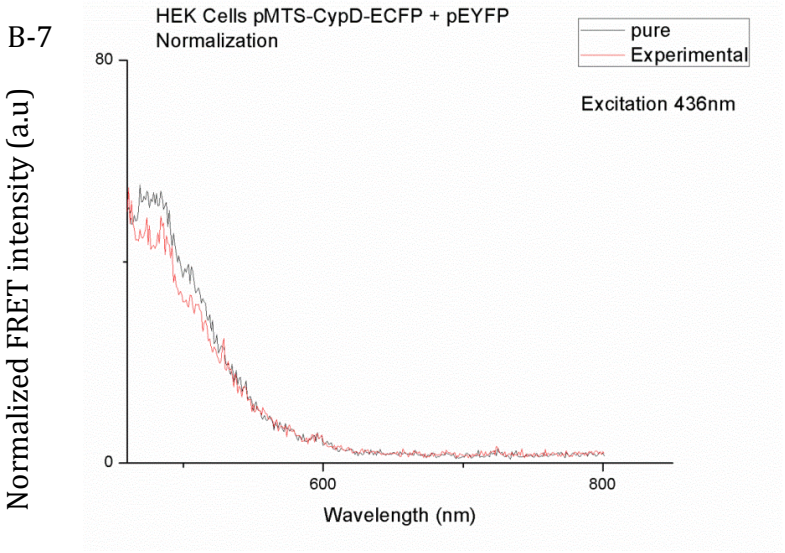

B-8

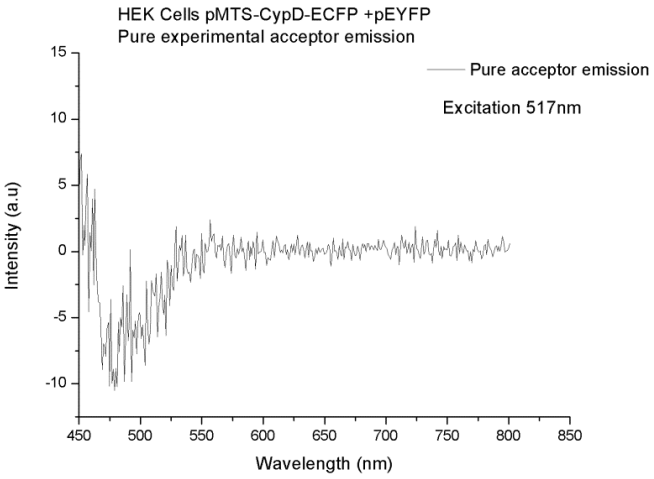

HEK cells expressing EYFP and MTS-CypD-ECFP, **B-6)** emission spectra when donor fluorophore is excited in the presence of an acceptor EYFP. **B-7)** Normalisation of emission spectra from figure B-1 & B-6 to allow for determination of ratio A. **B-8)** excitation of acceptor fluorophore EYFP (517nm) for evaluation of (E) ratio A.

POSITIVE CONTROL SPECTRA

B-12

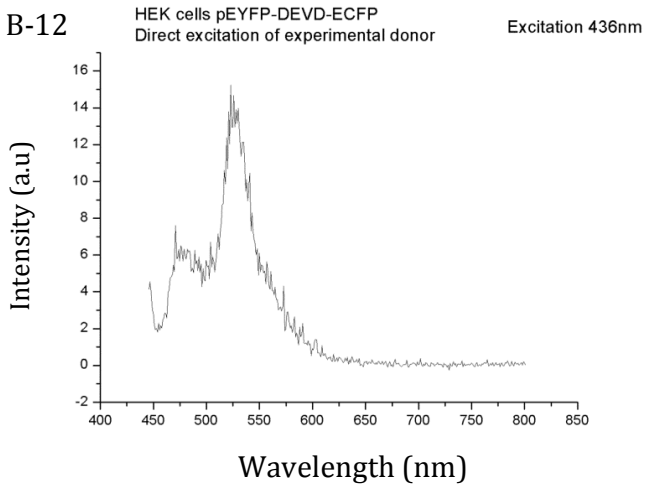

B-13

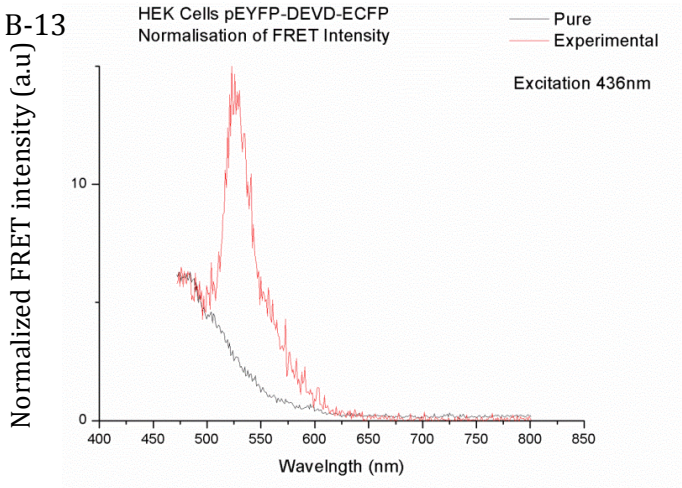

B-14

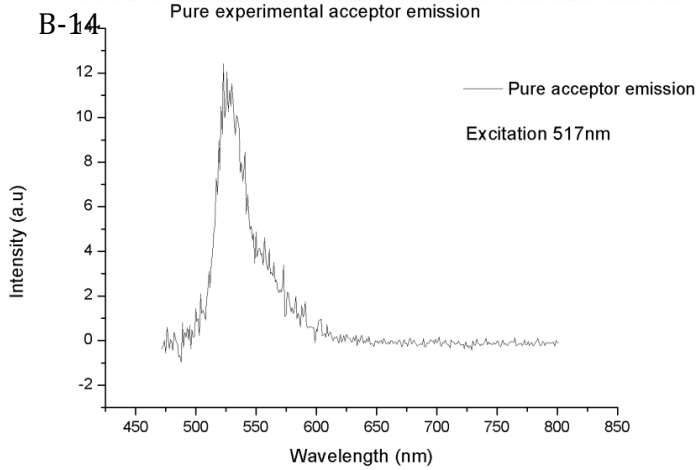

HEK cells expressing EYFP-DEVD-ECFP, **B-12)** emission spectra when donor fluorophore is excited in the presence of an acceptor EYFP. **B-13)** Normalisation of emission spectra from figure B-1 & B-8 to allow for determination of ratio A. **B-14)** emission spectra of acceptor fluorophore when excited at 517nm, for value E for the ratio A equation.

FLUOROPHORE EMISSION SPECTRA

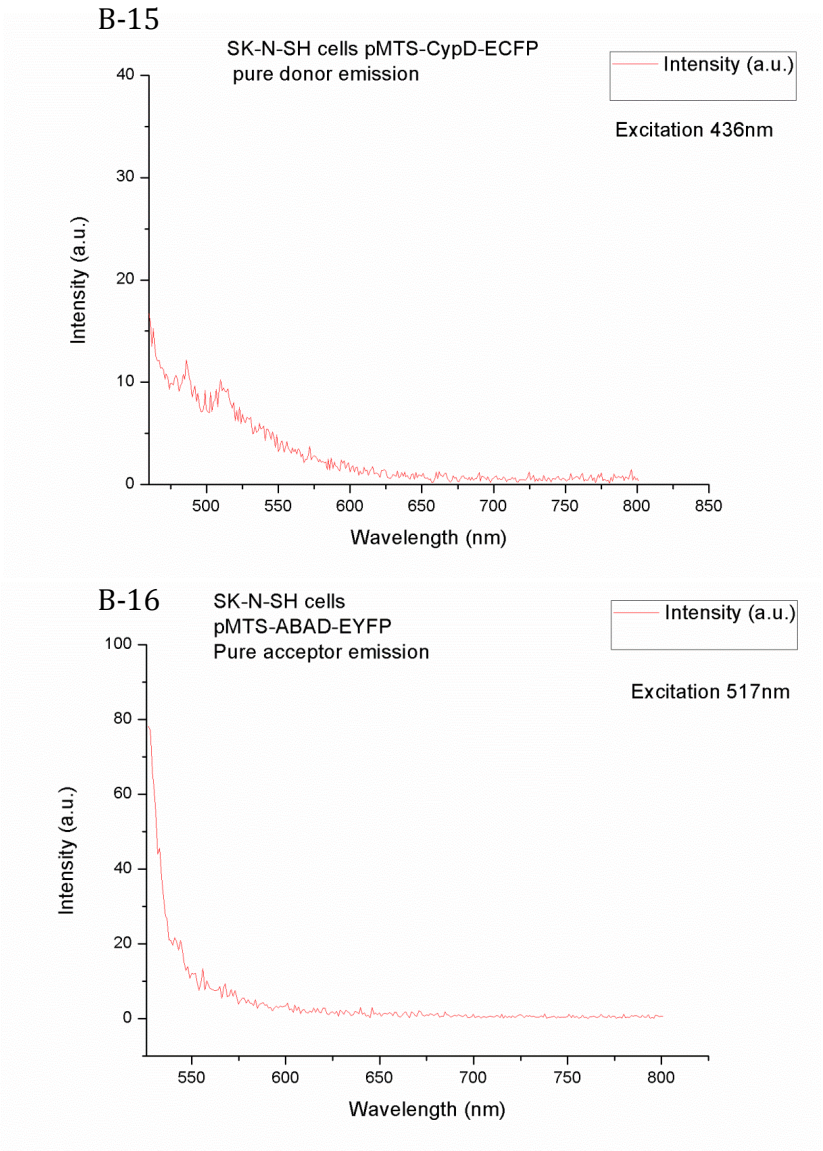

SK-N-SH cells expressing B-15) MTS-CypD-ECFP or B-16) MTS-ABAD-EYFP. **B-15)** Donor fluorophore (ECFP) emission when excited at 436nm. **B-16)** Acceptor fluorophore (EYFP) emission when excited at 517nm.

EXPERIMENTAL SPECTRA

B-17

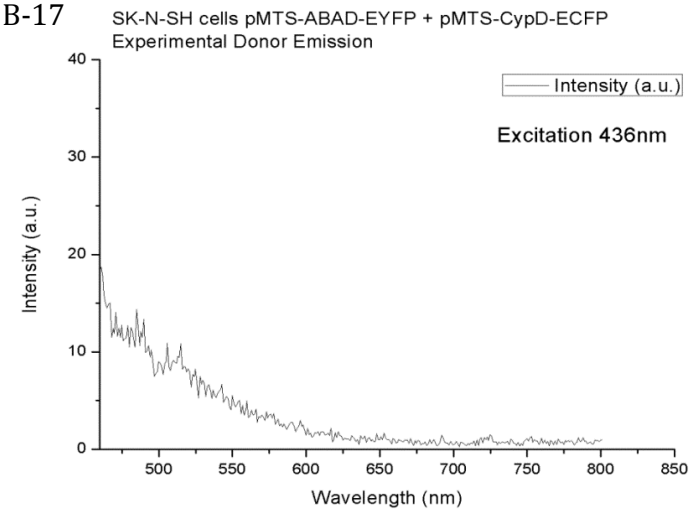

B-18

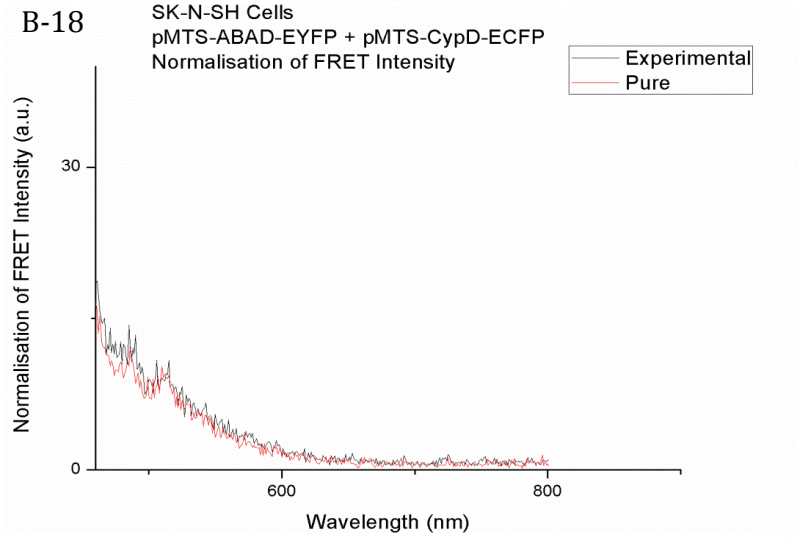

B-19

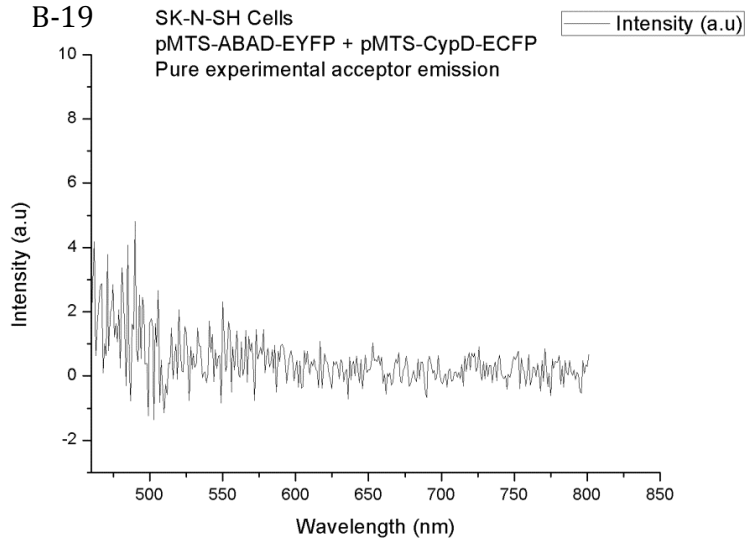

SK-N-SH cells expressing MTS-ABAD-EYFP and MTS-CypD-ECFP. **B-17)** Donor emission spectra when excited at 436nm. **B-18)** Normalisation of emission spectra B-15 and B-17 in order to calculate D (B-A) for Ratio A. **B-19)** acceptor emission when excited at 517nm, given values for E to calculate (D/E) ratio A.

NEGATIVE CONTROL SPECTRA

B-20

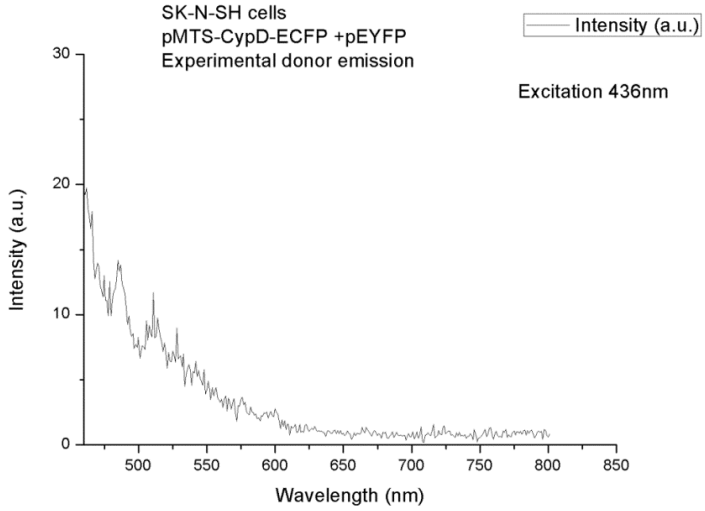

B-21

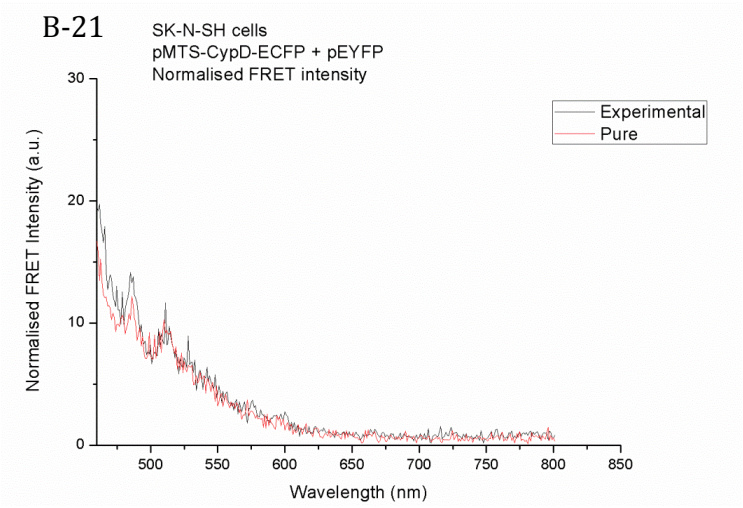

B-22

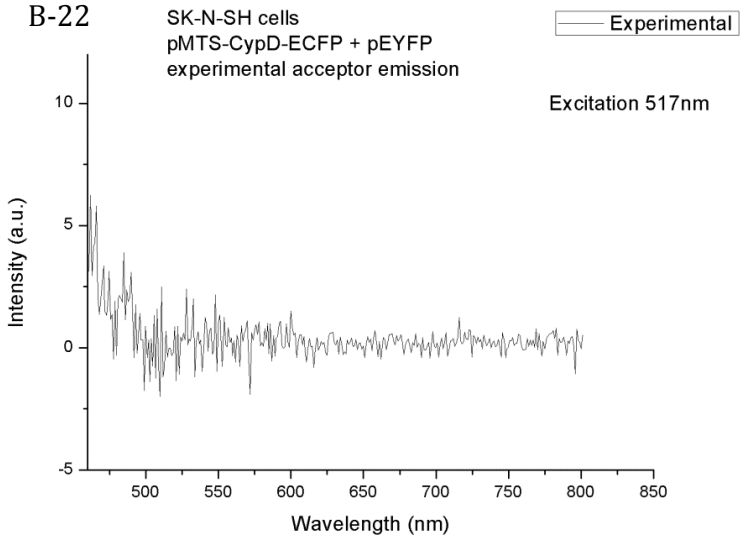

SK-N-SH cells expressing EYFP and MTS-CypD-ECFP. **B-20)** Donor emission spectra when excited at 436nm. **B-21)** Normalisation of emission spectra B-15 and B-20 in order to calculate D (B-A) for Ratio A. **B-22)** acceptor emission when excited at 517nm, given values for E to calculate (D/E) ratio A.

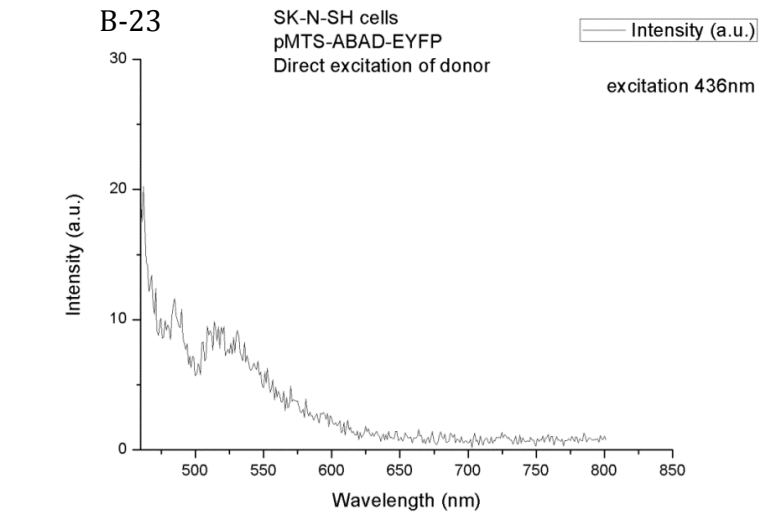

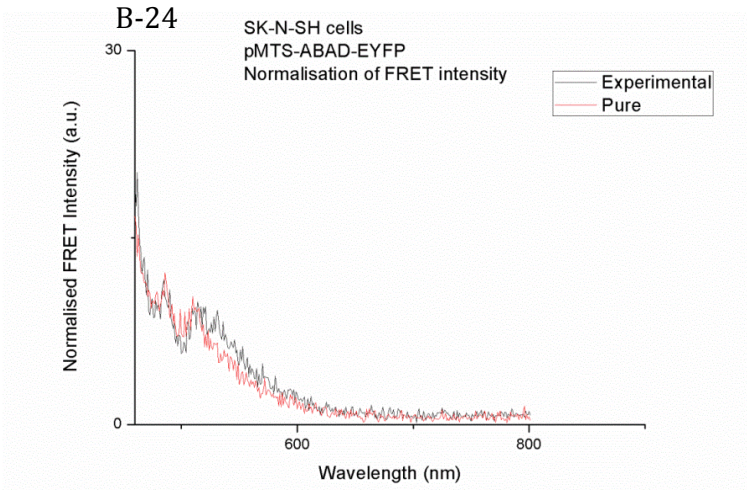

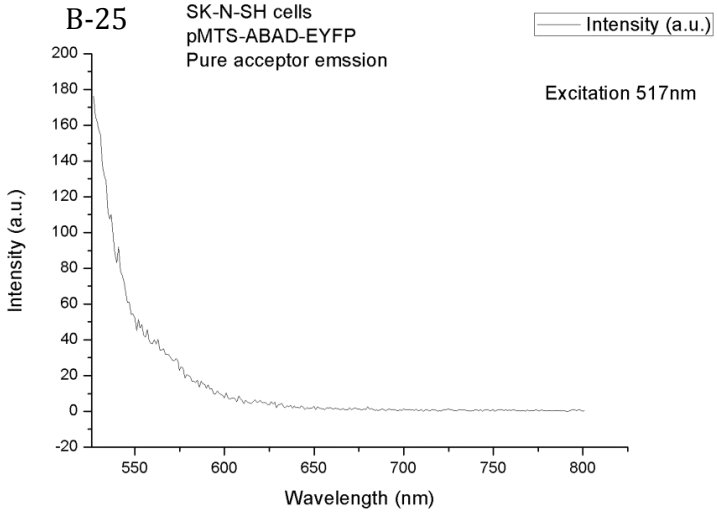

SK-N-SH cells expressing MTS-ABAD-EYFP. **B-23)** Donor emission spectra when excited at 436nm. **B-24)** Normalisation of emission spectra B-15 and B-23 in order to calculate D (B-A) for Ratio A. **B-25)** acceptor emission when excited at 517nm, given values for E to calculate (D/E) ratio A.

POSITIVE CONTROL SPECTRA

B-26

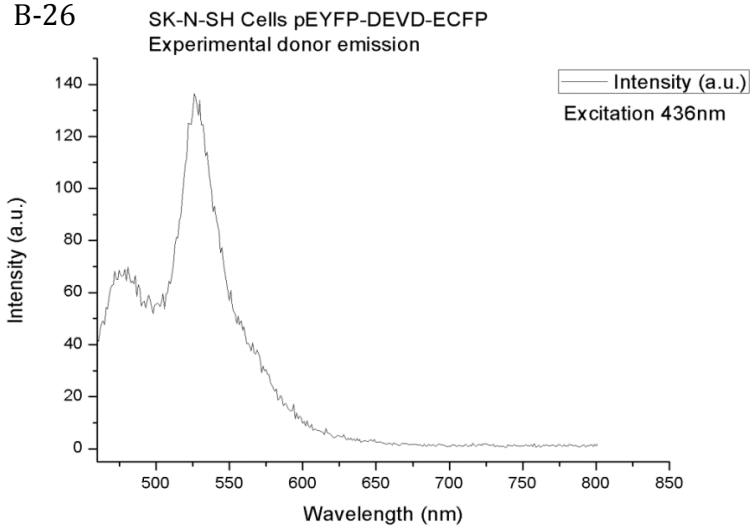

B-27

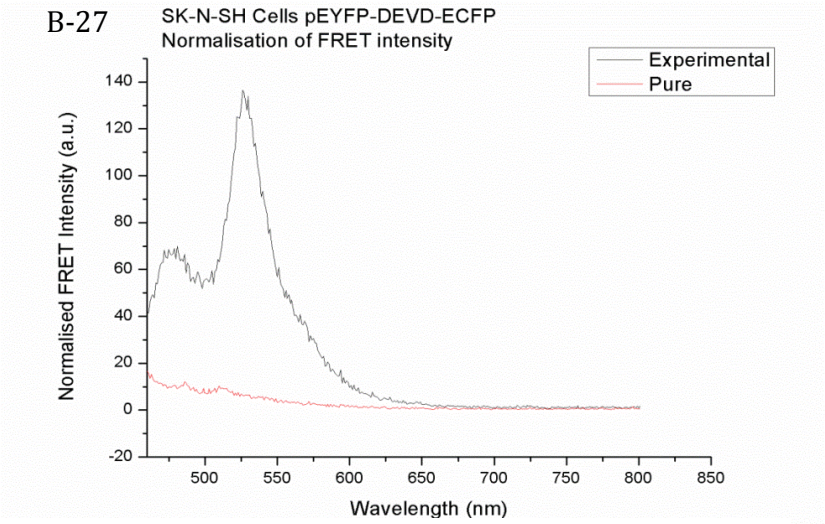

B-28

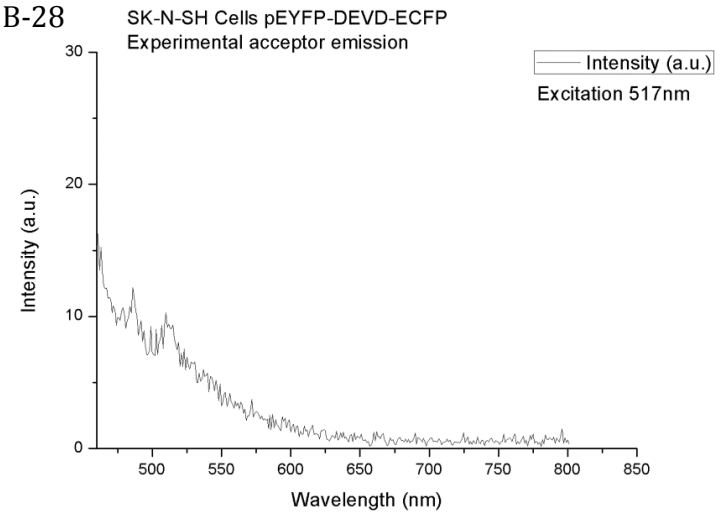

SK-N-SH cells expressing EYFP-DEVD-ECFP. **B-26)** Donor emission spectra when excited at 436nm. **B-27)** Normalisation of emission spectra B-15 and B-26 in order to calculate D (B-A) for Ratio A. **B-28)** acceptor emission when excited at 517nm, given values for E to calculate (D/E) ratio A.

APPENDIX C: CHAPTER 4: FLUORESCENT EMISSION TRACES FROM (-)-CHANA ASSAY

a) Fluorescence emission over 60

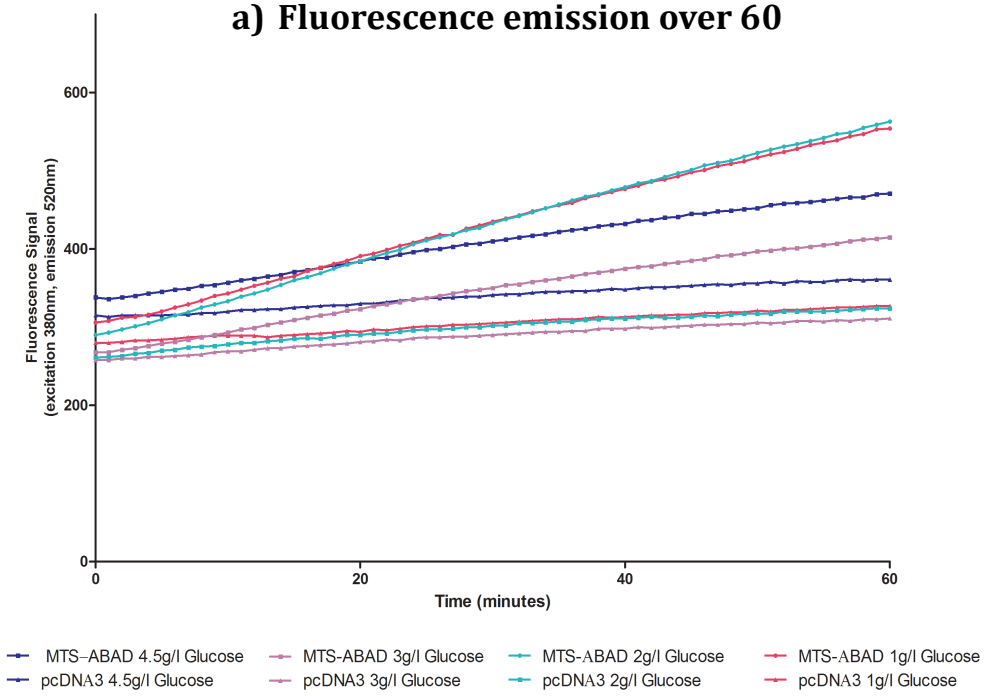

b) Fluorescence over 8 hours, SKNSH cell line

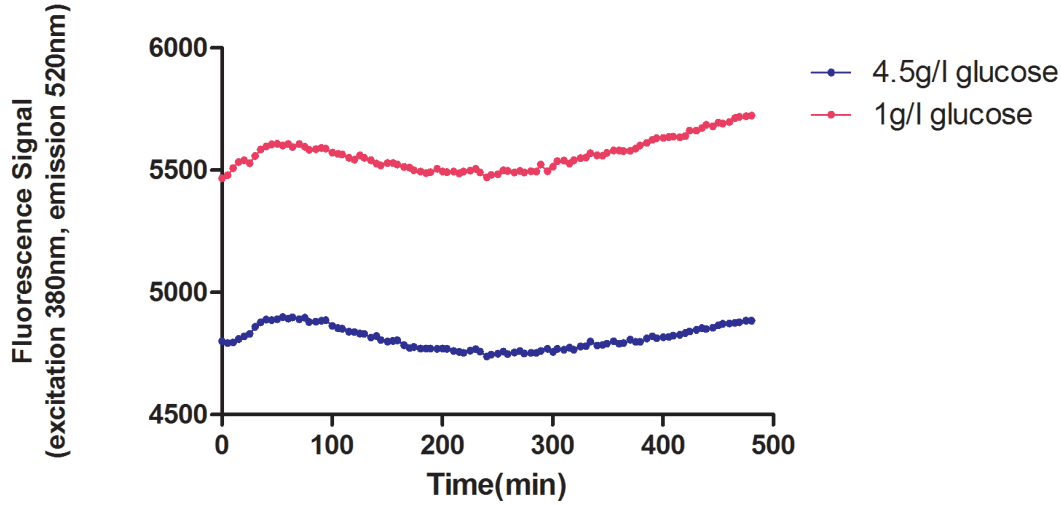

APPENDIX D: PUBLICATION

Biochemical Society Transactions www.biochemsoctrans.org

Mitochondrial β-amyloid in Alzheimer's disease

Eva Borger*, Laura Aitken*, Kirsty E.A. Muirhead*, Zoe E. Allen*, James A. Ainge†, Stuart J. Conway‡ and Frank J. Gunn-Moore*[1]

*School of Biology, Biological and Medical Sciences Building, University of St Andrews, North Haugh, St Andrews, Fife KY16 9TF, U.K., †School of Psychology, St. Mary's College, University of St Andrews, South Street, St Andrews, Fife KY16 9JP, U.K., and ‡Department of Chemistry, Chemistry Research Laboratory, University of Oxford, Mansfield Road, Oxford OX1 3TA, U.K.

Abstract

It is well established that the intracellular accumulation of Aβ (amyloid β-peptide) is associated with AD (Alzheimer's disease) and that this accumulation is toxic to neurons. The precise mechanism by which this toxicity occurs is not well understood; however, identifying the causes of this toxicity is an essential step towards developing treatments for AD. One intracellular location where the accumulation of Aβ can have a major effect is within mitochondria, where mitochondrial proteins have been identified that act as binding sites for Aβ, and when binding occurs, a toxic response results. At one of these identified sites, an enzyme known as ABAD (amyloid-binding alcohol dehydrogenase), we have identified changes in gene expression in the brain cortex, following Aβ accumulation within mitochondria. Specifically, we have identified two proteins that are up-regulated not only in the brains of transgenic animal models of AD but also in those of human sufferers. The increased expression of these proteins demonstrates the complex and counteracting pathways that are activated in AD. Previous studies have identified approximate contact sites between ABAD and Aβ; on basis of these observations, we have shown that by using a modified peptide approach it is possible to reverse the expression of these two proteins in living transgenic animals and also to recover mitochondrial and behavioural deficits. This indicates that the ABAD–Aβ interaction is potentially an interesting target for therapeutic intervention. To explore this further we used a fluorescing substrate mimic to measure the activity of ABAD within living cells, and in addition we have identified chemical fragments that bind to ABAD, using a thermal shift assay.

Introduction

A link between mitochondrial dysfunction and neurodegenerative conditions, such as AD (Alzheimer's disease), has long been suggested to exist. Observations of altered cerebral blood flow and bioenergetic deficits in dementia patients, made using positron electron tomography [1,2], initiated research into the function of mitochondria in neurodegeneration as they are central to cellular energy metabolism. Evidence of the pivotal role of metabolic pathways and free-radical turnover in mitochondria in normal aging and neurodegenerative diseases has since accumulated [3,4]. For example, Parker et al. detected reduced cytochrome *c* oxidase activity in platelets [5] and the brains of AD patients [6], whereas Sayre et al. found increased levels of 4-HNE (4-hydroxynonenal), a product of lipid peroxidation, in AD brain tissue in comparison with controls [7]. Due to the proximity of mitochondrial DNA to ROS (reactive oxygen species), which are naturally produced in the electron transport chain, this DNA is thought to accumulate mutations over time, which can lead to increasing mitochondrial dysfunction and increased production of ROS with age [8–10]. Key mitochondrial enzymes that are affected by AD include cytochrome *c* oxidase [5,11], the pyruvate dehydrogenase complex, α-ketoglutarate dehydrogenase and isocitrate dehydrogenase [12,13].

Lustbader et al. [14] used immunoelectron microscopy to show that mitochondrial Aβ (amyloid β-peptide) (both the 1–40 and 1–42 forms) localizes inside the mitochondria of Tg-mAPP [mAPP (mutant amyloid precursor protein)-overexpressing transgenic] animals and, significantly, the human AD brain. A further study showed that Aβ accumulation in the mitochondria from Tg-mAPP mice and the cerebral cortex of human AD brains is significantly higher than that in non-transgenic mice and non-AD brains [15]. More recent studies indicate that mitochondrial dysfunction and the accumulation of mitochondrial Aβ [and ABAD (amyloid-binding alcohol dehydrogenase): see below] can be observed in the early stages of AD in other commonly used transgenic animal strains, including the popular triple transgenic mouse model (human APP_{SWE}, Tau_{P301L} and $PS1_{M146V}$ [16]).

The origin of this mitochondrial Aβ is still under debate and there is experimental evidence of the local production (e.g. the presence of the γ-secretase complex within mitochondria) and/or the import of Aβ from the

Key words: Alzheimer's disease (AD), amyloid-binding alcohol dehydrogenase (ABAD), cyclohexenyl amine naphthalene alcohol (CHANA), cyclophilin D (CypD), intracellular amyloid β-peptide (intracellular Aβ), mitochondrial dysfunction.

Abbreviations used: Aβ, amyloid β-peptide; ABAD, amyloid-binding alcohol dehydrogenase; AD, Alzheimer's disease; Cdk5, cyclin-dependent kinase 5; CHANA, cyclohexenyl amine naphthalene alcohol; CHANK, cyclohexenyl amine naphthalene ketone; CypD, cyclophilin D; DP, decoy peptide; EFHD 2, EF-hand domain containing protein 2; Ep-1, endophilin-1; ER, endoplasmic reticulum; JNK, c-Jun-N-terminal kinase; mAPP, mutant amyloid precursor protein; ROS, reactive oxygen species; SPR, surface plasmon resonance; mPTP, mitochondrial permeability transition pore; Tg-mAPP, mAPP-overexpressing transgenic; TOM, translocase of outer mitochondrial membrane; TRX, thioredoxin 1.

[1]To whom correspondence should be addressed (email fjg1@st-andrews.ac.uk).

cytosol via the TOM (translocase of outer mitochondrial membrane) [17–19]. In addition to the ongoing efforts to determine how Aβ occurs within mitochondria, the other key question regards the action of Aβ once it is located within mitochondria. The addition of Aβ to cell cultures induces the dysfunction of mitochondrial respiration, ATP depletion and production of ROS [20,21]; the exposure of isolated mitochondria to Aβ reduces complex IV activity [22] and induces the formation of the permeability transition pore, which is linked to cell death [23]. In addition to these organelle-level changes, in the last decade attention has been increasingly focused on two mitochondrial proteins, ABAD (amyloid binding alcohol dehydrogenase) and CypD (cyclophilin D), both of which appear able to mediate the toxicity of the Aβ peptide. The binding of both proteins to Aβ (both the 1–40 and 1–42 forms) has been demonstrated at nanomolar Aβ concentrations, and Aβ accumulation within cells is known to result in an increase in the expression of both these proteins [23–25].

CypD

CypD, a peptidylprolyl isomerase F, is found in the mitochondrial matrix and it translocates to the inner mitochondrial membrane during times of oxidative stress where it is thought to play a role in the opening of the mPTP (mitochondrial permeability transition pore) [26]. CypD is considered to be a part of the mPTP as it associates with ANT (adenine nucleotide translocase) and possibly other factors, such as the VDAC (voltage-dependent anion channel) and the PiC (mitochondrial phosphate carrier), to contribute to the opening of the pore [27]. Using a variety of methods such as immunoprecipitation, co-localization and SPR (surface plasmon resonance) assays it was shown that CypD can bind to Aβ at nanomolar concentrations of Aβ. However, no direct contact sites have yet been identified [23]. Du et al. [23] also reported that under Aβ-rich conditions in the aging brain, CypD expression levels are increased and coincide with increased levels of ROS production. Further studies using Tg-mAPP mice deficient in the gene encoding CypD, revealed that the interaction of CypD with Aβ can result in cellular stress and cell death [23,25]. Notably, neurons derived from CypD-deficient animals are resistant to Aβ-induced opening of the mPTP and are thus protected against Aβ- and oxidative stress-induced cell death. These animals also exhibited significantly improved learning and memory functions in comparison with transgenic mAPP mice with normal expression of CypD [25].

ABAD

ABAD is the most characterized intracellular Aβ-binding protein and it was first identified in 1997 using a yeast two-hybrid screen [24]. It was originally identified within the ER (endoplasmic reticulum) and was termed ERAB (ER-associated amyloid-binding protein) [24]; however, later studies confirmed its presence inside mitochondria [28]. The action of this enzyme is primarily to catalyse the reduction of aldehydes and ketones or the reverse reaction of oxidation from alcohols for energy production. As described in more detail by Muirhead et al. [29] ABAD acts on a range of substrates, indicating the variety of functions it can have within the cell. This variety of potential substrates correlates with the finding that ABAD appears to act as a molecular switch. In the presence of low levels of Aβ, ABAD can exhibit neuroprotective effects, and its increased expression is protective in animal models of Parkinsonism [30] and metabolic stress [31]; however, as Aβ levels rise, it appears that ABAD loses its ability to protect and that it enhances Aβ toxicity [32]. X-ray crystallography studies of human and rat ABAD have provided a clear representation of the catalytic core of ABAD and enabled the identification of key residues involved in substrate binding and interaction with Aβ [33]. However, the precise identity of the residues involved in the Aβ–ABAD interaction could not be identified by means of crystallography, since loop D, the region that is thought to bind Aβ, was disordered in the structure [14]. Interaction with Aβ not only inhibits ABAD's enzyme function (though notably only at micromolar concentrations) [28,34], but also causes severe mitochondrial dysfunction and cellular toxicity [14,32], which cannot be attributed to a loss of enzyme function alone. Proteomics studies on mice overexpressing ABAD and mAPP revealed that in the living brain the ABAD–Aβ interaction also affects the expression of proteins. Proteins that were specifically identified were Ep-1 (endophilin-1) [35] and Prdx-2 (peroxiredoxin-2) [36], both of which were found to be more abundant in human AD brains in comparison with controls [35,36]. To date, the link between these two proteins and mitochondrial dysfunction remains unclear. However, evidence exists that increased levels of Ep-1 can cause the activation of JNK (c-Jun-N-terminal kinase) [35,37]. JNK is a stress kinase that has been linked to Aβ production in neuronal cells [38,39], whose action is associated with the early stages of AD [40]. Conversely, Prdx-2 is an antioxidant protein and an increase in its expression can protect against Aβ-induced toxicity [36]. Thus the increased expression of these two proteins typifies competing pathways that are activated in an AD afflicted brain.

Another important metabolic function located in mitochondria is Ca^{2+} homoeostasis. Evidence of disturbed Ca^{2+} homoeostasis [41] and alterations in Ca^{2+} regulated proteins, especially the neuronal proteinase calpain and its targets, has been detected in human AD brains, in human cortical neuron cultures *in vitro* [42,43] and in transgenic mice [44]. Interestingly, a link between the calpain-regulated Cdk5 (cyclin-dependent kinase 5) and Prdx-2 inactivation by phosphorylation has been discovered in a model of Parkinson's disease [45]. In addition, Cdk5 had been earlier identified as a candidate kinase for the mediation of neuronal toxicity in AD [46–48]. The relevance of this pathway to Prdx-2 function in AD has not been investigated so far. Our own studies indicate that the phosphorylation of Thr^{89} in Prdx-2 can regulate the observed protection against Aβ-induced toxicity (E. Borger, unpublished work). More

recently a novel Ca^{2+}-binding protein, EFHD 2 (EF-hand domain containing protein 2; swiprosin 1) was also linked to one of the hallmarks of AD [49]. EFHD 2 is associated with hyperphosphorylated tau protein in a mouse tauopathy model and in human AD brains to a greater degree than it is in control tissues [49]. Additionally, it was reported that protein levels of EFHD 2 were found to have increased in AD cases in comparison with those in controls [49], and our own studies suggest that this is also the case in the Tg-mAPP mouse model, which does not develop tauopathy (E. Borger, unpublished work). The function of EFHD 2 in neuronal cells is still unknown, but its association with two of AD hallmarks points towards its potential importance in AD pathology.

Taken together, research on human dementia patients and studies using animal as well as *in vitro* models for AD have shown that all key functions of mitochondria are affected in AD. A detrimental link between impaired brain energy metabolism, ROS production and disturbed Ca^{2+} homoeostasis has also been established in the case of other neuropathological conditions such as delirium, ischaemia and hypoglycaemia. Consequently, Blass [50,51] and Lin and Beal [52] have proposed the role of a downward 'mitochondrial spiral' in the development of neurodegenerative diseases, in particularly with regard to AD.

Therapeutic targets and development of assays

The proposed binding site of Aβ on ABAD, 'loop D', was identified through a range of complimentary techniques including X-ray crystallography and mutagenesis studies [14]. It has been shown that a synthetic peptide consisting of residues 92–120, which forms this loop, can be used as a DP (decoy peptide), which competes with ABAD as a partner that binds to Aβ. Using SPR, it was shown that this DP was able to prevent the binding of Aβ to ABAD [14]. The same region of ABAD, identified independently through an antisense peptide approach, was found to bind biotinylated Aβ with a K_d (dissociation constant) of 107 nM, using ELISA [53]. Cellular studies of the DP effects, using a Tat-DP fusion peptide to allow the peptide to cross the cell membrane, found that the application of the peptide protected neurons (from wild-type, Tg-ABAD and Tg-ABAD/mAPP mice) against Aβ-induced toxicity [14]. Similarly, the introduction of DP-TRX (thioredoxin 1; an enzyme introduced here in order to stabilize the peptide) into cell cultures using a lentiviral approach, revealed that DP-TRX-transfected cells showed decreased apoptosis, decreased LDH (lactate dehydrogenase) release and increased cell viability after treatment with Aβ in comparison with controls [54]. Compelling evidence of the effectiveness of the peptide was provided by *in vivo* studies in transgenic animals, where a fusion peptide consisting of amino acids 93–116 of loop D with a Tat sequence and a mitochondrial-targeting sequence [Tat-mito-DP(93–116)] was found to alter levels of AD biomarker proteins Prdx-2 and Ep-1 [35,36]. Intraperitoneal injection of Tat-mito-DP(93–116) into Tg-mAPP mice resulted in a reduction in Prdx-2 levels in these mice to levels that were comparable with those in non-transgenic mice [36]. Similarly, Ep-1 levels were elevated in double transgenic ABAD/mAPP mice and were found to return to basal levels when the mice were treated with Tat-mito-DP(93–116) [35]. In addition, behavioural studies revealed that treatment with the DP improved short-term memory performance in transgenic AD mouse models. Recently, Yao et al. demonstrated that double transgenic mAPP/Tat-mito-DP(91–119) mice as well as mAPP mice when systemically treated with the DP, showed significant improvement in the radial-arm water maze test of short-term memory performance in comparison with untreated mAPP mice [55].

In order to develop therapeutic compounds that target the Aβ–ABAD interaction, a robust method for monitoring the activity of the desired drug target is required. The use of purified ABAD protein to measure enzyme activity *in vitro* is well documented [29]. Utilizing the absorption of NADH at 340 nm, the rate of reduction in substrate can be measured by means of spectroscopy. Recently, we and our collaborators developed a cell-based assay that enables the study of ABAD activity in intact living cells. The assay uses a fluorescent ABAD substrate mimic, CHANA (cyclohexenyl amine naphthalene alcohol), which is based on the endogenous ABAD substrate oestradiol. CHANA is a non-fluorescent substrate under assay conditions, whereas the reaction product, CHANK (cyclohexenyl amine naphthalene ketone) fluoresces in non-aqueous environments, e.g. in cell membranes [56]. Due to these different photochemical properties, the selective detection of the accumulation of CHANK is possible. Thus the conversion of CHANA to CHANK, and hence ABAD activity, can be monitored by means of fluorescence microscopy. This novel approach has recently been improved upon by the means of synthesis of the individual stereoisomers of CHANA. (−)-CHANA was found to be selectively metabolized by ABAD, whereas (+)-CHANA showed a much higher level of background oxidation by other cellular dehydrogenases [57]. Thus, using (−)-CHANA, we have laid the foundations for a cell-based assay monitoring of ABAD activity. When using (−)-CHANA, metabolism was seen to be substantially diminished in cells treated with a known ABAD inhibitor, AG18051 [33]. Importantly, it was also demonstrated that Aβ can inhibit ABAD activity in living cells. Upon addition of 22 μM Aβ(1–42), HEK-293 cells (human embryonic kidney cells) were shown to exhibit a significant decrease in (−)-CHANA metabolism of approximately 20%. It is hoped that further development of this system will provide a robust cell-based assay for use in the identification of potential modulators of ABAD function [57].

The future

AD is a complex disease, and likewise it becomes more and more apparent that the toxicity of the Aβ peptide is also a complex process. Indeed, although many approaches to explain AD pathology have centred on extracellular Aβ, there

Figure 1 | **Consequences of mitochondrial Aβ**

APP (amyloid precursor protein) can be transported to mitochondria, where it interacts with TOM and TIM (translocase of the inner membrane), disturbing mitochondrial protein import (1). Aβ can be imported into mitochondria via TIM and TOM and is found associated with the inner mitochondrial membrane, disrupting mitochondrial respiration and leading to an excess production of ROS (2). Aβ has been found to interact with ABAD in the mitochondrial matrix, inhibiting enzyme activity (3). The Aβ–ABAD interaction also leads to an up-regulation of AD biomarkers Ep-1 (4) and Prdx-2 (5). At the inner mitochondrial membrane, Aβ can interact with CypD, which is involved in the formation of mPTP and Ca^{2+}-release from mitochondria (6). Aβ can be found in the cytosol, disturbing cell signalling, protein degradation and causing ROS production, which leads to an increase in cytosolic Ca^{2+} (7). Ca^{2+}-mediated Cdk5 activation has been found to inhibit Prdx-2's antioxidant function.

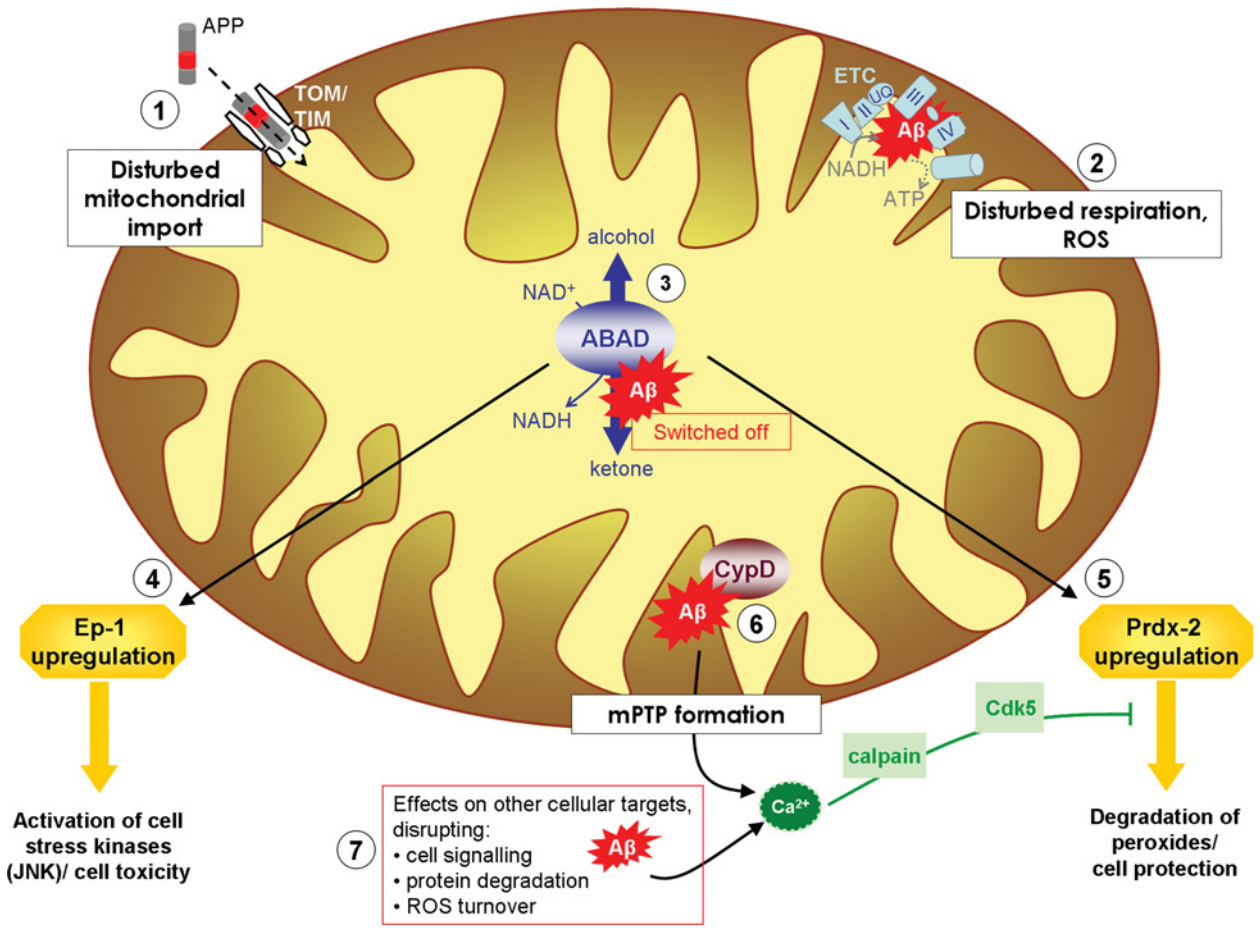

has been lesser focus on the involvement of intracellular species of Aβ. Our studies with our collaborators have focused on these events (summarized in Figure 1). They suggest that the one-drug and one-target approaches for the treatment of AD are unlikely to constitute an effective strategy of treatment of AD. Consequently, the treatment of this disease will probably require a three-pronged approach, targeting, for example: (i) the formation/clearance of Aβ and that of hyperphosphorylated tau; (ii) the support and stabilization of the remaining neuronal networks; and (iii) protection of potential sensitive intracellular targets. The integrity and function of mitochondria is one such sensitive intracellular target, and though ABAD and CypD are not classical drug targets they are important players in the sequence of events resulting in mitochondrial dysfunction. Therefore future approaches for the treatment of AD will greatly benefit from an understanding of their involvement in AD.

Funding

Our work is funded by an Alzheimer's Research UK William Lindsay Ph.D. Scholarship and Wellcome Trust Value in People award to K.E.A.M. and the Biotechnology and Biological Sciences Research Council. S.J.C. thanks St Hugh's College, Oxford, for research support.

References

1 Foster, N.L., Chase, T.N., Fedio, P., Patronas, N.J., Brooks, R.A. and Di Chiro, G. (1983) Alzheimer's disease: focal cortical changes shown by positron emission tomography. Neurology **33**, 961–965

2 Duara, R., Grady, C., Haxby, J., Sundaram, M., Cutler, N.R., Heston, L., Moore, A., Schlageter, N., Larson, S. and Rapoport, S.I. (1986) Positron emission tomography in Alzheimer's disease. Neurology **36**, 879–887
3 Beal, M.F. (1995) Aging, energy, and oxidative stress in neurodegenerative diseases. Ann. Neurol. **38**, 357–366
4 Bowling, A.C. and Beal, M.F. (1995) Bioenergetic and oxidative stress in neurodegenerative diseases. Life Sci. **56**, 1151–1171
5 Parker, Jr, W.D., Mahr, N.J., Filley, C.M., Parks, J.K., Hughes, D., Young, D.A. and Cullum, C.M. (1994) Reduced platelet cytochrome *c* oxidase activity in Alzheimer's disease. Neurology **44**, 1086–1090
6 Parker, Jr, W.D., Parks, J., Filley, C.M. and Kleinschmidt-DeMasters, B.K. (1994) Electron transport chain defects in Alzheimer's disease brain. Neurology **44**, 1090–1096
7 Sayre, L.M., Zelasko, D.A., Harris, P.L.R, Perry, G., Salomon, R.G. and Smith, M.A. (1997) 4-Hydroxynonenal-derived advanced lipid peroxidation end products are increased in Alzheimer's disease. J. Neurochem. **68**, 2092–2097
8 Richter, C., Park, J.W. and Ames, B.N. (1988) Normal oxidative damage to mitochondrial and nuclear DNA is extensive. Proc. Natl. Acad. Sci. U.S.A. **85**, 6465–6467
9 Beal, M.F. (2005) Mitochondria take center stage in aging and neurodegeneration. Ann. Neurol. **58**, 495–505
10 Liu, J., Head, E., Gharib, A.M., Yuan, W., Ingersoll, R.T., Hagen, T.M., Cotman, C.W. and Ames, B.N. (2002) Memory loss in old rats is associated with brain mitochondrial decay and RNA/DNA oxidation: partial reversal by feeding acetyl-L-carnitine and/or *R*-α-lipoic acid. Proc. Natl. Acad. Sci. U.S.A. **99**, 2356–2361
11 Cottrell, D.A., Blakely, E.L., Johnson, M.A., Ince, P.G. and Turnbull, D.M. (2001) Mitochondrial enzyme-deficient hippocampal neurons and choroidal cells in AD. Neurology **57**, 260–264
12 Bubber, P., Haroutunian, V., Fisch, G., Blass, J.P. and Gibson, G.E. (2005) Mitochondrial abnormalities in Alzheimer brain: mechanistic implications. Ann. Neurol. **57**, 695–703
13 Gibson, G.E., Park, L.C., Zhang, H., Sorbi, S. and Calingasan, N.Y. (1999) Oxidative stress and a key metabolic enzyme in Alzheimer brains, cultured cells, and an animal model of chronic oxidative deficits. Ann. N.Y. Acad. Sci. **893**, 79–94
14 Lustbader, J.W., Cirilli, M., Lin, C., Xu, H.W., Takuma, K., Wang, N., Caspersen, C., Chen, X., Pollak, S., Chaney, M. et al. (2004) ABAD directly links Aβ to mitochondrial toxicity in Alzheimer's disease. Science **304**, 448–452
15 Caspersen, C., Wang, N., Yao, J., Sosunov, A., Chen, X., Lustbader, J.W., Wei Xu, H., Stern, D., McKhann, G. and Yan, S.D. (2005) Mitochondrial Aβ: a potential focal point for neuronal metabolic dysfunction in Alzheimer's disease. FASEB J. **19**, 2040–2041
16 Yao, J., Irwin, R.W., Zhao, L., Nilsen, J., Hamilton, R.T. and Brinton, R.D. (2009) Mitochondrial bioenergetic deficit precedes Alzheimer's pathology in female mouse model of Alzheimer's disease. Proc. Natl. Acad. Sci. U.S.A. **106**, 14670–14675
17 Anandatheerthavarada, H.K., Biswas, G., Robin, M.A. and Avadhani, N.G. (2003) Mitochondrial targeting and a novel transmembrane arrest of Alzheimer's amyloid precursor protein impairs mitochondrial function in neuronal cells. J. Cell Biol. **161**, 41–54
18 Devi, L., Prabhu, B.M., Galati, D.F., Avadhani, N.G. and Anandatheerthavarada, H.K. (2006) Accumulation of amyloid precursor protein in the mitochondrial import channels of human Alzheimer's disease brain is associated with mitochondrial dysfunction. J. Neurosci. **26**, 9057–9068
19 Hansson Petersen, C.A., Alikhani, N., Behbahani, H., Wiehager, B., Pavlov, P.F., Alafuzoff, I., Leinonen, V., Ito, A., Winblad, B., Glaser, E. and Ankarcrona, M. (2008) The amyloid β-peptide is imported into mitochondria via the TOM import machinery and localized to mitochondrial cristae. Proc. Natl. Acad. Sci. U.S.A. **105**, 13145–13150
20 Casley, C.S., Land, J.M., Sharpe, M.A., Clark, J.B., Duchen, M.R. and Canevari, L. (2002) β-Amyloid fragment 25–35 causes mitochondrial dysfunction in primary cortical neurons. Neurobiol. Dis. **10**, 258–267
21 Chen, J.X. and Yan, S.D. (2007) Amyloid-β-induced mitochondrial dysfunction. J. Alzheimer's Dis. **12**, 177–184
22 Canevari, L., Clark, J.B. and Bates, T.E. (1999) β-Amyloid fragment 25–35 selectively decreases complex IV activity in isolated mitochondria. FEBS Lett. **457**, 131–134
23 Du, H., Guo, L., Fang, F., Chen, D., Sosunov, A.A., McKhann, G.M., Yan, Y., Wang, C., Zhang, H., Molkentin, J.D. et al. (2008) Cyclophilin D deficiency attenuates mitochondrial and neuronal perturbation and ameliorates learning and memory in Alzheimer's disease. Nat. Med. **14**, 1097–1105
24 Yan, S.D., Fu, J., Soto, C., Chen, X., Zhu, H., Al-Mohanna, F., Collison, K., Zhu, A., Stern, E., Saido, T. et al. (1997) An intracellular protein that binds amyloid-β peptide and mediates neurotoxicity in Alzheimer's disease. Nature **389**, 689–695
25 Du, H., Guo, L., Zhang, W., Rydzewska, M. and Yan, S. (2011) Cyclophilin D deficiency improves mitochondrial function and learning/memory in aging Alzheimer disease mouse model. Neurobiol. Aging **32**, 398–406
26 Connern, C.P. and Halestrap, A.P. (1994) Recruitment of mitochondrial cyclophilin to the mitochondrial inner membrane under conditions of oxidative stress that enhance the opening of a calcium-sensitive non-specific channel. Biochem. J. **302**, 321–324
27 Crompton, M., Virji, S. and Ward, J.M. (1998) Cyclophilin-D binds strongly to complexes of the voltage-dependent anion channel and the adenine nucleotide translocase to form the permeability transition pore. Eur. J. Biochem. **258**, 729–735
28 Oppermann, U.C., Salim, S., Tjernberg, L.O., Terenius, L. and Jornvall, H. (1999) Binding of amyloid β-peptide to mitochondrial hydroxyacyl-CoA dehydrogenase (ERAB): regulation of an SDR enzyme activity with implications for apoptosis in Alzheimer's disease. FEBS Lett. **451**, 238–242
29 Muirhead, K.E.A., Borger, E., Aitken, L., Conway, S.J. and Gunn-Moore, F.J. (2010) The consequences of mitochondrial amyloid β-peptide in Alzheimer's disease. Biochem. J. **426**, 255–270
30 Tieu, K., Perier, C., Vila, M., Caspersen, C., Zhang, H.-P., Teismann, P., Jackson-Lewis, V., Stern, D.M., Yan, S.D. and Przedborski, S. (2004) L-3-hydroxyacyl-CoA dehydrogenase II protects in a model of Parkinson's disease. Ann. Neurol. **56**, 51–60
31 Yan, S.D., Zhu, Y., Stern, E.D., Hwang, Y.C., Hori, O., Ogawa, S., Frosch, M.P., Connolly, Jr, E.S., McTaggert, R., Pinsky, D.J. et al. (2000) Amyloid β-peptide-binding alcohol dehydrogenase is a component of the cellular response to nutritional stress. J. Biol. Chem. **275**, 27100–27109
32 Takuma, K., Yao, J., Huang, J., Xu, H., Chen, X., Luddy, J., Trillat, A.C., Stern, D.M., Arancio, O. and Yan, S.S. (2005) ABAD enhances Aβ-induced cell stress via mitochondrial dysfunction. FASEB J. **19**, 597–598
33 Kissinger, C.R., Rejto, P.A., Pelletier, L.A., Thomson, J.A., Showalter, R.E., Abreo, M.A., Agree, C.S., Margosiak, S., Meng, J.J., Aust, R.M. et al. (2004) Crystal structure of human ABAD/HSD10 with a bound inhibitor: implications for design of Alzheimer's disease therapeutics. J. Mol. Biol. **342**, 943–952
34 Yan, S.D., Shi, Y., Zhu, A., Fu, J., Zhu, H., Zhu, Y., Gibson, L., Stern, E., Collison, K., Al-Mohanna, F. et al. (1999) Role of ERAB/L-3-hydroxyacyl-coenzyme a dehydrogenase type II activity in Aβ-induced cytotoxicity. J. Biol. Chem. **274**, 2145–2156
35 Ren, Y., Xu, H.W., Davey, F., Taylor, M., Aiton, J., Coote, P., Fang, F., Yao, J., Chen, D., Chen, J.X. et al. (2008) Endophilin I expression is increased in the brains of Alzheimer disease patients. J. Biol. Chem. **283**, 5685–5691
36 Yao, J., Taylor, M., Davey, F., Ren, Y., Aiton, J., Coote, P., Fang, F., Chen, J.X., Yan, S.D. and Gunn-Moore, F.J. (2007) Interaction of amyloid binding alcohol dehydrogenase/Aβ mediates up-regulation of peroxiredoxin II in the brains of Alzheimer's disease patients and a transgenic Alzheimer's disease mouse model. Mol. Cell. Neurosci. **35**, 377–382
37 Ramjaun, A.R., Angers, A., Legendre-Guillemin, V., Tong, X.-K. and McPherson, P.S. (2001) Endophilin regulates JNK activation through its interaction with the germinal center kinase-like kinase. J. Biol. Chem. **276**, 28913–28919
38 Colombo, A., Bastone, A., Ploia, C., Sclip, A., Salmona, M., Forloni, G. and Borsello, T. (2009) JNK regulates APP cleavage and degradation in a model of Alzheimer's disease. Neurobiol. Dis. **33**, 518–525
39 Tamagno, E., Parola, M., Bardini, P., Piccini, A., Borghi, R., Guglielmotto, M., Santoro, G., Davit, A., Danni, O., Smith, M.A. et al. (2005) β-Site APP cleaving enzyme up-regulation induced by 4-hydroxynonenal is mediated by stress-activated protein kinases pathways. J. Neurochem. **92**, 628–636
40 Lagalwar, S., Guillozet-Bongaarts, A.L., Berry, R.W. and Binder, L.I. (2006) Formation of phospho-SAPK/JNK granules in the hippocampus is an early event in Alzheimer disease. J. Neuropathol. Exp. Neurol. **65**, 455–464
41 Mattson, M.P., Cheng, B., Davis, D., Bryant, K., Lieberburg, I. and Rydel, R.E. (1992) β-Amyloid peptides destabilize calcium homeostasis and render human cortical neurons vulnerable to excitotoxicity. J. Neurosci. **12**, 376–389

42 Kuwako, K.-I., Nishimura, I., Uetsuki, T., Saido, T.C. and Yoshikawa, K. (2002) Activation of calpain in cultured neurons overexpressing Alzheimer amyloid precursor protein. Mol. Brain Res. **107**, 166–175
43 Saito, K., Elce, J.S., Hamos, J.E. and Nixon, R.A. (1993) Widespread activation of calcium-activated neutral proteinase (calpain) in the brain in Alzheimer disease: a potential molecular basis for neuronal degeneration. Proc. Natl. Acad. Sci. U.S.A. **90**, 2628–2632
44 Liang, B., Duan, B.-Y., Zhou, X.-P., Gong, J.-X. and Luo, Z.-G. (2010) Calpain activation promotes BACE1 expression, amyloid precursor protein processing, and amyloid plaque formation in a transgenic mouse model of Alzheimer disease. J. Biol. Chem. **285**, 27737–27744
45 Qu, D., Rashidian, J., Mount, M.P., Aleyasin, H., Parsanejad, M., Lira, A., Haque, E., Zhang, Y., Callaghan, S., Daigle, M. et al. (2007) Role of Cdk5-mediated phosphorylation of Prx2 in MPTP toxicity and Parkinson's disease. Neuron **55**, 37–52
46 Cole, A.R., Noble, W., van Aalten, L., Plattner, F., Meimaridou, R., Hogan, D., Taylor, M., LaFrancois, J., Gunn-Moore, F., Verkhratsky, A. et al. (2007) Collapsin response mediator protein-2 hyperphosphorylation is an early event in Alzheimer's disease progression. J. Neurochem. **103**, 1132–1144
47 Cruz, J.C., Kim, D., Moy, L.Y., Dobbin, M.M., Sun, X., Bronson, R.T. and Tsai, L.-H. (2006) p25/cyclin-dependent kinase 5 induces production and intraneuronal accumulation of amyloid β *in vivo*. J. Neurosci. **26**, 10536–10541
48 Smith, P.D., Crocker, S.J., Jackson-Lewis, V., Jordan-Sciutto, K.L., Hayley, S., Mount, M.P., O'Hare, M.J., Callaghan, S., Slack, R.S., Przedborski, S. et al. (2003) Cyclin-dependent kinase 5 is a mediator of dopaminergic neuron loss in a mouse model of Parkinson's disease. Proc. Natl. Acad. Sci. U.S.A. **100**, 13650–13655
49 Vega, I.E., Traverso, E.E., Ferrer-Acosta, Y., Matos, E., Colon, M., Gonzalez, J., Dickson, D., Hutton, M., Lewis, J. and Yen, S.H. (2008) A novel calcium-binding protein is associated with tau proteins in tauopathy. J. Neurochem. **106**, 96–106
50 Blass, J.P. (2000) The mitochondrial spiral: an adequate cause of dementia in the Alzheimer's syndrome. Ann. N.Y. Acad. Sci. **924**, 170–183
51 Blass, J.P. (2001) Brain metabolism and brain disease: is metabolic deficiency the proximate cause of Alzheimer dementia? J. Neurosci. Res. **66**, 851–856
52 Lin, M.T. and Beal, M.F. (2006) Mitochondrial dysfunction and oxidative stress in neurodegenerative diseases. Nature **443**, 787–795
53 Milton, N.G., Mayor, N.P. and Rawlinson, J. (2001) Identification of amyloid-β binding sites using an antisense peptide approach. NeuroReport **12**, 2561–2566
54 Yang, X., Yang, Y., Wu, J. and Zhu, J. (2007) Stable expression of a novel fusion peptide of thioredoxin-1 and ABAD-inhibiting peptide protects PC12 cells from intracellular amyloid-β. J. Mol. Neurosci. **33**, 180–188
55 Yao, J., Du, H., Yan, S., Fang, F., Wang, C., Lue, L.-F., Guo, L., Chen, D., Stern, D., Gunn-Moore, F.J. et al. (2011) Inhibition of ABAD–Aβ interaction reduces Aβ accumulation and improves mitochondrial function in a mouse model of Alzheimer's disease. J. Neurosci. **31**, 2313–2320
56 Froemming, M.K. and Sames, D. (2007) Harnessing functional plasticity of enzymes: a fluorogenic probe for imaging 17β-HSD10 dehydrogenase, an enzyme involved in Alzheimer's and Parkinson's diseases. J. Am. Chem. Soc. **129**, 14518–14522
57 Muirhead, K.E.A., Froemming, M., Li, X., Musilek, K., Conway, S.J., Sames, D. and Gunn-Moore, F.J. (2010) (−)-CHANA, a fluorogenic probe for detecting amyloid binding alcohol dehydrogenase HSD10 activity in living cells. ACS Chem. Biol. **5**, 1105–1114

Received 6 December 2010
doi:10.1042/BST0390868